# The geomicrobiology of iron, cobalt, nickel and manganese in lateritic tropical soils from the Santa Elena Peninsula, Costa Rica

A thesis submitted to the University of Manchester for the degree of

Doctor of Philosophy

in the Faculty of Science and Engineering

**2019**

**Agustín F Solano Arguedas**

School of Natural Sciences

Department of Earth and Environmental Sciences

# List of contents

Final word count: 71805 words

# List of figures

---

**Chapter 2**

**Chapter 6 Supplementary**

**Appendix 1**

# List of tables

**Chapter 6**



**Appendix 1**

## List of abbreviations

| | |
|---|---|
| ACG | Área de Conservación Guanacaste (Guanacaste Conservation Area) |
| AGW | Artificial Ground Water |
| ALS | Advance Light Source |
| ANOVA | Analysis of Variances |
| $CoG^3$ | Cobalt Geology, Geometallurgy and Geomicrobiology |
| CONAGEBIO | Comisión Nacional para la Gestión de la Biodiversidad (National Commission for Biodiversity Management) |
| Cpx | Clinopyroxene |
| DLS | Diamond Light Source |
| EDS | Energy Dispersive Spectroscopy |
| EDTA | Ethylenediaminetetraacetic Acid |
| $E_h$ | Redox potential |
| EPMA | Electron Probe Micro Analysis |
| EXAFS | Extended X-ray Absorption Fine Structure |
| GC-TCD | Gas Chromatography-Thermal Conductivity Detector |
| GGC | Geochemical/Geographical Classification |
| GIS | Geographic Information System |
| HC | Hierarchical Cluster Analysis |
| IC | Ion Chromatography |
| ICDD | International Centre for Diffraction Data |
| ICP-AES | Inductively Coupled Plasma Atomic Emission Spectroscopy |
| ICP-MS | Inductively Coupled Plasma Mass Spectroscopy |
| ITCZ | Intertropical Convergence Zone |
| ITS | Internal Transcribed Spacer gene |
| LOI | Loss on Ignition |
| Masl | Metres Above Sea Level |
| MAT | Middle America Trench |

| | |
|---|---|
| MICITT | Ministerio de Ciencia, Tecnología y Telecomunicaciones (Ministry of Science, Technology and Telecommunications) |
| NERC | Natural Environment Research Council |
| NHM | Natural History Museum |
| Ol | Olivine |
| Opx | Orthopyroxene |
| OTU | Operational Taxonomic Unit |
| PCA | Principal Component Analysis |
| PCR | Polymerase Chain Reaction |
| qPCR | Quantitative Real Time Polymerase Chain Reaction |
| ReForesta | Unidad de Recursos Forestales (Forest Resources Unit) |
| SAED | Selected Area Electron Diffraction |
| SEES | School of Earth and Environmental Sciences |
| SINAC | Sistema Nacional de Áreas de Conservación (National System of Conservation Areas) |
| TEM | Transmission Electron Microscopy |
| TOC | Total Organic Carbon |
| UCR | Universidad de Costa Rica (University of Costa Rica) |
| UNESCO | United Nations Educational Scientific and Cultural Organization |
| VFA | Volatile Fatty Acid |
| WDS | Wavelength Dispersive Spectrometers |
| XANES | X-ray Apsorption Near Edge Spectroscopy |
| XAS | X-ray Absorption Spectroscopy |
| XMCD | X-ray Magnetic Circular Dichroism Spectroscopy |
| XRD | X-ray Diffraction Spectroscopy |
| XRF | X-ray Fluorescence Spectroscopy |

## Thesis abstract

There is an increasing interest in the biogeochemistry of metals, like cobalt, fuelled by the growing need for batteries and other high technology products. Bioprocessing of Co has been proposed to improve its recovery from Ni-rich laterites, but the natural biogeochemistry of Co and other metals associated such as Fe, Ni and Mn in laterites is still relatively unexplored. In Costa Rica, the Santa Elena Peninsula is closely associated with the Santa Elena Ophiolite, and the tropical climate alongside the lack of anthropogenic alteration for nearly 50 years, make this a unique area to study natural biogeochemical processes in a laterite/serpentine context. This thesis therefore aimed to understand the biogeochemical cycling of Fe, Co, Ni and Mn in the lateritic soils of the Santa Elena Peninsula. The geochemical composition, mineralogy and microbial structure (prokaryotic and fungal) of these soils were described for the first time, considering a landscape approach. Three types of lateritic soils were identified based on the geochemistry, geography and microbial composition: *mountain* soils, *inner ophiolite lowland* soils and *north lowland* soils. Each type of soil was studied using fluctuating redox microcosm experiments to emulate a complete anaerobic-aerobic cycle. With glucose biostimulation, bioweathering and biomineralisation of Fe/Mg minerals were more intense in the mountain soils and mediated by microbial Fe redox cycling, while methanogenesis was enhanced in the lowland soils, highlighting the potential importance of these lateritic systems for carbon fluxes. For a better understanding of the natural conditions underpinning those biogeochemical cycles, the fluctuating redox microcosm experiments were extended by using samples from both dry and wet seasons and using cellulose as an electron donor analogous to the natural plant matter found in the soils. Under anoxic conditions mobilisation of Co, Ni and Mn was enhanced by microbial cellulose degradation and linked to microbial Fe(III) reduction and bioweathering of Fe-oxides. However, when oxic conditions were imposed, Co, Ni and Mn solubilisation increased, likely associated with the bioweathering of Mg minerals including hydrous silicates or clays but still linked to cellulose degradation. Organisms affiliated with the Firmicutes played a key role in these processes, likely degrading cellulose into smaller molecules bioavailable for other microbial processes such as Fe redox cycling (or metal chelation). Other microorganisms found that could be directly or indirectly associated with the cycling of Co, Ni and Mn included Fe(III) and Mn(IV) reducing bacteria, methanogens and fungi. Seasonal precipitation was key to induce redox processes in the serpentine soils by facilitating the development of anoxic conditions, and the impact depended on the soil geographical/geochemical origin. Despite the unique environment of the Santa Elena Peninsula, some of the results of this thesis supported previous observations in laterites and serpentine areas worldwide, evidencing the potential of the Santa Elena Peninsula as a model location to understand natural biogeochemical cycles in tropical serpentine ecosystems; but with outcomes that can also be extrapolated to other sites, landscapes and ecological contexts.

## Declaration

The author of this thesis declares that no portion of the work referred to in this thesis has been submitted in support of an application for another degree or qualification of this or any other university or other institute of learning.

## Copyright statement

i. The author of this thesis (including any appendices and/or schedules to this thesis) owns certain copyright or related rights in it (the “Copyright”) and s/he has given The University of Manchester certain rights to use such Copyright, including for administrative purposes.

ii. Copies of this thesis, either in full or in extracts and whether in hard or electronic copy, may be made only in accordance with the Copyright, Designs and Patents Act 1988 (as amended) and regulations issued under it or, where appropriate, in accordance with licensing agreements which the University has from time to time. This page must form part of any such copies made.

iii. The ownership of certain Copyright, patents, designs, trademarks and other intellectual property (the “Intellectual Property”) and any reproductions of copyright works in the thesis, for example graphs and tables (“Reproductions”), which may be described in this thesis, may not be owned by the author and may be owned by third parties. Such Intellectual Property and Reproductions cannot and must not be made available for use without the prior written permission of the owner(s) of the relevant Intellectual Property and/or Reproductions.

iv. Further information on the conditions under which disclosure, publication and commercialisation of this thesis, the Copyright and any Intellectual Property and/or Reproductions described in it may take place is available in the University IP Policy (seehttp://documents.manchester.ac.uk/DocuInfo.aspx?DocID=24420), in any relevant Thesis restriction declarations deposited in the University Library, The University Library’s regulations (seehttp://www.library.manchester.ac.uk/about/regulations/) and in The University’s policy on Presentation of Theses.

## Dedication

---

This thesis is dedicated to my family Mami, Papi, Feli, Dani and Fer, your unconditional support, good vibes and love during these years have been vital to keep wheels on track, peace of mind and a warm heart, you made this possible;

To my fiancée Fer, because distance was just a word that made us stronger and opened the door to an exciting future together,

And to Tita and Tito, because this journey commenced with them…

## Acknowledgements

I would like to start by extending my gratitude to my supervisor Jon, for believing in my project since the first time we talked long time ago and opening this incredible opportunity to develop my ideas in the Geomicro group of the University of Manchester and in the CoG$^3$ project. I also want to thank my co-supervisors, Clare for the guidance and support, and Richard for introducing me to the colourful world of rocks. A special acknowledgement is to Laura, for being my laboratory mentor, for the patience, help and support through the years, you were also a co-supervisor to me. Finally, thanks to my examiners Vicky and Heather for your valuable comments to improve this thesis. To all of you many thanks for your teachings and making me a better scientist!

I am very grateful to the Ministerio de Ciencia, Tecnología y Telecomunicaciones (MICITT) of the Gobierno de Costa Rica and to the Universidad de Costa Rica (UCR) for funding and supporting my PhD studies in Manchester, United Kingdom. I also want to acknowledge the CoG$^3$ Consortium Project (CoG3 NE/M011518/1), funded by the Natural Environment Research Council (NERC), for including me in the project and supporting this investigation too. Special thanks to the academic units of the UCR that supported my PhD: Unidad de Recursos Forestales, Instituto de Investigaciones en Ingeniería and Escuela de Química, and also to Oficina de Asuntos Internacionales y Cooperación Externa (OAICE).

I want to thank to María Marta Chavarría Diaz and Róger Blanco Segura from the Research Programme of the ACG for permitting the development of this research in the stunning Santa Rosa National Park and for support and advice during the field campaigns. Similar thanks to the Comisión Nacional para la Gestión de la Biodiversidad Costa Rica (CONAGEBIO).

I am also very grateful to my uncle Daniel Arguedas Quesada and my dad Francisco Solano Soto, for being such amazing assistants during field campaigns. Dany, I know the stories of rocks and digging holes will be told for years, but we learned a lot together during the expeditions, thanks!

Thanks to the personnel of SEES in the UoM Alastair Bewsher, John Waters, Paul Lythgoe, Chris Boothman, Stephen Stockley and Jonathan Fellowes for the laboratory support during my thesis, and to Dave Norwood for the administrative support for fieldwork and conferences. Also, thanks to the Geomicro group and other fellow PhD students (Late Lunchers LL) for being part of this.

A special thanks to my fellow CoGers, Sul, Dawn and Laura for sharing the cobalt exploration through lab work, meetings, conferences, beamtimes, trains, flights, continents; it has been an amazing adventure guys, hope we can keep collaborating in the future!

Thanks to the great G43, Ellen, Tom, Yusuf, Dawn, Katrina, Sarah, Matt, Franky, Elliot, Elspeth; for the conversations, laughs, birthdays (and really cool presents!), lunches/drinks, group support (and therapy)! it's been great sharing the office and working alongside you guys.

Gracias to my latin family Javi, Gianfranco, Rebe, Jeannette y Luzita, you made this journey a lot, much, more, easier to me, I will really miss our chats, lunches, Spanish discussions, but especially our wuntu (rat) adventures! You will be always in my heart amigos! Gracias de todo corazón.

And finally, the biggest thanks to my rocks, that held me strong through the entire journey of this PhD despite oceans apart. Mami, Papi, Feli (mi apoderada), Dani, Fer and Sebas, thanks for being always there for me, for making distances feel like nothing, and for reminding me why the family always comes first. I know it has been an incredible experience for all of us, thanks for encouraging me to give this step. Gracias por todo familia linda! And Fer, linda, thanks for sailing through this adventure with me, for all the teachings, support, love, time, and for always be...

¡Pura vida!

## About the Author

---

The Author of this thesis obtained a Bachelor's degree in Chemistry (BSc) in the Universidad de Costa Rica (UCR) in 2013. He later graduated from the Universidad de Costa Rica with a Bachelor's degree in Biology (BSc) in 2014, and in 2016 he obtained a Master's degree in Chemistry (MSc) in the same University. In 2013 the author earned a position as a graduate research student in the Centre of Electrochemistry and Chemical Energy of the UCR where he worked until 2015. During 2015 he also worked as an Instructor of General Chemistry Laboratories in the School of Chemistry of the UCR. Since 2014 he has been a Research Instructor in the Unit of Forest Resources (ReForesta) at the University of Costa Rica, working as the main person responsible for the chemistry laboratory and as a collaborator in the Research Programme in Forest Resources until he joined the Geomicrobiology research group in the University of Manchester in 2016, where the work of this thesis was undertaken. After his PhD studies in Manchester, he will return to the UCR to start a Lecturer position in ReForesta and in the School of Chemistry.

# Chapter 1. Project context and thesis structure

## 1.1 Context

Costa Rica is one of the most biologically diverse sites in the world and in the north-western part of the country is the Santa Elena Peninsula, an area with unique biological, ecological and geological characteristics. The geology of the peninsula comprises an ultramafic complex composed mainly of serpentinized peridotites, dunites and gabbros (Sánchez-Murillo et al., 2014), and is tightly related to the serpentine ecosystems present in its landscape. However, among its vast biodiversity, only few groups of organisms have been related to the ultramafic elements, for example the associate flora has been described and some microbial activity was related to the serpentinization process of the peridotites, but a wider approach must be done (Denyer and Gazel, 2009; Reeves et al., 2007).

In humid tropical areas, intensive weathering of serpentinized ultramafic rocks induces the formation of nickel laterites with different iron and magnesium minerals (Butt and Cluzel, 2013), and the Santa Elena Peninsula has the appropriate weather conditions to induce them. Thus, Fe and Mg containing minerals are the most common components of lateritic soils formed due to the weathering of ultramafic rocks, as well as other associated trace elements including manganese, nickel, cobalt or chromium (Reeves et al., 2007). The presence of Co and Ni has been reported in rocks and in soils from the Peninsula of Santa Elena, but the biogeochemical cycle of Fe, Co, Ni and Mn in these lateritic soils derived from ultramafic rocks is still widely unexplored.

## 1.2 The CoG3 Project, Cobalt Geology, Geometallurgy and Geomicrobiology

The current Natural Environment Research Council (NERC) project, $CoG^3$ (Cobalt Geology, Geometallurgy and Geomicrobiology) involves the Natural History Museum, The University of Manchester and other institutions, and looks to identify new environmentally benign extraction

and recovery processes for cobalt (Natural History Museum, n.d.). The project also seeks to understand how cobalt minerals and ores are formed and how cobalt behaves in the crust of the Earth and aims to promote a greater understanding of the distribution and behaviour of cobalt in natural systems. One of its work packages is more related to geomicrobiology and seeks to increase the knowledge of trace element cycling of Co-rich ores, including Ni-laterites, understanding the natural biogeochemistry of cobalt in oxic and anoxic environments. The research presented in this thesis, given the levels of Co and other trace elements in the soils of Santa Elena Peninsula, was aligned with this wider NERC consortium grant within the geomicrobiological work package based in the University of Manchester.

### 1.3 Research aims and hypotheses

The principal aim of this project was to study the biogeochemical cycling of iron, cobalt, nickel and manganese in the lateritic soils from the Santa Elena Peninsula. The geomicrobiological controls associated with Fe, Mg, Co, Ni and Mn cycling were explored in sediment microcosms, focusing on the impact of redox processes and a range of carbon sources/electron donors. Also, a detailed geochemical characterisation of the lateritic soils from the Santa Elena Peninsula was performed including geochemical, mineralogical and microbiological analyses, considering a landscape approach. The results presented in this thesis provide underpinning knowledge on the biogeochemistry of lateritic soils from the serpentine ecosystem in Santa Elena Peninsula, and more generally, have generated new knowledge associated with the biogeochemical cycling of Co, Ni and other trace elements in laterites and other natural environments. Three objectives of the thesis were:

1. To describe the nature of iron, cobalt, nickel and manganese in lateritic soil samples from the Santa Elena Peninsula, understanding their geological origin and the effect on the soil microbial community.
2. To analyse the relationship between anaerobic and aerobic microbial processes during the biogeochemical cycling of Fe, Co, Ni and Mn.
3. To determine the potential impact of seasonal rainfall on the biogeochemical cycling of Fe, Co, Ni and Mn in the lateritic soils of Santa Elena Peninsula.

The main hypothesis proposed for this thesis were:

1. The geochemistry and microbial composition of the lateritic soils vary depending on the geographical position within the Santa Elena Peninsula, associated with landscape features such as altitude or vegetation.
2. Anaerobic/aerobic microbially-mediated processes determine the cycling of Fe, Co, Ni and Mn in the lateritic soils via weathering of Fe minerals.
3. Seasonal rainfall influences the dominancy of aerobic or anaerobic processes in the soils of Santa Elena Peninsula by producing more local anoxic conditions during the wet season and more oxic conditions in the dry season.

### 1.4 Thesis structure

The thesis consists of seven chapters, commencing with this introductory chapter (Chapter 1) where the research context is briefly explained, and the aims and main hypothesis are presented.

Chapter 2 provides a literature review of scientific knowledge to support the research described in this thesis, including an introduction to the Santa Elena Peninsula, geological and geomicrobiological concepts.

Chapter 3 includes a brief description of the experimental methods and the analytical techniques used in this research.

Chapter 4 is the first research chapter and explores the hypothesis of differences in the geochemistry and microbial composition of the soils when considering the main landscapes observed in the Santa Elena Peninsula. The chapter presents the first geochemical and microbiological description of the lateritic soils from the Santa Elena Peninsula within a landscape approach. Here, mineralogical and geochemical data were recorded from both serpentinite rocks and lateritic soils and correlated with the native prokaryotic and fungal communities of the soils. All the soils sampled were clearly lateritic, but there were measurable variations in geochemical compositions, resulting in three types of lateritic soils identified: *mountain* soils, *inner ophiolite lowland* soils and *north lowland* soils, that were also supported by their native microbial

composition. This chapter is presented as a lead author manuscript to be submitted to the journal Geoderma.

Author contributions:

- A.F Solano-Arguedas: principal author, experimental concept and design, fieldwork, main experimental work (geochemical sampling preparation and analyses), geochemical data analysis, statistical analysis, manuscript writing.
- C. Boothman: performed DNA extraction, Illumina sequencing (prokaryotic and fungal) and associated data analysis.
- L. Newsome: input to experimental design, conceptual and experimental guidance, manuscript review.
- R.A.D. Pattrick: input to experimental design, conceptual and experimental guidance for mineralogical and rock sections, extensive manuscript review.
- D. Arguedas-Quesada: extensive fieldwork assistance.
- C.H. Robinson: input to experimental design, manuscript review.
- J.R. Lloyd: Principal supervisor, input to experimental design, conceptual and experimental guidance, extensive manuscript review.

Chapter 5 is the second research chapter and builds up from Chapter 4, considering a soil sample from every one of the three different locations defined on that chapter based on their geographical/geochemical characterisation. The Chapter 5 explores the hypothesis that microbially-mediated anaerobic/aerobic processes participate in the cycling of Fe and Mg in the lateritic soils through the weathering of Fe minerals. In this chapter, the biogeochemical cycling of Fe and Mg is studied in those lateritic soils, as they were largely represented in the geochemistry of the soils. To study their cycling, fluctuating redox microcosm experiments were performed using glucose and acetate-lactate as electron donors to promote reducing conditions, followed by oxidation in air. Changes in aqueous geochemistry, mineralogy and microbial communities were analysed, and evidence of bioweathering of Fe/Mg minerals, biomineralisation of Fe/Mg carbonate minerals, and methanogenesis was recorded as a direct and/or indirect consequence of microbially-mediated Fe redox cycling, with differences between geographical

locations. This chapter is presented as a lead author manuscript to be submitted to the journal Frontiers in Environmental Science.

Author contributions:

- A.F. Solano-Arguedas: principal author, experimental concept and design, fieldwork, all experimental work (experiment set up, monitoring and sampling, sample preparation for geochemical analyses), data analysis, manuscript writing.
- L. Newsome: experimental concept and design, conceptual and experimental guidance, extensive manuscript review.
- C. Boothman: performed DNA extraction, Illumina sequencing and associated data analysis.
- J.R. Lloyd: Principal supervisor, input experimental concept and design, conceptual and experimental guidance, extensive manuscript review.

Chapter 6 is the third research chapter and continues the exploration of biogeochemical cycles occurring in the lateritic soils of Santa Elena Peninsula initiated in Chapter 5 where a strong microbial influence was evidenced in the mobilisation of major elements (Fe and Mg). However, Chapter 6 focuses on understanding the cycling of cobalt, nickel and manganese that were strongly associated with Fe biogeochemistry in Chapter 5. For a better comprehension of the natural cycling of those elements in the lateritic soils, soil samples were collected during both seasons (dry and wet season) to include different seasonal redox environments. This chapter explores the hypothesis of differences in the dominancy of anaerobic or aerobic microbially-mediated processes associated with those biogeochemical cycles, where the seasonality could determine the presence of oxic/anoxic local environments. Fluctuating redox microcosm methodology successfully tested in Chapter 5 was also used in this chapter, but cellulose was used as electron donor instead to emulate a natural carbon source from plant matter. Co, Ni and Mn microbially-mediated cycling in these lateritic soils were closely associated with cellulose degradation, both under anoxic and oxic conditions and showing seasonal variations. This chapter is presented as a lead author manuscript to be submitted to the journal Geochimica et Cosmochimica Acta.

Author contributions:

- A.F. Solano-Arguedas: principal author, experimental concept and design, fieldwork, all experimental work (experiment set up, monitoring and sampling, sample preparation for geochemical analyses), data analysis, manuscript writing.
- L. Newsome: input to experimental design, conceptual and experimental guidance, extensive manuscript review.
- C. Boothman: performed DNA extraction, Illumina sequencing and associated data analysis.
- J.R. Lloyd: Principal supervisor, input to experimental concept and design, conceptual and experimental guidance, extensive manuscript review.

Chapter 7 includes general conclusions from this thesis, summarising the research presented in chapters 4, 5 and 6, and highlights the relevance of this investigation to understand the biogeochemical processes of the Santa Elena Peninsula within its ecological context and more widely to the general knowledge of natural behaviour of Fe, Ni, Co and Mn in serpentine ecosystems and laterites. Future work from this research is also discussed in terms of the local context of Santa Elena Peninsula, but also considering a broader scale.

Each section contains a reference list and supplementary information.

Appendices include contributions to other work, supplementary material to the thesis and a summary of conference presentations, awards, field work and external experimental work collaborations. Appendix 1 is a research manuscript titled “Manganese and cobalt redox cycling in laterites; biogeochemical and bioprocessing implications”, submitted to Chemical Geology journal and is currently in revision. The author of this thesis is a co-author of this manuscript (2$^{nd}$ author) and contributed to this research performing the experimental work with microcosm experiments using Brazilian laterites from Piauí, and also cooperated with manuscript revisions. The input for experimental work included the experiment set up, monitoring and sampling during the entire experiment, and sample preparation for geochemical analyses and DNA extraction. This research was included in this thesis because is the methodological base for the microcosm experiments performed in this project, but more importantly includes results related to Mn and Co cycling from laterites worldwide that support some of the outcomes from this thesis (especially

Chapter 5), confirming the importance of the Santa Elena Peninsula as a model lateritic site with a great potential to understand natural biogeochemical processes in laterites and serpentine ecosystems overall.

### 1.5 References


Butt, C.R.M., Cluzel, D., 2013. Nickel Laterite Ore Deposits: Weathered Serpentinites. Elements 9, 123–128. https://doi.org/10.2113/gselements.9.2.123

Denyer, P., Gazel, E., 2009. The Costa Rican Jurassic to Miocene oceanic complexes: Origin, tectonics and relations. J. South Am. Earth Sci. 28, 429–442. https://doi.org/10.1016/j.jsames.2009.04.010

Natural History Museum, n.d. CoG3 Consortium: Investigating the recovery of cobalt | Natural History Museum [WWW Document]. URL https://www.nhm.ac.uk/our-science/our-work/sustainability/cog3-cobalt-project.html (accessed 8.13.19).

Reeves, R.D., Baker, A.J.M., Romero, R., 2007. The ultramafic flora of the Santa Elena peninsula, Costa Rica: A biogeochemical reconnaissance. J. Geochemical Explor. 93, 153–159. https://doi.org/10.1016/j.gexplo.2007.04.002

Sánchez-Murillo, R., Gazel, E., Schwarzenbach, E.M., Crespo-Medina, M., Schrenk, M.O., Boll, J., Gill, B.C., 2014. Geochemical evidence for active tropical serpentinization in the Santa Elena Ophiolite, Costa Rica: An analog of a humid early Earth? Geochemistry, Geophys. Geosystems 15, 1783–1800. https://doi.org/10.1002/2013GC005213

# Chapter 2. Literature review

## 2.1 Costa Rica, biodiversity and conservation

Costa Rica is a country in Central America, between latitude 8°22'26" and 11°13'12" North and longitude 82°33'48" and 85°57'57" West, limited to the North with Nicaragua, to the south with Panamá, the Caribbean Sea to the East and the Pacific Ocean to the West (Figure 2.1) (Herrera, 2016). The terrestrial surface area of the country comprises 51,100 km$^2$ which is equivalent to 0.03% of global land surface; while its marine territory is eleven times bigger, containing 570,000 km$^2$ in the Pacific Ocean and 24,000 km$^2$ in the Caribbean (Kappelle, 2016).

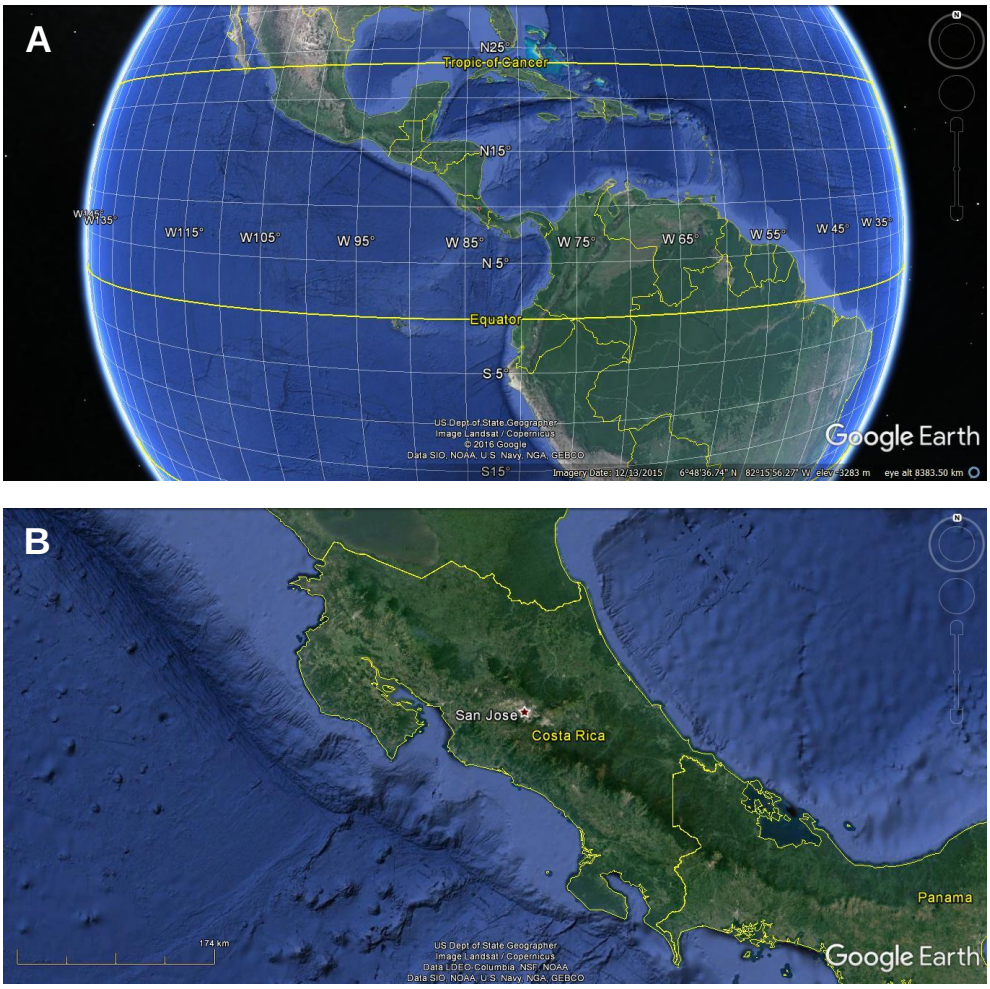


**Figure 2.1.** Map of tropical region of America (A) and Costa Rica (B).

The territory is divided into 11 Conservation Areas under the surveillance of the Sistema Nacional de Áreas de Conservación (National System of Conservation Areas, SINAC) (SINAC, n.d.). Within them, ~25% of the total surface of the country are protected wildlife areas, covering a rich set of ecosystems whose classification has been widely discussed and interpreted according to different parameters. One of the most inclusive classifications was proposed by Kappelle (2016), stating 15 different ecosystems within the Costa Rican territory, where 8 are terrestrial and 7 from fresh water or marine-coastal regions. The enormous variance in ecosystems, is influenced by several factors including the unique location of Costa Rica in the neotropic (tropical region in America) (Figure 2.1), the orography and geology of the country and the isthmic geography between the Caribbean Sea and the Pacific Ocean. Additionally, the diversity of ecosystems is driven by the large range of climatic groups found in Costa Rica (that are also determined by latitude, orography and isthmic geography) (Herrera, 2016). All these facts explain why Costa Rica is one of the most biologically diverse sites in the world, where 5% of the total known biodiversity on Earth can be found (Kappelle, 2016). The latter added to its small surface, makes Costa Rica as the most biodiversity dense country in the world.

One of those areas is the Area de Conservación Guanacaste (Guanacaste Conservation Area, ACG) allocated in the north-western part of the country (Figure 2.2). The ACG has 1,630 $km^2$ of protected wildlife area and despite its small protected area, it has approximately 335,000 terrestrial species, which is equivalent to 2.6% of the world biodiversity (ACG, 2014).

The ACG includes four of the five major tropical ecosystems: dry forest, cloud forest, rain forest and marine ecosystem; only desert is not present (Janzen and Hallwachs, 2016). Following Kappelle classification, several of the Costa Rican tropical ecosystems are present: the seasonal dry forest, the montane cloud forests of the volcanic *cordilleras* (mountain ranges), the evergreen moist forest of the Caribbean lowlands, the coastal-marine ecosystem of the Pacific Ocean and almost all the freshwater ecosystems (Kappelle, 2016). The significant relevance in developing ecological and biological processes were the main reasons why the ACG Wildlife Protected Area was declared as World Heritage by UNESCO in 1999 (ACG, 2014).

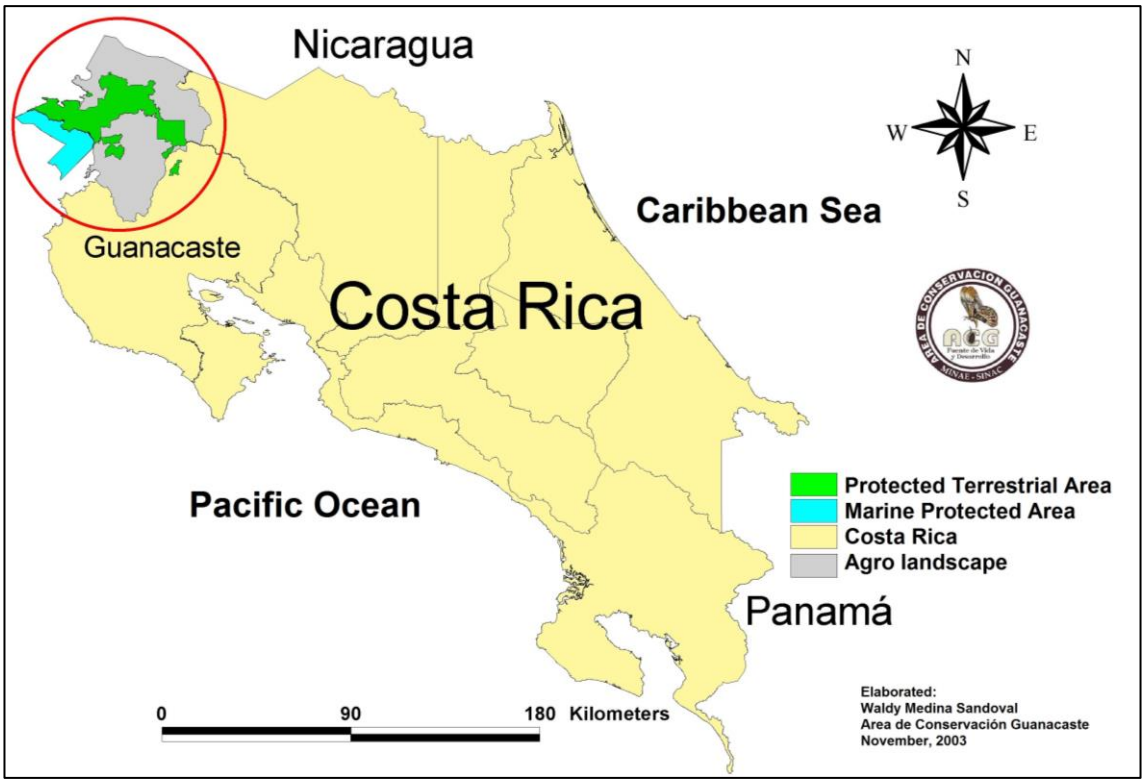


**Figure 2.2.** Location of ACG in Costa Rica and its division between protected and unprotected areas (Medina Sandoval, 2003).

### 2.2 Santa Elena Peninsula

In the west of the ACG protrudes the Santa Elena Peninsula, which is totally protected within the Santa Rosa National Park. The current research is based in this National Park, and further information as the geography, climate, vegetation, soils and geology will be described.

#### 2.2.1 Geography

The Santa Rosa National Park comprises three sectors spread all over the peninsula named as Murciélago, Santa Elena and Santa Rosa (Figure 2.3). The following research involves samples only from Murciélago (A) and from Santa Elena (B) sectors.

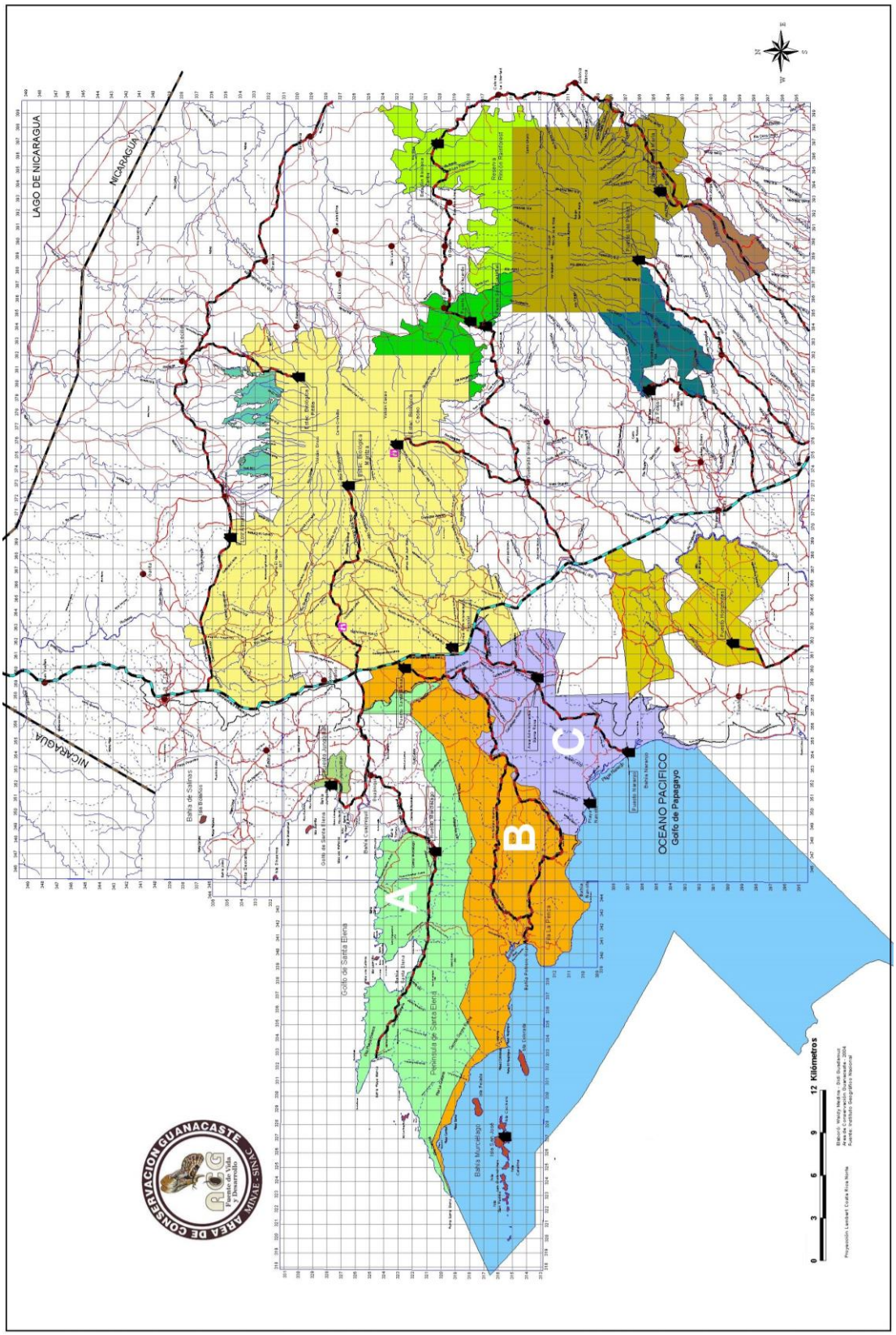


**Figure 2.3.** Detail of the Protected Wildlife Areas within the ACG. The Santa Rosa National Park comprises 3 sectors: Murciélago (A), Santa Elena (B) and Santa Rosa (C). Adapted from Medina and Guadamuz (2004).

The peninsula has a group of mountain ranges with hills lower than 700 masl (metres above sea level) resulting in a rugged topography. Several creeks and rivers of relative short length flow among the cliffs ending in one of the multiple bays surrounding the peninsula. The longest river, called Potrero Grande, runs by the middle of the peninsula and flows to the southwest into the mangrove and the bay with the same name (Figure 2.4).

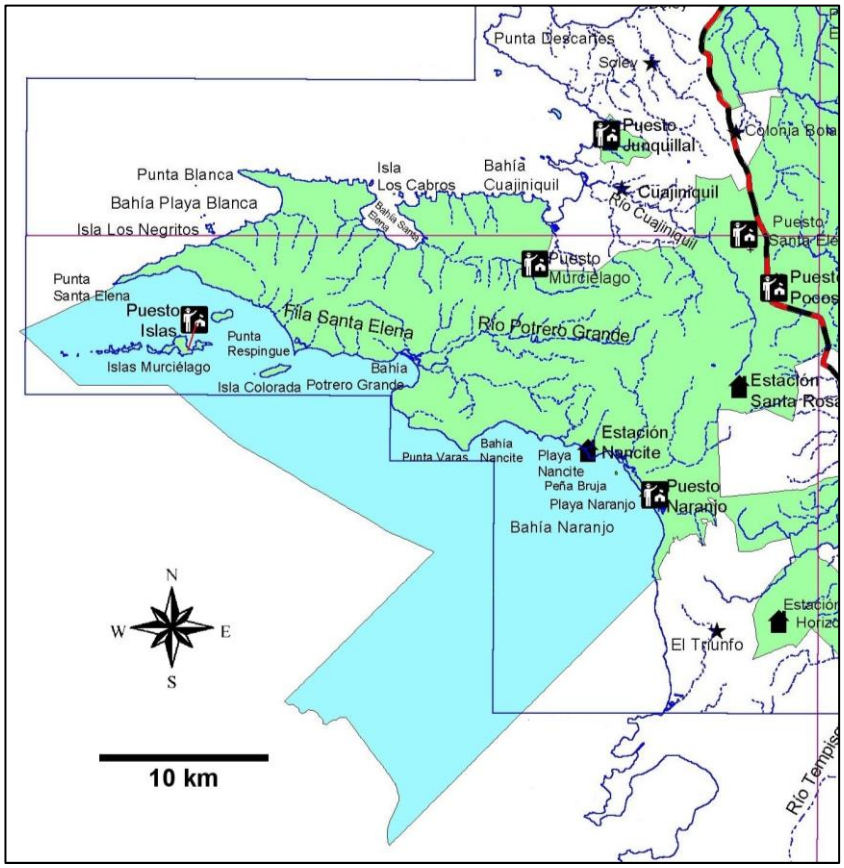


**Figure 2.4.** Map of the hydrographic network in the Santa Elena Peninsula. Adapted from Medina (2001).

### 2.2.2 Climate

The climate in the peninsula is very similar to all the seasonal dry forest lowlands in the northern Pacific of Costa Rica, a mostly dry to sub-humid climate with marked rain seasonality during the year. The dry and the wet season are the only two seasons present and are determined by the north-south shifts of the Intertropical Convergence Zone (ITCZ). The ITCZ is where the trade winds from both hemispheres converge in the tropical region, the north-eastern trade winds from the north and the south-eastern trade winds from the south (Herrera, 2016; Jiménez M. et al., 2016).

On the Santa Elena Peninsula, the dry season lasts for four months from December to March but may be extended to almost six if the transition months to the rainy season (April and May) are considered. During this season only 5% of the total annual precipitation is registered and the north-eastern trade winds flow over the area (Herrera, 2016; Instituto Meteorológico Nacional, n.d.; Jiménez M. et al., 2016).

The further 95% of annual precipitation falls during the rainy season and can be divided into two periods with similar proportions of precipitation. The first one is from May to August and the second from August to November, with November as a transition month to the dry season. During the first period, the ITCZ is over Costa Rica and the winds from the south-east bring cloud systems that generate storms and strong rains. The second stage has also south-eastern winds due to the return of the ITCZ but it is more influenced by cyclonic events. A small dry interval is present between both periods called *Veranillo* (small summer) or *canícula*, favoured by an increasing presence of the north-eastern winds and occurs during July-August (Instituto Meteorológico Nacional, n.d.; Janzen and Hallwachs, 2016). Despite the latter, the annual precipitation registered is still low, with 1,528 mm in the Santa Rosa National Park. Indeed, the Santa Elena Peninsula is the driest part of Costa Rica (Jiménez M. et al., 2016).

The average annual temperature during day is 33 °C while during the night it is 22 °C with an average day temperature amplitude of ~9 °C (Instituto Meteorológico Nacional, n.d.). In general, the northern dry lowlands are among the hottest areas of Costa Rica; even in the Santa Elena Peninsula the monthly average can reach 36 °C (Jiménez M. et al., 2016).

### 2.2.3 Vegetation and soils

In the northern Pacific dry lowlands, the characteristic vegetation is the "dry tropical forest" in general terms. However, several vegetation macrotypes are present in this area (Jiménez M. et al., 2016). The macrotype vegetation along the peninsula is mainly semi-deciduous/deciduous forest composed of xerophytic shrubs in the exposed areas or the hilltops, but in the lower lands or near water courses a semi-deciduous and/or evergreen vegetation is present. In the alluviums of Potrero Grande river and across other rivers in Murciélago sector, the vegetation changes completely to a seasonal evergreen forest of lowlands (Figure 2.5A and Figure 2.6) (Gómez and Herrera, 1986).

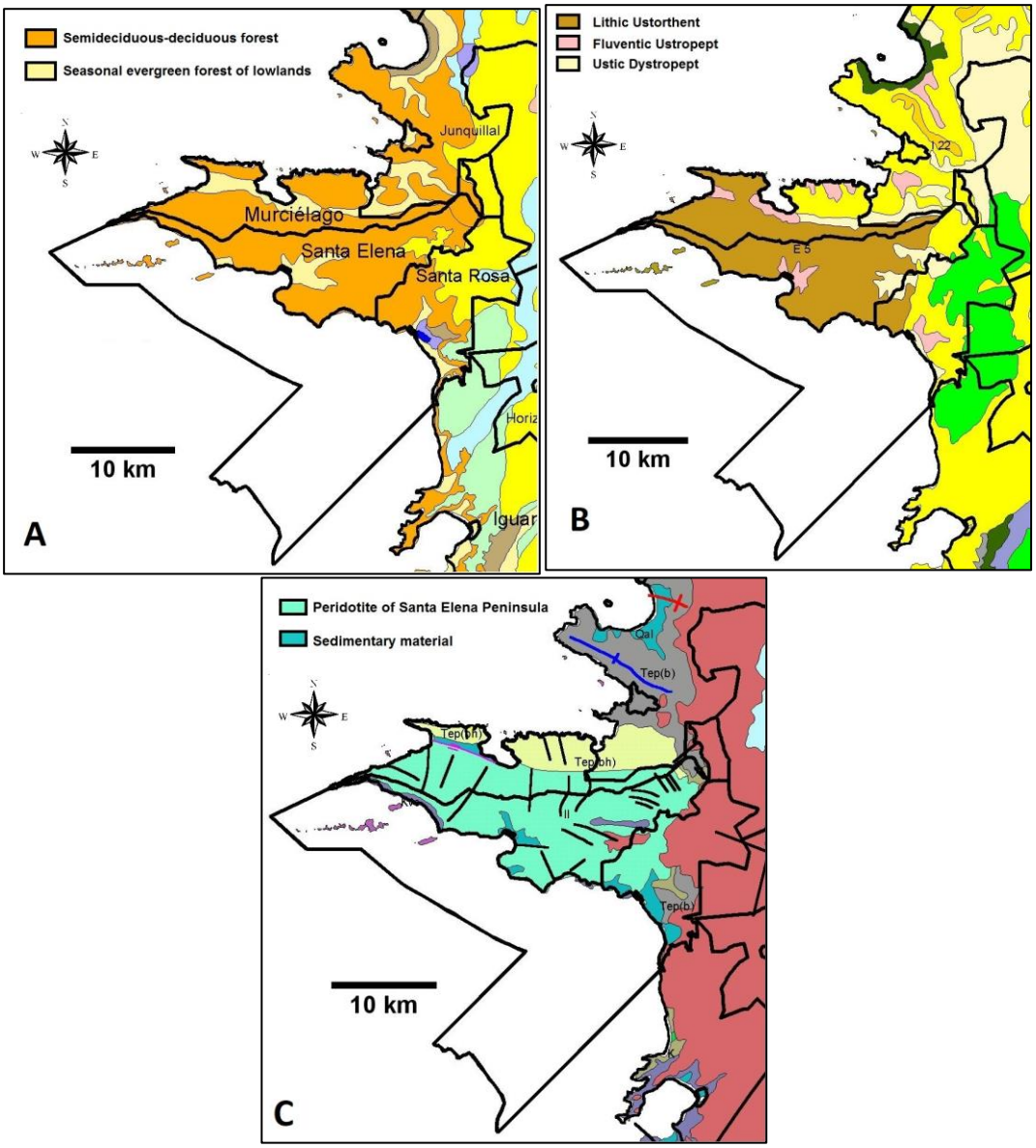


**Figure 2.5.** Map of the vegetation (A), soils (B) and geology (C) in the Santa Elena Peninsula. Only the relevant colours have been labelled. Adapted, respectively, from Medina (1999a, 1999b, 1999c).

The vegetation macrotype in the hilltops and the higher sides of the hills is meant to be a semi-deciduous/deciduous forest with a well-established forest canopy as occurs in the cliffs or water courses between mountains or in lower lands. The *nance* (*Byrsonima crassifolia*) is a representative tree of this kind of vegetation, however those characteristic trees are scarce, less biologically diverse and smaller than the ones occurring in the slopes or near water streams and instead the vegetation is herbaceous and shrubby, dominated in many areas by a native grass

(*Trachypogon plumosus*) (Figure 2.6). This change in the flora composition is mainly due to centuries of seasonal burns anthropogenically originated, in addition to the dry climate and to the eroded, dry and highly porous serpentine soils present all over the Peninsula (Janzen and Hallwachs, 2016; Jiménez M. et al., 2016).

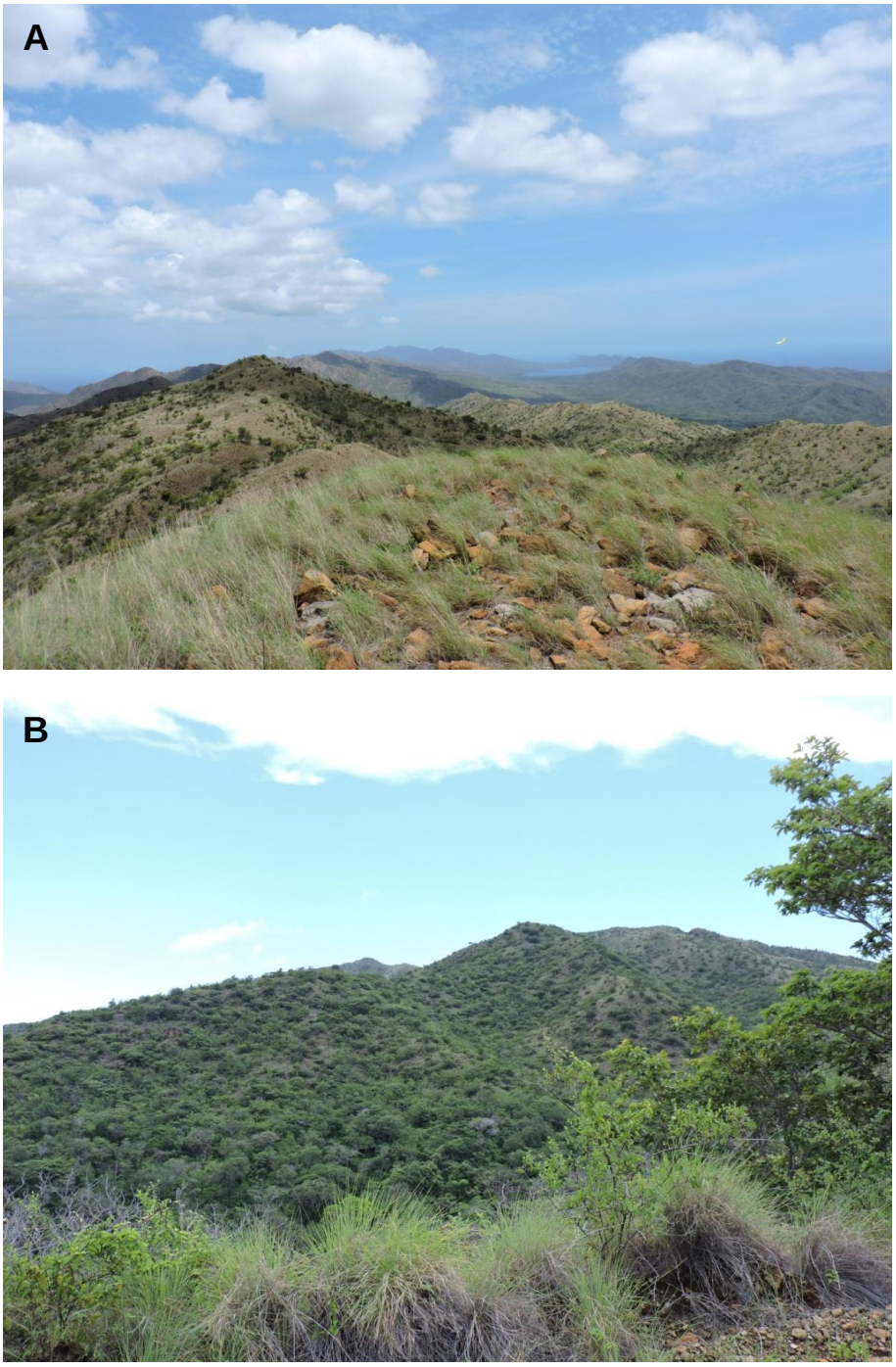


**Figure 2.6.** Characteristic vegetation in the Peninsula of Santa Elena. (A) The hilltops and the upper sections of the hills show a semi-deciduous/deciduous forest with scarce and small *nance* trees and dominated by a yellowish grass (*Trachypogon plumosus*) (observed at the front of the

picture). (B) In the slopes, the deciduous forest is denser and changes to an evergreen forest. Picture (B) was taken during the rainy season, therefore the deciduous trees *have* leaves; however on the slope of the far hill to the right, the change in the vegetation is still easy to observe.

Moreover, the vegetation type is closely related to the soil (Figure 2.5B). The soil under the semi-deciduous/deciduous forest mainly is a poorly developed soil called Lithic Ustorthent (a type of Entisol) and is the dominant soil in the peninsula. The seasonal evergreen forest of lowlands (Figure 2.5A) can be related to two similar types of Inceptisols: Fluventic Ustropept and Ustic Dystropept (Figure 2.5A) (Medina, 1999b, 1999a).

The Entisols comprise a group of recent soils with mineral nature that have little or no evidence of the development of pedogenic horizons due to their minimal development, reflecting many of the properties of their parent material. Among the Entisols, is a group called Orthents present on recent erosive surfaces or related to shallow soils on hard rock; and its subgroup Ustorthent has a warm soil temperature regime and an ustic soil moisture regime. This moisture regime is present in soils with average temperature over 22 °C and with limited moisture, dry for 90 or more days but present enough to plant growth when conditions are suitable. Among them, the subgroup *Lithic* have a lithic contact within 50 cm of the mineral soil surface (Alvarado and Mata, 2016; Soil Survey Staff, 2014). In summary, the characteristics of the most common soils in the peninsula, Lithic Usthortents, have: (1) a mineral nature due to recent erosion but with a thin layer of regolith with lithic contact within 50 cm, (2) warm temperature and (3) are dry for at least 3 months per year.

In general, the Inceptisols are difficult to define due to its wide range of characteristics, however they commonly occur on relatively active landscapes as river valleys or mountain slopes and have a weak horizon development. The Fluventic Ustropept and the Ustic Dystropept in particular, also have the ustic moisture regime described above and a warm soil temperature regime (Medina, 1999b; Soil Survey Staff, 2014). They are associated with fluvial parental material (Fluventic) or with the weathering of alluvial and/or colluvial fans (Dystropept) (Alvarado and Mata, 2016).

Finally, the soil composition in the peninsula can be associated with its geologic composition as can be seen in the Figure 2.5C. The weathering of peridotites seems to lead to the serpentine soils described above (Lithic Ustorthents), while the sedimentary materials due to alluvial and

colluvial deposits seems to be the basis for the Inceptisols. This will be discussed in more detail below.

### 2.2.4 Geology

The geology in Costa Rica is complex and very active, as it is located in the triple junction of the three plates beneath it, Cocos, Nazca and Caribe. The subduction of the Cocos Plate into the Caribe has created the Middle America Trench (MAT) whose southern border is in front of all the Pacific coast of Costa Rica (Figure 2.7A). Moving from the MAT to the East into the continental land of Costa Rica, several oceanic complexes can be observed along the Pacific coast, that were accreted as a result of subduction processes (Figure 2.7B) (Denyer and Gazel, 2009). These complexes or *ophiolites* are composed of igneous lithologies containing mafic/ultramafic rocks that were formed in the oceanic mantle and later uplifted by tectonic processes (Escuder-Viruete et al., 2015; Madrigal et al., 2015). The ophiolites in Costa Rica have ages within 200 and 40 million years (Ma) (Cretaceous-Eocene). Indeed, the oldest exposed rocks known from Costa Rica have been found there; while the ophiolite of Santa Elena is the oldest portion of land in Costa Rica and in all Central America, as it was an island long before the isthmus was completely formed (Alvarado and Cárdenes, 2016; Janzen and Hallwachs, 2016; Jiménez M. et al., 2016).

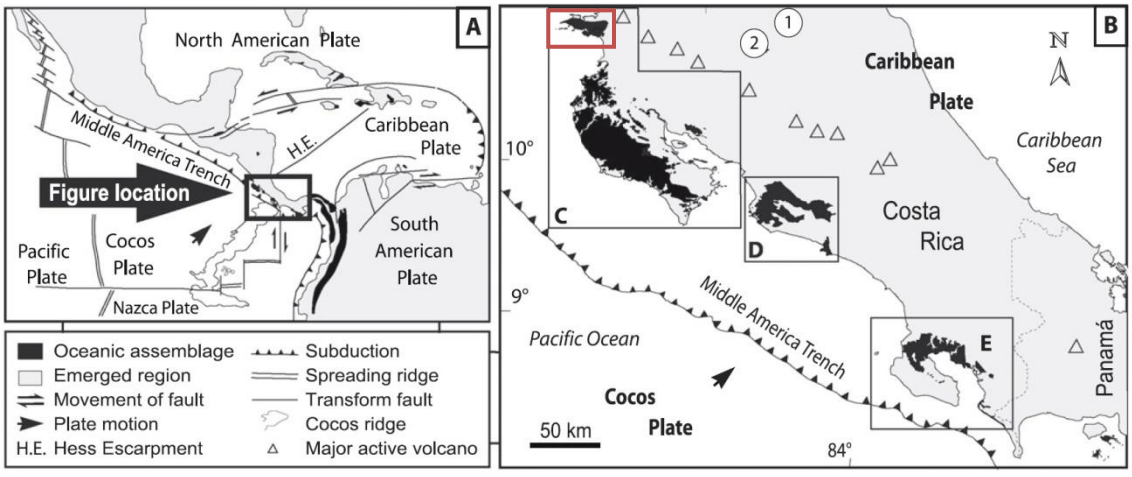


**Figure 2.7.** Tectonic Plates in Costa Rica. (A) Detail of the plates in Central America, (B) Oceanic complexes of Costa Rica: the Santa Elena-Nicoya Peninsulas (C), Herradura-Quepos (D) and Osa-Burica (E). In the Northern most section of C is the Peninsula of Santa Elena (in red). Adapted from Denyer and Gazel (2009).

The ophiolites can be described as an assemblage of several layers. The base is composed of ultramafic rocks, specifically peridotites as dunites, harzburgites and lherzolites that might be transformed to serpentinite in different grades. The next stage is characterized by the presence of mafic rocks as gabbros and diabases, followed by extrusive rocks as basalts, originated due to the flow of lavas under water with typical pillow-shapes. Finally, the top layer is commonly composed of deep-sea sediments. Indeed, as the Santa Elena ophiolite is covered by limestones of reef-rudists from the Campanian (Cretaceous), strongly suggests that it was emplaced during the Upper Cretaceous (Madrigal et al., 2015; Thorpe and Brown, 1993).

As observed in Figure 2.8, the Peninsula of Santa Elena is almost totally conformed by the Santa Elena Ophiolite, which is mainly composed of serpentinized peridotites (lherzolites, harzburgites and dunites) with mafic dikes of diabase that intrude the peridotites (Denyer and Gazel, 2009; Madrigal et al., 2015; Schwarzenbach et al., 2016). The same figure shows the presence of more recent alluvial deposits (Quaternary), easily associated with the alluviums of Potrero Grande River (in the centre of the map) and the course of several rivers in the Murciélago sector (in the northern boundaries of the Santa Elena Ophiolite). Moreover, these areas are also the same covered with Inceptisols, confirming the tight relationship between soil and geological composition along the peninsula. The similar comparison can be done with the Entisols and the Santa Elena Ophiolite. The latter can be better observed if compared with Figures 2.4 and 2.5.

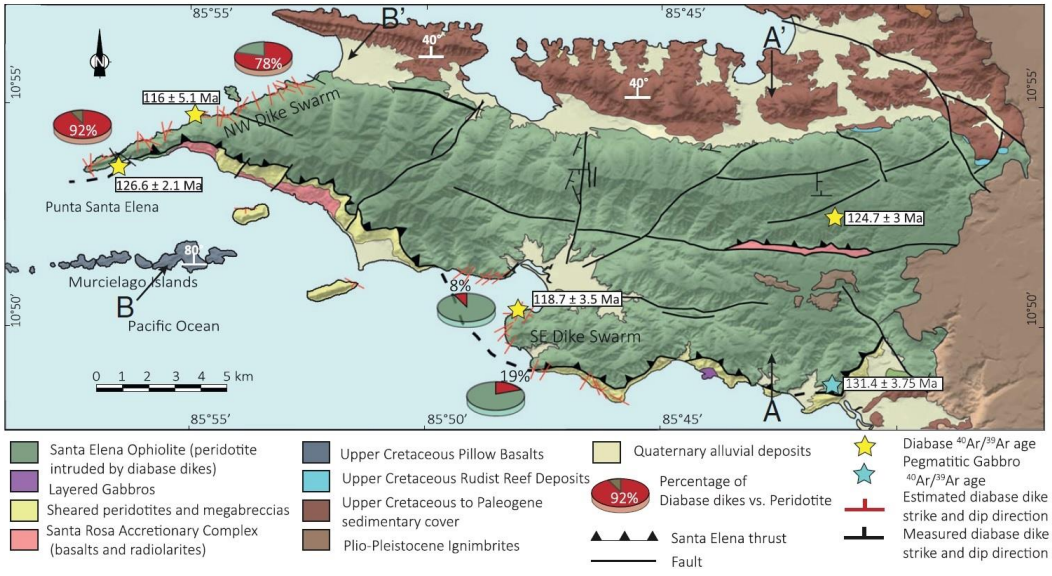


**Figure 2.8.** Detailed map of the geology of the Santa Elena Peninsula. Adapted from Madrigal *et al.* (2015).

### 2.3 Serpentine ecosystems: adaptation, specialisation and endemism

The presence of serpentinites and their geological history from a particular ultramafic rock influence the nature and composition of the soils formed from them, and thus the ecology of the biological communities associated, resulting in areas with 'serpentine' ecosystems (Moores, 2011). The serpentine soils show steep ecological gradients that promote several levels of habitat specialisation in the plants inhabiting those soils resulting in three types of serpentine plant species: endemic, tolerant and non-tolerant (Anacker, 2011).

Serpentine soils show difficult conditions for plant growth such as low Ca:Mg ratio, scarcity of essential macronutrients, high concentrations of heavy metals, low capacity of water retention, and are rocky and shallow soils susceptible to erosion (Kay et al., 2011; Kazakou et al., 2008). Thus, plant endemic lineages are those restricted to the serpentine soils that have developed an adaptation to those inherent serpentine conditions, while tolerant plants are those that could be found on serpentine conditions but not exclusively, as they are also present in other soils and ecosystems (Anacker, 2011). Serpentine adaptation and endemism have evolved multiple times in plants and following independent routes, resulting in differences of endemism in serpentine ecosystems across the world (Table 2.1). Higher ratios of endemism are found in tropical areas such as Cuba or New Caledonia due to their tropical climates, although in temperate zones large numbers of endemics can be found in areas like California due to the spatial variation in climate and topography (Anacker, 2011).

**Table 2.1.** Endemic diversity patters in six serpentine floras. Adapted from Anacker (2011).

| Area | No. Endemic Taxa | No. Families | Mean Tax on Richness per Family | No. Orders | Area ($km^2$) |
|---|---|---|---|---|---|
| Endemic-rich | | | | | |
| California | 215 | 39 | 5.5 | 24 | 6000 |
| Cuba | 854 | 24 | 35.6 | 14 | 7500 |
| New Caledonia | 1150 | 64 | 18.0 | 31 | 5500 |
| Endemic-poor | | | | | |
| Great Dyke | 14 | 8 | 1.8 | 6 | 3000 |
| Japan | 50 | 19 | 2.6 | 13 | 5256 |
| New Zealand | 32 | 18 | 1.8 | 13 | 309 |

Plants adapted to serpentine soils are typically smaller than their analogous in other soil types and are also adapted to dry soils, the so-called ‘serpentine syndrome’ (Kay et al., 2011), and as previously described in section 2.2.3, the vegetation in Santa Elena Peninsula shares those characteristics of the serpentine syndrome. Amongst the adaptations developed by serpentine flora are: developed root systems or restricted lateral root growth, selective translocation of Ca against Mg, exclusion of metals (e.g. by restricting them to roots), compartmentalisation of metals, and/or toxicity tolerance (Kay et al., 2011; Kazakou et al., 2008). The serpentine flora in the Santa Elena Peninsula has been described but only few local or regional endemics were found and no evidence of Ni hyperaccumulation was found (Reeves et al., 2007).

## 2.4 From ultramafic rocks to cobalt and nickel

As mentioned in section 2.2.4, several igneous rocks with mafic and ultramafic lithologies are present in the Peninsula of Santa Elena within the ophiolite or in the surroundings. A brief description of their definition and formation will be discussed below.

### 2.4.1 Description and geological origin of ultramafic rocks

The igneous rocks are the result of the solidification of magma, which is a mixture of molten or partially molten rocks and other materials beneath the Earth surface. When the magma is erupted at the surface of the Earth as lava, the molten fluid is rapidly solidified, and the dissolved components are crystallised quickly into minerals of small size, then the formed rock is extrusive or volcanic. But, if they are slowly crystallised beneath the surface, the crystals obtained in the rock are bigger, forming a rock called intrusive or plutonic. The size of the crystal or grain leads to another classification where the rock has an aphanitic texture if the grain is too small to be seen by the human eye, like in basalts, or a phaneritic texture when the crystals are visible to the naked eye, e.g. gabbros or peridotites (Thorpe and Brown, 1993; Turner and Verhoogen, 1960; Winter, 2001).

Once the igneous rocks are formed, they can be classified according to their colour, which is tightly related to the colour of the conforming minerals. Almost all the igneous rocks are composed of silicate minerals, but some of them have light colouration as the quartz, plagioclase or feldspar;

while others are darker, like hornblende, pyroxene or olivine. If the rock is rich in light-colour minerals then it is felsic (*fel*despar+*sil*ica), but if it is rich in darker colours it should be classified as mafic (*ma*gnesium+*f*erric iron, widely present in pyroxenes, olivine, etc.). If the rock is composed of more than 90% of mafic minerals, then it is an ultramafic rock (Thorpe and Brown, 1993; Winter, 2001).

Also, as the silicates are central in almost all the igneous rocks, the silica content is useful to separate them. In this case, a rock with more than 65% of $SiO_2$ is acid, within 52-65% is intermediate, from 52% to 45% is basic and with less than 45% is ultrabasic. This classification might be related to the colour, as the more mafic a rock is the less silica it contains, following a homologation of the basic/mafic and ultrabasic/ultramafic terms (Thorpe and Brown, 1993; Winter, 2001).

### 2.4.2 Peridotites and serpentinization

As explained before, the ophiolite of Santa Elena is mainly composed of peridotites. The peridotites are a group of intrusive igneous rocks with phaneritic texture. They are ultramafic rocks as they are mainly composed of olivines [$(Mg,Fe)_2SiO_4$] rich in magnesium and less than 40% of pyroxenes [$(Mg,Fe)SiO_3$]. The ratio of these two minerals will determinate the type of peridote present: harzburgite, lherzolite, wehrlite and dunite which is almost entirely composed of olivine (Figure 2.9). The peridotites might also contain hornblende at less than 40% (Streckeisen, 1976; Turner and Verhoogen, 1960; Winter, 2001).

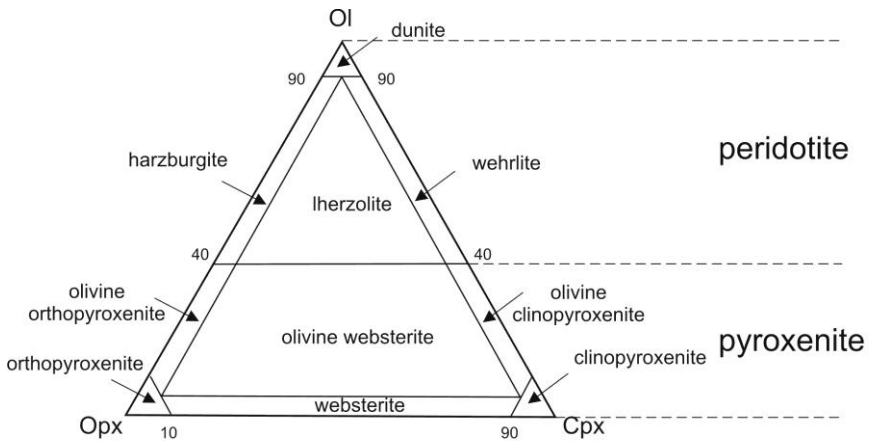


**Figure 2.9.** Classification of ultramafic rocks containing olivine (Ol), orthopyroxene (Opx) and clinopyroxene (Cpx) (Streckeisen, 1976).

The peridotites are the main constituents of the upper mantle. When the ophiolites are thrust onto the edge of continents or incorporated into mountain belts, the peridotites are exposed at the surface of Earth and represent the residues of the oceanic upper mantle produced after several geological processes like mantle melting or crust-mantle interaction. Therefore, the exposed peridotites allow the study of all these processes and at a bigger scale, the lithosphere generation (Escuder-Viruete et al., 2015; Winter, 2001).

The peridotites are also exposed to metamorphism, as a result of the orogenic processes occurring around them, and more especially in a subduction zone. The metamorphism is the result of changes in the mineralogy, texture and/or composition of a rock occurred predominantly in solid state and caused by agents such as pressure, temperature or metamorphic fluids, for example water behaving as a super-critical fluid (Winter, 2001).

When the peridotites are exposed to hydrotermal circulation through the upper mantle at temperatures below 450-500 °C, the pyroxenes and olivines become hydrated, forming a new mineral called serpentine [$(Mg,Fe)_3Si_2O_5(OH)_4$] (lizardite is the most common serpentine mineral). This process is called serpentinization and can produce other groups of minerals during the metamorphic progression. The iron that is not incorporated into serpentine can lead to the formation of magnetite ($Fe_3O_4$), while brucite is another product of the reaction [$(Mg,Fe)(OH)_2$] [Equation 1]. Further metamorphic products can include diopside [$CaMgSi_2O_6$], talc [$Mg_3Si_4O_{10}(OH)_2$], enstatite [$MgSiO_3$], anthophyllite [$Mg_7Si_8O_{22}(OH)_2$], quartz [$SiO_2$], and amphiboles such as tremolite [$Ca_2Mg_5Si_8O_{22}(OH)_2$] and other Mg-rich hornblendes (Malvoisin and Brunet, 2014; Winter, 2001).

$$2\ Mg_2SiO_4 + 3\ H_2O \rightarrow Mg_3Si_2O_5(OH)_4 + Mg(OH)_2 \quad [1]$$

Forsterite (Olivine) Serpentine Brucite

### 2.4.3 Laterites, cobalt and nickel

Laterites have been defined based on different classifications according to their mineralogy, geochemistry, morphology or geographical location. In a broad sense, a laterite can be defined as a “highly weathered natural material with high concentration of hydrated oxides of iron or aluminium, as a consequence of residual accumulation and/or absolute enrichment, by components transported in solution or as detrital material” (Stoops and Marcelino, 2018). Another

definition describes a laterite as a “superficial/near-superficial consolidated product of humid tropical weathering/oxidation and supergene enrichment as a result of physical and chemical processes on felsic/mafic/ultramafic/clay rocks” (Haldar, 2018).

The mineralogy of laterites lies between a ternary diagram with a Fe axis (hematite, goethite), an Al axis (bauxite) and a clay-axis (kaolinite); and a typical lateritic profile consists from bottom to top of parent rock, a saprolite layer, a lateritic layer and a gravel-free layer (Stoops and Marcelino, 2018). Geochemical variations during the residual enrichment process of Fe and Al can result in the formation of different weathering products. Fe enrichment from tropical weathering of acidic rocks leads to laterite formation regardless of their original Al/Fe ratio, indicating that Al and Si are removed; thus, resulting in laterites rich in goethite, hematite and kaolinite. However, under stronger leaching processes gibbsite [$\alpha$-$Al(OH)_3$] is favoured instead of kaolinite as a result of less dissolved silica, and therefore the weathering product is bauxite instead of laterite (Schellmann, 1994).

Laterites are analogous to other consolidated weathered covers such as calcrete, silcrete or ferricrete. Calcrete occurs in arid regions and is a cemented mixture of sand and silt by calcite, dolomite or other minerals. Silcrete also occurs in semiarid regions and is similar to calcrete but cemented by silica. Finally, the ferricrete is a layer of sedimentary rocks, such as conglomorates or breccia, cemented by iron oxides (Haldar, 2018).

Magnesium, iron and silicon are the main constituents in the elemental composition of the ultramafic rocks, but some other metals can be found within them in minor proportions including chromium, manganese, cobalt or nickel, etc. In particular, nickel can represent ~0.2% of the forsterite, while cobalt may be present between 0.06-0.09% in the ultramafic rocks (Roberts and Gunn, 2014; Thorne et al., 2012).

In the tropical and sub-tropical zones in particular, when these rocks are exposed to the rainfall cycles with precipitation over 1000 mm and seasonal temperatures range between 15-33°C, the weathering may facilitate the formation of Ni-laterites. These laterites tend to have a richer composition of certain metals than their parental rocks. If these laterites were formed from ultramafic rocks containing nickel within their olivine or serpentine minerals for example, then the laterite will be rich in nickel (Thorne et al., 2012). Thus, the Santa Elena Peninsula can be

considered an area of active lateritic soil formation, given its association with the Santa Elena Ophiolite, and the adequate climate conditions to develop them.

In general terms, the lateritization process starts with the dissolution of the olivine and serpentine minerals, following the leaching of mobile elements such as silicon and magnesium, among others (Thorne et al., 2012). Iron, nickel, cobalt and other heavy metals in these minerals, precipitate as insoluble oxides. Nickel for example, is commonly found associated with iron in limonite (Fe,Ni)O(OH) which is a common laterite mineral enriched with nickel (Weller et al., 2014).

The nickel laterites have economic importance as they contain more than 70% of the nickel resource in the lithosphere (Hallberg et al., 2011). However, the laterites only represent 40% of the world production of Ni, the rest comes from others sources of nickel such as the sulphide ores of millerite (NiS) or pentlandite $(Fe,Ni,Co)_9S_8$. But nickel is not the only metal economically important that can be obtained, as Co is an important by-product of nickel mining, and copper mining as well. Cobalt can represent between 0.025 and 0.18% of these laterites (Roberts and Gunn, 2014; Thorne et al., 2012; Weller et al., 2014).

### 2.4.4 Occurrence in Costa Rica

In Costa Rica, the presence of ultramafic rocks is restricted to the ophiolites shown in Figure 2.7. Three major complexes are shown: Santa Elena-Nicoya Peninsula in the North Pacific, Herradura-Quepos in the middle Pacific and Osa-Burica in the South Pacific. However recent researchers separate the Santa Elena Peninsula as a different ophiolite, although still related to Nicoya (Denyer and Gazel, 2009; Madrigal et al., 2015; Schwarzenbach et al., 2016).

Co, Ni and Mn have been reported in the ultramafic rocks of some these complexes. In the Santa Elena Peninsula in particular, those elements have been scarcely documented (Table 2.2). Remarkably, the content of these elements seems to be higher in the soil than in the rocks, which might be in accord with the lateritization process. However, a wider approach must be done to understand how the weathering of the peridotites in the Peninsula of Santa Elena relates to the presence of these metals in the lateritic soils.

**Table 2.2.** Iron, nickel, cobalt and manganese reports in the Peninsula of Santa Elena.

| Reference | Sample type | Iron | Nickel | Cobalt | Manganese |
|---|---|---|---|---|---|
| Marín Guzmán (1985) | Sediments | 5.6-6.8% | >100 ppm | 34-70 ppm | 560-920 ppm |
| Reeves *et al*. (2007) | Soil | 10.2-16.0% | 3240-5910 ppm | 152-325 ppm | 1450-2600 ppm |
| Denyer and Gazel (2009) | Peridotite | -- | 1993-2380 ppm | -- | -- |
| Madrigal *et al.* (2015) | Basalt/diabase | 8.9-15.1% | 14-106 ppm | 23-36 ppm | 130-250 ppm |

### 2.5 Soils, microorganisms and geomicrobiology

A soil might be defined as a "natural body comprised of solids (minerals and organic matter), liquid, and gases that occurs on the land surface, occupies space, and is characterized by one or both of the following: horizons, or layers, that are distinguishable from the initial material... or the ability to support rooted plants in natural environment" (Soil Survey Staff, 2014). The soil environment is one of the most complex habitats on Earth as its biodiversity is estimated to contain a third of all living organisms, and also regulates the activity of the other organisms in the ecosystems. Only the prokaryotic biomass has been estimated as $2.6x10^{29}$ cells in soil (Voroney and Heck, 2015). Even in the subsurface, held beneath soil zone, the total carbon biomass is estimated between $10^{16}$-$10^{17}$ grams, representing 2-19% of total biomass on Earth (Wilkins and Fredrikson, 2016).

Soil plays an important role as an interface where organisms (biosphere) interact with the rocks and minerals (lithosphere), water (hydrosphere) and air (atmosphere), while climate regulates the intensity of those interactions. Therefore, the soil ecosystem can be defined as "the totality of living organisms inhabiting soil, including plants, animals, and microorganisms, and their abiotic environment." Factors like the geology, climate and plant composition will affect the nature of a specific soil habitat and the composition of organisms within it (Voroney and Heck, 2015). These organisms might be prokaryotes (bacteria and archaea), algae, fungi, and many other groups such as protozoa, rotifers, nematodes, oligochaetes (earthworms) and arthropods (Coleman and Wall, 2015; Ehrlich, 2016a; Killham and Prosser, 2015; Taylor and Sinsabaugh, 2015).

The habitat in the soil is heterogeneous across its chemical, physical and biological characteristics, and the importance of one or other characteristic might change depending the scale, space and the organisms to be considered. Amongst these properties are the soil texture, related to the grain size and the aggregation of the particles; the pore size and the aeration, the temperature, moisture content, and chemical properties as the acidity and the redox potential (Voroney and Heck, 2015).

The redox potential in particular ($E_h$), is a good indicator of the soil aeration level as it measures the difference between the oxidized and reduced chemical species. When the soils are well aerated, the oxygen ($O_2$) acts as an electron acceptor of the electrons produced as a result of the metabolic activity of the soils organisms, for example when oxidising organic matter. Under anoxic conditions, alternative electron acceptors are used, and the anaerobic microorganisms are dominant. These processes, known together as anaerobic respiration, involve the reduction of other elements present in soil, such as iron, sulphur, manganese or nitrogen, or $CO_2$ in the methanogenesis process (Voroney and Heck, 2015).

Microorganisms contribute to soil evolution with their metabolism of organic matter or inorganic minerals. These organic and inorganic substrates and nutrients required by soil microbes are distributed between the surface of mineral particles and the soil solution. Consequently, several processes are developed to acquire those nutrients, such as absorption, ionic exchange, dissolution, oxidation-reduction reactions, etc. The metabolism of all these nutrients leads to the production of organic and inorganic acids, carbon dioxide, ammonia, and the dissolution or precipitation of new minerals; and therefore contributes to the soil formation (Ehrlich, 2016a).

### 2.5.1 Soil microbial biodiversity

Bacterial communities from different soils across the world are dominated by similar groups regardless of geographical location or ecosystem type, although only few soil bacterial phylotypes are dominant and most of them are rare (Figure 2.10) (Delgado-Baquerizo et al., 2018). The three major dominant bacterial clades found in soils worldwide are Proteobacteria, Actinobacteria and Acidobacteria (Figure 2.10C). When comparing ecosystems such as forests but from different climatic conditions, dry forests have a higher relative abundance of the dominant phylotypes compared to temperate forests, and to a larger extent when compared to cold forests (Figure

2.10B). Tropical forests have the lowest abundance of dominant bacterial soil phylotypes according to Delgado-Baquerizo *et al.* (2018) suggesting that tropical forest bacterial soil communities could be very distinct.

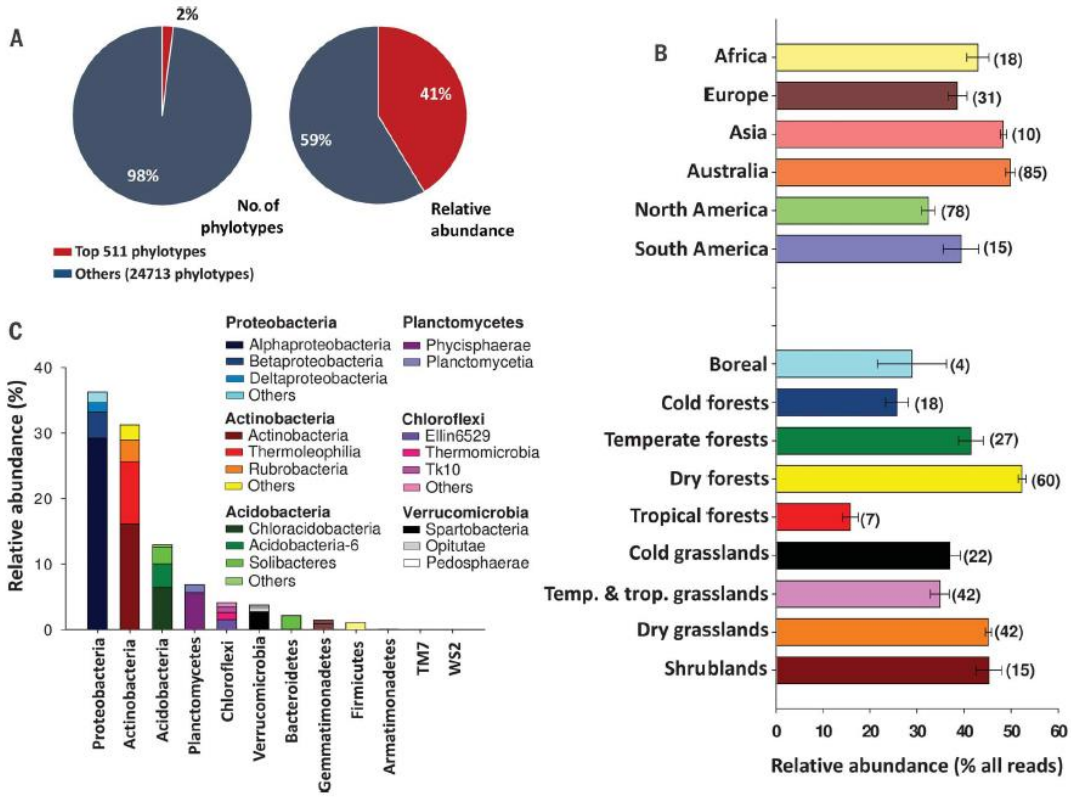


**Figure 2.10.** Abundance and composition of dominant soil bacterial phylotypes across the globe. (A) Percentage of phylotypes and relative abundance of 16S rRNA genes representing the dominant versus the remaining bacterial phylotypes. (B) Relative abundance of dominant phylotypes across continents and ecosystem types. (C) Taxonomic composition of the dominant phylotypes (Delgado-Baquerizo et al., 2018).

Soil microbial biodiversity is highly associated with climatic factors such as aridity index, maximum temperature and precipitation seasonality, and also to plant productivity. However, there are other potential driving factors to microbial distribution patterns such as other environmental predictors that are difficult to measure (e.g. soil C availability) or the ecological relationships of microorganisms with other organisms such as fungi or animals (Delgado-Baquerizo et al., 2018). In soils with organic horizons, fungi generally dominate the microbial mass and activity, especially in forests. They are also higher in proportion relative to bacteria, in acidic, low-nutrient soils with

high C-N ratios. The bacteria are much more dominant in alkaline, anoxic and carbon-phosphorus rich soils (Taylor and Sinsabaugh, 2015). However is important to consider that the majority of prokaryote groups and strains that are abundant and important for soil processes have not been characterised yet, similar to many mechanisms between soil-prokaryotes that have not been elucidated (Killham and Prosser, 2015).

### 2.5.2 Biodiversity in serpentine soils

Microbial communities in serpentine soils have been described and related to environmental and geographical factors. In New Caledonia tropical rainforests, bacterial communities of the ultramafic soils were dominated by Proteobacteria (31% of relative abundance), but unlike other soil types (Figure 2.10) Planctomycetes was the second most abundant clade (19%), followed by Acidobacteria (12%) and Actinobacteria (9%). Here, microbial richness, composition and abundance were related to plant cover type and dominant plant species; and the association was explained due to host preference, litter quality or root exudates (Bordez et al., 2016; Gourmelon et al., 2016). In serpentine soils from the Iberian Peninsula, the presence of vegetation such as Ni-hyperaccumulating or Ni-excluding plants affected the bacterial communities related to nutrient availability, especially for the Alphaproteobacteria profile; while non-vegetated soils were more affected by intrinsic soil properties resulting in different soil microbial communities (Touceda-González et al., 2018).

Similarly, host preference and density were also described as factors that influenced ectomycorrhizal community composition in New Caledonian rainforests (Carriconde et al., 2019). Ectomycorrhizal fungal colonisation was suggested to be facilitated by the plants in serpentine soils from Portugal, but the serpentine characteristics of the soil did not limit the mycorrhizal fungal diversity and the specialisation to serpentine soils might be occurring only in the plant ecotypes (Branco and Ree, 2010). Fungal communities of the ultramafic soils in New Caledonia were also related to several plant species, but Basidiomycota clades were more abundant in the areas covered with rainforest while Ascomycota groups were more abundant in more disturbed areas (Gourmelon et al., 2016).

However, edaphic parameters also influence soil bacterial and fungal communities in serpentine soils but to a lesser extent when compared to floristic predictors (Bordez et al., 2016; Gourmelon

et al., 2016). Soil properties such as pH, nitrogen and calcium content affected distribution patterns of bacterial and fungal communities in New Caledonian ultramafic soils (Bordez et al., 2016). Also, the abundance of nutrients and litter decomposition rates have been proposed as important characteristics affecting microbial communities in ultramafic soils, especially those in tropical regions (Gourmelon et al., 2016).

The high content of metals, especially nickel, is another important edaphic parameter in serpentine soils that determines microbial communities. The presence of this metal indirectly affected the microbial composition of ultramafic soils mediated by the presence or absence of Ni-hyperaccumulating or Ni-excluding plants as previously described (Touceda-González et al., 2018). Also, high Ni-content in New Caledonian ultramafic soils influenced the presence of symbiotic associations such as arbuscular mycorrhizal fungi and ectomycorrhizal fungi improving plant tolerance to this metal; and Ni-resistant and Ni-hyperaccumulating bacterial strains have been found in these ultramafic soils too (Gourmelon et al., 2016).

Finally, some other ecological parameters have been described as potential factors affecting microbial communities in serpentine soils. The relationship between bacterial and fungal soil communities was evidenced in New Caledonian ultramafic soils; and site effects in microbial communities for the same area were also hypothesised in the context of the biogeographical island theory, based on the geographical distribution of the ultramafic substrates into a large massif and several isolated islets (Gourmelon et al., 2016).

In summary, microbial communities in serpentine soils are the result of complex interactions between abiotic and biotic factors, highly influenced by the plant coverage. Thus, recent studies have demonstrated that the serpentine-ultramafic soils do not limit bacterial and fungal diversity, and they have evidenced the biological complexity of these ecosystems (Bordez et al., 2016; Branco and Ree, 2010; Carriconde et al., 2019; Gourmelon et al., 2016).

### 2.5.3 Geomicrobiological processes

Geomicrobiology studies focus on the role of microbes in fundamental geologic processes on Earth; the importance of microorganisms in soil formation and transformation briefly explained above is just a part of its approach. Other processes considered within geomicrobiology are: the

cycling of organic and inorganic matter at the surface and subsurface of Earth; weathering of rocks and minerals through production and excretion of metabolic products or redox reactions; formation of minerals as iron sulphides, iron and manganese oxides, calcium carbonate or silica; diagenesis of minerals, lithification of particles to form sedimentary rocks; accumulation of sediment as calcium carbonate tests from foraminifera or silica tests from radiolaria, and formation, preservation and degradation of fossil fuels (Ehrlich, 2016b; Ehrlich et al., 2016).

Microorganisms can act as geologic agents, serving as agents of concentration, dispersion or fractionation. When they accumulate inorganic matter through deposition of inorganic products in specific parts of the cell, passive accumulation, or precipitation of insoluble compounds, then they are concentration agents. As dispersion agents, microbes can dissolve minerals or produce soluble compounds as by-products of other processes. Finally, as fractionation agents, the microorganisms may selectively mobilise one or more compounds from a mixture of insoluble inorganic compounds. Hence, their influence may be direct, as enzyme mediated processes, or indirect due to the chemical action of their metabolic products, or through the alteration of the conditions in their environment as pH or $E_h$ (Ehrlich, 2016b).

Many of the processes mentioned above are related to the metabolism of the microorganisms mediating them. They are developed either through catabolic or anabolic reactions. The catabolic reactions in particular, can be separated into aerobic and anaerobic processes depending on the terminal electron acceptor in the reaction. In aerobic processes, organic compounds or inorganic species are oxidized via several biochemical reactions within an electron transport system, using oxygen as the ultimate acceptor of electrons, and then transformed into water. The anaerobic reactions are performed with other reducible species as the terminal electron acceptor, such as nitrate, iron(III), sulphate, carbon dioxide, or organic compounds such as fumarate (Ehrlich, 2016b; Voroney and Heck, 2015). One example of an anaerobic process is the oxidation of organic acids with Fe(III) as the only electron acceptor (Kappler et al., 2016; Lovley and Phillips, 1988).

#### 2.5.3.1 Dissimilatory Fe(III) and Mn(IV) reduction

Iron is used by a diverse set of microorganisms both physiologically and phylogenetically either acting as an electron donor for microbial processes when present as Fe(II) or as an electron

acceptor for Fe(III)-reducing microorganisms during anaerobic respiration (Kappler et al., 2016). With this mechanism of respiration, called dissimilatory iron(III) reduction, microorganisms can generate energy from Fe(III) reduction when coupled to the oxidation of a large range of organic compounds or even $H_2$ (Lovley et al., 2004). Ferric iron, on the other hand, can be reduced from several iron (III) minerals including goethite (α-$Fe^{3+}OOH$) or hematite (α-$Fe_2O_3$)(Kappler et al., 2016). Many organisms that reduce Fe(III) also reduce Mn(IV), and are present both in Bacteria and Archaea, with *Geobacter* sp. and *Shewanella* sp. as classic examples of them. The dissimilatory Fe(III) and Mn(IV) reduction are important processes in a diversity of environments that have anoxic conditions, and availability of both organic matter and Fe(III) and Mn (IV) (Lovley et al., 2004). Thus, in the Santa Elena Peninsula dissimilatory Fe(III) reduction could be an important microbial mechanism in the lateritic soils if anoxic conditions are developed, as large concentrations of iron and manganese are expected due to the lateritic nature, and given the strong seasonality with a large rainy season, waterlogging of soils can lead to the development of these mechanisms.

However, as said before, dissimilatory Fe(III) reduction is not the only mechanism involving geomicrobiological cycling of iron, and in oxic conditions other microorganisms could be relevant in the context of Santa Elena Peninsula such as acidophilic aerobic iron(II)-oxidising bacteria. Therefore, understanding the geomicrobiology associated with Fe in the lateritic soils of Santa Elena is a key point to considerate for any other biogeochemical cycle in the site.

#### 2.5.3.2 Geomicrobiology of Co and Ni

Although the geomicrobiology of elements such as iron, manganese, phosphorus, nitrogen, sulphur and others, has been widely studied and characterized, other elements have not been considered in such detail (Fike et al., 2016; Francis and Casciotti, 2016; Hansel and Learman, 2016; Kappler et al., 2016; Schink and Simeonova, 2016). Among these elements, cobalt and nickel have little understanding of their geomicrobiology, although some insights can be found. For example, in laboratory experiments, the bacteria *Desulfovibrio desulfuricans* was capable of produce cobalt sulphide and nickel sulphide in a culture containing lactate from salts of cobalt and nickel, respectively. Also, *Acidithiobacillus ferrooxidans* has been reported to oxidize sulphides including the millerite (NiS) (Ehrlich, 2016c).

Moreover, the geomicrobiology of nickel is often associated with the biomining processes in laterite ores. The aim of such biomining processes is the acceleration of the dissolution of sulphide minerals to enhance the recovery of metals mediated by microorganisms. This process occurs by oxidative dissolution, for example with acidophilic prokaryotes that are capable of oxidising reduced sulphide minerals. Therefore, biomining emerges as an important alternative in low-grade deposits of certain metals such as nickel or cobalt, and is also useful to re-process waste materials from mining operation, among other benefits (Hallberg et al., 2011).

However, in some of these investigations, instead of targeting the nickel directly, the aim was to accelerate the dissolution of ferric iron minerals, supposing that other metals associated with the iron (as nickel) can be released into solution, and later recovered in acid media using acidophilic microorganisms. Following this focus, the use of *A. ferrooxidans,* an iron and sulphur-oxidizing chemolithotroph, demonstrated that the extraction of nickel from a limonitic laterite ore was accelerated due to the reductive dissolution of the ferric iron minerals (Hallberg et al., 2011). This same approach was reported as a potential method to extract other metals from oxidised ores, as copper, cobalt or manganese (Johnson and du Plessis, 2015). Nevertheless, other research proved than aerobic reductive dissolution using *Acidithiobacillus thiooxidans* was more efficient in extracting total iron, ferrous iron, and dissolving manganese, cobalt and nickel than the anaerobic reductive dissolution with *A. ferrooxidans* (Marrero et al., 2017). Fungi as *Aspergillus* and *Penicillium* also have been used to leach metals as copper, nickel and cobalt from low-grade mineral ores through metal-chelating metabolic by-products as oxalic or citric acid, although is thought not to be a viable option due to the low yields, high operational features and high costs (Gadd et al., 2014; Johnson and du Plessis, 2015).

### 2.5.4 Studies in the Santa Elena Peninsula

No research has been reported regarding the geomicrobiology of nickel, cobalt or any other trace element found in the soils. Indeed, only three investigations have studied the living organisms inhabiting the ultramafic rocks and their associated soils (Crespo-Medina et al., 2017; Reeves et al., 2007; Sánchez-Murillo et al., 2014).

The first one was a description of the flora associated with the ultramafic soils, where the main result was the report of several plant genera also represented in other Latin-American regions

where ultramafic rocks can be found. They also reported the chemical ultramafic composition of the soils in the 6 locations sampled. However, the authors emphasised that only a small area of the peninsula was covered in the investigation and large areas of the peninsula remain biogeochemically unexplored (Reeves et al., 2007).

The other two studies had a more geomicrobiological focus, but were oriented to the study of hyper alkaline springs and their relationship with the serpentinization process and methane cycling in serpentinization-influenced fluids (Crespo-Medina et al., 2017). They found signatures of methanogenic archaea from the orders Methanobacteriales, Methanocellales, and Methanomicrobiales and proposed a relationship between these microorganisms and an active serpentinization process, although they did not prove their exact role in the system. Nevertheless, the authors were more focused in the possible implications of the study as a scenario analogue to humid early Earth or Mars through the water supply conditions, the serpentinizing solute transport and in the modelling of hydrogeochemical responses, rather than in the possible geomicrobiological processes occurring there (Sánchez-Murillo et al., 2014).

In conclusion, despite being so well studied in its geology and ecology, the Peninsula of Santa Elena has been widely overlooked in the matter of the geomicrobiological processes occurring in the soils. These processes might have important geological implications and are crucial to the development of the soil habitat and to the serpentine ecosystems occurring over it.

### 2.6 References

ACG, 2014. ¿Qué es el ACG? - Área de Conservación Guanacaste [WWW Document]. URL http://www.acguanacaste.ac.cr/acg/que-es-el-acg (accessed 12.8.16).

Alvarado, A., Mata, R., 2016. Soils fo Costa Rica: An Agroecological Approach, in: Kappelle, M. (Ed.), Costa Rican Ecosystems. The University of Chicago Press, p. 774.

Alvarado, G.E., Cárdenes, G., 2016. Geology, Tectonics, and Geomorphology of Costa Rica: A Natural History Approach, in: Kappelle, M. (Ed.), Costa Rican Ecosystems. The University of Chicago Press, p. 744.

Anacker, B.L., 2011. Phylogenetic patterns of endemism and diversity, in: Harrison, S., Rajakaruna, N. (Eds.), Serpentine: The Evolution and Ecology of a Model System. University of California Press, Berkeley, p. 446.

Bordez, L., Jourand, P., Ducousso, M., Carriconde, F., Cavaloc, Y., Santini, S., Claverie, J.M., Wantiez, L., Leveau, A., Amir, H., 2016. Distribution patterns of microbial communities in ultramafic landscape: a metagenetic approach highlights the strong relationships between

diversity and environmental traits. Mol. Ecol. 25, 2258–2272. https://doi.org/10.1111/mec.13621

Branco, S., Ree, R.H., 2010. Serpentine Soils Do Not Limit Mycorrhizal Fungal Diversity. PLoS One 5, e11757. https://doi.org/10.1371/journal.pone.0011757

Carriconde, F., Gardes, M., Bellanger, J.-M., Letellier, K., Gigante, S., Gourmelon, V., Ibanez, T., McCoy, S., Goxe, J., Read, J., Maggia, L., 2019. Host effects in high ectomycorrhizal diversity tropical rainforests on ultramafic soils in New Caledonia. Fungal Ecol. 39, 201–212. https://doi.org/10.1016/j.funeco.2019.02.006

Coleman, D.C., Wall, D.H., 2015. Soil Fauna: Occurence, Biodiversity, and Roles in Ecosystem Function, in: Paul, E.A. (Ed.), Soil Microbiology, Ecology, and Biochemistry. Academic Press, p. 582.

Crespo-Medina, M., Twing, K.I., Sánchez-Murillo, R., Brazelton, W.J., McCollom, T.M., Schrenk, M.O., 2017. Methane Dynamics in a Tropical Serpentinizing Environment: The Santa Elena Ophiolite, Costa Rica. Front. Microbiol. 8, 916. https://doi.org/10.3389/fmicb.2017.00916

Delgado-Baquerizo, M., Oliverio, A.M., Brewer, T.E., Benavent-González, A., Eldridge, D.J., Bardgett, R.D., Maestre, F.T., Singh, B.K., Fierer, N., 2018. A global atlas of the dominant bacteria found in soil. Science. 359, 320–325. https://doi.org/10.1126/science.aap9516

Denyer, P., Gazel, E., 2009. The Costa Rican Jurassic to Miocene oceanic complexes: Origin, tectonics and relations. J. South Am. Earth Sci. 28, 429–442. https://doi.org/10.1016/j.jsames.2009.04.010

Ehrlich, H.L., 2016a. Uppermost Lithosphere as a Microbial Habitat, in: Ehrlich, H.L., Newman, D.K., Kappler, A. (Eds.), Ehrlich's Geomicrobiology. CRC Press, p. 635.

Ehrlich, H.L., 2016b. Geomicrobial Processes: a Physiological and Biochemical Overview, in: Ehrlich, H.L., Newman, D.K., Kappler, A. (Eds.), Ehrlich's Geomicrobiology. CRC Press, p. 635.

Ehrlich, H.L., 2016c. Biogenesis and Biodegradation of Sulfide Minerals in the Earth's Surface, in: Ehrlich, H.L., Newman, D.K., Kappler, A. (Eds.), Ehrlich's Geomicrobiology. CRC Press, p. 635.

Ehrlich, H.L., Newman, D.K., Kappler, A., 2016. Introduction, in: Ehrlich, H.L., Newman, D.K., Kappler, A. (Eds.), Ehrlich's Geomicrobiology. CRC Press, p. 635.

Escuder-Viruete, J., Baumgartner, P.O., Castillo-Carrión, M., 2015. Compositional diversity in peridotites as result of a multi-process history: The Pacific-derived Santa Elena ophiolite, northwest Costa Rica. Lithos 231, 16–34. https://doi.org/10.1016/j.lithos.2015.05.019

Fike, D.A., Bradley, A.S., Leavitt, W.D., 2016. Geomicrobiology of Sulfur, in: Ehrlich, H.L., Newman, D.K., Kappler, A. (Eds.), Ehrlich's Geomicrobiology. CRC Press, p. 635.

Francis, C.A., Casciotti, K.L., 2016. Geomicrobiology of Nitrogen, in: Ehrlich, H.L., Newman, D.K., Kappler, A. (Eds.), Ehrlich's Geomicrobiology. CRC Press, p. 635.

Gadd, G.M., Bahri-Esfahani, J., Li, Q., Rhee, Y.J., Wei, Z., Fomina, M., Liang, X., 2014. Oxalate production by fungi: significance in geomycology, biodeterioration and bioremediation. Fungal Biol. Rev. https://doi.org/10.1016/j.fbr.2014.05.001

Gómez, L.D., Herrera, W., 1986. Clave para Macrotipos de Vegetación de Costa Rica [WWW Document]. Veg. y clima Costa Rica. URL http://www.inbio.ac.cr/es/biod/minae/Estudio_Pais/estudio/macrotipos.html

Gourmelon, V., Maggia, L., Powell, J.R., Gigante, S., Hortal, S., Gueunier, C., Letellier, K., Carriconde, F., 2016. Environmental and Geographical Factors Structure Soil Microbial Diversity in New Caledonian Ultramafic Substrates: A Metagenomic Approach. PLoS One

11, 1–25. https://doi.org/10.1371/journal.pone.0167405

Haldar, S.K., 2018. Chapter 5 - Exploration Geochemistry, in: Haldar, S.K. (Ed.), Mineral Exploration, Principles and Applications. Elsevier, pp. 85–101. https://doi.org/10.1016/B978-0-12-814022-2.00005-8

Hallberg, K.B., Grail, B.M., Plessis, C.A. du, Johnson, D.B., 2011. Reductive dissolution of ferric iron minerals: A new approach for bio-processing nickel laterites. Miner. Eng. 24, 620–624. https://doi.org/10.1016/j.mineng.2010.09.005

Hansel, C.M., Learman, D.R., 2016. Geomicrobiology of Manganese, in: Ehrlich, H.L., Newman, D.K., Kappler, A. (Eds.), Ehrlich's Geomicrobiology. CRC Press, pp. 401–452.

Herrera, W., 2016. Climate of Costa Rica, in: Kappelle, M. (Ed.), Costa Rican Ecosystems. The University of Chicago Press, p. 744.

Instituto Meteorológico Nacional, n.d. Clima en Costa Rica-Pacífico Norte [WWW Document]. URL https://www.imn.ac.cr/documents/10179/31165/PacificoNorte.pdf/4a0e8960-8c51-4390-8a8d-73d9d825d59b (accessed 1.24.17).

Janzen, D.H., Hallwachs, W., 2016. Biodiversity Conservation History and Future in Costa Rica: The Case of Área de Conservación Guanacaste (ACG), in: Kappelle, M. (Ed.), Costa Rican Ecosystems. The University of Chicago Press, p. 744.

Jiménez M., Q., Carrillo J., E., Kappelle, M., 2016. The Northern Pacific Lowland Seasonal Dry Forest of Ganacaste and the Nicoya Peninsula, in: Kappelle, M. (Ed.), Costa Rican Ecosystems. The University of Chicago Press, p. 744.

Johnson, D.B., du Plessis, C.A., 2015. Biomining in reverse gear: Using bacteria to extract metals from oxidised ores. Miner. Eng. 75, 2–5. https://doi.org/10.1016/j.mineng.2014.09.024

Kappelle, M., 2016. Costa Rica's Ecosystems: Setting the Stage, in: Kappelle, M. (Ed.), Costa Rican Ecosystems. The University of Chicago Press, p. 744.

Kappler, A., Emerson, D., Gralnick, J.A., Roden, E.E., Muehe, E.M., 2016. Geomicrobiology of Iron, in: Ehrlich, H.L., Newman, D.K., Kappler, A. (Eds.), Ehrlich's Geomicrobiology. CRC Press, pp. 343–399.

Kay, K.M., Ward, K.L., Watt, L.R., Schemske, D.W., 2011. Plant Speciation, in: Harrison, S., Rajakaruna, N. (Eds.), Serpentine: The Evolution and Ecology of a Model System. University of California Press, Berkeley, p. 446.

Kazakou, E., Dimitrakopoulos, P.G., Baker, A.J.M., Reeves, R.D., Troumbis, A.Y., 2008. Hypotheses, mechanisms and trade-offs of tolerance and adaptation to serpentine soils: from species to ecosystem level. Biol. Rev. 83, 495–508. https://doi.org/10.1111/j.1469-185X.2008.00051.x

Killham, K., Prosser, J.I., 2015. The Bacteria and Archaea, in: Paul, E.A. (Ed.), Soil Microbiology, Ecology, and Biochemistry. Academic Press, Boston, p. 582. https://doi.org/10.1016/B978-0-12-415955-6.00003-7

Lovley, D.R., Holmes, D.E., Nevin, K.P., 2004. Dissimilatory Fe(III) and Mn(IV) Reduction. Adv. Microb. Physiol. 49, 219–286. https://doi.org/10.1016/S0065-2911(04)49005-5

Lovley, D.R., Phillips, E.J.P., 1988. Novel Mode of Microbial Energy Metabolism: Organic Carbon Oxidation Coupled to Dissimilatory Reduction of Iron or Manganese. Appl. Envir. Microbiol. 54, 1472–1480.

Madrigal, P., Gazel, E., Denyer, P., Smith, I., Jicha, B., Flores, K.E., Coleman, D., Snow, J., 2015. A melt-focusing zone in the lithospheric mantle preserved in the Santa Elena Ophiolite, Costa Rica. Lithos 230, 189–205. https://doi.org/10.1016/j.lithos.2015.04.015

Malvoisin, B., Brunet, F., 2014. Water diffusion-transport in a synthetic dunite: Consequences for

oceanic peridotite serpentinization, Earth and Planetary Science Letters. https://doi.org/10.1016/j.epsl.2014.07.004

Marín Guzmán, F., 1985. Levantamiento geoquímico regional de la hoja Liberia 1:200.000 (Costa Rica). Rev. Geológica América Cent. 1–21. https://doi.org/10.15517/rgac.v0i02.10479

Marrero, J., Coto, O., Schippers, A., 2017. Anaerobic and aerobic reductive dissolutions of iron-rich nickel laterite overburden by Acidithiobacillus. Hydrometallurgy 168, 49–55. https://doi.org/10.1016/J.HYDROMET.2016.08.012

Medina Sandoval, W., 2003. Ubicación del Area de Conservación Guanacaste [WWW Document]. ACG Maps - Mapas del ACG - Área Conserv. Guanacaste. URL http://www.acguanacaste.ac.cr/images/phocagallery/mapas/galeria-mapas/thumbs/phoca_thumb_l_4acg_costarica.jpg (accessed 12.11.16).

Medina, W., 2001. Area de Conservación Guanacaste Red Hidrográfica [WWW Document]. Sist. Inf. Geográfica - Área Conserv. Guanacaste. URL http://www.investigadoresacg.org/IMAGES/MAPFILES/maps/general_ACG/RIOS_ACG.JPG (accessed 12.11.16).

Medina, W., 1999a. Tipos de vegetación: Hoja Liberia - Area de Conservación Guanacaste [WWW Document]. Sist. Inf. Geográfica - Área Conserv. Guanacaste. URL http://www.investigadoresacg.org/IMAGES/MAPFILES/maps/physical_biological/vegetacion_acg.jpg (accessed 12.11.16).

Medina, W., 1999b. Suelos: Hoja Liberia - Area de Conservación Guanacaste [WWW Document]. Sist. Inf. Geográfica - Área Conserv. Guanacaste. URL http://www.investigadoresacg.org/IMAGES/MAPFILES/maps/physical_biological/suelos_acg.jpg (accessed 12.11.16).

Medina, W., 1999c. Geología: Hoja Liberia - Area de Conservación Guanacaste [WWW Document]. Sist. Inf. Geográfica - Área Conserv. Guanacaste. URL http://www.investigadoresacg.org/IMAGES/MAPFILES/maps/physical_biological/geologia_acg.jpg (accessed 12.11.16).

Medina, W., Guadamuz, D., 2004. Area de Conservación Guanacaste [WWW Document]. Sist. Inf. Geográfica - Área Conserv. Guanacaste. URL http://www.acguanacaste.ac.cr/biodesarrollo/sistemas-de-informacion-geografica (accessed 12.11.16).

Moores, E.M., 2011. Serpentinites and other ultramafic rocks, in: Harrison, S., Rajakaruna, N. (Eds.), Serpentine: The Evolution and Ecology of a Model System. University of California Press, Berkeley, p. 446.

Reeves, R.D., Baker, A.J.M., Romero, R., 2007. The ultramafic flora of the Santa Elena peninsula, Costa Rica: A biogeochemical reconnaissance. J. Geochemical Explor. 93, 153–159. https://doi.org/10.1016/j.gexplo.2007.04.002

Roberts, S., Gunn, G., 2014. Cobalt, in: Gunn, G. (Ed.), Critical Metals Handbook. John Wiley & Sons, Oxford, pp. 122–149. https://doi.org/10.1002/9781118755341.ch6

Sánchez-Murillo, R., Gazel, E., Schwarzenbach, E.M., Crespo-Medina, M., Schrenk, M.O., Boll, J., Gill, B.C., 2014. Geochemical evidence for active tropical serpentinization in the Santa Elena Ophiolite, Costa Rica: An analog of a humid early Earth? Geochemistry, Geophys. Geosystems 15, 1783–1800. https://doi.org/10.1002/2013GC005213

Schellmann, W., 1994. Geochemical differentiation in laterite and bauxite formation. CATENA 21, 131–143. https://doi.org/10.1016/0341-8162(94)90007-8

Schink, B., Simeonova, D.D., 2016. Geomicrobial Interactions with Phosphorus, in: Ehrlich, H.L., Newman, D.K., Kappler, A. (Eds.), Ehrlich's Geomicrobiology. CRC Press, p. 635.

Schwarzenbach, E.M., Gill, B.C., Gazel, E., Madrigal, P., 2016. Sulfur and carbon geochemistry of the Santa Elena peridotites: Comparing oceanic and continental processes during peridotite alteration. Lithos 252, 92–108. https://doi.org/10.1016/j.lithos.2016.02.017

SINAC, n.d. Sistema Nacional de Áreas de Conservación (SINAC) [WWW Document]. URL http://www.sinac.go.cr/ES/conozca/Paginas/default.aspx (accessed 12.8.16).

Soil Survey Staff, 2014. Keys to Soil Taxonomy, 12th ed. USDA-Natural Resources Conservation Service, Washington D.C.

Stoops, G., Marcelino, V., 2018. Chapter 24 - Lateritic and Bauxitic Materials, in: Stoops, G., Marcelino, V., Mees, F.B.T.-I. of M.F. of S. and R. (Second E. (Eds.), . Elsevier, pp. 691–720. https://doi.org/10.1016/B978-0-444-63522-8.00024-3

Streckeisen, A., 1976. To each plutonic rock its proper name. Earth-Science Rev. 12, 1–33. https://doi.org/10.1016/0012-8252(76)90052-0

Taylor, D.L., Sinsabaugh, R.L., 2015. The Soil Fungi: Occurrence, Phylogeny, and Ecology, in: Paul, E.A. (Ed.), Soil Microbiology, Ecology, and Biochemistry. Academic Press, p. 582.

Thorne, R.L., Roberts, S., Herrington, R., 2012. Climate change and the formation of nickel laterite deposits. Geology 40, 331–334. https://doi.org/10.1130/G32549.1

Thorpe, R.S., Brown, G.C., 1993. The Field Description of Igneous Rocks, Second. ed. John Wiley & Sons, Ltd.

Touceda-González, M., Kidd, P.S., Smalla, K., Prieto-Fernández, A., 2018. Bacterial communities in the rhizosphere of different populations of the Ni-hyperaccumulator Alyssum serpyllifolium and the metal-excluder Dactylis glomerata growing in ultramafic soils. Plant Soil 431, 317–332. https://doi.org/10.1007/s11104-018-3767-6

Turner, F.J., Verhoogen, J., 1960. Igneous and Metamorphic Petrology, Second. ed. McGraw-Hill Book COmpany, Inc.

Voroney, R.P., Heck, R.J., 2015. The Soil Habitat, in: Paul, E.A. (Ed.), Soil Microbiology, Ecology, and Biochemistry. Academic Press, p. 582.

Weller, M., Overton, T., Rourke, J., Armstrong, F., 2014. Inorganic Chemistry, 6th ed. Oxford University Press, Oxford.

Wilkins, M., Fredrikson, J.K., 2016. Terrestrial Subsurface Ecosystem, in: Ehrlich, H.L., Newman, D.K., Kappler, A. (Eds.), Ehrlich's Geomicrobiology. CRC Press, p. 635.

Winter, J.D., 2001. An Introduction to Igneous and Metamorphic Petrology. Prentice Hall Inc, New Jersey.

# Chapter 3. Methodology

This chapter briefly describes the analytical techniques and experimental methods used in this thesis, however a more detailed description of the parameters and specifications used for each technique are described in the methodological sections of each research chapter (4, 5 and 6). When required, all chemical reagents were analytical grade and used as received, and aqueous solutions were prepared in deionised water (18 MΩ). Soil and rock samples were collected by the author of this thesis from the Santa Elena Peninsula in Costa Rica, during several field campaigns between 2016-2018 (see Appendix 3 for detail). All of the soil samples were tested in triplicate, where each replicate corresponded to one replicate from the sampling area in the Santa Elena Peninsula. For details of sampling methodology see also Chapters 4, 5 and 6.

### 3.1 Petrographic examination, and electron probe micro analysis (EPMA)

Rock samples were analysed with a polarised microscope and later with EPMA to analyse chemical distribution and quantification within minerals, these techniques were used in chapter 4. Thin sections of the rock samples collected were prepared using low viscosity optical epoxy resin, cut to 30 μm thickness with a Buehler PetroThin thin sectioning system and polished with 1 μm diamond paste. The EPMA technique is based on collecting X-ray photons emitted at a characteristic wavelength after bombarding a sample with an electron beam; the X-rays emitted are recorded and identified with wavelength dispersive spectroscopy (Figure 3.1) (CAMECA, n.d.).

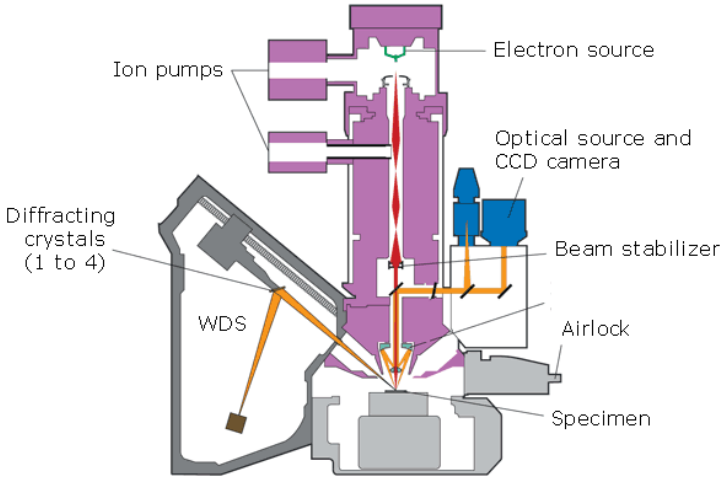


**Figure 3.1.** Detail of a EPMA analyser (CAMECA, n.d.).

Petrographic analysis was undertaken using a Nikon Eclipse LV100NPOL petrographic microscope equipped with a Nikon DS-Fi2 camera and DS-U3 camera control software. The polished thin sections were carbon coated prior to EPMA. EPMA was carried out using a Cameca SX100 electron probe microanalyser equipped with 5 wavelength dispersive spectrometers (WDS). Elemental distribution maps were created for Fe, Mg, Si, Al, Cr, Mn, Co, Ni, Ca, Ti, Cl, K, Na and S, and points were analysed at 20 kV, 5 nA with a 10 µm beam using the standards fayalite (Fe), periclase (Mg), anorthite (Si, Al), $Cr_2O_3$, tephrolite (Mn), Co-metal, NiO, wollastonite (Ca), rutile (Ti), sodalite (Cl), orthoclase (K), jadeite (Na) and pyrite (S). Thin sections were prepared by Mr. Stephen Stockley, and EPMA analysis was performed by Dr. Jon Fellowes (University of Manchester).

### 3.2 X-ray fluorescence spectroscopy (XRF)

In Chapter 4, for both rock powder and soil samples, bulk elemental composition of major and trace metals was analysed using XRF. Prior to XRF, samples were prepared as pellets from dry fine powder of the samples, and the total carbon content was determined by loss on ignition (LOI). This technique is based on the characteristic fluorescence emitted (fluorescence X-rays) by a particular material when it is irradiated with X-rays. The X-rays force the inner electrons of the atoms to move to an outer shell, creating a void that is filled by outer electrons and thus emitting X-rays in the process (Figure 3.2) (HITACHI, n.d.).

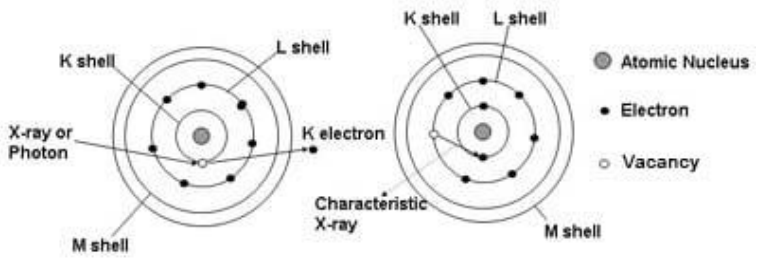


**Figure 3.2.** Principle of creation of X-Rays (HITACHI, n.d.).

Measurements were carried out on an Axios Panalytical XRF spectrometer equipped with a Rh X-ray source. Samples were scanned, identifying both major (*Omnian program*) and trace elements (*Pro-Trace program*). Sample preparation involved 12 g of dry sample and 3 g of Hoechst Wax™ ground together in an agate ball mill and then pressed into a pellet with a pneumatic press. The total carbon content in the samples was also calculated by loss on ignition (LOI), weighing exactly 1.000 g of sample and determining the mass after heating first at 105 °C for 1 h and then at 1000°C for 1 h. Sample preparation and LOI was done by the author of this thesis; XRF was performed by Mr. Paul Lythgoe (University of Manchester).

### 3.3 X-ray diffraction spectroscopy (XRD)

Bulk mineralogy was studied for soil and rock samples collected from the Santa Elena Peninsula with XRD. The mineralogy in the soils after biostimulation in redox cycling microcosm experiments of chapters 5 and 6, both under anoxic and oxic conditions, was also analysed with this technique. This technique is based on measuring the diffraction angles and intensities of an incident X-ray that is diffracted when it reaches a crystalline structure, following Bragg's Law (International Union of Crystallography, 1999).

Measurements were carried out on a Bruker D8 Advance diffractometer, equipped with a Göbel Mirror, a Lynxeye detector and a copper X-ray tube, providing $CuK_{\alpha 1}$ X-rays with a wavelength of 1.5406 Å. Samples were scanned from 5-70$^{o}$ 2θ, with a step size of 0.02$^{o}$ and a count time of 0.2 s per step. The resulting patterns were evaluated using EVA version 4 software, which compares experimental data to standard XRD patterns of minerals from the ICDD (International Centre for

Diffraction Data) Database. Anaerobic XRD samples were prepared by the author of this thesis; XRD analysis was performed by Dr. John Waters (University of Manchester).

### 3.4 Fluctuating redox microcosm experiments

Fluctuating redox microcosm experiments were developed to study the biogeochemical cycling of metals in lateritic soils from the Santa Elena Peninsula, and they were used in chapters 5 and 6. Redox cycling experiments were set up using 120 mL serum bottles where 10 g of the soil to be tested was added, followed by 100 mL of artificial groundwater (AGW) (Wilkins et al., 2007) and the electron donor required. AGW was prepared (per litre of deionised water) with 0.0066 g KCl, 0.0976 g $MgSO_4 \cdot 7H_2O$, 0.810 g $MgCl_2 \cdot 6H_2O$, 0.1672 g $CaCO_3$, 0.0275 $NaNO_3$, 0.0094 g NaCl and 0.2424 $NaHCO_3$. The electron donors tested in this thesis were glucose, acetate and lactate used at a concentration of 10 mM and nanocrystalline cellulose. Controls were also prepared without electron donors.

The bottles were degassed with a mixture of 80:20 $N_2$ and $CO_2$ and incubated under anoxic conditions at 30 °C for ten months. Oxic conditions were later imposed by decapping the serum bottles, replacing the rubber bung with a sterilised foam bung and foil cap, and incubating on a shaking incubator at 30 °C and 100 *g* for 5 months (Figure 3.1). The length of each stage (anoxic and oxic) was determined considering the moment when all the monitoring conditions were stabilised (pH, redox potential and Fe(II) bioavailable). Based on previous microcosm experiments with Brazilian laterites (Appendix 1), the stabilisation was expected to happen after few months of incubation and that was the original plan with these microcosm experiments. However, the samples from Santa Elena Peninsula were more active than previous samples from Appendix 1 and stabilisation took more time than expected.

Each microcosm was sampled monthly using sterile syringes and needles to extract 0.6mL of slurry. Prior to extraction, the microcosm bottles were shaken up to homogenise the slurry. Samples were monitored monthly based on the procedure of previous microcosm experiments (Appendix 1), and also because this sampling periodicity optimised the number of time points to observe the changes in the geochemistry of the microcosm without cumulating a large number of samples for further geochemical analysis. The aliquots were monitored measuring pH, the redox potential, and by using the ferrozine assay to determine the Fe(II) bioavailable content. Aliquots

were taken for further aqueous geochemistry and stored at 30 °C until analysis. Slurry samples were taken for DNA extraction and frozen immediately. Samples for ion chromatography were also frozen to measure volatile fatty acids concentration (VFAs). VFAs are common fermentation products when Fe(II) bacteria metabolises substrates such as glucose (Lovley and Phillips, 1986), thus VFAs are used as a proxy for breakdown of the electron donor amendments. When necessary, samples of headspace gas were also taken and analysed. By the end of the experiment, approximately 15 mL of the initial microcosm volume (100 mL of AGW) was extracted, considering both the slurry samples for monitoring and the slurry samples for DNA. This volume was not replaced during the microcosm experiment. It was considered that the extracted volume did not affect significatively the chemistry of the experiments in a large scale, considering that the aliquots were taken from a pre-homogenised serum bottle where aliquots included both liquid and sediment in a proportional amount from each microcosm sampled.


**Figure 3.3.** Detail of fluctuating redox microcosm experiments during anoxic conditions (left) and oxic conditions (right).

### 3.5 Ferrozine colorimetric assay

The ferrozine assay is a colorimetric method widely used in geomicrobiology to determine the concentration of Fe(II) and total iron in solution, and as explained in Section 3.4 it was used monthly to monitor the fluctuating redox microcosm experiments. The method uses a complexation reaction between ferrozine (3-(2-Pyridyl)-5,6-diphenyl-1,2,4-triazine-*p*,*p'*-disulfonic acid monosodium) and Fe(II) forming a violet complex, which concentration can be later determined spectrophotometrically at 560 nm (Braunschweig et al., 2012). Fe(II) is extracted

from the sample using HCl (0.5 M) during one hour before first spectrophotometric measurement (to determine Fe(II) ), and then is subsequently extracted with a solution of hydroxylamine hydrochloride to reduce any Fe(III) in solution during another hour prior to a second measurement to determine total content of Fe. The standards used were prepared using $FeSO_4 \cdot 7H_2O$. A typical ferrozine assay of the microcosm samples used in this thesis is shown in figure 3.4.

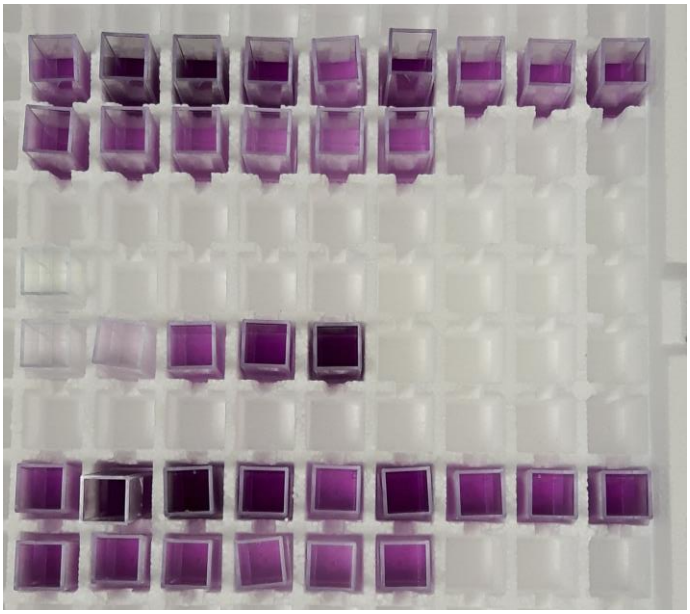

**Figure 3.4.** Detail of a typical ferrozine assay, blank and Fe(II) standards are in the middle rows of the picture.

### 3.6 Inductively coupled plasma atomic emission spectroscopy (ICP-AES) and mass spectroscopy (ICP-MS)

ICP-AES was used to analyse aqueous concentration of Mg and Fe in the microcosm experiments across time. ICP-MS was used for Mn, Co and Ni. In this technique the liquid sample is nebulised to form an aerosol with argon that is passed through a plasma stream where the aerosol evaporates and molecules dissociate producing photons that are quantified later by the spectrometer (Heckel and Dombek, 2009).

Supernatant slurry samples from the microcosm experiments described in section 3.4 were prepared with 2% $HNO_3$. Mg and Fe measurements were carried out on a Perkin-Elmer Optima 5300DV spectrometer, equipped with a concentric glass nebulizer system fitted to a cyclonic

spray chamber, and based on an echelle polychromator with a segmented-array charge-coupled-device detector. Mn, Co and Ni concentrations in solution were analysed using an Agilent Technologies 7700x spectrometer, equipped with a concentric MicroMist nebuliser, a quartz Peltier-cooled Scott-type double pass spray chamber, a 3rd generation Octopole Reaction System (ORS3) and an electron multiplier detector. Sample preparation was done by the author of this thesis, and ICP-AES analysis was done by Mr. Paul Lythgoe.

### 3.7 Ion chromatography (IC)

IC was used to determined organic and inorganic anions in the aqueous phase of the microcosm experiments. Organic molecules included different organic acids or volatile fatty acids (VFAs), and inorganic anions studied were sulphate, nitrate and chloride. As a chromatography technique it is based on an ion exchange separator column where the eluent is introduced, and the ions are retained by the column, and the charge and size of the ions sets the order in which the ions are retained and elute, to be further detected by a conductivity detector (Heckel and Dombek, 2009).

Supernatant slurry aliquots prepared in deionised water from the microcosm samples described in section 3.4 were analysed. Measurements were carried out on an ICS5000 dual channel ion chromatographer equipped with a conductivity detector. One channel incorporated a microbore Dionex AS18 column to determine inorganic anions including chloride, nitrate and sulphate; the other channel was equipped with a IonPac AS11-HC Hydroxide-Selective Anion-Exchange capillary column to determine VFAs as gluconate, lactate, acetate, formate, propionate, iso- and n-butyrate, iso- and n-valerate. VFA data in chapters 5 and 6 is presented as the total VFAs concentration, considered as the molar sum of all the organic acids mentioned before and presented per unit of volume. Samples were prepared by the author of this thesis during monitoring of microcosm experiments, but analysis was performed by Mr. Alastair Bewsher.

### 3.8 Gas chromatography (GC-TCD)

When gas was produced in the microcosm serum bottles the accumulation was easy to observe as bubbles were present inside the bottles generating a positive pressure over the rubber cap

that had to be released every month. Here the samples were taken with a syringe to measure the approximate volume of gas, and later introduced in a vial with argon. GCTCD was used to determine the presence of hydrogen, oxygen, nitrogen and methane. Gas chromatography is also based on a separation column where the gas is retained or not depending on the affinities with the column and the volatility of the sample (Heckel and Dombek, 2009). Samples were prepared by the author of this thesis and analysis was done by Mr. Paul Lythgoe.

Headspace gas produced in the microcosm serum bottles described in section 3.4 was collected using sterile 50 mL syringes and sterile needles, by puncturing the septum and allowing the pressure of the incoming gas to move the piston of the syringe. The gas was transferred to an argon filled vial, leaving the sampling gas to replace the argon in the vial. Gas samples were analysed in an Agilent 7890 Gas Chromatography system equipped with a 7890 Thermal Conductivity Detector (TCD) and a HP Molesieve column 30 m long and 0.53 mm diameter, for the detection of hydrogen, oxygen, nitrogen and methane.

### 3.9 Polymerase Chain Reaction (PCR)

PCR is a method to synthesise a strand of DNA from a template strand and using the DNA polymerase (from *Thermis aquaticus* if TaqDNA polymerase, or from *Pyrococcus furiosus* if PfuDNA polymerase). PCR consists of several consecutive steps (Figure 3.5), starting with the denaturalisation of the DNA template with high temperature, followed by the binding of the primer where the polymerase will start the synthesis. Synthesis is the next step and occurs with the addition of nucleotides and once finished, the last step is the amplification of the new DNA strand by repeating the process (National Center for Biotechnology Information, n.d.). In this research project, PCR was used to amplify the DNA extracted from the soil samples, specifically the 16S rRNA for prokaryotes and ITS2 gene for fungi. The DNA extraction, PCR and further sequencing were performed by Mr. Chris Boothman (University of Manchester).

The PCR amplicons of 16S rRNA were sequenced using the Illumina MiSeq platform (Illumina, San Diego, CA, USA) targeting the V4 hyper variable region (forward primer, 515F, 5′-GTGYCAGCMGCCGCGGTAA-3′; reverse primer, 806R, 5′-GGACTACHVGGGTWTCTAAT-3′)

for 2 × 250-bp paired-end sequencing (Illumina). These primers have been widely tested for Illumina sequencing of 16S rRNA (Caporaso et al., 2012, 2011).

Sequencing of PCR amplicons of the ITS2 region of nuclear ribosomal DNA was conducted with the Illumina MiSeq platform (Illumina, San Diego, CA, USA), targeting the ITS2 internal transcribed spacer region between the large subunit (LSU) and the 5.8S ribosomal genes (forward primer, ITS4F, 5′- AGCCTCCGCTTATTGATATGCTTAART -3′, reverse primer, 5.8SR, 5′- AACTTTYRRCAAYGGATCWCT -3′;). These primers were designed and tested for the Illumina protocol to maximise coverage within Fungi kingdom while minimising nontarget eukaryotes (Taylor et al., 2016).

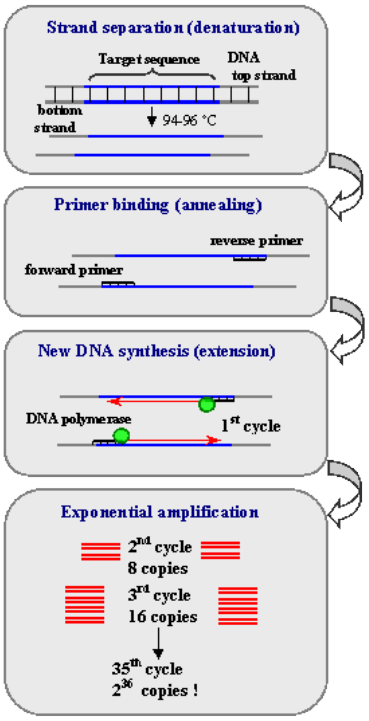


**Figure 3.5.** Polymerase chain reaction (National Center for Biotechnology Information, n.d.).

### 3.10 Statistical analyses

In general, data is reported as an average of three replicates ± standard deviation across the chapters 4, 5 and 6 of this thesis (unless otherwise explained on the text). Different statistical analyses were developed on chapters 4, 5 and 6 using JMP14 statistical software (SAS Institute Inc, 2018), and α=0.05 was used in the statistical tests. In chapter 4, XRF data sets of the bulk

geochemical composition of the soils and rocks from Santa Elena Peninsula were used to test correlations between metals. Moreover, the soil samples were analysed to test if there were differences between the two landscapes observed (mountains and lowlands) in terms of the water content, the pH and total carbon content. ANOVA was done for water content and total carbon content. Wilcoxon test was done for pH because this variable did not fulfil the assumptions of normal distribution nor equal variances (Dytham, 2011). In chapter 4, a linear model was proposed to explain the variation of Ni and Co concentration with altitude. Finally, hierarchical cluster analysis (HC) and principal component analysis (PCA) were performed using the XRF soil geochemical data set and the prokaryotic-fungal OTUs data set to study the relationships between the geographical locations of the samples in terms of those variables. Ward method was used for HC. For PCA, the analysis was performed on the correlation matrix due to the different variances and scales of the variables. The number of components explained ~75% of the total variation of the original variables and were chosen based on the eigenvalues, an individual contribution to the total variation higher than 5% and graphically with the change of slope of the scree plot (Everitt and Hothorn, 2011).

### 3.11 Diversity indices and rarefaction curves

Measuring diversity in microbial communities is challenging for several reasons like using an operational taxonomic unit (OTU) as a way to define a 'microbial species', and also, the much larger size of microbial communities when compared to plant or animal communities, generally resulting in a underrepresented sample of the microbial community (Haegeman et al., 2013). In ecology in general, there are several statistical methods to describe the biodiversity of a community, derived from different theoretical justifications and measuring different assemblages to their calculations. Similarity indices, like the Jaccard or Sørensen indices, are based on presence/absence of species and consider the number of species shared between assemblages, and those that are unique to each assemblage (Chao et al., 2006). Other methods are the Chao estimator, which is an abundance-based estimator of species richness of a community (Haegeman et al., 2013), and the Simpson index and the Shannon index, both considering the species richness (total number of species in the community) and the species evenness of the

community (Figure 3.6A, B) (Hill, 1973). All the indices have strengths and weaknesses, and in a microbiological context the major problem is still associated with the disparity between community and sample; yet they are still widely used to estimate microbial communities using the OTUs as a 'microbial species' definition (Haegeman et al., 2013; Kim et al., 2017; Louis et al., 2016).

Rarefaction curve is a statistical technique where the number of species of a community is plotted as a function of the sample size (Figure 3.6C) (Haegeman et al., 2013), and in a microbiological context can be used to approximate the number of OTUs expected in a random sample of individuals (Kim et al., 2017). In chapters 4, 5 and 6 rarefaction curves were plotted for prokaryotic and fungal communities, using both the Shannon index and the number of OTUs (species richness).

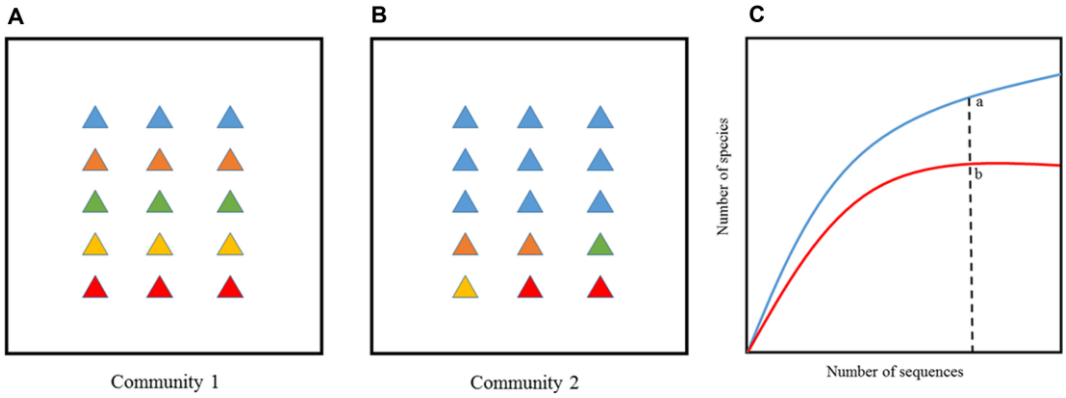


**Figure 3.6.** Graphical description of species richness and evenness. Species richness is the same in community (A) and (B), although (A) is more evenly distributed than (B). (C) Rarefaction curve for (A) and (B) communities, being less diverse the second one (Kim et al., 2017).

### 3.12 References


Braunschweig, J., Bosch, J., Heister, K., Kuebeck, C., Meckenstock, R.U., 2012. Reevaluation of colorimetric iron determination methods commonly used in geomicrobiology. J. Microbiol. Methods 89, 41–48. https://doi.org/10.1016/j.mimet.2012.01.021

CAMECA, n.d. Introduction to Electron Probe Microanalysis (EPMA) [WWW Document]. URL https://www.cameca.com/products/epma/technique (accessed 8.15.19).

Caporaso, J.G., Lauber, C.L., Walters, W.A., Berg-Lyons, D., Huntley, J., Fierer, N., Owens, S.M., Betley, J., Fraser, L., Bauer, M., Gormley, N., Gilbert, J.A., Smith, G., Knight, R., 2012. Ultra-high-throughput microbial community analysis on the Illumina HiSeq and MiSeq platforms. Isme J. 6, 1621. https://doi.org/10.1038/ismej.2012.8

Caporaso, J.G., Lauber, C.L., Walters, W.A., Berg-Lyons, D., Lozupone, C.A., Turnbaugh, P.J., Fierer, N., Knight, R., 2011. Global patterns of 16S rRNA diversity at a depth of millions of sequences per sample. Proc. Natl. Acad. Sci. 108, 4516–4522. https://doi.org/10.1073/PNAS.1000080107

Chao, A., Chazdon, R.L., Colwell, R.K., Shen, T.-J., 2006. Abundance-Based Similarity Indices and Their Estimation When There Are Unseen Species in Samples. Biometrics 62, 361–371. https://doi.org/10.1111/j.1541-0420.2005.00489.x

Dytham, C., 2011. Choosing and using statistics: a biologist's guide, 3rd ed. Wiley-Blackwell, Oxford.

Everitt, B., Hothorn, T., 2011. An introduction to applied multivariate analysis with R. Springer, New York. https://doi.org/10.1007/978-1-4419-9650-3

Haegeman, B., Hamelin, J., Moriarty, J., Neal, P., Dushoff, J., Weitz, J.S., 2013. Robust estimation of microbial diversity in theory and in practice. ISME J. 7, 1092–1101. https://doi.org/10.1038/ismej.2013.10

Heckel, P., Dombek, T., 2009. Chapter 9 - Monitoring Inorganic Compounds, in: Ahuja, S.B.T.-H. of W.P. and Q. (Ed.), . Academic Press, Amsterdam, pp. 197–212. https://doi.org/10.1016/B978-0-12-374192-9.00009-1

Hill, M.O., 1973. Diversity and Evenness: A Unifying Notation and Its Consequences. Ecology 54, 427–432. https://doi.org/10.2307/1934352

HITACHI, n.d. Principle of XRF Analysis : Hitachi High-Technologies GLOBAL [WWW Document]. URL https://www.hitachi-hightech.com/global/products/science/tech/ana/xrf/descriptions/ (accessed 8.15.19).

International Union of Crystallography, 1999. (IUCr) Chapter 6. The principles of X-ray diffraction [WWW Document]. URL https://www.iucr.org/publ/50yearsofxraydiffraction/full-text/principles (accessed 8.15.19).

Kim, B.-R., Shin, J., Guevarra, R.B., Lee, J.H., Kim, D.W., Seol, K.-H., Lee, J.-H., Kim, H.B., Isaacson, R.E., 2017. Deciphering Diversity Indices for a Better Understanding of Microbial Communities. J. Microbiol. Biotechnol. 27, 2089–2093. https://doi.org/10.4014/jmb.1709.09027

Louis, B.P., Maron, P.-A., Menasseri-Aubry, S., Sarr, A., Lévêque, J., Mathieu, O., Jolivet, C., Leterme, P., Viaud, V., 2016. Microbial Diversity Indexes Can Explain Soil Carbon Dynamics as a Function of Carbon Source. PLoS One 11, e0161251. https://doi.org/10.1371/journal.pone.0161251

Lovley, D.R., Phillips, E.J.P., 1986. Organic Matter Mineralization with Reduction of Ferric Iron in Anaerobic Sediments. Appl. Envir. Microbiol. 51, 683–689.

National Center for Biotechnology Information, n.d. Polymerase Chain Reaction (PCR) [WWW Document]. URL https://www.ncbi.nlm.nih.gov/probe/docs/techpcr/ (accessed 8.15.19).

SAS Institute Inc, 2018. JMP.

Taylor, D.L., Walters, W.A., Lennon, N.J., Bochicchio, J., Krohn, A., Caporaso, J.G., Pennanen, T., 2016. Accurate Estimation of Fungal Diversity and Abundance through Improved Lineage-Specific Primers Optimized for Illumina Amplicon Sequencing. Appl. Environ. Microbiol. 82, 7217–7226. https://doi.org/10.1128/AEM.02576-16

Wilkins, M.J., Livens, F.R., Vaughan, D.J., Beadle, I., Lloyd, J.R., 2007. The influence of microbial redox cycling on radionuclide mobility in the subsurface at a low-level radioactive waste storage site. Geobiology 5, 293–301. https://doi.org/10.1111/j.1472-4669.2007.00101.x

# Chapter 4. Geochemistry and microbiology of lateritic soils from the Santa Elena Ophiolite, a geographical-landscape approach

---

Agustín F. Solano-Arguedas[a*], Christopher Boothman[a], Laura Newsome[ab], Richard A.D. Pattrick[a], Daniel Arguedas-Quesada[c], Clare H. Robinson[a] and Jonathan R. Lloyd[a]

[a] Williamson Research Centre, School of Earth and Environmental Sciences, University of Manchester, Manchester, M13 9PL, United Kingdom

[b] Camborne School of Mines and Environment and Sustainability Institute, University of Exeter, Penryn, Cornwall, TR10 9FE, United Kingdom

[c] Verdiazul Sumate al Cambio, Playa Junquillal de Santa Cruz, Guanacaste, Costa Rica

[*] Corresponding author: agustin.solanoarguedas@postgrad.manchester.ac.uk

## 4.1 Abstract

The Santa Elena Ophiolite in the north-west of Costa Rica is an ultramafic system comprised mainly of peridotites, exposed to active lateritization processes accelerated by the tropical climatic conditions of the region. However, despite their well-studied geology, the resulting lateritic soils are still poorly understood both in their geochemical composition and in the microbial communities that they host. The aim of this study was to characterise these two interlinked factors, relating them to contrasting landscapes in the region and their characteristic soil types and vegetation cover. The soils were confirmed as Ni-rich lateritic soils but as expected, they showed a differentiation depending on their geographical location within the ophiolite area, both in their geochemistry and in their microbiology. Three main lateritic soil types were identified within the Santa Elena Ophiolite area considering geographical/biogeochemical characteristics: *mountain* soils, *inner ophiolite lowland* soils and *north lowland* soils. Towards the mountains, altitude-related factors influenced weathering processes, resulting in soils dominated by lizardite and iron oxides and richer in iron and trace metals as cobalt, manganese and nickel, the latter even with levels comparable to nickel ore laterites. The lowlands, although sharing similar landscapes, showed

variations in their geochemistry, separating those from the northern boundaries of the ophiolite from those inside the ophiolite area that were closer to the mountain soils. Amongst the last group, within the same riparian basin, concentrations of trace metals were higher downstream towards the mangrove areas of Potrero Grande. Microbial communities showed a similar separation across the locations sampled, with iron redox cycling bacteria more abundant in the mountain soils and fungal groups restricted to these areas, while manganese-oxidising bacteria were more abundant in the lowlands, with the highest relative abundance in the mangrove areas. To our knowledge this is the first detailed description of the mineralogy and the geochemistry of these soils, and also the first report of the microbial communities in the lateritic soils of Santa Elena Peninsula. The biotic-abiotic associations recorded in these actively-forming lateritic soils, underpinning its potential as a hotspot for serpentinization endemism, make the Santa Elena Peninsula a model area to study the geomicrobiology and ecology of serpentine ecosystems undergone tropical conditions.

**Keywords:** Mineralogy, serpentinite, nickel-laterite, prokaryotes, fungi, geomicrobiology.

**Highlights:**

The geomicrobiological evolution of geographically distinct lateritic soils from the Santa Elena Ophiolite of Costa Rica was analysed.

Mountain soils were richer in Fe, Ni and Co and abundant in Fe-redox cycling bacteria.

Lowland soils differed geochemically between the north and the inner area of the ophiolite.

Mangrove soils downstream in the Potrero Grande basin acted as a metal-sink.

Mn-oxidising bacteria were more abundant in the mangrove lowland soils.

## 4.2 Introduction

The peninsula of Santa Elena is on the north-western Pacific coast of Costa Rica within the Area of Conservation Guanacaste, and has a rugged topography including several mountain ranges (elevation >700 m) and small riparian basins. The majority of the peninsula is composed of the Santa Elena Ophiolite, one of the oceanic complexes found along the Pacific coast of Costa Rica,

formed as a result of accretionary processes during the Upper Cretaceous (Denyer and Gazel, 2009; Madrigal et al., 2015). The Santa Elena Ophiolite is composed mainly of ultramafic serpentinized peridotites (lherzolites, harzburgites and dunites) in association with mafic lithologies such as gabbros, diabases and basalts (Denyer and Gazel, 2009; Madrigal et al., 2015; Schwarzenbach et al., 2016; Whattam et al., 2016).

In the tropical and sub-tropical zones, the weathering of ultramafic rocks exposed to annual precipitation of over 1000 mm and seasonal temperatures ranges between 15-33°C, leads to development of nickeliferous laterites (Roberts and Gunn, 2014; Thorne et al., 2012). Such climatic conditions prevail in the peninsula of Santa Elena, a tropical region mostly dry to sub-humid where the average annual temperature during the day is 33°C and 22°C at night, and the average annual precipitation is 1528 mm. There is a marked dry-wet seasonality where only 5% of the precipitation occurs during the dry season (December-mid May)(Herrera, 2016; Instituto Meteorológico Nacional, n.d.; Jiménez M. et al., 2016) and thus the Santa Elena Peninsula is an active area of lateritic soil formation.

The dominant soil type covering the Santa Elena Ophiolite is defined as a lateritic Lithic Ustorthent and its distribution on the Santa Elena Peninsula closely corresponds to the area underlain by the peridotite (harzburgite) (Figure 4.4.1A, B) (Medina, 1999b, 1999c). The soil has a thin regolith layer but can be characterised as a laterite due to its oxidised and clayey mineralogy and its water retention capacity (Alvarado et al., 2011; Soil Survey Staff, 2014). Recently developed fluvial and alluvial deposits (Quaternary) are found associated with the rivers on the south-centre of the peninsula (as Potrero Grande River) and on the northern margin of the ophiolite (Figure 4.1B), resulting in soils of fluvial origin (Fluventic Ustropept) and alluvial and colluvial origins sourced from the surrounding mountains (Ustic Dystropept) (Madrigal et al., 2015; Medina, 1999b).

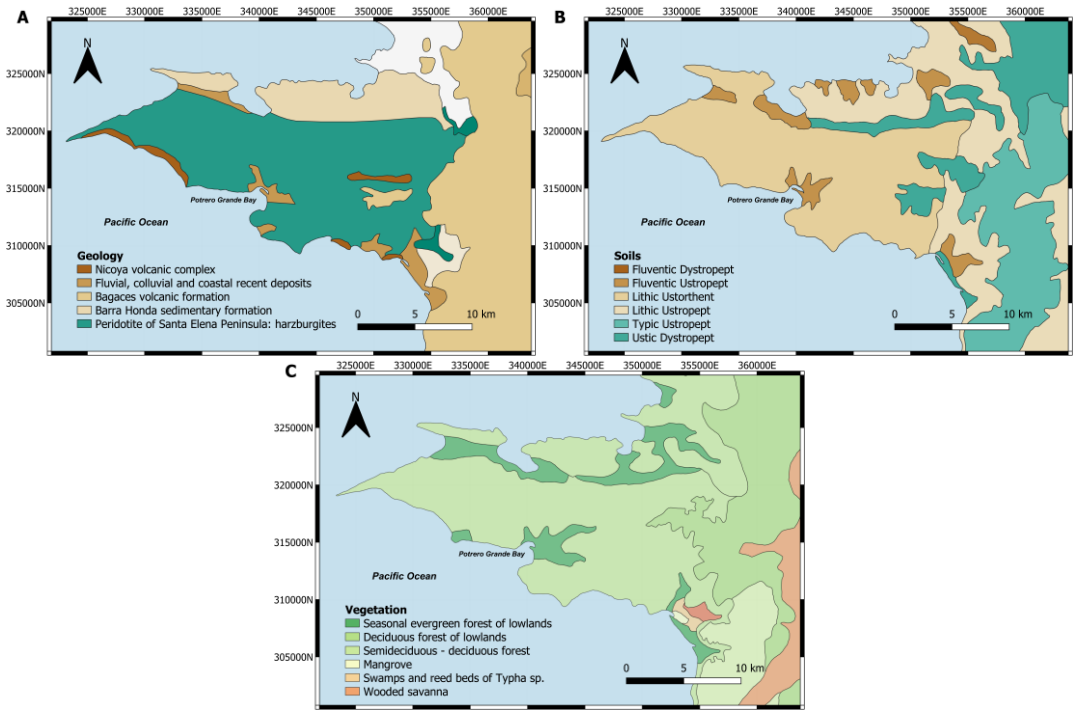


**Figure 4.1.** Maps of the geology (A), soils (B) and vegetation (C) in the Santa Elena Peninsula. Only the relevant colours are labelled. Adapted, respectively, from Medina (1999a, 1999b, 1999c).

The predominant vegetation macrotype along the peninsula is a semi-deciduous/deciduous forest, with its distribution closely related to the area of the Santa Elena Ophiolite (Figure 4.1C). However, the composition changes with the topography of the peninsula; it is dominated by xerophytic shrubs and herbaceous vegetation in the exposed areas or the mountain tops, and in the lower altitudes or near water courses a semi-deciduous/deciduous and/or evergreen vegetation is present. In the alluvia of the Potrero Grande River and across other rivers in the north of the Peninsula, the vegetation changes completely to a seasonal evergreen lowland forest (Gómez and Herrera, 1986; Jiménez M. et al., 2016). The resulting landscape in the Santa Elena Peninsula overlying the ophiolite area can thus be separated into a predominant *mountain* landscape with scarce shrubby vegetation, closely related to the lateritic soils, and the *lowland* landscape with more complex vegetation and alluvial soil deposits (Figure 4.2).

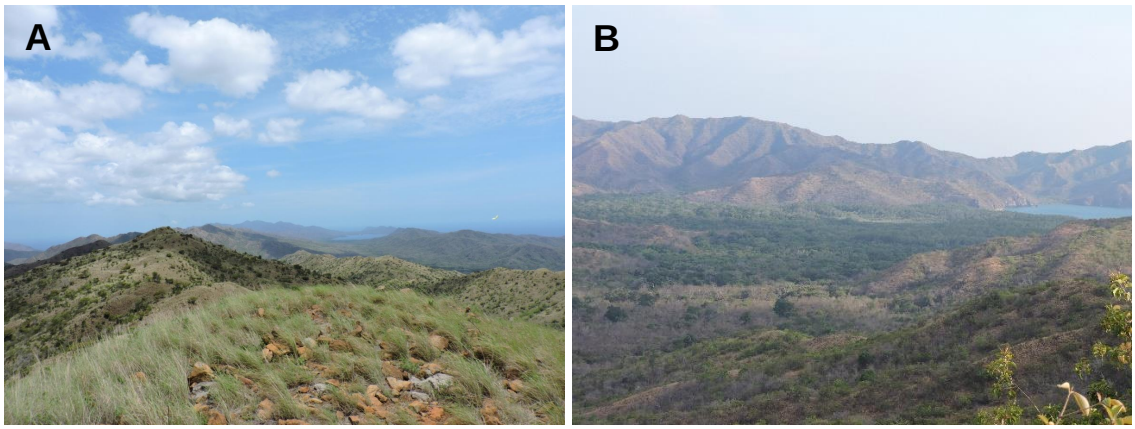


**Figure 4.2.** Characteristic landscapes in the Santa Elena Peninsula. (A) In the *mountains* such as Cerro el Inglés, the hilltops and the upper sections of the hills show a semi-deciduous/deciduous forest with scarce and low-stature trees and dominated (foreground) by grasses (Poaceae) with areas of exposed soils. (B) In the *lowlands* such as in Potrero Grande Basin (centre), the deciduous forest is denser and changes to an evergreen forest in some areas; the *mountain* landscape can be seen in the foreground and background.

Lateritic soils have higher concentrations of metals including cobalt and nickel than their parental rocks as a result of weathering processes. Depending on metal concentrations and the minerals present, laterites can be economically viable, for example nickel laterites are the source of 40% of global Ni production and 20-30% of Co (Butt and Cluzel, 2013; Roberts and Gunn, 2014; Thorne et al., 2012). Bioprocessing of laterites has been studied as either an alternative method of extraction from low-grade deposits of cobalt and nickel or to re-process waste materials from mining operations. This extraction process has been examined using model acidophilic Fe(III)-reducing bacteria fungi such as *Aspergillus* sp. and *Penicillium* sp. (Gadd et al., 2014; Hallberg et al., 2011; Johnson and du Plessis, 2015; Marrero et al., 2017). However, the indigenous microorganisms in lateritic soils and their natural geochemical association are poorly defined.

In the Santa Elena Peninsula, reports of Co, Ni and other metals associated with the laterites are very limited and research has focussed on the ultramafic source rocks; in previous references to soils or sediments the geographical distribution of the samples was not clear or involved a small area of the peninsula (Denyer and Gazel, 2009; Gazel et al., 2006; Madrigal et al., 2015; Marín Guzmán, 1985; Reeves et al., 2007). Additionally, the peninsula is protected as a National Park within an area declared as a World Heritage by UNESCO due to its significance in developing

ecological and biological processes where ore exploitation is prohibited. Nonetheless the Santa Elena Peninsula is a unique area to study the natural conditions underlying the active formation of lateritic soils and developing an understanding of both the geochemical processes and the associated microbial communities. This fundamental work could also help inform future bioprocessing work at other sites.

The aim of this study was to characterise the geochemistry of the lateritic soils in the Santa Elena Peninsula and the associated microbial communities, using a landscape and geographical location approach. Here we describe the mineralogy and the geochemical composition of the soils from ten different locations within the area of the Santa Elena Ophiolite. For a better understanding of the lateritic soil system overall, the geochemistry of serpentinite rocks prior to regolith formation was also determined. The composition of the prokaryotic and fungal communities in the same samples were also characterised. To our knowledge this is the first report of both the geochemistry and microbiology of the lateritic soils associated with the Santa Elena Ophiolite, and we extend this work to consider our data in the context of different landscapes, soil types, topographies and the geographical location within the ophiolite area, resulting in the first multidisciplinary study of its type.

## 4.3 Material and methods

### 4.3.1 Sampling

Samples were collected in the Santa Elena Peninsula, Costa Rica, within the National Park Santa Rosa of the Area de Conservación Guanacaste (ACG), during the dry seasons of 2016 (May) and 2017 (April). Ten locations along the Peninsula were chosen, including five sites from mountain landscapes and five from lowlands (Figure 4.3, Table 4.1). In each site, a sampling area of 5x5 m was traced wherein 3 randomly distributed (replicate) sections were taken at a depth of 10-15 cm. For each sample, the soil from the surface was carefully removed. When the depth was achieved, between 1 and 1.5 kg of soil at the same depth was extracted and stored into a re-sealable plastic bag at 4°C. Large rock fragments (>5 cm) or large roots were separated from the sample. Serpentinite rocks found loose at the same depth (representing weathered protolith)

within the soil sampling areas were also collected. Additionally, relatively unweathered rocks were collected from outcrops as close to the sampling locations as possible.

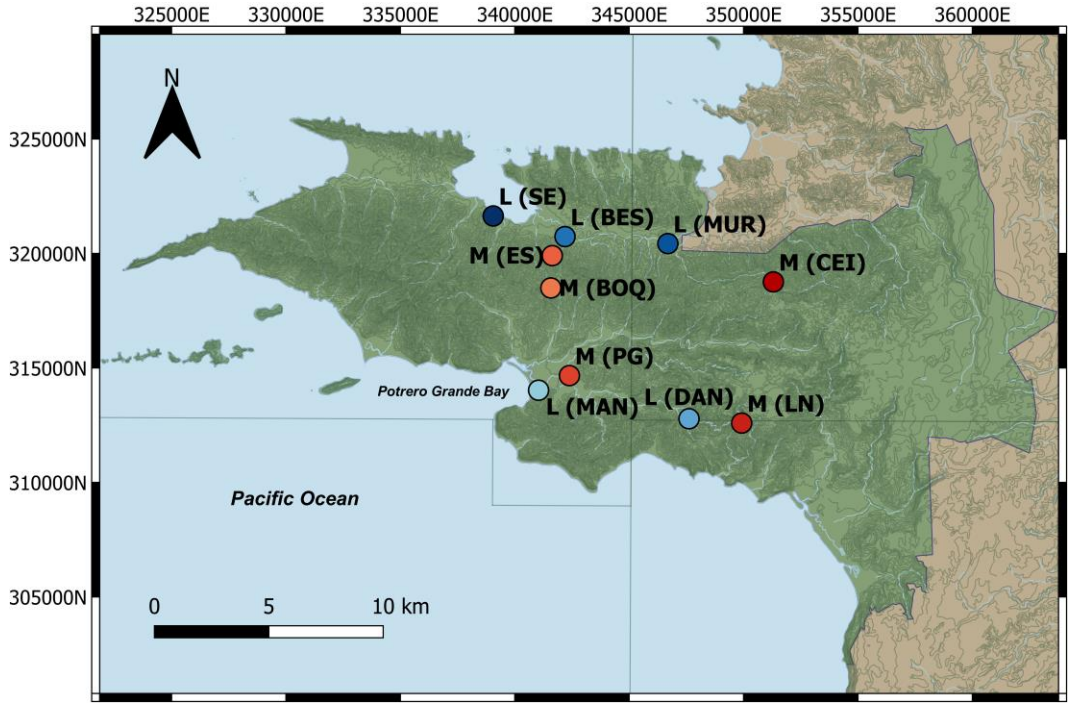


**Figure 4.3.** Geographical distribution of the 10 locations sampled within the Santa Elena Peninsula (green area: National Park Santa Rosa). Mountain (M) landscapes are in red-to-orange colours and lowland (L) landscapes in light-to-dark blue (see labels in Table 4.1).

**Table 4.1.** Summary of the locations sampled within the Santa Elena Peninsula and their main characteristics. Letters in brackets in first column correspond to photographs shown in Figure 4.4.

| Location | Coordinates | Altitude | Vegetation* | Soil type* | Geology* | Topography |
|---|---|---|---|---|---|---|
| Mountain (CEI) (A) | N10° 53.198' W85° 41.490' | 495 m | Grass only but scarce, with patches of exposed soils | Entisol (Lithic ustorthent) | Ophiolite | Near the top of a hill (Cerro el Inglés) |
| Mountain (LN) (B) | N10° 49.849' W85° 42.236' | 309 m | Grass only but scarce, with exposed soils | Entisol (Lithic ustorthent) | Ophiolite | Top of a hill, small terrace. |
| Mountain (PG) (C) | N10° 50.957' W85° 46.372' | 17 m | Semi-deciduous/ deciduous forest mixed with grass | Entisol (Lithic ustorthent) | Ophiolite | Lower side of a hill, near Potrero Grande (PG) river |

| Location | Coordinates | Altitude | Vegetation* | Soil type* | Geology* | Topography |
|---|---|---|---|---|---|---|
| Mountain (ES) (D) | N10° 53.797' W85° 46.796' | 197 m | Grass dominated, Semi-deciduous/ deciduous forest | Entisol (Lithic ustorthent) | Ophiolite | Top of a hill (El Silencio road) |
| Mountain (BOQ) (E) | N10° 53.030' W85° 46.826' | 269 m | Grass dominated, Semi-deciduous/ deciduous forest | Entisol (Lithic ustorthent) | Ophiolite | Top of a hill (Loma Boquerones) |
| Lowland (DAN) (F) | N10° 49.947' W85° 43.499' | 69 m | Semi-deciduous/ deciduous forest, no grass present | Entisol (Lithic ustorthent) | Ophiolite | River terrace surrounded by steep hills, ~10 km upstream from MAN location. |
| Lowland (MAN) (G) | N10° 50.606' W85° 47.110' | -4 m | Seasonal evergreen forest of lowlands, no grass present | Inceptisol (Fluventic ustropept) | Sedimentary deposits | Flat area between the base of a hill and the mangrove flooded area, close to PG river mouth |
| Lowland (BES) (H) | N10° 54.249' W85° 46.493' | 18 m | Seasonal evergreen forest of lowlands no grass present | Inceptisol (Ustic dystropept) | Ophiolite (close to the margin) | Flat area on a river valley, close to a river, base of the ES hills |
| Lowland (MUR) (I) | N10° 54.094' W85° 44.025' | 52 m | Seasonal evergreen forest of lowlands no grass present | Inceptisol (Ustic dystropept) | Ophiolite (close to the margin) | Small terrace, close to a creek in Murciélago sector, lower side of a small hill |
| Lowland (SE) (J) | N10° 54.730' W85° 48.217' | 25 m | Seasonal evergreen forest of lowlands, no grass present | Inceptisol (Fluventic ustropept) | Sedimentary deposits/ Ophiolite (margin) | Lower side of a hill, on a very steep area. |

* The vegetation, soil type and geology classifications are based on vegetation, soils, and geology maps of ACG (Medina, 2014). (For details of the sampling points see Figure 4.S1).


**Figure 4.4**. Detail of the locations sampled within the Santa Elena Peninsula. Mountain (M) landscapes were: CEI (A), LN (B), PG (C), ES (D), BOQ (E); while lowlands (L) samples were collected in DAN (F), MAN (G), BES (H), MUR (I) and SE (J).

### 4.3.2 Geochemical characterisation

Prior to bulk geochemical characterisation, rock samples were ground into fine powder using a Tema® mill (tungsten), while soil samples were dried at 105°C prior to grinding. Approximately 20 g of each soil sample were weighed and heated at 105 °C for 24 h. They were weighed again once cooled and the water content was calculated as a percentage of the mass lost. Additionally, the pH of the soils was measured with 10 g of fresh sample in 10 mL of deionised water, stirred and left to stand and settle for 1 h before measuring the pH (Allen, 1989).

#### 4.3.2.1 X-ray diffraction spectroscopy (XRD)

For both rock powder and soil samples, measurements were carried out on a Bruker D8 Advance diffractometer, equipped with a Göbel Mirror, a Lynxeye detector and a copper X-ray tube, providing $CuK_{\alpha 1}$ X-rays with a wavelength of 1.5406 Å. Samples were scanned from 5-70$^{o}$ 2θ, with a step size of 0.02$^{o}$ and a count time of 0.2 s per step. The resulting patterns were evaluated using EVA version 4 software, which compares experimental data to standard XRD patterns of minerals from the ICDD (International Centre for Diffraction Data) Database.

#### 4.3.2.2 X-ray fluorescence spectroscopy (XRF)

For both rock powder and soil samples, measurements were carried out on an Axios Panalytical XRF spectrometer equipped with a Rh X-ray source. Samples were scanned, identifying both major (*Omnian program*) and trace elements (*Pro-Trace program*). Sample preparation involved 12 g of dry sample and 3 g of Hoechst Wax™ ground together in an agate ball mill and then pressed into a pellet with a pneumatic press. The total carbon content in the samples was also calculated by loss on ignition (LOI), weighing exactly 1.000 g of sample and determining the mass after heating first at 105 °C for 1 h and then at 1000°C for 1 h.

#### 4.3.2.3 Petrographic examination, and electron probe micro analysis (EPMA)

Polished thin sections (30 µm) of rock samples were prepared using standard techniques. Petrographic analysis was undertaken using a Nikon Eclipse LV100NPOL petrographic microscope equipped with a Nikon DS-Fi2 camera and DS-U3 camera control software. Mineral and textural analysis was undertaken and phases suitable for EPMA identified. The polished thin sections were carbon coated prior to EPMA. EPMA was carried out using a Cameca SX100

electron probe microanalyser equipped with 5 wavelength dispersive spectrometers (WDS). Elemental distribution maps were created for Fe, Mg, Si, Al, Cr, Mn, Co, Ni, Ca, Ti, Cl, K, Na and S, and points were analysed at 20 kV, 5 nA with a 10 µm beam using the standards fayalite (Fe), periclase (Mg), anorthite (Si, Al), $Cr_2O_3$, tephrolite (Mn), Co-metal, NiO, wollastonite (Ca), rutile (Ti), sodalite (Cl), orthoclase (K), jadeite (Na) and pyrite (S).

#### 4.3.2.4 Mapping and statistical analyses

The processing of map data was done using QGIS 3.10.0 A Coruña software (QGIS Development Team, 2019). GIS layers were taken from the ACG GIS-maps database (Medina, 2014) and Costa Rica Lambert Norte was used as the coordinate reference system. Statistical analyses on XRF data sets were developed with JMP14 statistical software (SAS Institute Inc, 2018). For ANOVA and Wilcoxon tests and for correlations, $\alpha=0.05$ was considered appropriate. Hierarchical cluster analysis (HC) and principal component analysis (PCA) were also performed.

### 4.3.3 Microbial community analysis

#### 4.3.3.1 DNA extraction

One replicate core from every location was chosen, and DNA was extracted from 200 µl of sediment slurry using a DNeasy PowerLyzer PowerSoil Kit (Qiagen, Manchester, U.K). 16S rRNA genes were amplified via PCR (polymerase chain reaction) using 8F (5'-AGAGTTTGATCCTGGCTCAG-3'), and 1492R (5'-TACGGYTACCTTGTTACGACTT-3')(Lane, 1991). Following amplification via PCR, the DNA was stained with SYBR Safe DNA Gel Stain (Thermo Fisher Scientific) before placement in an agarose gel, where it was subsequently separated using electrophoresis. The stained DNA was viewed under UV light, and target ~1500 base pair products were identified by comparison to a ladder of DNA fragments of varying lengths.

#### 4.3.3.2 Prokaryotic community analysis

The PCR amplicons of 16S rRNA were sequenced using the Illumina MiSeq platform (Illumina, San Diego, CA, USA) targeting the V4 hyper variable region (forward primer, 515F, 5′-GTGYCAGCMGCCGCGGTAA-3′; reverse primer, 806R, 5′-GGACTACHVGGGTWTCTAAT-3′) for 2 × 250-bp paired-end sequencing (Illumina) (Caporaso et al., 2012, 2011). PCR amplification was performed using Roche FastStart High Fidelity PCR System (Roche Diagnostics Ltd,

Burgess Hill, UK) in 50 µl reactions under the following conditions: initial denaturation at 95°C for 2 min, followed by 36 cycles of 95°C for 30 s, 55°C for 30 s, 72°C for 1 min, and a final extension step of 5 min at 72°C. The PCR products were purified and normalised to ~20 ng each using the SequalPrep Normalization Kit (Fisher Scientific, Loughborough, UK). The PCR amplicons from all samples were pooled in equimolar ratios. The run was performed using a 4 pM sample library spiked with 4 pM PhiX to a final concentration of 10% following the method of Schloss and Kozich (Kozich et al., 2013).

Raw sequences for prokaryotes were divided into samples by barcodes (up to one mismatch was permitted) using a sequencing pipeline. Quality control and trimming was performed using Cutadapt (Martin, 2011), FastQC (Babraham Bioinformatics, n.d.), and Sickle (Joshi and Fass, 2011). MiSeq error correction was performed using SPADes (Nurk et al., 2013). Forward and reverse reads were incorporated into full-length sequences with Pandaseq (Masella et al., 2012). Chimeras were removed using ChimeraSlayer (Haas et al., 2011), and operational taxonomic units (OTUs) were generated with UPARSE (Edgar, 2013). OTUs were classified by Usearch (Edgar, 2010) at the 97% similarity level, and singletons were removed. Rarefaction analysis was conducted using the original detected OTUs in Qiime (Caporaso et al., 2010). The taxonomic assignment was performed by the RDP classifier (Wang et al., 2007).

#### 4.3.3.2 Fungal community analysis

Sequencing of PCR amplicons of the ITS2 region of nuclear ribosomal DNA was conducted with the Illumina MiSeq platform (Illumina, San Diego, CA, USA), targeting the ITS2 internal transcribed spacer region between the large subunit (LSU) and the 5.8S ribosomal genes (forward primer, ITS4F, 5′- AGCCTCCGCTTATTGATATGCTTAART -3′, reverse primer, 5.8SR, 5′-AACTTTYRRCAAYGGATCWCT -3′;) (Taylor et al., 2016) for 2 × 300-bp paired-end sequencing (Illumina) (Caporaso et al., 2012, 2011). PCR amplification was performed using Roche FastStart High Fidelity PCR System (Roche Diagnostics Ltd, Burgess Hill, UK) in 50 µl reactions under the following conditions: initial denaturation at 95°C for 2 min, followed by 36 cycles of 95°C for 30 s, 56°C for 45 s, 72°C for 2 min, and a final extension step of 5 min at 72°C. The PCR products were purified and normalised to ~20 ng each using the SequalPrep Normalization Kit (Fisher Scientific, Loughborough, UK). The PCR amplicons from all samples were pooled in equimolar ratios. The

run was performed using a 10 pM sample library spiked with 10 pM PhiX to a final concentration of 10% following the method of Schloss and Kozich (Kozich et al., 2013).

The ITS sequencing data produced by the Miseq platform was analysed using the PIPITS automated pipeline (Gweon et al., 2015). Chimeras were removed by reference based chimera detection using UCHIME (Edgar et al., 2011) in conjunction with the UNITE UCHIME reference data set. The taxonomic assignment was performed by the RDP classifier (Wang et al., 2007) using the UNITE fungal ITS reference data set.

## 4.4 Results and Discussion

### 4.4.1 Geochemical characterisation of rocks

Serpentinite clasts within the regolith at 10 cm depth were analysed to determine the geochemistry and mineral composition of the parent rock for the lateritic soils. Bulk geochemical composition of all the rock samples were determined by XRF (Figure 4.5). Co showed a strong positive correlation with Mn ($r=0.8765$, $p<0.0001$) and Ni ($r=0.8530$, $p<0.0001$), to a lesser degree to Fe ($r=0.5959$, $p=0.0071$), and Cr ($r=0.4655$, $p=0.0438$). Mn was correlated to Fe ($r=0.5112$, $p=0.0253$) similarly than Co, while Cr and Ni showed a closer association with Fe ($r=0.8428$, $p<0.0001$; $r=0.7790$, $p<0.0001$, respectively). Cr was also positively correlated with Al ($r=0.7139$, $p=0.0006$) (Table 4.S1, Figure 4.S2). Moreover, Fe, Ni and Cr had a similar inverse correlation with Mg close to $r=-0.6$; the same as with Si although only Fe was significantly negative correlated ($r=-0.4802$, $p<0.0375$) (Table 4.S1, Figure 4.S2).

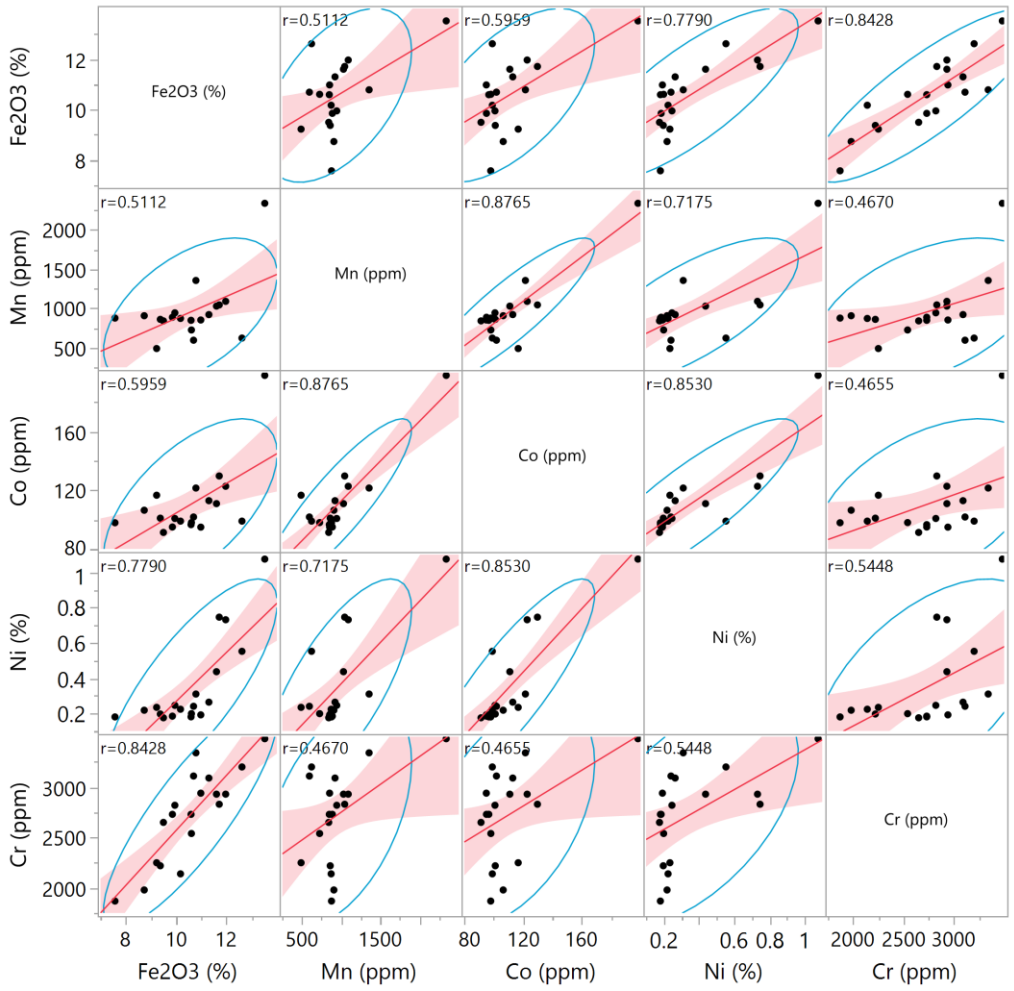


**Figure 4.5.** Bulk elemental correlations in serpentinites of the Santa Elena Peninsula for $Fe_2O_3$, Mn, Co, Ni, and Cr determined by XRF. All the rock samples collected were analysed and these elements all show a positive correlation between them ($p<0.05$; Density ellipses $\alpha=95\%$). Full details of the correlation matrix, including Al, Si and Mg and all the correlations and probabilities associated are shown in Table 4.S1 and Figure 4.S2.

XRD (Figure 4.6) revealed the bulk mineralogy of these rocks to mainly comprise the serpentine-group mineral lizardite [$Mg_3Si_2O_5(OH)_4$] irrespective of geomorphological location and soil type. Despite the high degree of serpentinization, minerals of the parental peridotite, notably forsteritic olivine [$(Mg,Fe)Si_2O_4$] and enstatite [$MgSiO_3$] were present in different amounts in the bulk mineralogy; the clinopyroxenes augite [$(Ca,Na)(Mg,Fe,Al,Ti)(Si,Al)_2O_6$] and diopside [$(Ca,Mg,Fe)SiO_3$] were also present to a lesser extent. This confirmed the peridotitic nature of the parent rock and the presence of extensive lizardite and olivine, along with enstatite as the predominant pyroxene, suggest a harzburgite protolith. Clinochlore [$(Mg,Fe)_5Al_2Si_3O_{10}(OH)_8$] was

also present in minor proportions. Rocks collected from superficial (transported) deposits close to the sampling locations revealed the same mineral suite but with a greater concentration of forsterite in some cases and the absence of clinochlore.

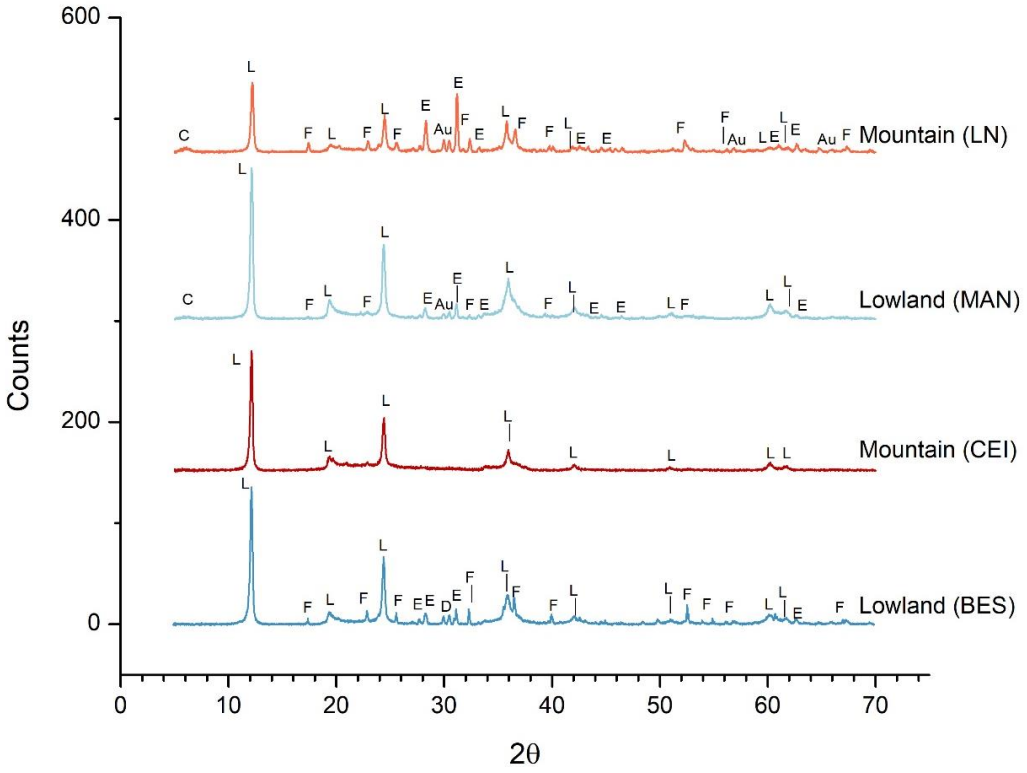


**Figure 4.6.** Bulk mineralogy of rock clasts from the soils (10 cm depth) of the Santa Elena Peninsula. Main minerals found with XRD were: Lizardite (L), Enstatite (E), Forsterite (F), Augite (Au), Diopside (D) and Clinochlore (C). The samples shown (LN and MAN) are representative of all the rocks collected in both Mountain and Lowland areas and from the superficial outcrops (CEI and BES) close to sampling locations.

The petrographic data confirmed a very high degree of serpentinization of the rocks from mountain locations (Figure 4.7A) with pervasive lizardite surrounding relict ferromagnesian minerals; the resistate mineral, a ferrite spinel was also identified, likely to be a ferrite chrome spinel [$(Mg,Fe)(Al,Cr)_2O_4$] due to the positive Fe:Cr correlation (Figure 4.5). The *in situ* physical and chemical weathering of the parent peridotite to produce the mountain soils was found to be more intense than that observed in the lowland soils. In the latter, a higher proportion of relict olivine and pyroxene was observed although they were still dominated by serpentine minerals (lizardite) (Figure 4.7B) suggesting that the rock clasts in these lowland colluvial and alluvial

deposits will have been brought in by erosion and have had less exposure to the more intense weathering processes in the mountain areas. In rock samples collected from outcrops close to the soil sampling locations, the proportion of the peridotite parental minerals, olivine and pyroxene, to serpentine minerals was much greater than in the soil-hosted clasts (Figure 4.7C,D).

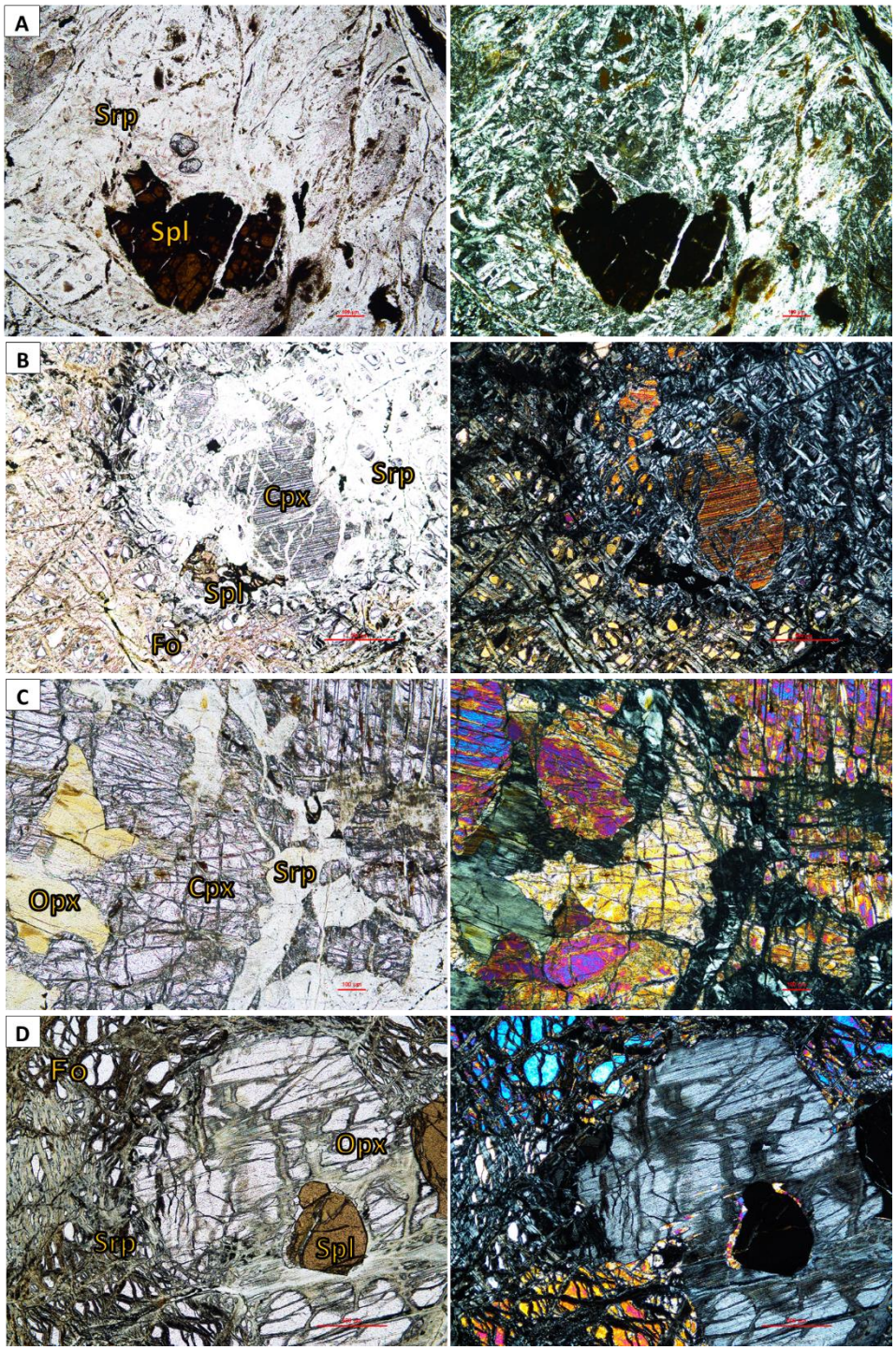


**Figure 4.7.** Photomicrographs from polished thin sections of representative serpentinite rocks from Santa Elena Peninsula under plane-polarized light (left) and crossed polars (right). Rock

clasts from within the soil collected at 10 cm depth from (A) the Mountain LN and (B) Lowland MAN sites. (C) Rocks from outcrops close to Mountain CEI and (D) Lowland BES site. Cpx: clinopyroxene, Fo: forsterite, Ol: olivine, Opx: orthopyroxene, Srp: serpentine, Spl: spinel. Scale 100µm (A,C), 500 µm (B,D).

The elemental distribution maps (Figures 4.8, 4.S3-S5) produced from the polished thin sections of the serpentinite clasts from the soils (Figure 4.7A, B) and of the serpentinized peridotites from outcrops (Figure 4.7C, D) supported correlations observed in the bulk geochemistry and mineralogy. Olivine was confirmed as forsterite (MgO: 48.8 ± 0.3 %, FeO: 9.5 ± 0.1 %, $SiO_2$: 40.3 ± 0.1 %) regardless of rock type (Figures 4.S3-S5), and lizardite covered a major proportion of Mg and Si in the serpentinite clasts (Figure 4.8 and 4.S3) and in the peridotites from outcrops to a lesser extent. Fe was ubiquitous in all minerals although concentrated in Fe oxide veinlets, and in the spinel minerals. Cr, and especially Al were co-located in the spinel with Fe and Mg, confirming the identification of this phase as a hercynite [$(Fe,Mg)(Al,Cr)_2O_4$.], also reflected in the positive correlations in the bulk geochemistry (Figure 4.5 and 4.S2), but with differences between locations. In the serpentinite clast of the mountain location LN (Figure 4.7A) was a Cr-rich hercynite (MgO: 12.8 ± 1.4 %, FeO: 19.6 ± 0.9 %, $Al_2O_3$: 30.1 ± 4.8 %, $Cr_2O_3$: 33.9 ± 5.2 %) (Figure 4.8), but in the serpentinite clast from the lowland MAN (Figure 4.7B) was an Al-rich hercynite (Figure 4.S3), same as in the peridotites from outcrops (MgO: 15.5 ± 0.1 %, FeO: 11.5 ± 0.1 %, $Al_2O_3$: 53.9 ± 0.3 %, $Cr_2O_3$: 15.5 ± 0.2 %) (Figure 4.7D, 4.S5).

Co was very strongly associated with Fe but mostly restricted to Fe-oxide veinlets and spinel minerals, with concentrations ranging from 0.016 wt% to 0.044 wt% in the spinels and slightly higher in the Fe-veinlets (Figures 4.8, 4.S3-S5); Mn had a similar association with Fe, although present in all minerals. Remarkably, in the spinel minerals Mn was more concentrated in the Cr-rich hercynite of the serpentinite clast from the mountain LN (0.245 ± 0.030 wt%) (Figure 4.8) than in the Al-rich hercynite from the lowland serpentinite and from the peridotites from outcrops (0.126 ± 0.016 wt%) (Figure 4.S3-S5). Both Co and Mn trends with Fe were also supported by their positive bulk elemental correlation (Figure 4.5). Ni was associated with serpentine and olivine areas with concentrations ranging from 0.2 wt% to 0.3 wt%, but was also present in spinels in similar concentration. However, in highly weathered serpentinite clasts as in Mountain LN, Ni was concentrated in Fe oxide veinlets and lower Al regions of the lizardite rather than in the spinels

(Figure 4.8), which can be related to the Ni-spinel/olivine partitioning in the parental peridotite. During lherzolite formation, such as those from the Santa Elena Ophiolite, $Ni^{2+}$ is stabilised in olivines and $Cr^{3+}$ in spinels, due to their high octahedral coordination site preferences (Burns, 1973). Additionally, in Mg-rich spinel peridotite xenoliths that have higher concentrations of Ni in the olivine than in the spinel or pyroxenes, and more Co in the spinel than the olivine or pyroxenes, the Ni partitioning is ruled by the major Al/Cr composition of the spinel (Stosch, 1981). In the serpentinite clasts of Santa Elena Peninsula both Al and Cr were strongly associated in the Cr-rich hercynite (Figure 4.8 and 4.S2, Table 4.S1) explaining the absence of Ni in the hercynite spinels and its presence in the lizardite, the serpentinized product of parental olivines. Finally, clinopyroxenes were confirmed as diopside, as in lowland MAN serpentinite clast (MgO: 16.1 ± 0.4 %, CaO: 21.3 ± 0.5 %, $Al_2O_3$: 6.4 ± 0.5 %, FeO: 2.8 ± 0.1 %, $SiO_2$: 50.8 ± 0.4 %) (Figure 4.7B and 4.S3), and orthopyroxenes as enstatite, as in peridodite from outcrop close to BES (MgO: 31.5 ± 0.5 %, CaO: 1.8 ± 0.6 %, $Al_2O_3$: 5.5 ± 0.3 %, FeO: 6.3 ± 0.2 %, $SiO_2$: 53.3 ± 3.5 %) (Figure 4.7D and 4.S5). Co and Ni concentrations in pyroxenes were considerably lower than in the other minerals present (Figures 4.S3-S5).

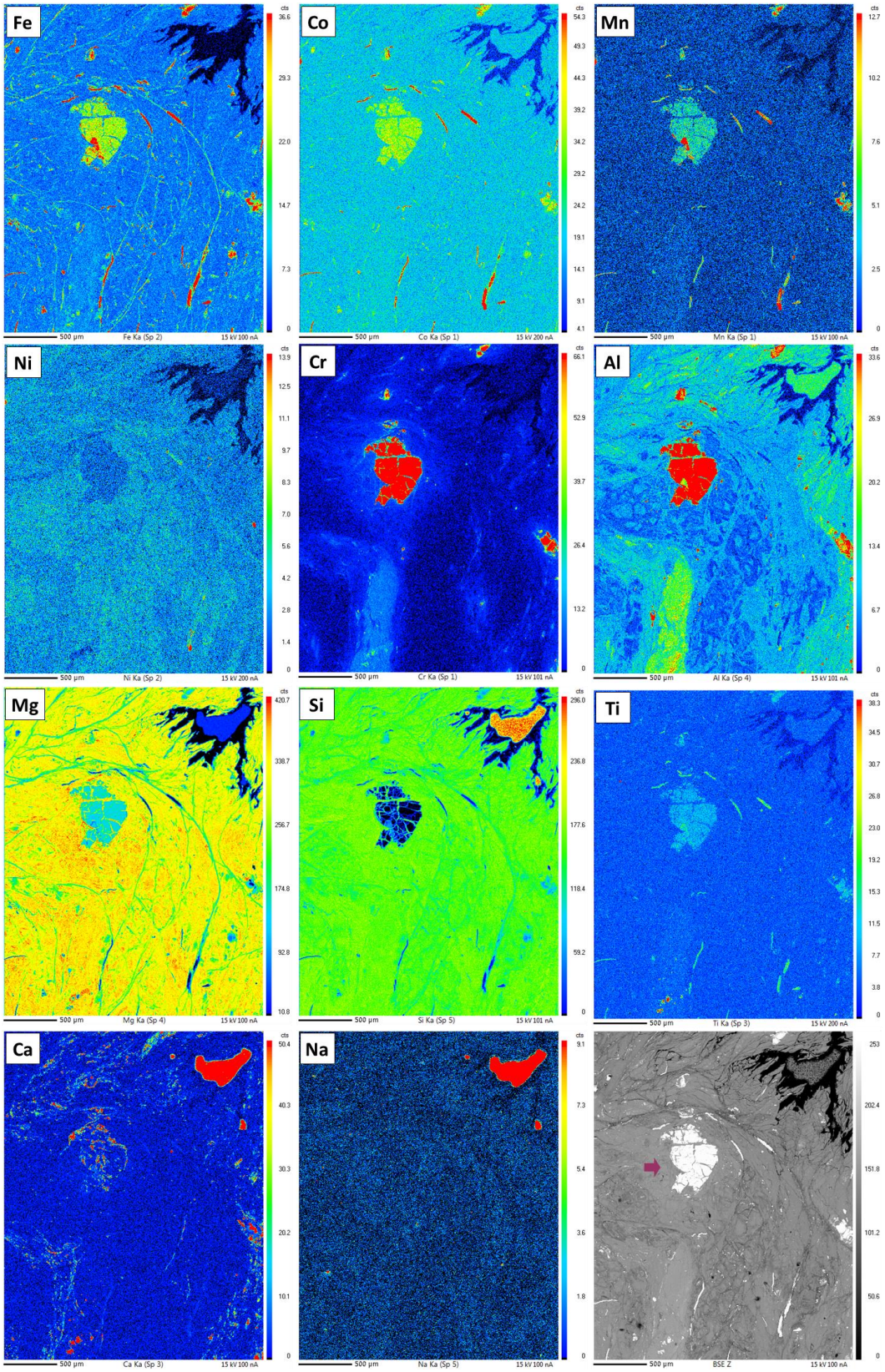


**Figure 4.8.** Elemental distribution determined on a polished thin section of a serpentinite clast from 10 cm depth (Mountain site LN), defined by EPMA. The area includes that covered by Figure 4.7A (rotated 90° counterclockwise). Count intensity colour scale (right of each micrograph)

decreases downwards; scale 500 µm. Analysis of a serpentinite from Lowland site (MAN) (Figure 4.7B) and of rocks from outcrops close to Mountain CEI (Figure 4.7C) and Lowland BES (7D) are shown in Figures 4.S3, S4 and S5, respectively.

In summary, the rock clasts found within the lateritic soils of the Santa Elena Peninsula were highly serpentinized peridotites regardless of the landscape or the location. However, relicts of the peridotite parental minerals were more common in rocks found in the rapidly transported lowland soils; rocks in the mountain sites showed a more advanced degree of serpentinization related to the more intense *in situ* degree of physical and chemical weathering. The geochemical analysis of these rocks, including also those from the outcrops, displayed positive correlations between Fe, Co, Ni, Mn and Cr. Co and Mn were concentrated in Cr-rich spinels and Fe-oxide veinlets, while Ni was present in those minerals too but in highly serpentinized rocks it was concentrated in the Fe-veinlets and in the serpentine minerals.

### 4.4.2 Geochemical characterisation of the lateritic soils

The geochemistry of the soils in the Santa Elena Peninsula was studied in the 10 different locations along the peninsula, 5 each from the mountain and lowland landscapes in the area of the Santa Elena Ophiolite. The water content of the soils was higher in the mountain locations (23.9 ± 4.3 %) than in the lowland ones (14.5 ± 4.5 %) ($F=33.52$, $p<0.0001$). There was no difference between the landscapes in terms of the total carbon content of the samples (Mountain: 13.4 ± 2.1 wt%, Lowland: 12.2 ± 1.9 wt%, $F=2.57$, $p=0.1204$), and pH was circumneutral for all the locations (Mountain: 7.01 ± 0.25, Lowland: 6.90 ± 0.49; $Z=0.83$, $p=0.4065$) (Table 4.2).

**Table 4.2.** Water content, total carbon content and pH of the soils sampled.

| Location | Water (wt%) | Total carbon (wt%)* | pH** |
|---|---|---|---|
| Mountain (CEI) | 27.1 ± 3.7 | 12.1 ± 1.3 | 6.94 ± 0.18 |
| Mountain (LN) | 26.1 ± 5.9 | 11.2 ± 0.8 | 7.21 ± 0.06 |
| Mountain (PG) | 20.8 ± 1.3 | 14.8 ± 0.2 | 6.95 ± 0.10 |
| Mountain (ES) | 26.3 ± 0.9 | 12.4 ± 0.1 | 7.15 ± 0.03 |
| Mountain (BOQ) | 19.4 ± 2.5 | 16.2 ± 1.2 | 6.85 ± 0.50 |
| Lowland (DAN) | 11.9 ± 3.2 | 15.1 ± 0.4 | 7.35 ± 0.21 |
| Lowland (MAN) | 15.4 ± 2.3 | 10.2 ± 0.5 | 7.49 ± 0.19 |
| Lowland (BES) | 17.2 ± 0.5 | 12.8 ± 0.2 | 6.47 ± 0.14 |

| Location | Water (wt%) | Total carbon (wt%)* | pH** |
|---|---|---|---|
| Lowland (MUR) | 19.5 ± 0.8 | 11.9 ± 0.3 | 6.35 ± 0.07 |
| Lowland (SE) | 8.6 ± 3.7 | 11.1 ± 1.5 | 6.83 ± 0.07 |

Results are shown as an average of the 3 replicates collected from every location and their standard deviation. *Total carbon content was calculated for dry weight. **pH was measured in fresh samples.

The mineralogy of the soils in the Santa Elena Peninsula was determined using XRD. All the soils sampled were mainly composed of magnesium silicates, iron oxides and clay silicates confirming the lateritic nature of all the soils, but with different proportions depending on the location (Figure 4.9). Lizardite was the only mineral found in all the locations although its incidence was considerably higher in the samples from the mountain landscapes, and the lowland samples inside the ophiolite area (DAN and MAN) (Table 4.1, Figure 4.S1), being the dominant mineral in all of them. The mountain locations also shared the presence of iron oxides as maghemite and goethite, and clay minerals such as clinochlore and smectite [$(1/2Ca,Na)_{0.3}(Mg, Fe, Al)_3(Si,Al)_4O_{10}(OH)_2 \cdot 4H_2O$], the latter closer to a Mg-rich smectite like stevensite [$Ca_{0.2}Mg_{2.9}Si_4O_{10}(OH)_2 \cdot 4H_2O$]. The presence of smectites could explain the higher content of water in the mountain soils because of their water retention capacities (Table 4.2). However, the BOQ location deviated from the other mountain landscapes as hematite, magnesio-hornblende [$Ca_2(Mg,Fe)_4AlSi_7AlO_{22}(OH)_2$] and kaolinite [$Al_2Si_2O_5(OH)_4$] were present.

In the lowland locations, kaolinite and hornblende-like minerals (close to Mg-rich members as magnesio-hornblende and edenite) were a common characteristic, also present in location BOQ as mentioned before (Figure 4.9). Another common feature was the presence of spinel-group minerals. Nevertheless, the lowlands from the inner ophiolite area (DAN and MAN) differed from the lowlands from the north boundary of the ophiolite (BES, MUR and SE) not only in the lizardite dominancy but also in the presence of smectite minerals. BES and MUR both had hematite as the main iron oxide and a low occurrence of clinochlore, while SE was the most dissimilar sample overall in terms of the mineralogy, being dominated by feldspars (albite) and clinochlore, and the only one without spinel minerals. Therefore, the mineralogy of the soils suggested three main groups of samples, those from the mountains dominated by lizardite and iron oxides, those from

inside the ophiolite area dominated by lizardite but with spinel and hornblende minerals, and the others from lowlands to the north boundary of the ophiolite where SE was slightly different.

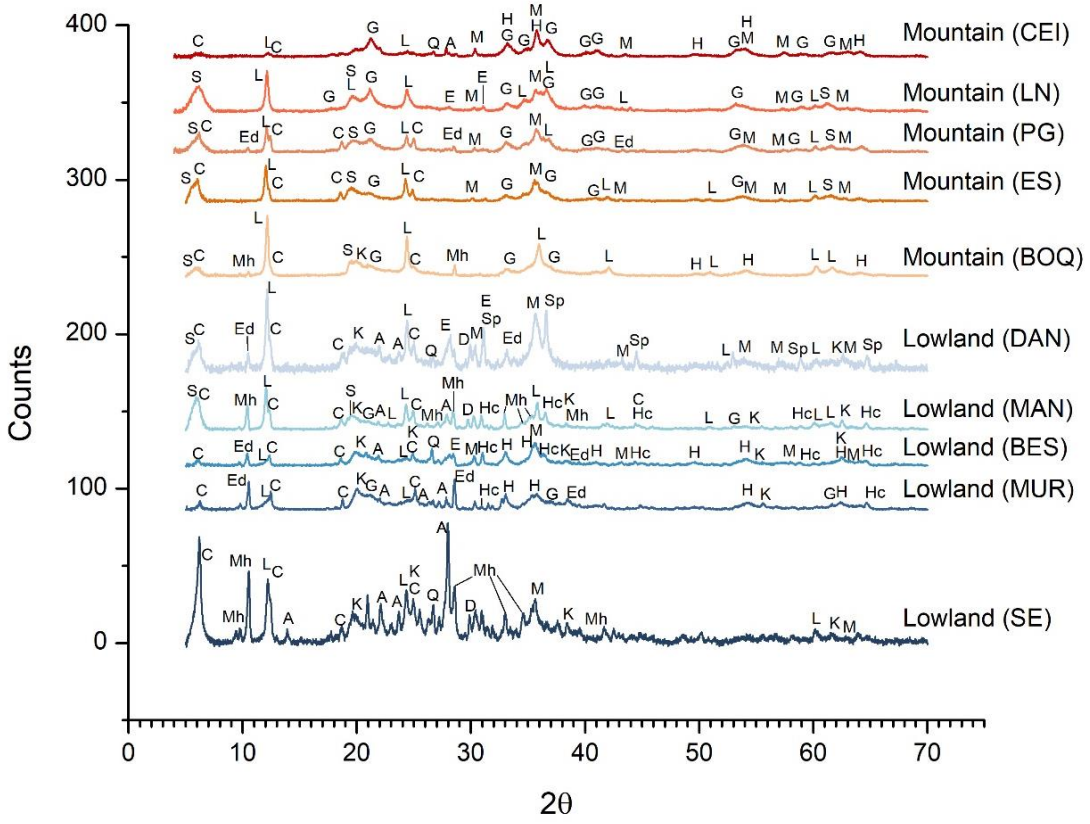


**Figure 4.9.** Mineralogy of the soils in the peninsula of Santa Elena. Main minerals found with XRD were: lizardite (L), goethite (G), hematite (H), maghemite (M), diopside (D), enstatite (E), hercynite (Hc), ferrite spinel (Sp), clinochlore (C), stevensite (S), magnesio-hornblende (Mh), edenite (Ed), kaolinite (K), quartz (Q) and albite (A). Red-to-orange colours were assigned to "mountain" landscapes and light-to-dark blue colours to "lowland" landscapes.

The bulk geochemical composition of the lateritic soil samples from the Santa Elena Peninsula was obtained by XRF analysis (Table 4.3), with data from 30 samples from ten locations spread along the eastern, central, northern and southern areas of the ophiolite (Table 4.1, Figure 4.S1). The location Cerro el Inglés (CEI in this study) was also included for comparison to a limited previous study (Reeves et al., 2007).

The soils are rich in Fe, Mn, Co, Ni, Cr and Mg, although the concentration varied with location origin (Table 4.S2). When comparing with other serpentinite derived soils, the Co and Mn contents

found here are comparable to serpentinite soils from Cuba and New Zealand, and laterites from Australia. However, the soils from the Santa Elena Peninsula were significantly richer in chromium and nickel when compared with those soils (Hallberg et al., 2011; Kabata-Prendias, 2001; Reeves et al., 2007, 1999). In two mountain locations in particular (CEI and LN), Ni had values comparable to those of oxide ore Ni laterite deposits, where percentages between 1-2% are extracted. These ore grades are expected below 10 m in depth and not as shallow as in the Santa Elena Peninsula (10 cm) (Butt and Cluzel, 2013; Roberts and Gunn, 2014). Nevertheless, the content of all the elements studied were considerably higher than those reported previously for the Santa Elena Peninsula (Table 4.3). The mountain CEI had the greatest values of the soils sampled (for all the elemental ranges), doubling or even quadrupling, as with Cr, the upper values previously reported for soils. In previous studies only three locations to the eastern side of the ophiolite were considered with 6 samples overall, and the authors emphasised the small area covered and the lack of biogeochemical information from the rest of the peninsula (Reeves et al., 2007).

**Table 4.3.** Iron, manganese, cobalt, nickel, chromium and magnesium in soils, sediments and rocks from the Santa Elena Peninsula.

| Sample (number of samples) | $Fe_2O_3$ (%) | MnO (ppm) | Co (ppm) | Ni (ppm) | Cr (ppm) | MgO (%) | Method, Reference |
|---|---|---|---|---|---|---|---|
| *Soils (30)* | *14.0-52.1* | *2000-6350* | *70-406* | *1660-13920* | *1000-12380* | *2.5-26.4* | *XRF, This study (Table 4.S2)* |
| Soils (6) | 10.2-16.0* | 1450-2600* | 152-325 | 3240-7220 | 1400-3640 | 3.8-15.6* | ICP-ES (Reeves et al., 2007) |
| Fluvial sediments (NR) | 5.6-6.8* | 560-920* | 34-70 | >100 | -- | -- | AAS (Marín Guzmán, 1985) |
| *Serpentinite (19)* | *7.6-13.5* | *488-2340** | *91-198* | *1759-10752* | *1870-3480* | *24.6-35.6* | *Bulk XRF, This study* |
| Peridotite and ultramafic rocks (NR) | -- | -- | -- | 1993-2380 | 1931-2471 | 34-45 | NR (Denyer and Gazel, 2009) |
| Diabase and basalt rocks (23) | 8.9-15.1 | 130-250 | 23-37 | 15-106 | 30-368 | 5.0-8.1 | XRF (majors) and LA-ICP-MS (traces) (Madrigal et al., 2015) |

* $Fe_2O_3$, MnO and MgO were reported as Fe, Mn and Mg %. / NR: Not reported, AAS: atomic absorption spectroscopy, ICP-ES: inductively coupled plasma emission spectroscopy, LA-ICP-MS: laser-ablation ICP mass-spectroscopy.

The bulk geochemistry of the soil samples from all the locations in the Santa Elena Peninsula, showed analogous patterns to those found in the parent serpentinite with positive correlations of Fe, Ni, Co, Mn and Cr overall (Figure 4.10). However, there were significant differences in the lateritic soils, especially with Co and Ni. Co had a very strong correlation with Mn in the serpentinite ($r=0.8765$, $p<0.0001$) but this decreased in the laterites ($r=0.7099$, $p<0.0001$), while its positive correlation with Fe increased from ($r=0.5959$, $p=0.0071$) to ($r=0.8229$, $p<0.0001$) in the soils. Ni correlated with Mn too although less strongly in the soils ($r=0.3940$, $p=0.0312$) compared to rocks ($r=0.7175$, $p=0.0005$). But unlike Co, Ni remained similarly related to Fe in the soils ($r=0.7339$, $p<0.0001$) as in rocks ($r=0.7790$, $p<0.0001$). The association of Co and Ni was also analogous in the soils ($r=0.8986$, $p<0.0001$) compared to the rocks ($r=0.8530$, $p<0.0001$).

Cr increased its association with Co, Ni and Mn ($r=0.8951$, $r=0.7201$, $r=0.7096$, respectively, all $p<0.0001$) when changing from the rocks to the soils, and in parallel decreased regarding to Fe ($r=0.7505$, $p<0.0001$). On the other hand, the negative correlations of Mg in the rocks were weakened in the soil, while a strong inverse association with Al emerged for Co ($r=-0.6862$, $p<0.0001$), Ni ($r=-0.7775$, $p<0.0001$) and Cr ($r=-0.6167$, $p=0.0003$). Finally, the negative correlation between Si and Fe was strengthened from the rocks ($r=-0.4802$, $p=0.0375$) to the soils ($r=-0.9319$, $p<0.0001$); a trend also observed for Si with Co, Ni, Cr and Mn ($r=-0.6993$, $r=-0.6340$, $r=-0.6555$, $r=-0.5399$, respectively, all with $p<0.002$) (Table 4.S3, Figure 4.S4).

The latter results suggested that during lateritic soil formation in the Santa Elena Peninsula, Co, Ni and Mn are more likely to be concentrated in oxide minerals rather than the hydrous Mg silicate or clay silicate minerals, hence their negative correlation with silicon (Butt and Cluzel, 2013). Therefore, in the lateritic soils the minerals bearing those elements could be the iron oxides (goethite, maghemite or hematite) and/or the spinel-like minerals (Cr-rich hercynite) according to the overall soil mineralogy (Figure 4.9) and to the mineralogy of the serpentinite clasts where Co was strongly associated with both minerals (Figure 4.8 and 4.S3-S5). Therefore, during lateritic soil formation, Co, Ni and Mn are concentrated in the Fe-oxides, hence increasing its correlation with Fe, and in the hercynite too, where Cr is also concentrated. Cr concentration in the spinel is largely likely to substitute Al, as their strong positive correlation in the rocks is completely inverted in the soils into a negative association; a similar trend occurred with the rocks when comparing serpentinite clasts with less weathered peridotite rocks (see previous rock section) suggesting

Cr-Al substitution in spinels as a characteristic feature of lateritic soil formation as a consequence of the serpentinite weathering. However the negative correlation of Fe, Co, Ni, Cr and Mn, with Si could be also strengthened due to the dilution of those metals in a major pool of Si in the soils resulting from the presence of quartz or other alumino-silicates as kaolinite or feldspars that might be the result of the weathering of other lithologies found in the Peninsula as gabbros or basalts (Whattam et al., 2016). The latter could also explain the strong negative association with Al. The presence of Co, Ni and Mn in the Mg-rich smectites, clinochlore or amphiboles cannot, therefore, be discarded entirely.

Additionally, Ni and Co in the soils had a weaker correlation with Mn if compared with the serpentinite clasts, suggesting that Mn could have been leached to some extent from the Fe-oxide minerals, leading to the concentration of Ni and Co, a mechanism that could be biologically mediated (Hansel and Learman, 2016). Moreover, correlations between Fe and Co increased in the soils, while Fe and Ni correlations remained similar. As with manganese, Fe weathering processes could also be microbially mediated (Kappler et al., 2016). When considered together, these data confirmed the complex processes underpinning mobilisation of trace elements during lateritic soil formation, processes that probably involved both geochemical and biological factors, and highlighting a multidisciplinary biogeochemical focus for future studies on soil processes within the Santa Elena Peninsula.

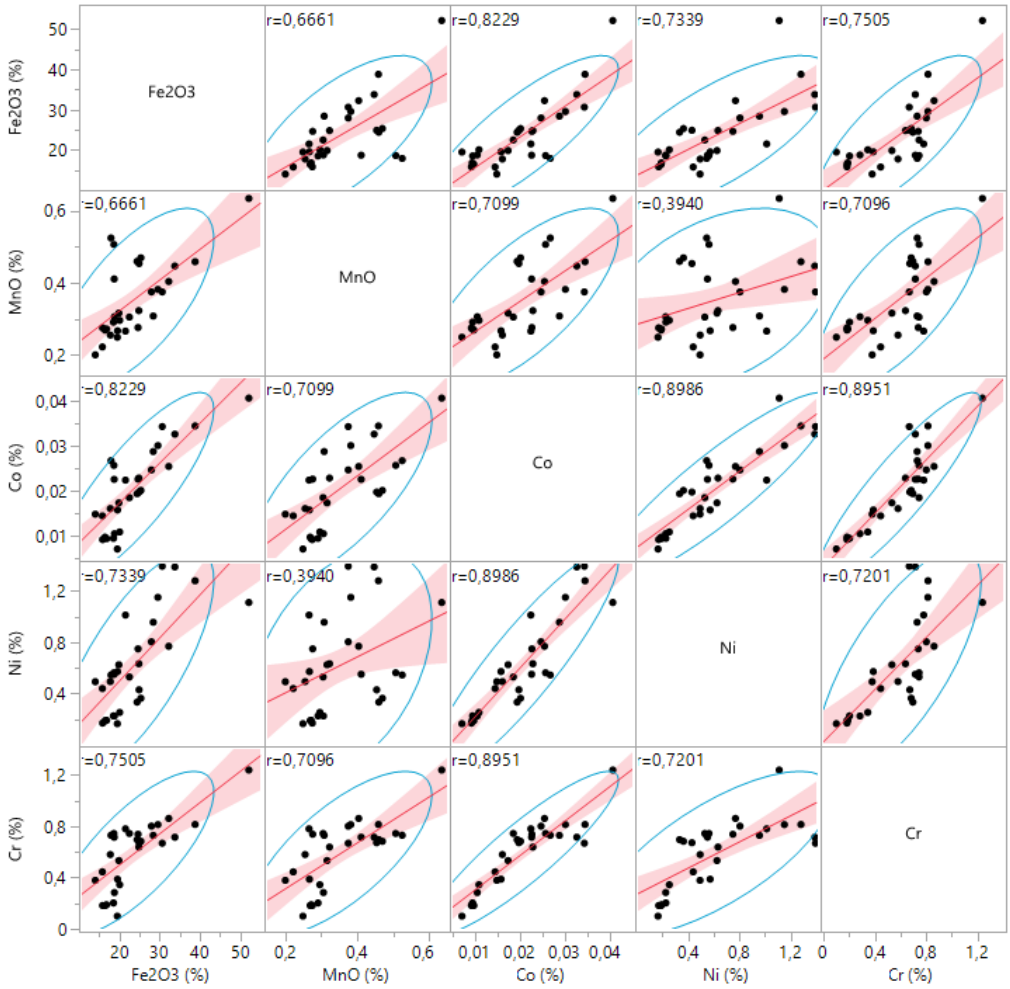


**Figure 4.10.** Elemental correlations in lateritic soils of Santa Elena Peninsula for Fe, Mn, Co, Ni, and Cr. All elements were positively correlated ($p<0.05$) (density ellipses $\alpha=95\%$). A broad analysis including Al, Si and Mg and all the correlations and probabilities associated are shown in Table 4.S3 and Figure 4.S6.

### 4.4.3 Geochemistry of the lateritic soils in a landscape context

The geochemical composition of the soil samples from the 10 locations in the Santa Elena Peninsula was also studied in a geographical-landscape context (Figure 4.11, 4.12). Fe and Si were the major components in all the soils accounting together for a ~60% of the total mass, followed by Mg and Al at between 15-25%. However, the Fe content was higher in the samples from the mountain landscapes, except in BOQ that had levels like those from the lowland soils. Al and Ca had the opposite trend, being lower in the mountains but with the BOQ soils representing an exception. Mg was considerably lower in the samples from the north limit of the

ophiolite (BES, MUR and SE) while the other lowland samples were more similar to the mountain landscapes (Figure 4.12).

In terms of the minor constituents, Ni, Cr and Co had greater levels in the mountain soils compared to the lowlands, similar to the trend observed with Fe, while Ti had the inverse tendency and Mn was relatively constant across the sites (Figure 4.11). Analogous to major elements, a difference could be observed in the lowland samples depending on their geographical position within the ophiolite, while the BOQ sample also differed from the other mountains (Figure 4.12). The sample from CEI (mountain landscape) was notable, as it was the soil with the highest quantities of Fe, Ni, Cr, Mn and Co and the lowest percentage of Si overall, and the smallest content of Mg amongst the mountains (Figure 4.11, 4.12). This was the sample collected at the highest altitude, from an area of scarce vegetation and patches of uncovered soils (Table 4.1), and therefore exposed to a higher extent of physical weathering from the harsh local conditions of temperature, rain and wind. Interestingly, the soil samples from the LN site were closest to the CEI samples with respect to Ni and Co content, and this was the second highest sampling site, also with scarce vegetation and patches of uncovered soils. An analogous case was reported in Italian alpine serpentine soils found above 2000 m altitude, where pedogenesis on serpentinite was very slow or absent when associated with factors such as low plant coverage and steep slopes that favoured high erosion rates; resulting in soils with higher amounts of exchangeable Ni compared to most developed soils under coniferous forest (D'Amico et al., 2015).

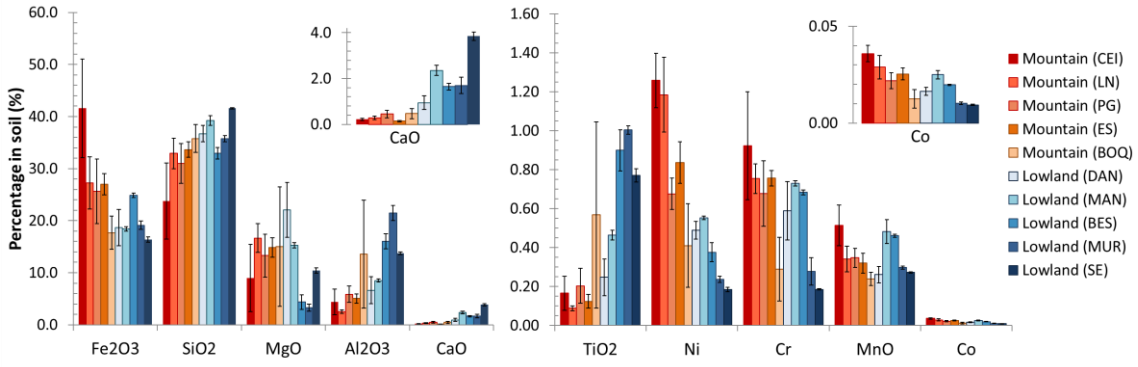


**Figure 4.11.** Geochemical composition of the soils in the Santa Elena Peninsula measured with XRF. Major elements and main trace metals are shown with their respective standard deviation per location. Mountain (M) landscapes are in red-to-orange colours and lowland (L) landscapes in light-to-dark blue. These 10 elements plus the carbon content (Table 4.1) corresponded to 93-

98% of the dry mass weight in all the locations sampled. CaO and Co are zoomed in the inset plots. The complete geochemical composition per location is presented in Table 4.S2.

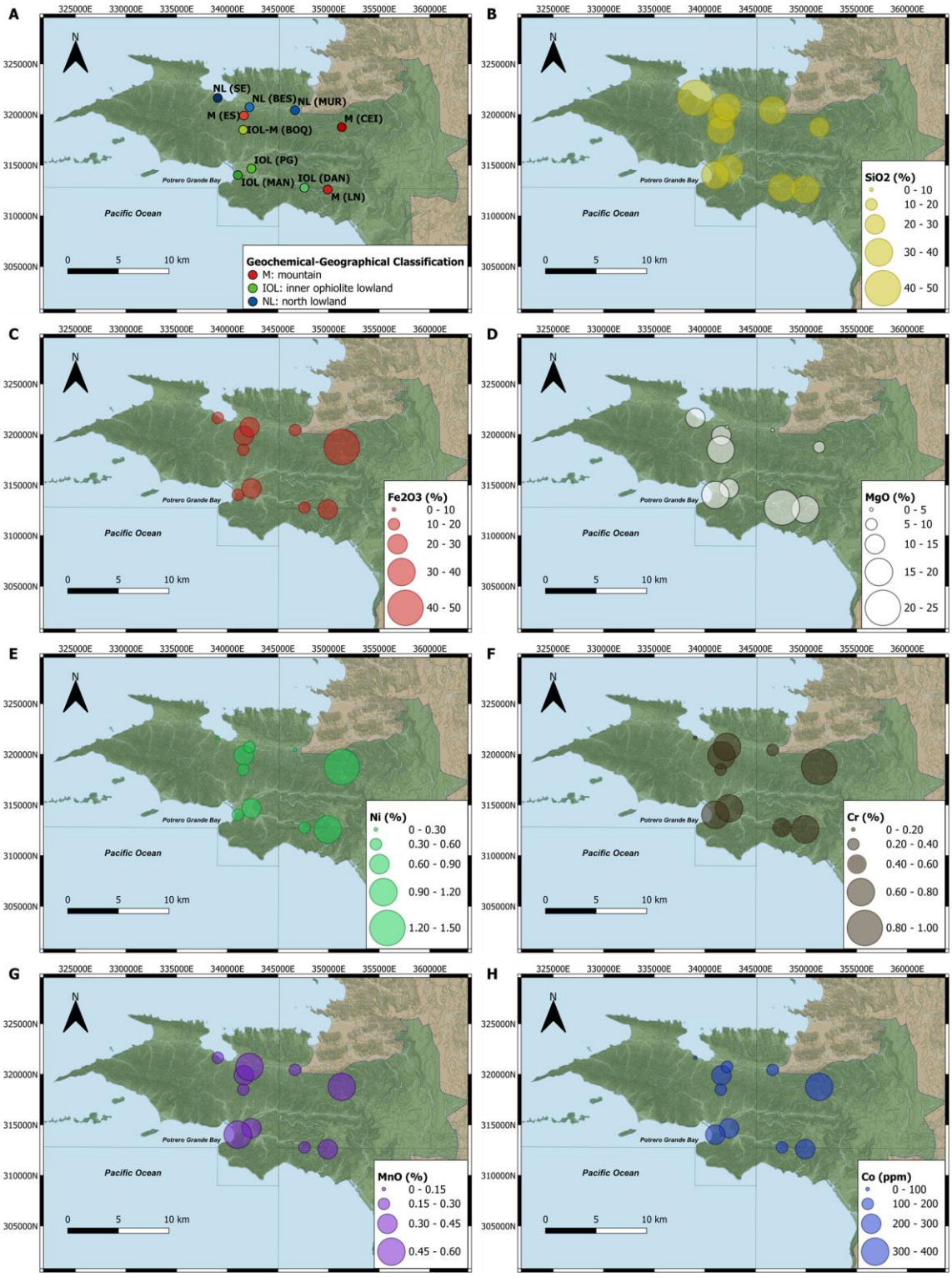


**Figure 4.12.** Geographical distribution of (A) the three serpentine soil groups found in the Santa Elena Peninsula based on geochemical clustering analysis (see Figure 4.13), and the distribution

of major elements: Si (B), Fe (C) and Mg (D), and main trace metals: Ni (E), Cr (F), Mn (G) and Co (H) in those lateritic soils.

Relationships between the geographical locations of the samples and their soil geochemistry were studied using a hierarchical clustering analysis (Figure 4.12A, 4.13). Three distinct groups could be identified according to their geochemistry, supporting the results based on mineralogical analyses. First, the soils from the higher mountain landscapes (CEI, LN and ES) were clustered together, consistent with their identification as lateritic soils rich in Fe, Ni, Cr and Co in a mineralogy dominated by lizardite and iron oxides. Interestingly, within this group of soils, the concentration of Ni and Co increased with altitude (Table 4.4); a trend that can be associated with erosive factors, as seen in non-tropical serpentine soils (D'Amico et al., 2015). In other non-serpentine soils, like in Galapagos Islands, weathering processes associated with climate increased with altitude (Taboada et al., 2016) and influenced larger amounts of secondary phases of Fe, Al and Si at higher elevations (Taboada et al., 2019). The latter highlights the necessity to further study the influence of the altitude-associated characteristics (vegetation coverage and climate exposure) in the serpentine soils of Santa Elena Peninsula.

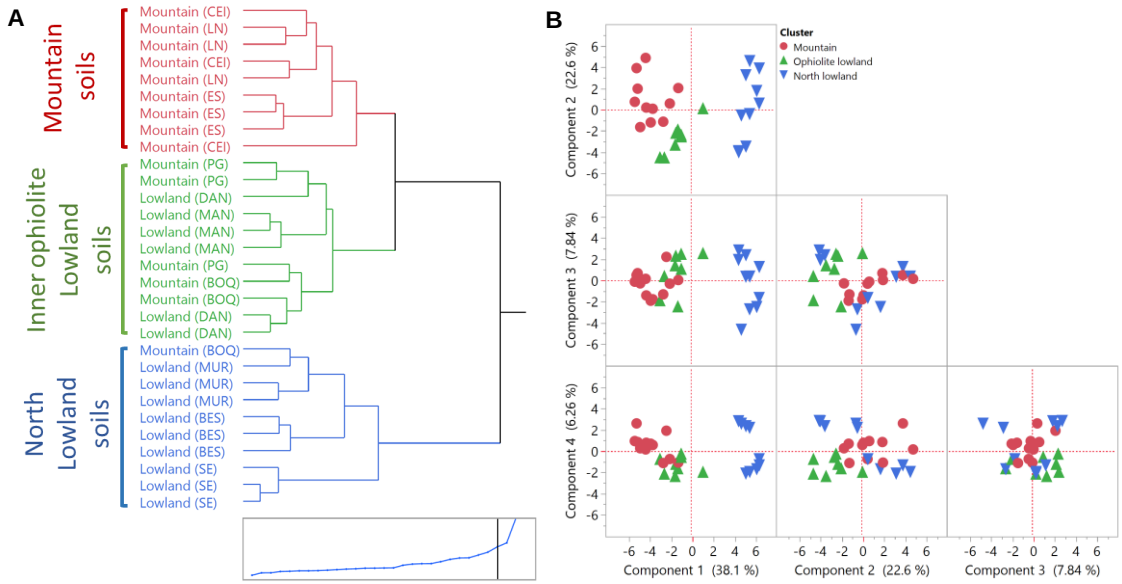


**Figure 4.13.** (A) Hierarchical clustering analysis (HC) and (B) principal components analysis (PCA) for the geochemistry of the soils. Three groups of soils can be considered in (A), top to bottom named as: mountain soils (●), inner ophiolite lowland soils (▲) and north lowland soils (▼). The geographical distribution of each sampling location per cluster can be seen in Figure

4.12A, for details within geology, soil and vegetation maps see Figure 4.S1. HC used Ward method, and considered the total carbon content, the water percentage, pH and geochemical XRF data (including both majors and traces elements), inset of (A) is the distance graph showing the cut point for three clusters. Four main components explained ~75% of the variance within the samples according to PCA (B): PC1 (38.1%), PC2 (22.6%), PC3 (7.8%) and PC4 (6.3%). The score of each variable within each component is in Figure 4.S7.

**Table 4.4.** Linear model of nickel and cobalt with altitude in the mountain soils.

| Element | Linear model* | $R^2$ | F ratio | Prob>F |
|---|---|---|---|---|
| Nickel | Ni (%) = 0.6536 + 0.0013*Altitude (masl) | 0.7407 | 28.56 | 0.0003 |
| Cobalt | Co (ppm) = 204.82 + 0.30*Altitude (masl) | 0.6493 | 18.51 | 0.0016 |

*Graphical regressions were plotted in Figure 4.S8. Masl: metres above sea level.

The second group of serpentine soils (Figure 4.13) contained locations from the inner ophiolite area (PG, BOQ, DAN and MAN) (Figure 4.12A, 4.S1), which can be viewed as a transition group from the mountain landscapes to lowlands (Table 4.1), although they are geochemically closer to the mountain soils than to the other lowlands sampled (Figure 4.12, 4.13). For example, PG was originally described as a mountain, but it was the mountain location with the lowest altitude (Table 4.1), BOQ was also a mountain location with relative high altitude (Table 4.1) but was highly heterogeneous in its geochemistry with compositions similar to the other mountain samples within uncertainties (Figure 4.11, 4.12), while DAN was a lowland sample inside the ophiolite area and surrounded by mountains (Figure 4.12A, 4.S1). Within this inner ophiolite lowland cluster were also the lowland soils from the mangrove area of Potrero Grande (Figure 4.12, 4.13). Surprisingly, despite being in the same hydrographic basin, MAN and DAN were geochemically distinct, with higher levels of Mg and total carbon upstream (DAN), while Ni, Mn, Co and Cr were more concentrated in the mangrove location (MAN), 10 km downstream from DAN (Table 4.2, Figure 4.12). In mangroves from New Caledonia located downstream a lateritic deposit a similar trend of concentration of Ni and Cr was reported, with average concentrations of Ni similar to those found in this mangrove from the Santa Elena Peninsula (Marchand et al., 2012; Noël et al., 2015). In fact, mangroves acting as metal-sinks or as buffer of metals have been largely reported, and not only in mangroves downstream lateritic soils such as those from New Caledonia that have high

concentrations of Fe and Ni (Marchand et al., 2016). In other mangroves worldwide within different geological and ecological contexts, metal accumulation occur in many cases associated with contamination from anthropogenic activities, such as mangroves in Australia (Holloway et al., 2016; Nath et al., 2013), Senegal (Bodin et al., 2013), Singapore (Cuong et al., 2005) or Brazil (Fonseca et al., 2013; Machado et al., 2002).

Finally, the last group of soils that were clustered together and contained soils from the north boundary of the ophiolite (BES, MUR and SE) (Figure 4.12, 4.13, 4.S1). In general, these were soils from lowlands and were poor in Mg but rich in Al, Ca and Ti. Their geochemical composition together with the mineralogy reflected more complex processes involved in their formation probably due to their geographical position between different geological units (Figure 4.S1), and collectively influenced by the laterite geochemistry of the ophiolite mountains (reflected in the lizardite common mineral). However, BES and MUR were slightly different to SE therefore subdividing the soils from the north boundary of the ophiolite in north lowland soils (BES and MUR) and northwest lowland soils (SE). This difference relied mainly on a higher amount of Si, Ca and Na (Figure 4.11, 4.12), and reinforced the different mineralogy observed in this location dominated by albite (Figure 4.9) and coincided with the soil type separation reported for those sites (Table 4.1, Figure 4.S1).

In summary, although all of the soils sampled were clearly lateritic, there were measurable variations in geochemical compositions, resulting in three types of lateritic soils. Within the ophiolite area the concentrations of Fe and trace elements including Co, Ni and Mn were higher in the *mountain* soils, and the concentration of Co and Ni increased with the altitude. In the lowland soils collected from inside the ophiolite area, the *inner ophiolite* soils retained characteristics from the surrounding mountains, and the concentration of the trace metals studied increased downstream, accumulating in the mangrove area. The *north lowland* soils at the northern boundaries of the ophiolite had the most dissimilar geochemistry although still influenced by the ophiolite.

### 4.4.4 Microbial characterisation of the lateritic soils

The microbial composition of the lateritic soils associated with the Santa Elena Ophiolite was studied by sequencing the V4 variable region of 16S rRNA for the prokaryotic communities and

the ITS2 region of nuclear ribosomal DNA for fungi. To our knowledge, this is the first report of both the prokaryotic and fungal communities of the lateritic soils along the Santa Elena Peninsula. Only two previous studies have reported indigenous microorganisms of this area but both were restricted to methane-related prokaryotes in three hyper alkaline springs (Crespo-Medina et al., 2017; Sánchez-Murillo et al., 2014).

#### 4.4.4.1 Prokaryotic communities in the soils

Regardless of the location or the landscape considered, the prokaryotic communities in all 10 samples studied seemed homogeneous in their composition at the phylum level (Figure 4.14A). The prokaryotic diversity was very similar among the sites as showed in rarefaction curves, although the communities were slightly less diverse in the mountain CEI sample (Figure 4.14B, S9), and in terms of the phylotype richness, there was no clear distinction between the two main landscapes studied ($F=0.3173$, $p=0.5887$). The prokaryotic communities in general were clearly dominated by Bacteria (Figure 4.14A), with only 4% of the total abundance corresponding to Archaea. The latter domain was represented by two phyla and 17 phylotypes, 13 were from the Thaumarchaeota (3% of the total relative abundance) and 4 phylotypes were affiliated with the Euryarcheota (1% relative abundance). Both groups are commonly found in soils worldwide, Euryarcheota in water-saturated soils principally (Gubry-Rangin et al., 2015; Stieglmeier et al., 2014; Whitman et al., 2014). When considering every location sampled, Thaumarcheota were ubiquitous along the peninsula but higher in in the mangrove location (4% relative abundance) and in the most geochemically dissimilar lowland sample (SE) (14% relative abundance), suggesting involvement in nitrogen cycling in those sites, as this group comprises ammonia-oxidizing microorganisms (Gubry-Rangin et al., 2015; Stieglmeier et al., 2014). Euryarcheota was represented by methanogenic individuals affiliated with the order Thermoplasmatales and were more represented in the mountain locations and the lowland soils from inside the ophiolite area (DAN).

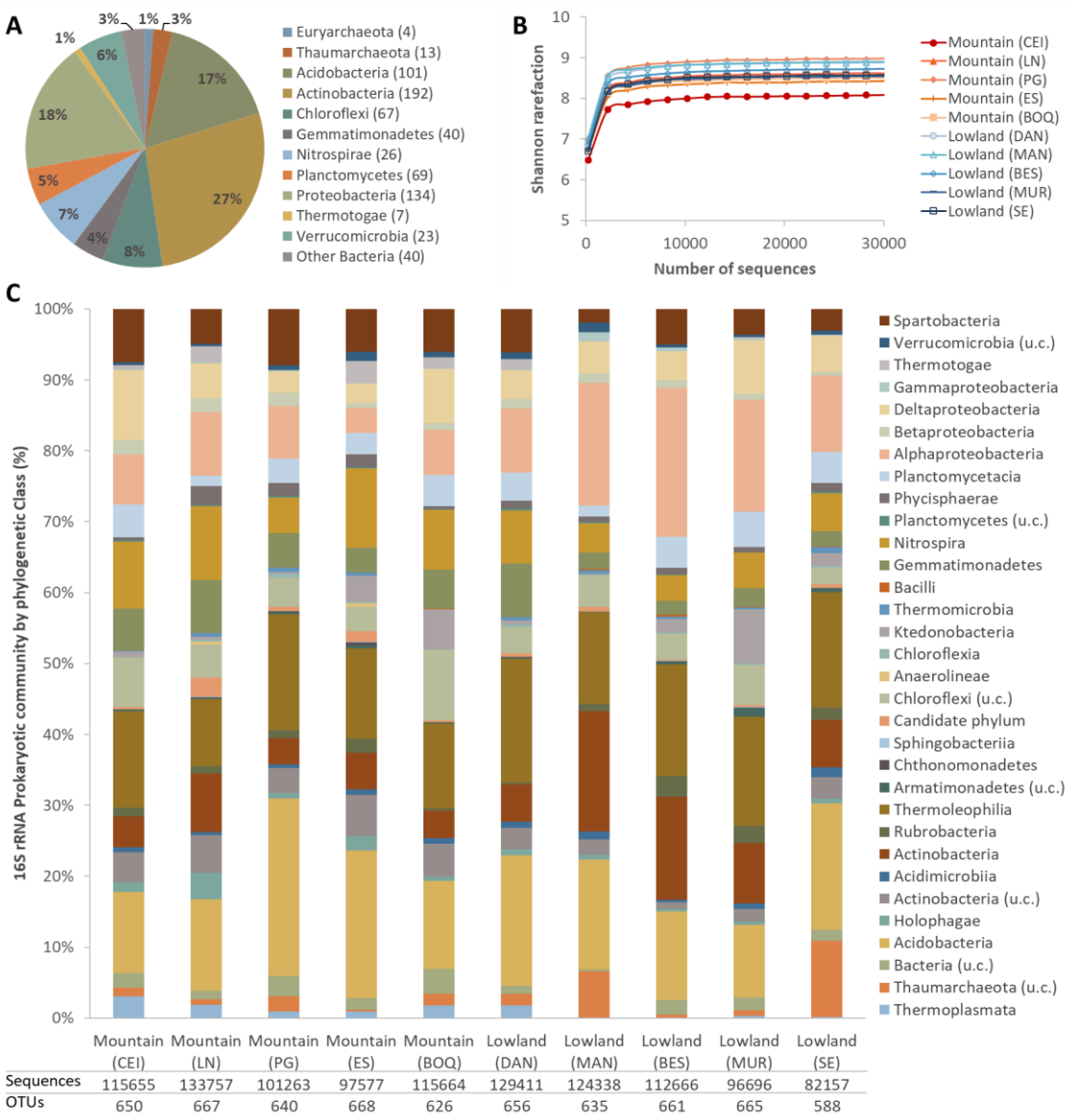


**Figure 4.14.** Prokaryotic communities in the lateritic soils sampled in the Santa Elena Peninsula obtained by the sequencing of the V4 region of 16S rRNA. (A) Relative abundance per phylum of all the sequences obtained in the entire sampling area associated with the Santa Elena Ophiolite. In brackets the number of prokaryotic phylotypes (OTUs). (B) Shannon rarefaction curve with red-to-orange colours assigned to “mountain” landscapes and light-to-dark blue colours to “lowland” landscapes. (C) Prokaryotic communities per phylogenetic class in the lateritic soils in each of the locations sampled. Total OTUs obtained: 716, total sequences read: 1109229; ‘u.c.’: unclassified class. In (A) “Other Bacteria” included Bacteroidetes (1 OTU, 379 sequences), Firmicutes (2 OTU, 718 sequences), Armatimonadetes (4 OTU, 5595 sequences), Candidate phylum (12 OTU,84655 sequences), and unclassified Bacteria (21 OTU, 20322 sequences).

Actinobacteria represented the major phylum within the lateritic soils in the Santa Elena Peninsula both in phylotype richness (192) and total abundance (27%), followed by representatives of the Proteobacteria (134 phylotypes, 18% of total abundance) and Acidobacteria (101 OTUs and 17% total abundance) (Figure 4.14A). Those three phyla are also the dominant clades in soils across the world although Proteobacteria tends to be the dominant group (Delgado-Baquerizo et al., 2018). In every location, Actinobacteria were also the major group detected ranging from 20-26% relative abundance both in the mountain and inner ophiolite samples, to 35-44% in samples from the north lowlands (Figure 4.14C). These levels were considerably higher than those reported from other ultramafic soils in New Caledonia, where actinobacteria only accounted for 8-10% in largely proteobacteria-dominated soils (Gourmelon et al., 2016). This group is also one of the largest clades recognised in manganese rich soils, and comprises several manganese-oxidising bacteria (Ghosh and Das, 2018; Yang et al., 2013), several of which were found in all the locations of the peninsula (*Mycobacterium* sp., *Arthrobacter* sp., *Actinophytocola* sp., *Pseudonocardia* sp., *Saccharopolyspora* sp., *Sciscionella* sp. and *Streptomyces* sp.). Generally, these were more abundant in the lowland soils (3-8% relative abundance) rather than in the mountain samples (0.6-2%), with the Mn-enriched mangrove (MAN) samples (Figure 4.9, 4.11, 4.12) containing the largest relative abundance (8%) (Figure 4.S10). Interestingly, many of these Actinobacteria genera are also associated with ultramafic soils rich in nickel and chromium in Spain (Touceda-González et al., 2018).

The other group of interest potentially associated with manganese oxidation was the second most common clade overall, Proteobacteria, which contains species of *Pedomicrobium* (Alphaproteobacteria), *Pseudomonas* (Gammaprotobacteria), and Burkholderiales (Betaproteobacteria) (Algora et al., 2015; Ghosh and Das, 2018; Hansel and Learman, 2016; Yang et al., 2013). In general, these represented 0.4-2.7% of the relative abundance per location, being less heavily represented in the mountains compared to the lowland soils (Figure 4.S10).

Potential iron-reducing bacteria were also detected, for example organisms affiliated with the Myxococcales (Deltaproteobacteria), where *Anaeromyxobacter* sp. was the major genus (Ding et al., 2017; Lovley et al., 2004; Treude et al., 2003). The group was better represented in the mountains (Figure 4.S10), but the highest proportion was found in the CEI mountain location (8% relative abundance), that was the site with the greatest quantity of iron, while the mangrove

location had the lowest relative abundance (0.1%)(Figure 4.11). Well-known iron-oxidising bacteria were also present at the different locations (Figure 4.S8), including those affiliated with the manganese-oxidising Betaproteobacteria mentioned before (that can also oxidise Fe(II) ) (Emerson et al., 2015), and phylotypes from the Nitrospira class (Daims, 2014). This group was better represented in the mountain soils ranging from 6% to 11% of relative abundance, although not so different from the lowlands (4-8% of relative abundance).

Finally, other bacteria found whose functionality could be inferred included organisms associated with the cycling of nitrogen as those from the order Nitrospirales (within the Nitrospira class) or the *Nitrospinaceae* family (Deltaproteobacteria) (Figure 4.14C) (Daims, 2014; Lücker and Daims, 2014) ranging from 4 to 11% of relative abundance; a group relatively ubiquitous across all the locations complimenting the ammonia oxidiser archaebacteria previously described (Figure 4.S10). Also, sulfur-cycling Deltaproteobacteria from the orders Desulfobacterales and Desulfurellales were found at all the locations but to a lesser extent (0.3-2.8% relative abundance)(Figure 4.S10) (Greene, 2014).

In summary, despite an apparent homogeneity across the sample area, the prokaryotic communities in the lateritic soils of the Santa Elena Peninsula had certain characteristics that related to their specific site of origin. The mountain locations shared many phylogenetic groups even in similar proportions, however those related to iron redox cycling were more abundant in those landscapes than in the lowlands; with the sample from the lowland to the inner ophiolite area (DAN) having communities more like those of the mountains, and the mountain CEI location, with the higher relative abundance of iron reducers and the lowest diversity overall. The lowlands were richer in potential manganese-oxidising bacteria, especially those from Actinobacteria, and the mangrove location had the greatest abundancy of them. These results were analogous to the geochemical relationships between the locations sampled, as higher concentrations of Fe and Fe(III) minerals were found in the mountain soils and the mangrove was one of the locations with the highest concentrations of Mn, reflecting the interdependence of the prokaryotic communities and the geochemistry of the lateritic soils.

#### 4.4.4.2 Fungal communities in the soils

The fungal communities in the ten samples of lateritic soils were also studied, by sequencing the ITS2 region of nuclear ribosomal DNA (Figure 4.15). In terms of the phylotype richness, soils from the lowland landscapes were richer and had more OTUs (155 ± 7) than in the mountain ones (108 ± 7) ($F=22.61$, $p=0.0014$) (Figure 4.15B, 4.S11), with the mountains CEI and LN the less diverse locations while lowlands BES and MAN were more diverse. In general, none of the locations were as rich or diverse as their prokaryotic communities previously discussed (Figure 4.S7). Over all the soils sampled across the Santa Elena Peninsula, the fungal communities were Ascomycota-dominated with 206 OTUs (61% of the total OTUs found) and 69% of the total sequences against 22 OTUs that were basidiomycetes (5% total sequences), with a high percentage of unclassified fungi (104 OTUs, 25% total sequences) (Figure 4.15A). Most of the locations had a similar phylum ratio when compared to the complete peninsula, but three sites had higher percentages of ascomycetes: the mountains CEI and LN (93% and 79% of relative abundance, respectively), and the mangrove location MAN (82%) (Figure 4.15C). Those were also the locations with the lower amount of unclassified fungi, although they had the larger quantities of unclassified Ascomycota (Figure 4.15C). On the other extreme, the mountain BOQ had the larger proportion of unclassified fungi, and the lower Ascomycota rate (31% of relative abundance). Large numbers of unclassified fungi could be explained both by the high unexplored diversity normally found in the tropics, where the ACG in particular is considered a hotspot of biodiversity, and the expected endemism associated with lateritic soils due to their high relative levels of trace metals and general abiotic stress; similar to the endemism broadly reported in plants from serpentine ecosystems (Anacker, 2011; Gourmelon et al., 2016).

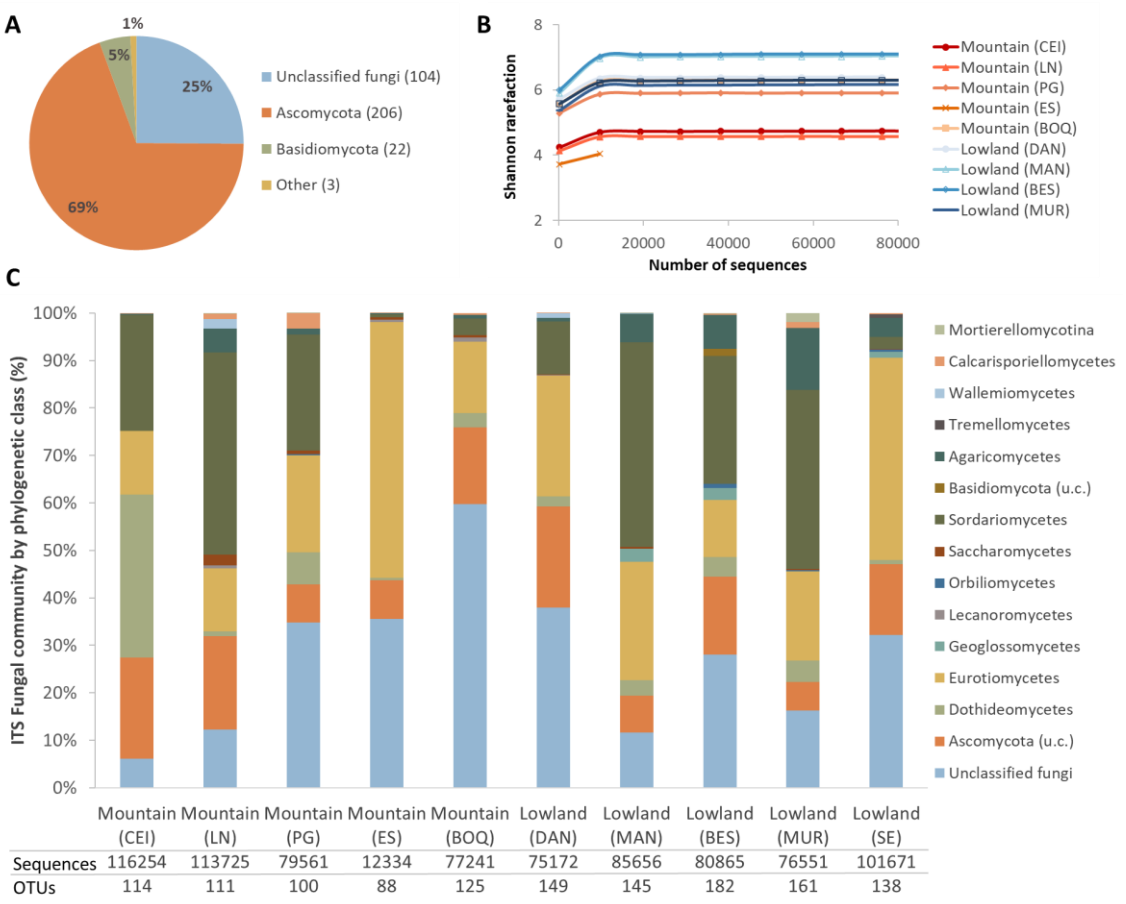


**Figure 4.15.** Fungal communities per phylogenetic class in the lateritic soils of the Santa Elena Peninsula obtained by ITS2 sequencing. (A) Relative abundance of all the sequences obtained per phylum in the entire sampling area associated with the Santa Elena Ophiolite. In brackets the number of fungal phylotypes (OTUs). (B) Shannon rarefaction curve with red-to-orange colours assigned to “mountain” landscapes and light-to-dark blue colours to “lowland” landscapes. (C) Fungal communities per phylogenetic class in each location sampled. Total OTUs obtained: 338, total sequences read: 818985; ‘u.c.’: unclassified class. In (A) Other included Calcarisporiellomycota (1 OTU, 5923 sequences) and Mortierellomycota (2 OTU, 1671 sequences). Total OTUs: 338, total sequences: 818985.

Amongst the ascomycetes, Dothideomycetes was the largest phylogenetic class found in the mountain CEI location (34% of relative abundance), much higher than any other site (Figure 4.15C). This group was mostly represented by Mycosphaerellaceae, a family widely studied because many fungal species are described as plant pathogens, although their members can also cover other niches and lifestyles (Videira et al., 2017). Soils from the mountain CEI location

was covered with Poaceae species (grasses), a plant family also associated with certain fungal species of Mycosphaerellaceae (Braun et al., 2015). Interestingly, these grasses were also present in the other mountain locations, but these fungi were absent regardless of their vegetation or altitude. As noted previously, the other main difference between the CEI and the other mountains was the highest levels of iron and trace metals overall, suggesting a more complex association between these fungi, the plants and the soil geochemistry that should be further addressed.

Eurotiomycetes was present in all the soils sampled (Figure 4.15C), including species of *Aspergillus* and *Penicillium* as the most common constituents. *Aspergillus* sp. had higher proportions in the mangrove sample (MAN) (12% of relative abundance) and in the mountains (PG, ES, CEI and LN) (4-10% of relative abundance). Those are fungi commonly isolated from heavy metal polluted areas (Gadd, 2007), and the lateritic soils from the mountains of the Santa Elena Peninsula here shown to have greater proportions of main trace elements, while the mangrove was geochemically distinct to the other lowlands due to its metal-accumulation characteristics (see section 4.4.3). *Penicillium* sp. was more common in the lowlands, with 2-11% of relative abundance, but the biggest ratio was in the mountain ES (43%) although it was the site with the lowest OTUs count, and the lowest sequences read.

The Sordariomycetes were the third important class of ascomycetes found, although their subsequent classification varied depending on the locations (Figure 4.15C). The Coniochaetales were the dominant sordariomycetes in the mountains CEI and LN and restricted to those two sites; a group that has been reported from different soils worldwide but that has undergone recent phylogenetic revision (García et al., 2006). The Hypocreales were represented by *Fusarium* sp. (4-11% of relative abundance) and *Purpureocillium* sp. (16-21%) in the lowland soils except in the location upstream in the ophiolite area (DAN) and the one to the northwest (SE) (Figure 4.S1). *Fusarium* sp. is also commonly isolated from heavy metal polluted areas (Gadd, 2007), while *Purpureocillium* sp. has been reported as endophyte in mangrove plants, where the fungus induced the complexation of Cu, Mn and Fe in the soil (Gong et al., 2017), highlighting the necessity to better understand the role of this fungal genus especially towards the mangrove of Potrero Grande here studied. Location PG had an analogous content of *Purpureocillium* sp. (11%), this was the mountain site with the lowest altitude (Table 4.1), geochemically classified

within the inner ophiolite lowland group (Figure 4.12, 4.13) and the one with the most different vegetation leading towards the type found in the lowland locations (Table 4.1), implying an influence of the vegetation type and the presence of this fungal group. The influence of vegetation cover in the microbial diversity of prokaryotes and fungi has been reported in ultramafic soils in New Caledonia, an issue of high interest to study in the Santa Elena Peninsula (Bordez et al., 2016; Carriconde et al., 2019; Gourmelon et al., 2016).

The other important fungal phylum in the soils of the peninsula of Santa Elena was Basidiomycota better represented in the lowland locations (5-13% of the total abundance) (Figure 4.15C). The lowland location inside the ophiolite area (DAN) had a lower content of basidiomycetes (2%) while the mountain location LN had a similar proportion to the other lowlands (7%), and all of them were dominated by Agaricomycetes. An interesting case was the presence of the macrofungi *Lycoperdon sp*. in mountain LN and lowland MAN (5% of relative abundance in each location), a fungal genus reported to accumulate metals as gold, mercury, lead, zinc and copper (Borovička et al., 2010; Gadd, 2007); and other metals such as iron, manganese chromium, nickel and cobalt (Sarikurkcu et al., 2015).

In summary, the composition of the fungal communities per location complimented some of the results previously described in the geochemistry of the lateritic soils of the peninsula of Santa Elena (Section 4.4.3). Amongst the mountains, CEI and LN, the two locations with the highest amounts of iron and main trace metals, had a different structure largely supported by fungal groups restricted to those two locations. The sample from the mangrove (MAN) had a very distinct fungal composition if compared with the location upstream (DAN), just as observed with their geochemical characterisation, where the mangrove acted as a metal-sink downstream. But in general, the presence of fungal groups that had been previously associated with metal cycling suggests that future work can further address fungal interactions with the lateritic soils in the Santa Elena Peninsula.

### 4.4.5 Microbial communities of the lateritic soils in a landscape context

Finally, all of the prokaryotic and fungal data were analysed using hierarchical clustering analysis to study the relationships between soil microbial ecology and soil origin within the Santa Elena Peninsula (Figure 4.16). Two major groups were clear, the first contained all the mountain

locations but also the lowland in the inner area of the ophiolite (DAN), while the second one included the rest of the lowland samples. This separation could be related to the vegetation because it corresponds, except for DAN location, to the landscape differentiation observed in the Santa Elena Peninsula (Table 4.1) which was proposed using vegetation type as one of the main characteristics of classification. Vegetation strongly influences microbial communities, including both prokaryotes and fungi, in tropical serpentine soils (Bordez et al., 2016; Carriconde et al., 2019; Gourmelon et al., 2016), non-tropical serpentine soils (Branco and Ree, 2010; D'Amico et al., 2015; Touceda-González et al., 2018) and non-serpentine soils in general (Delgado-Baquerizo et al., 2018). However, the differentiation of microbial communities can be associated with abiotic factors too. Altitudinal differences in soil microbial communities were found in subalpine forests of Montana where riparian zones and upland zones differed according to the soil water content (Du et al., 2015); and more generally, pH of soils and soil geochemistry can drive microbial communities both in serpentine and non-serpentine soils (Bordez et al., 2016; Delgado-Baquerizo et al., 2018; Gourmelon et al., 2016; Osborne et al., 2011).

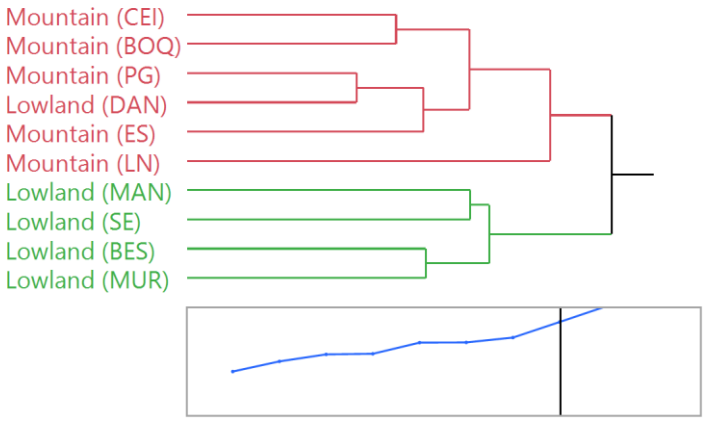


**Figure 4.16.** Hierarchical clustering analysis (HC) of the microbial composition of the lateritic soils in the Santa Elena Peninsula, considering the abundancies of sequences of prokaryotes and fungi, both by phylogenetic class.

In the serpentine soils of Santa Elena Peninsula here sampled, contrary to the geochemistry (Figure 4.13), for the microbial communities the clusters were not as distantly separated (Figure 4.16), mainly because of their relatively large compositional similarities both in the prokaryotic and fungal communities (Figure 4.14, 4.15); however, some relationships warrant comment. The mountain cluster represents a well-preserved group of soils characterised by a relatively high Fe

and trace metals content (Figure 4.11, 4.13), and therefore microorganisms associated with the iron redox cycling. The microbial communities of the mountains BOQ and PG, and lowland DAN had a closer composition to that of the other mountain samples (Figure 4.16) but differed slightly in the geochemistry, yet still close to the mountain samples (inner ophiolite lowland cluster in Figure 4.13), confirming their status as intermediate locations between the mountains and the lowlands. PG in particular was closer to DAN location than any other mountain site, and both were also classified together in terms of their geochemistry (Figure 4.13). This closeness between those two locations could be due to the similarities in altitude and vegetation between both sites (Table 4.1); in fact PG was the only mountain location which vegetation was not dominated by grasses and trees were more abundant and considerably higher (Figure 4.4), highlighting the close association between altitude, vegetation and microbial communities in these serpentine soils.

Within the other lowland samples, towards the northern boundaries of the ophiolite, BES and MUR locations were more similar to each other than to SE (to the northwest) both geochemically and microbiologically (Figure 4.13, 4.16). The mangrove location (MAN) emerged as a very interesting and particular location, geochemically closer to the other sites in the inner ophiolite lowland group (Figure 4.13) however, microbially closer to the other lowlands (Figure 4.16). Also, within the same riparian basin the composition of the microbial community upstream (DAN) was relatively dissimilar to the mangrove location (MAN) downstream (Figure 4.16). Despite having analogous geochemical composition (Figure 4.13), DAN and MAN locations had different vegetation (Table 4.1, Figure 4.4). Thus, the dissimilarity found in this basin of Santa Elena Peninsula suggested that vegetation could have a stronger influence driving soil microbial communities than the geochemical characteristics of the serpentine soils, a trend also observed in other tropical serpentine soils from New Caledonia (Bordez et al., 2016; Gourmelon et al., 2016).

In summary, all these results evidenced how microbial communities in serpentine soils can be affected by variations of biotic factors like vegetation type and coverage, and abiotic factors such as the geochemistry of the soils or the altitude, even within a small geographical area. Thus, despite the unique ecological characteristics of this area, the Santa Elena Peninsula has demonstrated its potential as a model site to study serpentine ecosystems undergone tropical

conditions, but also as an area of interest to understand biogeochemical cycles within various ecological and landscape contexts.

### 4.5 Conclusions

The geochemistry of the lateritic soils in the Santa Elena Peninsula was characterised considering a landscape geographical approach, and to our knowledge this was the first report of both the mineralogy and geochemical composition of the soils associated with the area of the Santa Elena Ophiolite within this context. The soils were Ni-rich laterites, but with geochemical variations depending on their geographical position within the ophiolite area, reflecting differences in the degree of serpentinization in soil-hosted rock clasts associated with different *in situ* weathering processes, and thus resulting in three different lateritic soil types: *mountain* soils, *inner ophiolite lowland* soils and *north lowland* soils. The content of Fe was positively correlated to Ni, Co and Mn, with higher concentrations in the mountain soils. The mountain soils were dominated by lizardite and iron oxide minerals, and the influence of altitude-associated characteristics, as the minor vegetation coverage and thus more direct climate exposure, favoured the concentration of cobalt and nickel in these soils. Even despite sharing the soil classification type in some cases, the lowlands in the inner ophiolite area were geochemically distinct to those at the northern margin of the ophiolite. The lateritic inner ophiolite lowland soils were like the soils present from surrounding mountains, and within a same riparian basin the concentration of trace metals increased downstream with higher concentrations towards the mangrove, acting as a metal-sink area. The north lowland soils had differences in geochemistry but were still influenced by the ophiolite. Therefore, when studying the soils of the Santa Elena Peninsula, both soil classification and also the geochemical composition of the soils should be considered, according to their geographical location within the ophiolite area, especially in inner ophiolite lowland areas or the top of the mountains.

The native microbial communities of these lateritic soils were also studied, and this research was the first to describe, to our knowledge, both the prokaryotic and the fungal composition of the soils associated with the Santa Elena Ophiolite**.** The microbial composition complimented the geochemical separation of the soils depending on the geographical location in the peninsula. In

the mountain locations, richer in Fe and associated trace metals, the abundance of prokaryotes related to Fe-redox cycling was higher, while the fungal communities were less diverse but with groups restricted only to those locations. In the lowlands, Mn-oxidising bacteria were more abundant, but the microbial communities in the inner area of the ophiolite were closer to the mountains soils communities, while those at the boundary were different again. However, the mangrove area of Potrero Grande was microbially closer to the north lowlands, and like with the geochemistry, it was microbially distinct when compared to the upstream location, registering the major abundance of Mn-oxidising bacteria overall and a distinct fungal community. Therefore, the dissimilarities found in the microbial communities of these serpentine soils could be associated with the soil geochemistry but results also suggested that the vegetation coverage could have an important influence driving the microbial communities that must be further studied. Also, in general, prokaryotes were more diverse the soils than fungi, although the large amounts of unclassified fungi indicated specialism in metal concentrated areas, presenting the Santa Elena Peninsula as a hotspot of serpentinization endemism that should be better studied.

The Santa Elena Peninsula has proven to be a unique place to study the relationships between the microbial communities and the geochemistry of lateritic soils and this research will serve as a basis for future work to better understand the role of both prokaryotes and fungi in the biogeochemical cycles of the serpentine soils of this site. Moreover, this study evidenced the complex associations between microbial communities, vegetation and abiotic factors such as the geochemistry of the soils or the altitude, occurring in serpentine environments and under active laterite formation processes due to tropical climate. Therefore, in a wider approach the Santa Elena Peninsula emerges as a potential model site to understand the natural interactions between biotic and abiotic factors occurring in tropical serpentine ecosystems, and more generally, to study the natural biogeochemical cycles of metals such as Fe, Ni, Co, Mn or Cr, under different ecological and landscape contexts.

### 4.6 Funding

This research was developed and funded by the scholarship for the PhD of AFSA granted by the Ministerio de Ciencia, Tecnología y Telecomunicaciones (MICITT) of the Government of Costa

Rica and the Universidad de Costa Rica (UCR). MICITT funded the fieldwork, while the CoG$^3$ Consortium Project (CoG3 NE/M011518/1), funded by the Natural Environment Research Council (NERC), partially supported this investigation through several analyses.

### 4.7 Acknowledgements

We want to thank to María Marta Chavarría Diaz and Róger Blanco Segura from the Research Programme of the ACG for giving the permissions to develop this research in the Santa Rosa National Park and for their support and advice with the sampling logistics during the field campaigns. We are also very grateful to Francisco Solano Soto for transport and logistics support, and general assistance to AFSA in the first field campaign. We want to thank to Paul Lythgoe, Alastair Bewsher, John Waters, Stephen Stockley and Jonathan Fellowes (University of Manchester) for analytical support with XRF, XRD, thin section preparation and EPMA. We also extend our gratitude to Dr. Heather Buss and Dr. Vicky Coker for useful inputs to the final version of this paper. Finally, we want to thank Carlos Rojas, Pedro Rojas and the personnel of Unidad de Recursos Forestales (ReForesta-UCR) for allowing AFSA to use their research laboratories while in Costa Rica. The authors declared that all the biological samples were collected under the authorised permission given to AFSA from the Comisión Nacional para la Gestión de la Biodiversidad Costa Rica (CONAGEBIO) to access the DNA of the samples collected.

### 4.8 References

Algora, C., Wasmund, K., Adrian, L., Trevisan, M., Vasileiadis, S., Krüger, M., Puglisi, E., 2015. Manganese and iron as structuring parameters of microbial communities in Arctic marine sediments from the Baffin Bay. FEMS Microbiol. Ecol. 91. https://doi.org/10.1093/femsec/fiv056

Allen, S.E., 1989. Chemical analysis of ecological materials, 2nd ed. Blackwell Scientific Publications, London.

Alvarado, G.E., Pérez, W., Vogel, T.A., Gröger, H., Patiño, L., 2011. The Cerro Chopo basaltic cone (Costa Rica): An unusual completely reversed graded pyroclastic cone with abundant low vesiculated cannonball juvenile fragments. J. Volcanol. Geotherm. Res. 201, 163–177. https://doi.org/10.1016/j.jvolgeores.2010.11.010

Anacker, B.L., 2011. Phylogenetic patterns of endemism and diversity, in: Harrison, S., Rajakaruna, N. (Eds.), Serpentine: The Evolution and Ecology of a Model System. University of California Press, Berkeley, p. 446.

Babraham Bioinformatics, n.d. FastQC.

Bodin, N., N'Gom-Kâ, R., Kâ, S., Thiaw, O.T., Tito de Morais, L., Le Loc'h, F., Rozuel-Chartier, E., Auger, D., Chiffoleau, J.-F., 2013. Assessment of trace metal contamination in mangrove ecosystems from Senegal, West Africa. Chemosphere 90, 150–157. https://doi.org/10.1016/j.chemosphere.2012.06.019

Bordez, L., Jourand, P., Ducousso, M., Carriconde, F., Cavaloc, Y., Santini, S., Claverie, J.M., Wantiez, L., Leveau, A., Amir, H., 2016. Distribution patterns of microbial communities in ultramafic landscape: a metagenetic approach highlights the strong relationships between diversity and environmental traits. Mol. Ecol. 25, 2258–2272. https://doi.org/10.1111/mec.13621

Borovička, J., Dunn, C.E., Gryndler, M., Mihaljevič, M., Jelínek, E., Rohovec, J., Rohošková, M., Řanda, Z., 2010. Bioaccumulation of gold in macrofungi and ectomycorrhizae from the vicinity of the Mokrsko gold deposit, Czech Republic. Soil Biol. Biochem. 42, 83–91. https://doi.org/10.1016/j.soilbio.2009.10.003

Branco, S., Ree, R.H., 2010. Serpentine Soils Do Not Limit Mycorrhizal Fungal Diversity. PLoS One 5, e11757. https://doi.org/10.1371/journal.pone.0011757

Braun, U., Crous, P.W., Nakashima, C., 2015. Cercosporoid fungi (Mycosphaerellaceae) 3. Species on monocots (Poaceae, true grasses). IMA Fungus 6, 25–97. https://doi.org/10.5598/imafungus.2015.06.01.03

Burns, R.C., 1973. The partitioning of trace transition elements in crystal structures: a provocative review with applications to mantle geochemistry. Geochim. Cosmochim. Acta 37, 2395–2403. https://doi.org/10.1016/0016-7037(73)90287-1

Butt, C.R.M., Cluzel, D., 2013. Nickel Laterite Ore Deposits: Weathered Serpentinites. Elements 9, 123–128. https://doi.org/10.2113/gselements.9.2.123

Caporaso, J.G., Kuczynski, J., Stombaugh, J., Bittinger, K., Bushman, F.D., Costello, E.K., Fierer, N., Peña, A.G., Goodrich, J.K., Gordon, J.I., Huttley, G.A., Kelley, S.T., Knights, D., Koenig, J.E., Ley, R.E., Lozupone, C.A., McDonald, D., Muegge, B.D., Pirrung, M., Reeder, J., Sevinsky, J.R., Turnbaugh, P.J., Walters, W.A., Widmann, J., Yatsunenko, T., Zaneveld, J., Knight, R., 2010. QIIME allows analysis of high-throughput community sequencing data. Nat. Methods 7, 335–336. https://doi.org/10.1038/nmeth.f.303

Caporaso, J.G., Lauber, C.L., Walters, W.A., Berg-Lyons, D., Huntley, J., Fierer, N., Owens, S.M., Betley, J., Fraser, L., Bauer, M., Gormley, N., Gilbert, J.A., Smith, G., Knight, R., 2012. Ultra-high-throughput microbial community analysis on the Illumina HiSeq and MiSeq platforms. Isme J. 6, 1621. https://doi.org/10.1038/ismej.2012.8

Caporaso, J.G., Lauber, C.L., Walters, W.A., Berg-Lyons, D., Lozupone, C.A., Turnbaugh, P.J., Fierer, N., Knight, R., 2011. Global patterns of 16S rRNA diversity at a depth of millions of sequences per sample. Proc. Natl. Acad. Sci. 108, 4516–4522. https://doi.org/10.1073/PNAS.1000080107

Carriconde, F., Gardes, M., Bellanger, J.-M., Letellier, K., Gigante, S., Gourmelon, V., Ibanez, T., McCoy, S., Goxe, J., Read, J., Maggia, L., 2019. Host effects in high ectomycorrhizal diversity tropical rainforests on ultramafic soils in New Caledonia. Fungal Ecol. 39, 201–212. https://doi.org/10.1016/j.funeco.2019.02.006

Crespo-Medina, M., Twing, K.I., Sánchez-Murillo, R., Brazelton, W.J., McCollom, T.M., Schrenk, M.O., 2017. Methane Dynamics in a Tropical Serpentinizing Environment: The Santa Elena Ophiolite, Costa Rica. Front. Microbiol. 8, 916. https://doi.org/10.3389/fmicb.2017.00916

Cuong, D.T., Bayen, S., Wurl, O., Subramanian, K., Shing Wong, K.K., Sivasothi, N., Obbard, J.P., 2005. Heavy metal contamination in mangrove habitats of Singapore. Mar. Pollut. Bull. 50, 1732–1738. https://doi.org/https://doi.org/10.1016/j.marpolbul.2005.09.008

D'Amico, M.E., Freppaz, M., Leonelli, G., Bonifacio, E., Zanini, E., 2015. Early stages of soil development on serpentinite: the proglacial area of the Verra Grande Glacier, Western

Italian Alps. J. Soils Sediments 15, 1292–1310. https://doi.org/10.1007/s11368-014-0893-5

Daims, H., 2014. The Family Nitrospiraceae, in: Rosenberg, E., DeLong, E.F., Lory, S., Stackebrandt, E., Thompson, F. (Eds.), The Prokaryotes, Other Major Lineages of Bacteria and the Archaea. Springer Berlin Heidelberg, Heidelberg, p. 1028. https://doi.org/10.1007/978-3-642-38954-2

Delgado-Baquerizo, M., Oliverio, A.M., Brewer, T.E., Benavent-González, A., Eldridge, D.J., Bardgett, R.D., Maestre, F.T., Singh, B.K., Fierer, N., 2018. A global atlas of the dominant bacteria found in soil. Science (80-. ). 359, 320–325. https://doi.org/10.1126/science.aap9516

Denyer, P., Gazel, E., 2009. The Costa Rican Jurassic to Miocene oceanic complexes: Origin, tectonics and relations. J. South Am. Earth Sci. 28, 429–442. https://doi.org/10.1016/j.jsames.2009.04.010

Ding, B., Li, Z., Qin, Y., 2017. Nitrogen loss from anaerobic ammonium oxidation coupled to Iron(III) reduction in a riparian zone. Environ. Pollut. 231, 379–386. https://doi.org/10.1016/j.envpol.2017.08.027

Du, Z., Riveros-Iregui, D.A., Jones, R.T., McDermott, T.R., Dore, J.E., McGlynn, B.L., Emanuel, R.E., Li, X., 2015. Landscape Position Influences Microbial Composition and Function via Redistribution of Soil Water across a Watershed. Appl. Environ. Microbiol. 81, 8457 LP – 8468. https://doi.org/10.1128/AEM.02643-15

Edgar, R.C., 2013. UPARSE: highly accurate OTU sequences from microbial amplicon reads. Nat. Methods 10, 996–998. https://doi.org/10.1038/nmeth.2604

Edgar, R.C., 2010. Search and clustering orders of magnitude faster than BLAST. Bioinformatics 26, 2460–2461. https://doi.org/10.1093/bioinformatics/btq461

Edgar, R.C., Haas, B.J., Clemente, J.C., Quince, C., Knight, R., 2011. UCHIME improves sensitivity and speed of chimera detection. Bioinformatics 27, 2194–2200. https://doi.org/10.1093/bioinformatics/btr381

Emerson, D., Scott, J.J., Benes, J., Bowden, W.B., 2015. Microbial Iron Oxidation in the Arctic Tundra and Its Implications for Biogeochemical Cycling. Appl. Environ. Microbiol. 81, 8066 LP – 8075. https://doi.org/10.1128/AEM.02832-15

Fonseca, E.F., Baptista Neto, J.A., Silva, C.G., 2013. Heavy metal accumulation in mangrove sediments surrounding a large waste reservoir of a local metallurgical plant, Sepetiba Bay, SE, Brazil. Environ. Earth Sci. 70, 643–650. https://doi.org/10.1007/s12665-012-2148-3

Gadd, G.M., 2007. Geomycology: biogeochemical transformations of rocks, minerals, metals and radionuclides by fungi, bioweathering and bioremediation. Mycol. Res. 111, 3–49. https://doi.org/10.1016/j.mycres.2006.12.001

Gadd, G.M., Bahri-Esfahani, J., Li, Q., Rhee, Y.J., Wei, Z., Fomina, M., Liang, X., 2014. Oxalate production by fungi: significance in geomycology, biodeterioration and bioremediation. Fungal Biol. Rev. https://doi.org/10.1016/j.fbr.2014.05.001

García, D., Stchigel, A.M., Cano, J., Calduch, M., Hawksworth, D.L., Guarro, J., 2006. Molecular phylogeny of Coniochaetales. Mycol. Res. 110, 1271–1289. https://doi.org/10.1016/j.mycres.2006.07.007

Gazel, E., Denyer, P., Baumgartner, P.O., 2006. Magmatic and geotectonic significance of Santa Elena Peninsula, Costa Rica. Geol. Acta 4, 193–202. https://doi.org/10.1344/105.000000365

Ghosh, S., Das, A.P., 2018. Metagenomic insights into the microbial diversity in manganese-contaminated mine tailings and their role in biogeochemical cycling of manganese. Sci. Rep. 8, 8257. https://doi.org/10.1038/s41598-018-26311-w

Gómez, L.D., Herrera, W., 1986. Clave para Macrotipos de Vegetación de Costa Rica [WWW Document]. Veg. y clima Costa Rica. URL http://www.inbio.ac.cr/es/biod/minae/Estudio_Pais/estudio/macrotipos.html

Gong, B., Liu, G., Liao, R., Song, J., Zhang, H., 2017. Endophytic fungus Purpureocillium sp. A5 protect mangrove plant Kandelia candel under copper stress. Brazilian J. Microbiol. 48, 530–536. https://doi.org/10.1016/J.BJM.2016.10.027

Gourmelon, V., Maggia, L., Powell, J.R., Gigante, S., Hortal, S., Gueunier, C., Letellier, K., Carriconde, F., 2016. Environmental and Geographical Factors Structure Soil Microbial Diversity in New Caledonian Ultramafic Substrates: A Metagenomic Approach. PLoS One 11, 1–25. https://doi.org/10.1371/journal.pone.0167405

Greene, A.C., 2014. The Family Desulfurellaceae, in: Rosenberg, E., DeLong, E.F., Lory, S., Stackebrandt, E., Thompson, F. (Eds.), The Prokaryotes: Deltaproteobacteria and Epsilonproteobacteria. Springer Berlin Heidelberg, Berlin, Heidelberg, pp. 135–142. https://doi.org/10.1007/978-3-642-39044-9_312

Gubry-Rangin, C., Kratsch, C., Williams, T.A., McHardy, A.C., Embley, T.M., Prosser, J.I., Macqueen, D.J., 2015. Coupling of diversification and pH adaptation during the evolution of terrestrial Thaumarchaeota. Proc. Natl. Acad. Sci. U. S. A. 112, 9370–9375.

Gweon, H.S., Oliver, A., Taylor, J., Booth, T., Gibbs, M., Read, D.S., Griffiths, R.I., Schonrogge, K., 2015. PIPITS: an automated pipeline for analyses of fungal internal transcribed spacer sequences from the Illumina sequencing platform. Methods Ecol. Evol. 6, 973–980. https://doi.org/10.1111/2041-210X.12399

Haas, B.J., Gevers, D., Earl, A.M., Feldgarden, M., Ward, D. V, Giannoukos, G., Ciulla, D., Tabbaa, D., Highlander, S.K., Sodergren, E., Methé, B., DeSantis, T.Z., Human Microbiome Consortium, T.H.M., Petrosino, J.F., Knight, R., Birren, B.W., 2011. Chimeric 16S rRNA sequence formation and detection in Sanger and 454-pyrosequenced PCR amplicons. Genome Res. 21, 494–504. https://doi.org/10.1101/gr.112730.110

Hallberg, K.B., Grail, B.M., Plessis, C.A. du, Johnson, D.B., 2011. Reductive dissolution of ferric iron minerals: A new approach for bio-processing nickel laterites. Miner. Eng. 24, 620–624. https://doi.org/10.1016/j.mineng.2010.09.005

Hansel, C.M., Learman, D.R., 2016. Geomicrobiology of Manganese, in: Ehrlich, H.L., Newman, D.K., Kappler, A. (Eds.), Ehrlich's Geomicrobiology. CRC Press, pp. 401–452.

Herrera, W., 2016. Climate of Costa Rica, in: Kappelle, M. (Ed.), Costa Rican Ecosystems. The University of Chicago Press, p. 744.

Holloway, C.J., Santos, I.R., Tait, D.R., Sanders, C.J., Rose, A.L., Schnetger, B., Brumsack, H.-J., Macklin, P.A., Sippo, J.Z., Maher, D.T., 2016. Manganese and iron release from mangrove porewaters: A significant component of oceanic budgets? Mar. Chem. 184, 43–52. https://doi.org/10.1016/j.marchem.2016.05.013

Instituto Meteorológico Nacional, n.d. Clima en Costa Rica-Pacífico Norte [WWW Document]. URL https://www.imn.ac.cr/documents/10179/31165/PacificoNorte.pdf/4a0e8960-8c51-4390-8a8d-73d9d825d59b (accessed 1.24.17).

Jiménez M., Q., Carrillo J., E., Kappelle, M., 2016. The Northern Pacific Lowland Seasonal Dry Forest of Ganacaste and the Nicoya Peninsula, in: Kappelle, M. (Ed.), Costa Rican Ecosystems. The University of Chicago Press, p. 744.

Johnson, D.B., du Plessis, C.A., 2015. Biomining in reverse gear: Using bacteria to extract metals from oxidised ores. Miner. Eng. 75, 2–5. https://doi.org/10.1016/j.mineng.2014.09.024

Joshi, N., Fass, J., 2011. Sickle: A sliding-window, adaptive, quality-based trimming tool for FastQ files.

Kabata-Prendias, A., 2001. Trace elements in soils and plants, 3rd ed. CRC Press, Boca Raton, Florida.

Kappler, A., Emerson, D., Gralnick, J.A., Roden, E.E., Muehe, E.M., 2016. Geomicrobiology of Iron, in: Ehrlich, H.L., Newman, D.K., Kappler, A. (Eds.), Ehrlich's Geomicrobiology. CRC Press, pp. 343–399.

Kozich, J.J., Westcott, S.L., Baxter, N.T., Highlander, S.K., Schloss, P.D., 2013. Development of a dual-index sequencing strategy and curation pipeline for analyzing amplicon sequence data on the MiSeq Illumina sequencing platform. Appl. Environ. Microbiol. 79, 5112–5120. https://doi.org/10.1128/AEM.01043-13

Lane, D.J., 1991. 16S/23S rRNA Sequencing, in: Stackebrandt, E., Goodfellow, M. (Eds.), Nucleic AcidTechniques in Bacterial Systematics. Wiley, New York, pp. 115–147.

Lovley, D.R., Holmes, D.E., Nevin, K.P., 2004. Dissimilatory Fe(III) and Mn(IV) Reduction. Adv. Microb. Physiol. 49, 219–286. https://doi.org/10.1016/S0065-2911(04)49005-5

Lücker, S., Daims, H., 2014. The Family Nitrospinaceae, in: Rosenberg, E., DeLong, E.F., Lory, S., Stackebrandt, E., Thompson, F. (Eds.), The Prokaryotes: Deltaproteobacteria and Epsilonproteobacteria. Springer Berlin Heidelberg, Berlin, Heidelberg, pp. 231–237. https://doi.org/10.1007/978-3-642-39044-9_402

Machado, W., Silva-Filho, E. V, Oliveira, R.R., Lacerda, L.D., 2002. Trace metal retention in mangrove ecosystems in Guanabara Bay, SE Brazil. Mar. Pollut. Bull. 44, 1277–1280. https://doi.org/10.1016/S0025-326X(02)00232-1

Madrigal, P., Gazel, E., Denyer, P., Smith, I., Jicha, B., Flores, K.E., Coleman, D., Snow, J., 2015. A melt-focusing zone in the lithospheric mantle preserved in the Santa Elena Ophiolite, Costa Rica. Lithos 230, 189–205. https://doi.org/10.1016/j.lithos.2015.04.015

Marchand, C., Fernandez, J.-M., Moreton, B., 2016. Trace metal geochemistry in mangrove sediments and their transfer to mangrove plants (New Caledonia). Sci. Total Environ. 562, 216–227. https://doi.org/10.1016/j.scitotenv.2016.03.206

Marchand, C., Fernandez, J.-M., Moreton, B., Landi, L., Lallier-Vergès, E., Baltzer, F., 2012. The partitioning of transitional metals (Fe, Mn, Ni, Cr) in mangrove sediments downstream of a ferralitized ultramafic watershed (New Caledonia). Chem. Geol. 300–301, 70–80. https://doi.org/10.1016/j.chemgeo.2012.01.018

Marín Guzmán, F., 1985. Levantamiento geoquímico regional de la hoja Liberia 1:200.000 (Costa Rica). Rev. Geológica América Cent. 1–21. https://doi.org/10.15517/rgac.v0i02.10479

Marrero, J., Coto, O., Schippers, A., 2017. Anaerobic and aerobic reductive dissolutions of iron-rich nickel laterite overburden by Acidithiobacillus. Hydrometallurgy 168, 49–55. https://doi.org/10.1016/J.HYDROMET.2016.08.012

Martin, M., 2011. Cutadapt removes adapter sequences from high-throughput sequencing reads. EMBnet.journal 17, 10–12. https://doi.org/10.14806/ej.17.1.200

Masella, A.P., Bartram, A.K., Truszkowski, J.M., Brown, D.G., Neufeld, J.D., 2012. PANDAseq: paired-end assembler for Illumina sequences. BMC Bioinformatics 13, 31. https://doi.org/10.1186/1471-2105-13-31

Medina, W., 2014. Capas SIG - Área de Conservación Guanacaste [WWW Document]. URL https://www.acguanacaste.ac.cr/biodesarrollo/sistemas-de-informacion-geografica/capas-sig (accessed 2.19.19).

Medina, W., 1999a. Suelos: Hoja Liberia - Area de Conservación Guanacaste [WWW Document]. Sist. Inf. Geográfica - Área Conserv. Guanacaste. URL http://www.investigadoresacg.org/IMAGES/MAPFILES/maps/physical_biological/suelos_acg.jpg (accessed 12.11.16).

Medina, W., 1999b. Geología: Hoja Liberia - Area de Conservación Guanacaste [WWW Document]. Sist. Inf. Geográfica - Área Conserv. Guanacaste. URL http://www.investigadoresacg.org/IMAGES/MAPFILES/maps/physical_biological/geologia_acg.jpg (accessed 12.11.16).

Medina, W., 1999c. Tipos de vegetación: Hoja Liberia - Area de Conservación Guanacaste [WWW Document]. Sist. Inf. Geográfica - Área Conserv. Guanacaste. URL http://www.investigadoresacg.org/IMAGES/MAPFILES/maps/physical_biological/vegetacion_acg.jpg (accessed 12.11.16).

Nath, B., Birch, G., Chaudhuri, P., 2013. Trace metal biogeochemistry in mangrove ecosystems: A comparative assessment of acidified (by acid sulfate soils) and non-acidified sites. Sci. Total Environ. 463–464, 667–674. https://doi.org/10.1016/j.scitotenv.2013.06.024

Noël, V., Morin, G., Juillot, F., Marchand, C., Brest, J., Bargar, J.R., Muñoz, M., Marakovic, G., Ardo, S., Brown, G.E., 2015. Ni cycling in mangrove sediments from New Caledonia. Geochim. Cosmochim. Acta 169, 82–98. https://doi.org/10.1016/j.gca.2015.07.024

Nurk, S., Bankevich, A., Antipov, D., Gurevich, A.A., Korobeynikov, A., Lapidus, A., Prjibelski, A.D., Pyshkin, A., Sirotkin, A., Sirotkin, Y., Stepanauskas, R., Clingenpeel, S.R., Woyke, T., Mclean, J.S., Lasken, R., Tesler, G., Alekseyev, M.A., Pevzner, P.A., 2013. Assembling single-cell genomes and mini-metagenomes from chimeric MDA products. J. Comput. Biol. 20, 714–737. https://doi.org/10.1089/cmb.2013.0084

Osborne, C.A., Zwart, A.B., Broadhurst, L.M., Young, A.G., Richardson, A.E., 2011. The influence of sampling strategies and spatial variation on the detected soil bacterial communities under three different land-use types. FEMS Microbiol. Ecol. 78, 70–79. https://doi.org/10.1111/j.1574-6941.2011.01105.x

QGIS Development Team, 2019. QGIS Geographic Information System.

Reeves, R.D., Baker, A.J.M., Borhidi, A., Berazaín, R., 1999. Nickel Hyperaccumulation in the Serpentine Flora of Cuba. Ann. Bot. 83, 29–38. https://doi.org/10.1006/anbo.1998.0786

Reeves, R.D., Baker, A.J.M., Romero, R., 2007. The ultramafic flora of the Santa Elena peninsula, Costa Rica: A biogeochemical reconnaissance. J. Geochemical Explor. 93, 153–159. https://doi.org/10.1016/j.gexplo.2007.04.002

Roberts, S., Gunn, G., 2014. Cobalt, in: Gunn, G. (Ed.), Critical Metals Handbook. John Wiley & Sons, Oxford, pp. 122–149. https://doi.org/10.1002/9781118755341.ch6

Sánchez-Murillo, R., Gazel, E., Schwarzenbach, E.M., Crespo-Medina, M., Schrenk, M.O., Boll, J., Gill, B.C., 2014. Geochemical evidence for active tropical serpentinization in the Santa Elena Ophiolite, Costa Rica: An analog of a humid early Earth? Geochemistry, Geophys. Geosystems 15, 1783–1800. https://doi.org/10.1002/2013GC005213

Sarikurkcu, C., Tepe, B., Kocak, M.S., Uren, M.C., 2015. Metal concentration and antioxidant activity of edible mushrooms from Turkey. Food Chem. 175, 549–555. https://doi.org/10.1016/j.foodchem.2014.12.019

SAS Institute Inc, 2018. JMP.

Schwarzenbach, E.M., Gill, B.C., Gazel, E., Madrigal, P., 2016. Sulfur and carbon geochemistry of the Santa Elena peridotites: Comparing oceanic and continental processes during peridotite alteration. Lithos 252, 92–108. https://doi.org/10.1016/j.lithos.2016.02.017

Soil Survey Staff, 2014. Keys to Soil Taxonomy, 12th ed. USDA-Natural Resources Conservation Service, Washington D.C.

Stieglmeier, M., Alves, R.J.E., Schleper, C., 2014. The Phylum Thaumarchaeota, in: Rosenberg, E., DeLong, E.F., Lory, S., Stackebrandt, E., Thompson, F. (Eds.), The Prokaryotes, Other Major Lineages of Bacteria and the Archaea. Springer Berlin Heidelberg, Heidelberg, p.

1028. https://doi.org/10.1007/978-3-642-38954-2

Stosch, H.-G., 1981. Sc, Cr, Co and Ni partitioning between minerals from spinel peridotite xenoliths. Contrib. to Mineral. Petrol. 78, 166–174. https://doi.org/10.1007/BF00373778

Taboada, T., Ferro-Vázquez, C., Stoops, G., Martínez-Cortizas, A., Rodríguez-Flores, R., Rodríguez-Lado, L., 2019. Secondary aluminium, iron and silica phases across a volcanic soil climosequence, Galápagos Islands. Eur. J. Soil Sci. 70, 540–549. https://doi.org/10.1111/ejss.12788

Taboada, T., Rodríguez-Lado, L., Ferro-Vázquez, C., Stoops, G., Martínez Cortizas, A., 2016. Chemical weathering in the volcanic soils of Isla Santa Cruz (Galápagos Islands, Ecuador). Geoderma 261, 160–168. https://doi.org/https://doi.org/10.1016/j.geoderma.2015.07.019

Taylor, D.L., Walters, W.A., Lennon, N.J., Bochicchio, J., Krohn, A., Caporaso, J.G., Pennanen, T., 2016. Accurate Estimation of Fungal Diversity and Abundance through Improved Lineage-Specific Primers Optimized for Illumina Amplicon Sequencing. Appl. Environ. Microbiol. 82, 7217–7226. https://doi.org/10.1128/AEM.02576-16

Thorne, R.L., Roberts, S., Herrington, R., 2012. Climate change and the formation of nickel laterite deposits. Geology 40, 331–334. https://doi.org/10.1130/G32549.1

Touceda-González, M., Kidd, P.S., Smalla, K., Prieto-Fernández, A., 2018. Bacterial communities in the rhizosphere of different populations of the Ni-hyperaccumulator Alyssum serpyllifolium and the metal-excluder Dactylis glomerata growing in ultramafic soils. Plant Soil 431, 317–332. https://doi.org/10.1007/s11104-018-3767-6

Treude, N., Rosencrantz, D., Liesack, W., Schnell, S., 2003. Strain FAc12, a dissimilatory iron-reducing member of the Anaeromyxobacter subgroup of Myxococcales. FEMS Microbiol. Ecol. 44, 261–269. https://doi.org/https://doi.org/10.1016/S0168-6496(03)00048-5

Videira, S.I.R., Groenewald, J.Z., Nakashima, C., Braun, U., Barreto, R.W., de Wit, P.J.G.M., Crous, P.W., 2017. Mycosphaerellaceae – Chaos or clarity? Stud. Mycol. 87, 257–421. https://doi.org/10.1016/J.SIMYCO.2017.09.003

Wang, Q., Garrity, G.M., Tiedje, J.M., Cole, J.R., 2007. Naive Bayesian classifier for rapid assignment of rRNA sequences into the new bacterial taxonomy. Appl. Environ. Microbiol. 73, 5261–5267. https://doi.org/10.1128/AEM.00062-07

Whattam, S.A., Gazel, E., Yi, K., Denyer, P., 2016. Origin of plagiogranites in oceanic complexes: A case study of the Nicoya and Santa Elena terranes, Costa Rica. Lithos 262, 75–87. https://doi.org/10.1016/j.lithos.2016.06.017

Whitman, W.B., Bowen, T.L., Boone, D.R., 2014. The Methanogenic Bacteria, in: Rosenberg, E., DeLong, E.F., Lory, S., Stackebrandt, E., Thompson, F. (Eds.), The Prokaryotes: Other Major Lineages of Bacteria and The Archaea. Springer Berlin Heidelberg, Berlin, Heidelberg, pp. 123–163. https://doi.org/10.1007/978-3-642-38954-2_407

Yang, W., Zhang, Zhen, Zhang, Zhongming, Chen, H., Liu, J., Ali, M., Liu, F., Li, L., 2013. Population structure of manganese-oxidizing bacteria in stratified soils and properties of manganese oxide aggregates under manganese-complex medium enrichment. PLoS One 8, e73778–e73778. https://doi.org/10.1371/journal.pone.0073778

## 4.9 Supplementary figures

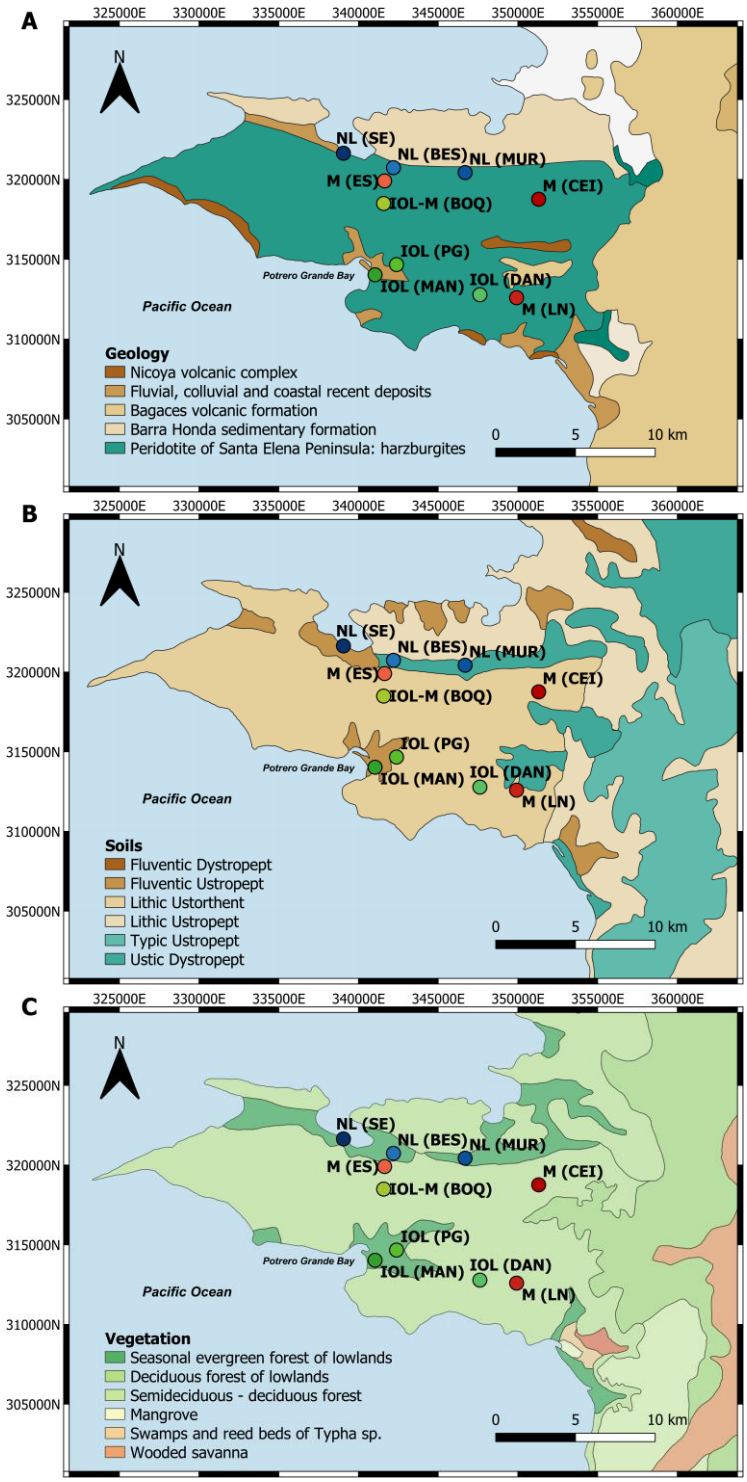


**Figure 4.S1.** Geographical distribution of the 10 locations sampled within the maps of the geology (A), soils (B) and vegetation (C) of the Santa Elena Peninsula. Colour code is based on hierarchical clustering analysis (Figure 4.13): red-to-orange colours assigned to mountain (M) landscapes, green colours to inner ophiolite lowlands (IOL) and light-to-dark blue colours to north lowlands (NL). Maps adapted from Medina (1999a, 1999b, 1999c).

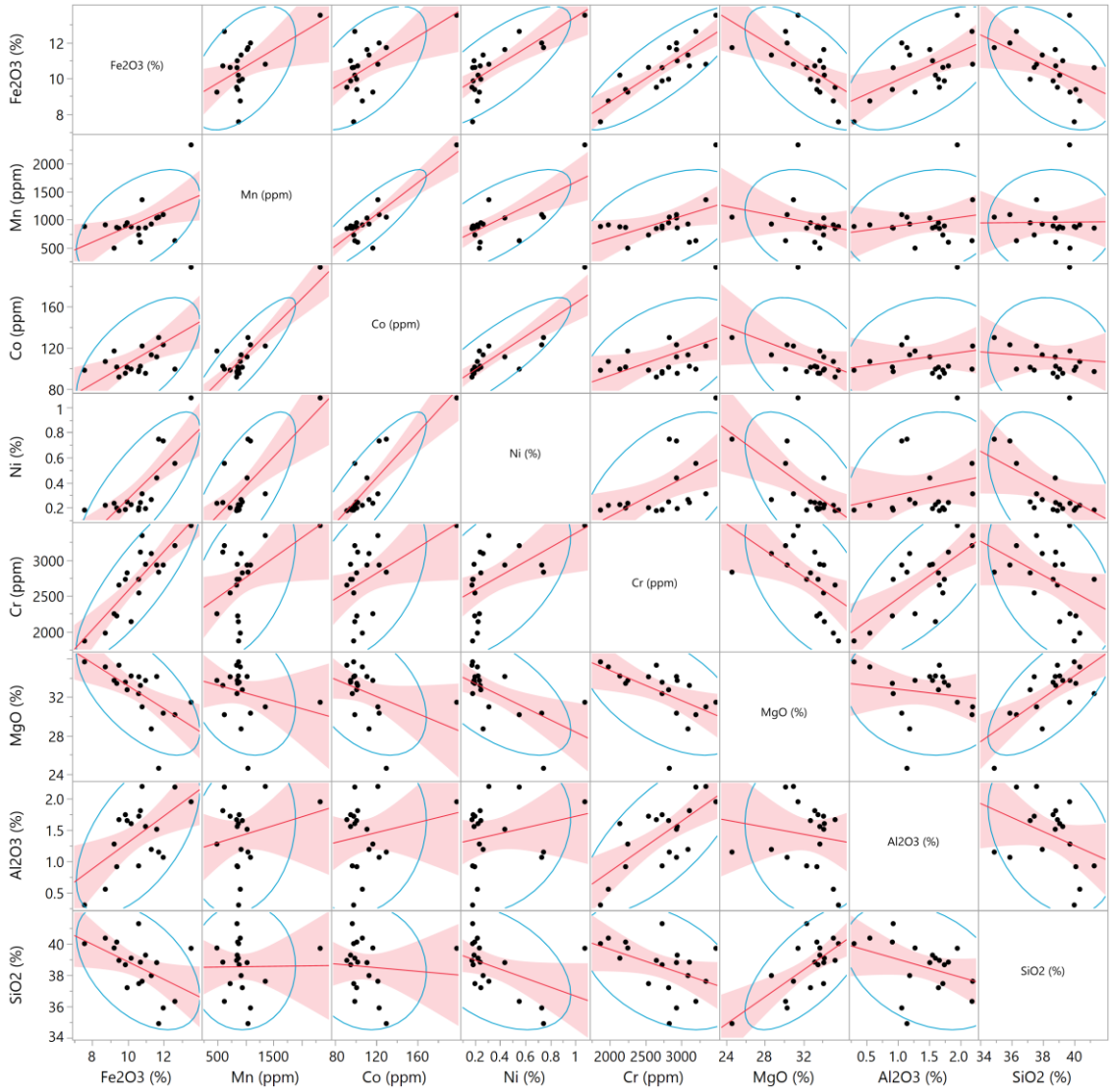


**Figure 4.S2.** Bulk elemental correlations in serpentinized rocks from the peninsula of Santa Elena for Fe, Mn, Co, Ni, Cr, Mg, Al, and Si, all of them analysed by XRF. All the rocks collected were considered for the analysis (α=95% for density ellipses and confidence curves).

**Table 4.S1**. Linear correlations and probabilities associated for the Fe, Mn, Co, Ni, Cr, Mg, Al and Si found in serpentinized rocks from the peninsula of Santa Elena, all of them analysed by XRF.

| **Corr.** | **$Fe_2O_3$** | **Mn** | **Co** | **Ni** | **Cr** | **MgO** | **$Al_2O_3$** | **$SiO_2$** |
|---|---|---|---|---|---|---|---|---|
| $Fe_2O_3$ | 1.0000 | 0.5112 | 0.5959 | 0.7790 | 0.8428 | -0.6234 | 0.5784 | -0.4802 |
| Mn | 0.5112 | 1.0000 | 0.8765 | 0.7175 | 0.4670 | -0.2330 | 0.2066 | 0.0113 |
| Co | 0.5959 | 0.8765 | 1.0000 | 0.8530 | 0.4655 | -0.3960 | 0.1864 | -0.0853 |
| Ni | 0.7790 | 0.7175 | 0.8530 | 1.0000 | 0.5448 | -0.5949 | 0.2235 | -0.4386 |
| Cr | 0.8428 | 0.4670 | 0.4655 | 0.5448 | 1.0000 | -0.5367 | 0.7139 | -0.4280 |
| MgO | -0.6234 | -0.2330 | -0.3960 | -0.5949 | -0.5367 | 1.0000 | -0.1466 | 0.7012 |
| $Al_2O_3$ | 0.5784 | 0.2066 | 0.1864 | 0.2235 | 0.7139 | -0.1466 | 1.0000 | -0.3575 |
| $SiO_2$ | -0.4802 | 0.0113 | -0.0853 | -0.4386 | -0.4280 | 0.7012 | -0.3575 | 1.0000 |
| **Prob.** | **$Fe_2O_3$** | **Mn** | **Co** | **Ni** | **Cr** | **MgO** | **$Al_2O_3$** | **$SiO_2$** |
| $Fe_2O_3$ | <.0001 | 0.0253 | 0.0071 | <.0001 | <.0001 | 0.0043 | 0.0095 | 0.0375 |
| Mn | 0.0253 | <.0001 | <.0001 | 0.0005 | 0.0438 | 0.3372 | 0.3961 | 0.9634 |
| Co | 0.0071 | <.0001 | <.0001 | <.0001 | 0.0446 | 0.0933 | 0.4448 | 0.7284 |
| Ni | <.0001 | 0.0005 | <.0001 | <.0001 | 0.0159 | 0.0072 | 0.3576 | 0.0603 |
| Cr | <.0001 | 0.0438 | 0.0446 | 0.0159 | <.0001 | 0.0178 | 0.0006 | 0.0675 |
| MgO | 0.0043 | 0.3372 | 0.0933 | 0.0072 | 0.0178 | <.0001 | 0.5494 | 0.0008 |
| $Al_2O_3$ | 0.0095 | 0.3961 | 0.4448 | 0.3576 | 0.0006 | 0.5494 | <.0001 | 0.1329 |
| $SiO_2$ | 0.0375 | 0.9634 | 0.7284 | 0.0603 | 0.0675 | 0.0008 | 0.1329 | <.0001 |

All the rocks collected were considered for the analysis. For correlations blue indicates the positive ones and red the negative ones. For probabilities, coloured numbers indicate $p<0.05$.

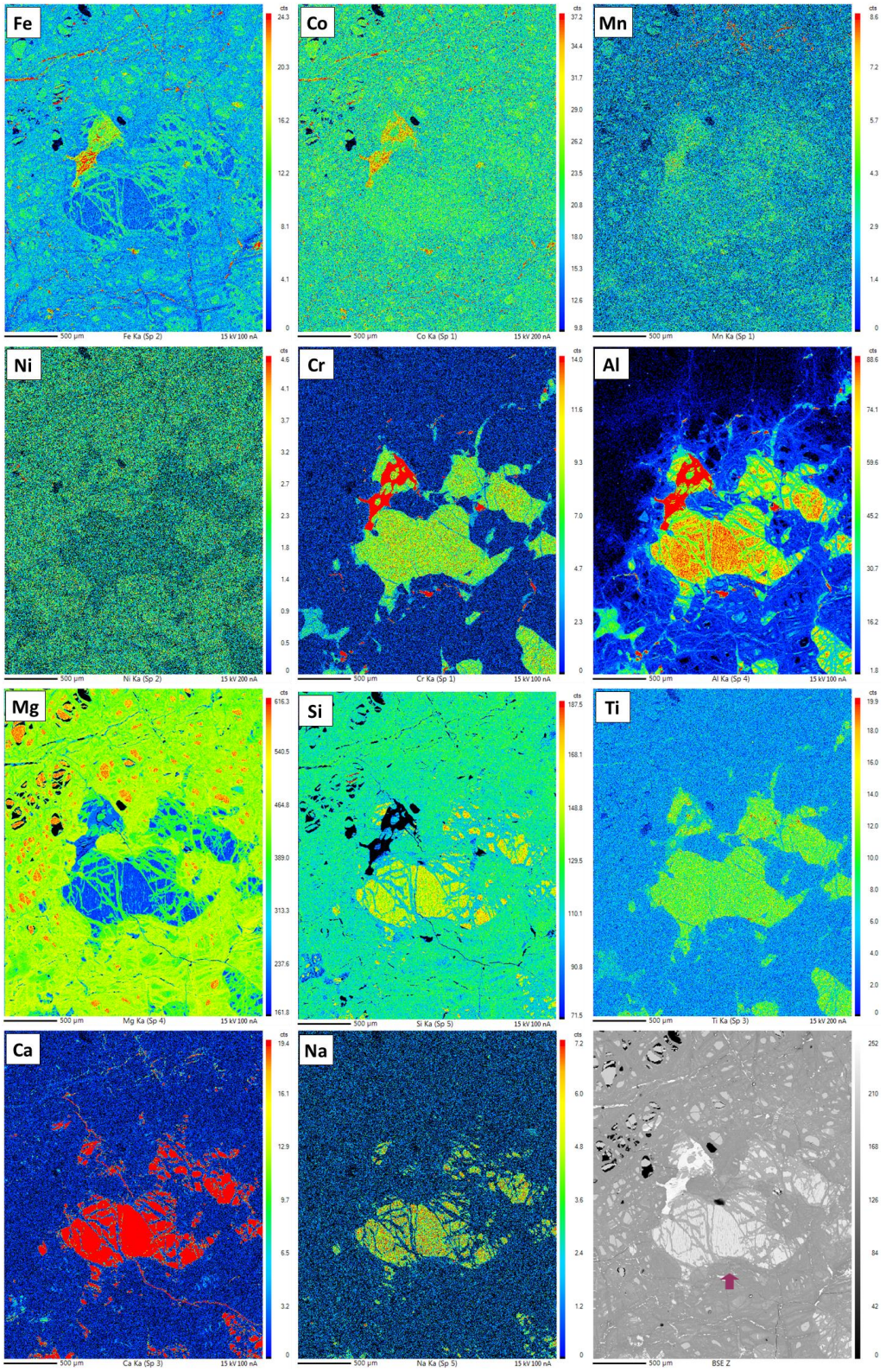


**Figure 4.S3.** Elemental distribution determined on a polished thin section of a serpentinite clast from 10 cm depth (Lowland site MAN), defined by EPMA. The area includes that covered by Figure 4.7B (rotated 90° clockwise). Count intensity colour scale (right of each micrograph) decreases downwards; scale 500 µm.

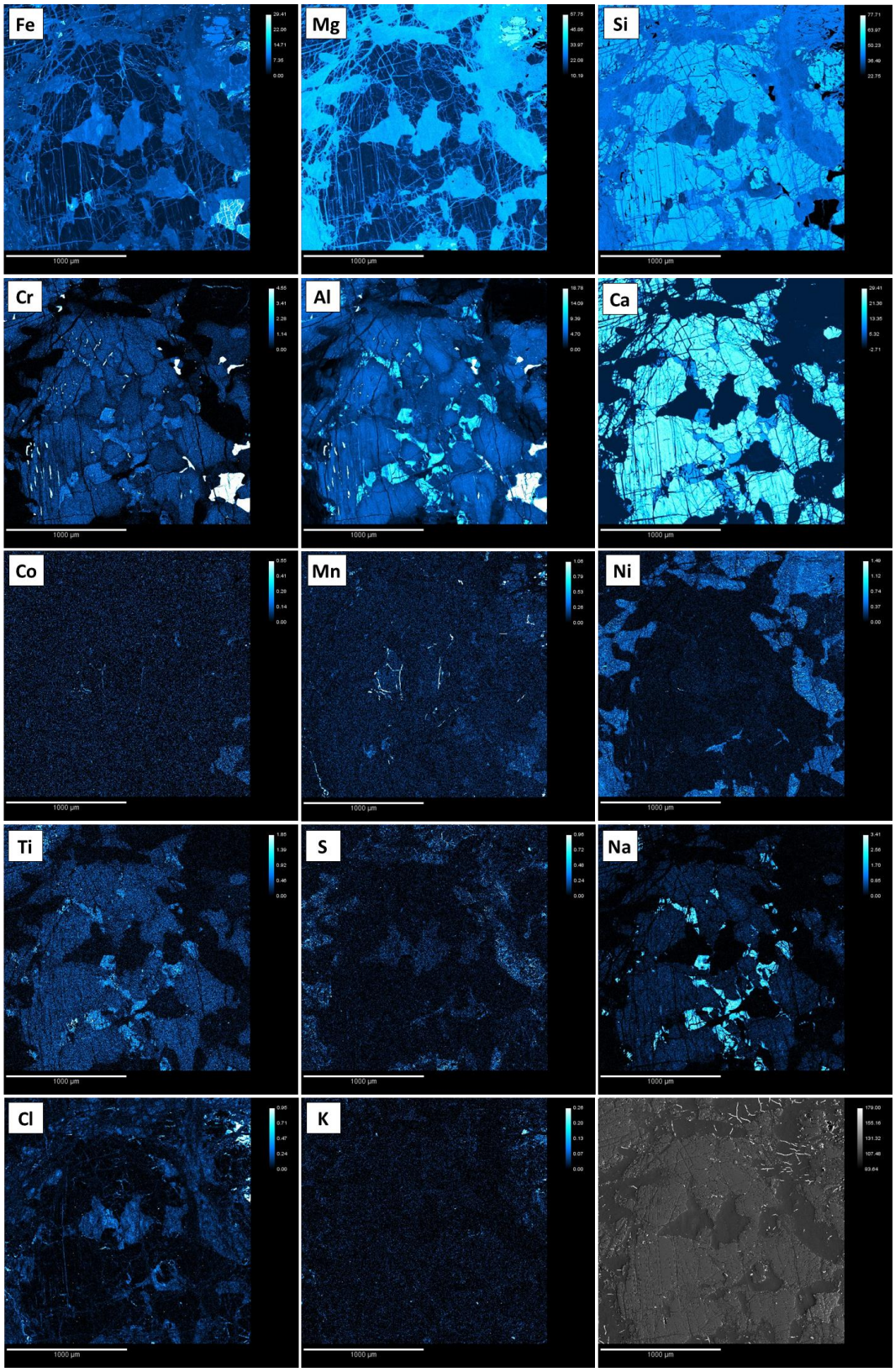


**Figure 4.S4.** Elemental distribution determined on a polished thin section of a rock from an outcrop close to Mountain CEI location, defined by EPMA. The area includes that covered by Figure 4.7C (rotated 90° counterclockwise). Count intensity colour scale (right of each micrograph) decreases downwards; scale 1000 µm.

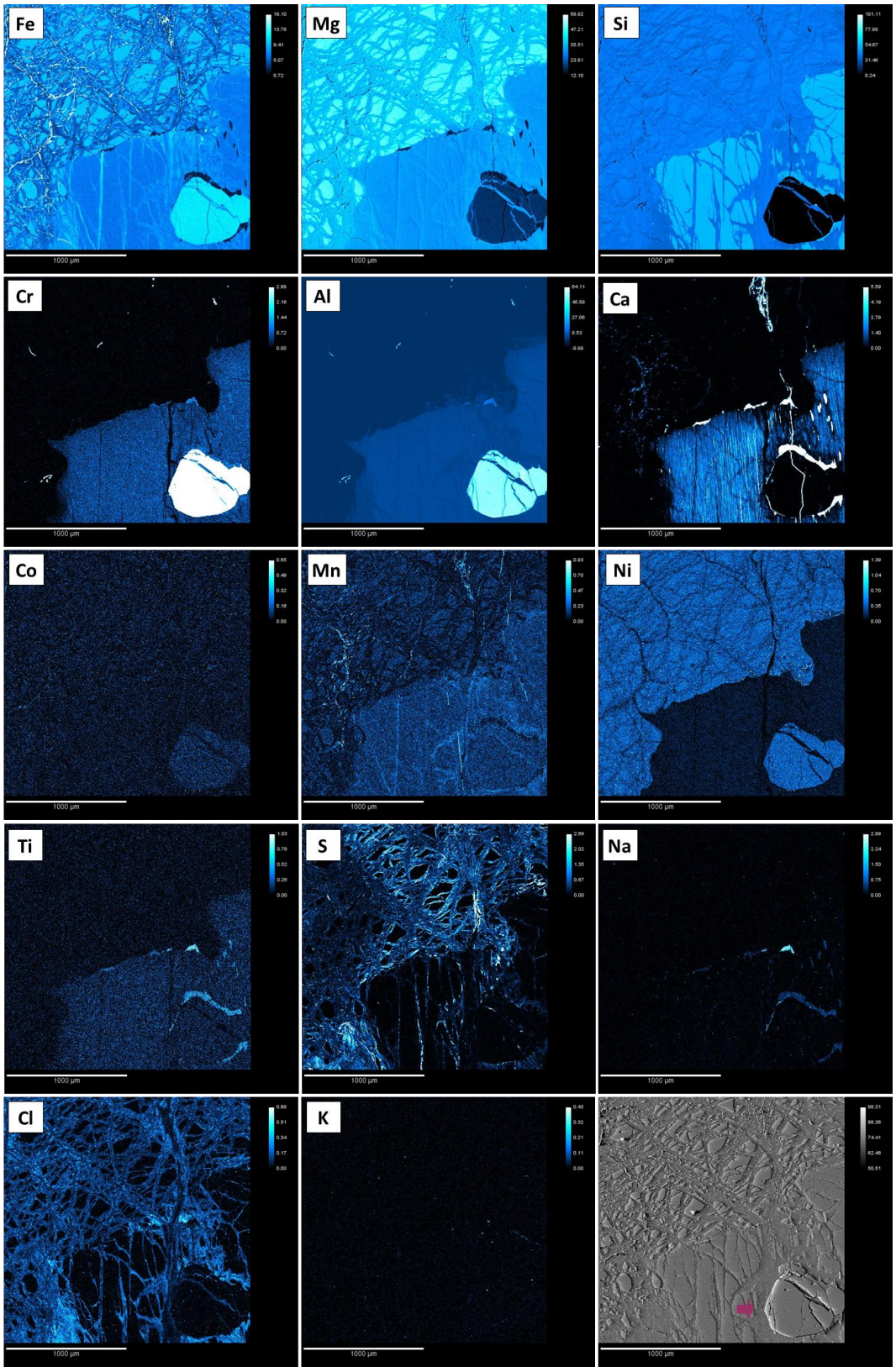


**Figure 4.S5.** Elemental distribution determined on a polished thin section of a rock from an outcrop close to Lowland BES location, defined by EPMA. The area includes that covered by Figure 4.7D (rotated 90° clockwise). Count intensity colour scale (right of each micrograph) decreases downwards; scale 1000 µm.

**Table 4.S2.** Elemental geochemical composition of the lateritic soils from 10 locations of the peninsula of Santa Elena, analysed by XRF majors (%) and traces (ppm).

| Site | $Fe_2O_3$ (%) | MgO (%) | $SiO_2$ (%) | $Al_2O_3$ (%) | CaO (%) | $TiO_2$ (%) | $Na_2O$ (%) | MnO (%) | Ni (%) | Cr (%) |
|---|---|---|---|---|---|---|---|---|---|---|
| Mountain (CEI) | 41.6 ± 9.5 | 9.0 ± 6.4 | 23.8 ± 7.3 | 4.4 ± 2.5 | 0.22 ± 0.05 | 0.17 ± 0.09 | 0.05 ± 0.01 | 0.51 ± 0.11 | 1.26 ± 0.14 | 0.92 ± 0.28 |
| Mountain (LN) | 27.2 ± 5.0 | 16.7 ± 2.8 | 32.9 ± 2.9 | 2.5 ± 0.3 | 0.28 ± 0.08 | 0.09 ± 0.01 | 0.02 ± 0.04 | 0.34 ± 0.07 | 1.18 ± 0.19 | 0.75 ± 0.08 |
| Mountain (PG) | 25.7 ± 6.2 | 13.3 ± 4.1 | 31.0 ± 3.8 | 5.6 ± 1.6 | 0.45 ± 0.16 | 0.20 ± 0.09 | 0.02 ± 0.03 | 0.35 ± 0.05 | 0.68 ± 0.08 | 0.68 ± 0.17 |
| Mountain (ES) | 27.0 ± 2.0 | 14.8 ± 1.9 | 33.7 ± 1.5 | 5.0 ± 0.9 | 0.14 ± 0.02 | 0.12 ± 0.04 | 0.04 ± 0.01 | 0.32 ± 0.05 | 0.84 ± 0.11 | 0.76 ± 0.04 |
| Mountain (BOQ) | 17.7 ± 3.2 | 15.0 ± 11.5 | 35.8 ± 2.7 | 13.6 ± 10.4 | 0.47 ± 0.22 | 0.57 ± 0.48 | 0.06 ± 0.01 | 0.24 ± 0.03 | 0.41 ± 0.22 | 0.29 ± 0.04 |
| Lowland (DAN) | 18.7 ± 3.5 | 22.1 ± 5.3 | 36.7 ± 1.6 | 6.6 ± 2.6 | 0.95 ± 0.30 | 0.25 ± 0.10 | 0.13± 0.05 | 0.26 ± 0.04 | 0.49 ± 0.05 | 0.59 ± 0.16 |
| Lowland (MAN) | 18.4 ± 0.4 | 15.3 ± 0.5 | 39.2 ± 1.0 | 8.5 ± 0.3 | 2.35 ± 0.22 | 0.46 ± 0.10 | 0.22 ± 0.04 | 0.48 ± 0.06 | 0.55 ± 0.01 | 0.73 ± 0.15 |
| Lowland (BES) | 24.9 ± 0.5 | 4.4 ± 1.4 | 32.9 ± 1.1 | 16.1 ± 1.5 | 1.64 ± 0.14 | 0.90 ± 0.03 | 0.14± 0.03 | 0.46 ± 0.01 | 0.38 ± 0.05 | 0.68 ± 0.01 |
| Lowland (MUR) | 19.1 ± 0.8 | 3.3 ± 0.6 | 35.8 ± 0.6 | 21.5 ± 1.5 | 1.70 ± 0.35 | 1.00 ± 0.11 | 0.13 ± 0.03 | 0.30 ± 0.01 | 0.24 ± 0.02 | 0.28 ± 0.07 |
| Lowland (SE) | 16.4± 0.5 | 10.4 ± 0.5 | 41.6 ± 0.1 | 13.8 ± 0.3 | 3.85 ± 0.19 | 0.77 ± 0.03 | 0.89 ± 0.03 | 0.272 ± 0.003 | 0.18 ± 0.01 | 0.185 ± 0.003 |

All soils are high in iron oxides

**Continuation. Table 4.S2.** Elemental geochemical composition of the lateritic soils from 10 locations of the peninsula of Santa Elena, analysed by XRF majors (%) and traces (ppm).

| Site | Co (ppm) | V (ppm) | Zn (ppm) | Cu (ppm) | Ba (ppm) | Te (ppm) | Sc (ppm) | Sr (ppm) | Zr (ppm) | I (ppm) |
|---|---|---|---|---|---|---|---|---|---|---|
| Mountain (CEI) | 359 ± 42 | 135 ± 53 | 131 ± 28 | 83 ± 27 | 74 ± 25 | 61 ± 2 | 33 ± 10 | 19 ± 4 | 22 ± 14 | 36 ± 8 |
| Mountain (LN) | 289 ± 60 | 116 ± 8 | 107 ± 5 | 56 ± 7 | 59 ± 17 | 59 ± 3 | 23 ± 1 | 17 ± 11 | 7 ± 1 | 11 ± 10 |
| Mountain (PG) | 219 ± 41 | 120 ± 39 | 79 ± 14 | 68 ± 14 | 60 ± 7 | 55 ± 3 | 28 ± 7 | 15 ± 4 | 16 ± 7 | 13 ± 4 |
| Mountain (ES) | 253 ± 31 | 98 ± 9 | 70 ± 8 | 59 ± 27 | 34 ± 10 | 55 ± 3 | 32 ± 5 | 7 ± 1 | 4 ± 1 | 18 ± 3 |
| Mountain (BOQ) | 125 ± 48 | 181 ± 104 | 48 ± 14 | 74 ± 29 | 46 ± 22 | 52 ± 2 | 32 ± 16 | 14 ± 15 | 35 ± 33 | 12 ± 8 |
| Lowland (DAN) | 163 ± 20 | 117 ± 39 | 85 ± 17 | 55 ± 19 | 102 ± 35 | 51 ± 2 | 19 ± 5 | 30 ± 23 | 23 ± 12 | 12 2 |
| Lowland (MAN) | 250 ± 22 | 160 ± 8 | 126 ± 25 | 64 ± 13 | 95 ± 12 | 52 ± 3 | 25 ± 1 | 21 ± 2 | 25 ± 1 | 0 |
| Lowland (BES) | 197 ± 4 | 254 ± 25 | 118 ± 9 | 110 ± 9 | 175 ± 11 | 55 ± 1 | 39 ± 3 | 43 ± 7 | 74 ± 10 | 26 ± 2 |
| Lowland (MUR) | 102 ± 7 | 290 ± 6 | 58 ± 9 | 106 ± 7 | 159 ± 7 | 53 ± 2 | 44 ± 2 | 42 ± 10 | 77 ± 5 | 14 ± 1 |
| Lowland (SE) | 94 ± 3 | 196 ± 4 | 86 ± 3 | 103 ± 7 | 59 ± 2 | 52 ± 1 | 29.7 ± 0.1 | 77 ± 3 | 53 ± 1 | 8 ± 2 |

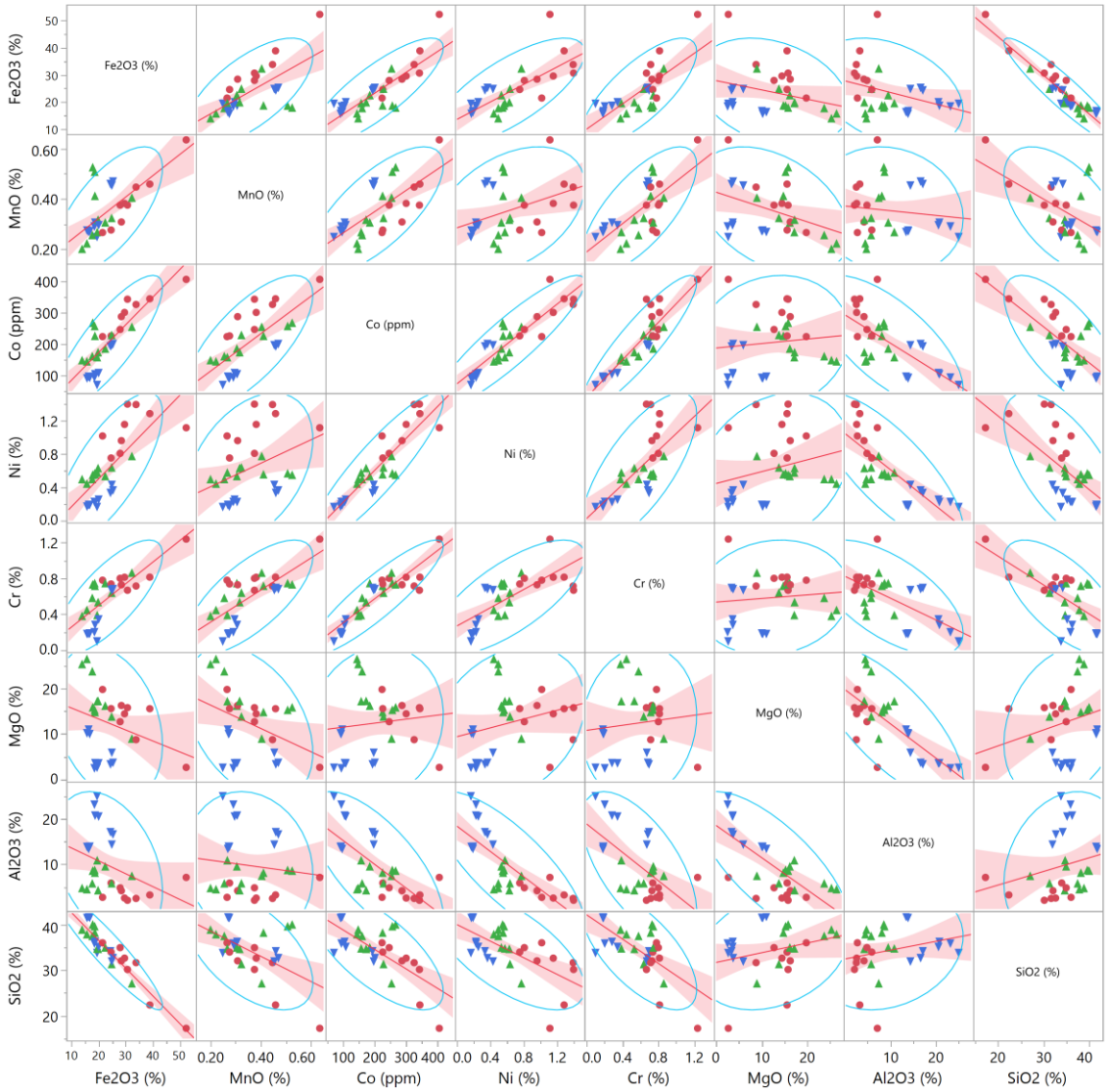


**Figure 4.S6.** Bulk elemental correlations in lateritic soils from the peninsula of Santa Elena for Fe, Mn, Co, Ni, Cr, Mg, Al, and Si, all of them analysed by XRF. All the soil samples collected were considered for the analysis (α=95% for density ellipses and confidence curves). Correlations and probabilities are shown in Table 4.S3. Markers correspond to clusters of Figure 4.13: mountain soils (●), inner ophiolite lowland soils (▲) and north lowland soils (▼).

**Table 4.S3.** Linear correlations and probabilities associated for the Fe, Mn, Co, Ni, Cr, Mg, Al and Si found in lateritic soils from the peninsula of Santa Elena, all of them analysed by XRF.

| Corr. | $Fe_2O_3$ | Mn | Co | Ni | Cr | MgO | $Al_2O_3$ | $SiO_2$ |
|---|---|---|---|---|---|---|---|---|
| $Fe_2O_3$ | 1.0000 | 0.6661 | 0.8229 | 0.7339 | 0.7505 | -0.2871 | -0.3478 | -0.9319 |
| Mn | 0.6661 | 1.0000 | 0.7099 | 0.3940 | 0.7096 | -0.3890 | -0.1192 | -0.5399 |
| Co | 0.8229 | 0.7099 | 1.0000 | 0.8986 | 0.8951 | 0.1121 | -0.6862 | -0.6993 |
| Ni | 0.7339 | 0.3940 | 0.8986 | 1.0000 | 0.7201 | 0.2619 | -0.7775 | -0.6340 |
| Cr | 0.7505 | 0.7096 | 0.8951 | 0.7201 | 1.0000 | 0.1056 | -0.6167 | -0.6555 |
| MgO | -0.2871 | -0.3890 | 0.1121 | 0.2619 | 0.1056 | 1.0000 | -0.7302 | 0.2731 |
| $Al_2O_3$ | -0.3478 | -0.1192 | -0.6862 | -0.7775 | -0.6167 | -0.7302 | 1.0000 | 0.2409 |
| $SiO_2$ | -0.9319 | -0.5399 | -0.6993 | -0.6340 | -0.6555 | 0.2731 | 0.2409 | 1.0000 |

| Prob. | $Fe_2O_3$ | Mn | Co | Ni | Cr | MgO | $Al_2O_3$ | $SiO_2$ |
|---|---|---|---|---|---|---|---|---|
| $Fe_2O_3$ | <.0001 | <.0001 | <.0001 | <.0001 | <.0001 | 0.1240 | 0.0596 | <.0001 |
| Mn | <.0001 | <.0001 | <.0001 | 0.0312 | <.0001 | 0.0336 | 0.5303 | 0.0021 |
| Co | <.0001 | <.0001 | <.0001 | <.0001 | <.0001 | 0.5553 | <.0001 | <.0001 |
| Ni | <.0001 | 0.0312 | <.0001 | <.0001 | <.0001 | 0.1621 | <.0001 | 0.0002 |
| Cr | <.0001 | <.0001 | <.0001 | <.0001 | <.0001 | 0.5786 | 0.0003 | <.0001 |
| MgO | 0.1240 | 0.0336 | 0.5553 | 0.1621 | 0.5786 | <.0001 | <.0001 | 0.1442 |
| $Al_2O_3$ | 0.0596 | 0.5303 | <.0001 | <.0001 | 0.0003 | <.0001 | <.0001 | 0.1998 |
| $SiO_2$ | <.0001 | 0.0021 | <.0001 | 0.0002 | <.0001 | 0.1442 | 0.1998 | <.0001 |

For correlations blue indicates the positive ones and red the negative ones. For probabilities, coloured numbers indicate $p<0.05$.

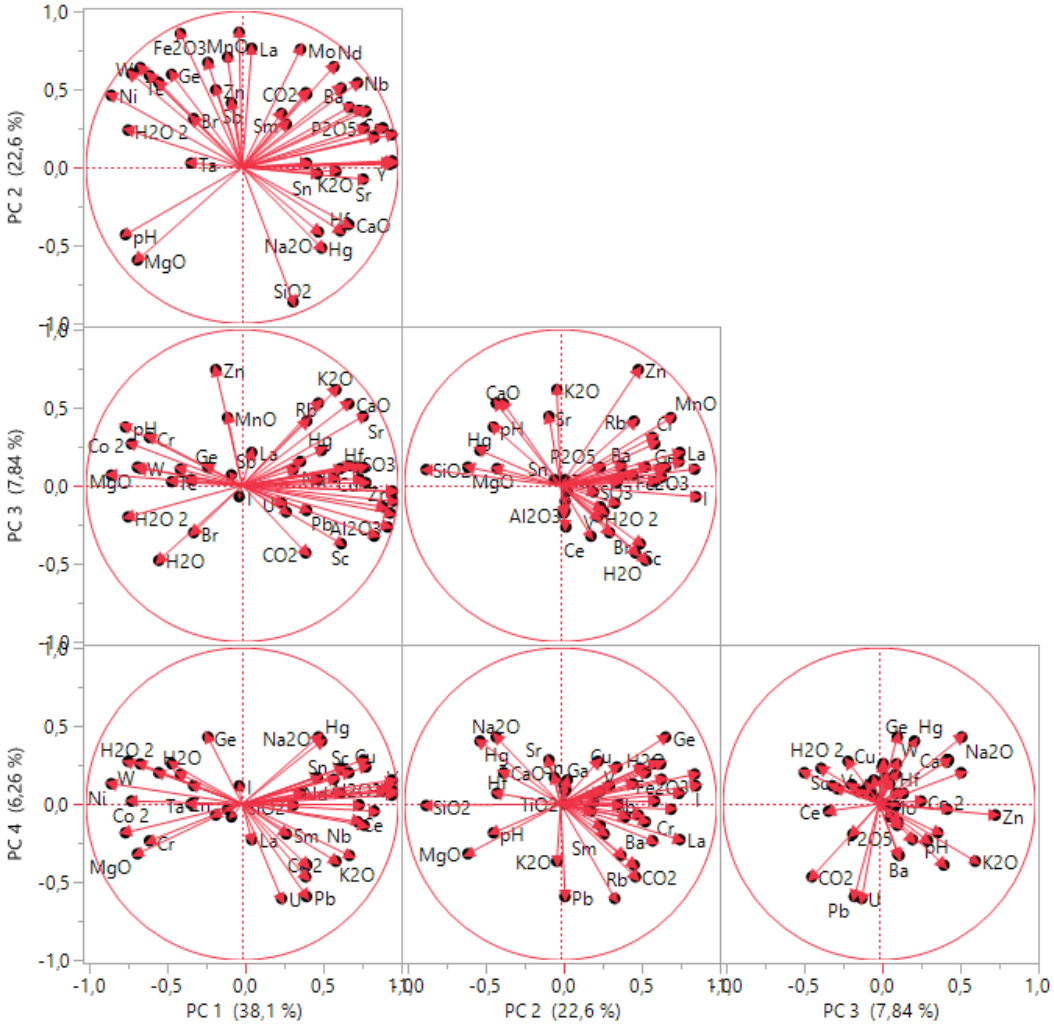


**Figure 4.S7.** Principal components analysis (PCA) for the geochemistry of the soils and the score of each variable within each component. Four main components explained ~75% of the variance within the samples according to PCA (right): PC1 (38.1%), PC2 (22.6%), PC3 (7.8%) and PC4 (6.3%).

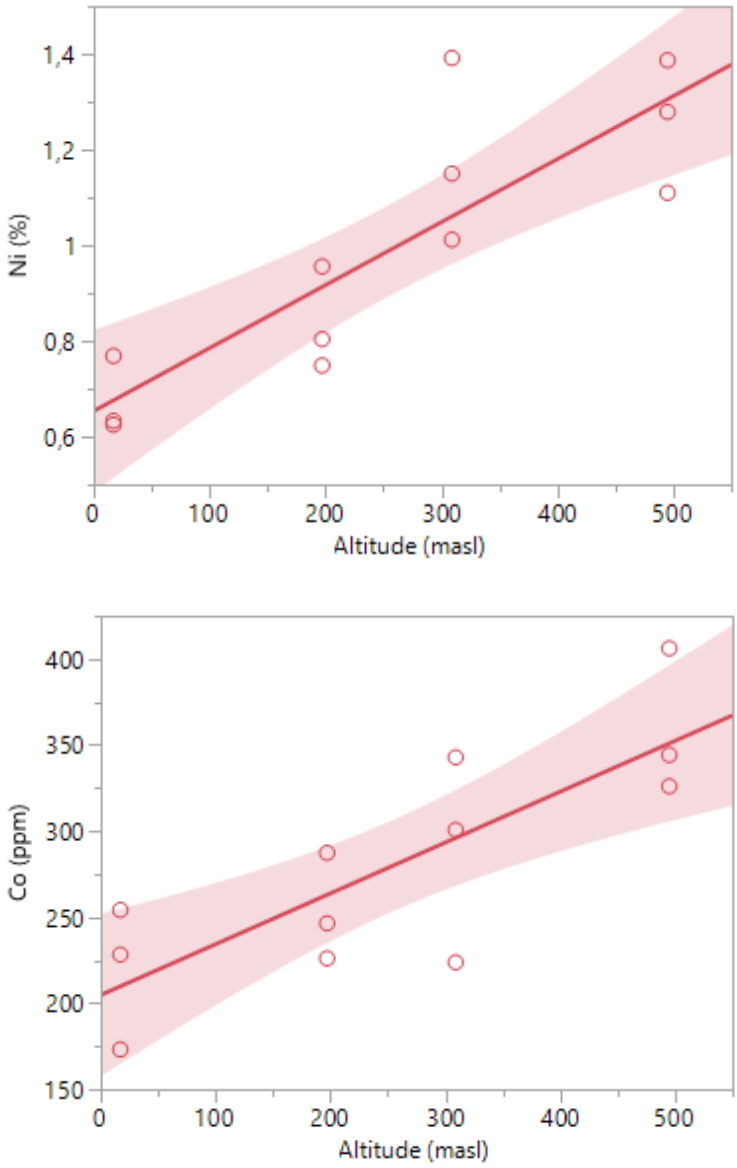


**Figure 4.S8.** Linear model of nickel (top) and cobalt (bottom) with altitude in the mountain soils. Graphical regressions were plotted in Figure 4.S5. Masl: metres above sea level. (α=0.05 for confidence curves).

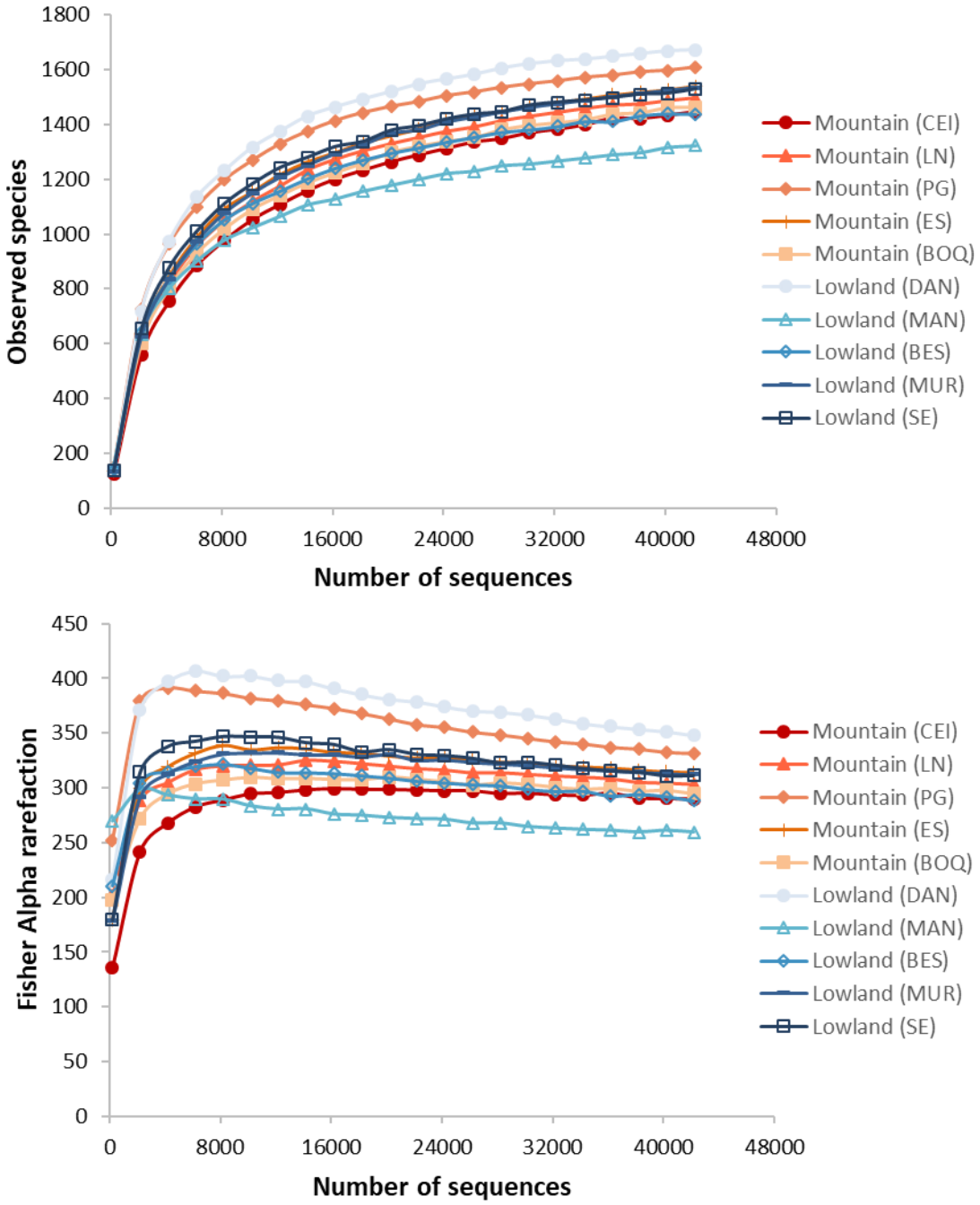


**Figure 4.S9.** Rarefaction curves for the prokaryotic communities in the lateritic soils overall the locations sampled in the peninsula of Santa Elena per observed species (top) and Fisher Alpha (bottom) after sequencing the V4 region of 16S rRNA.

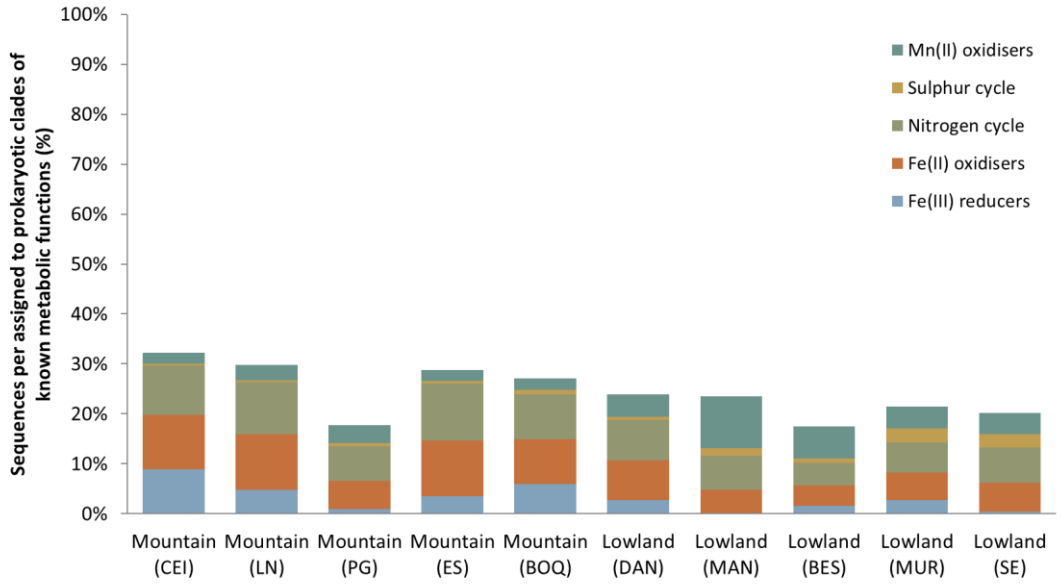


**Figure 4.S10.** Abundance of sequences per prokaryotic metabolic function assigned to phylogenetic clades after sequencing the V4 region of 16S rRNA in the lateritic soils overall the locations in the peninsula of Santa Elena.

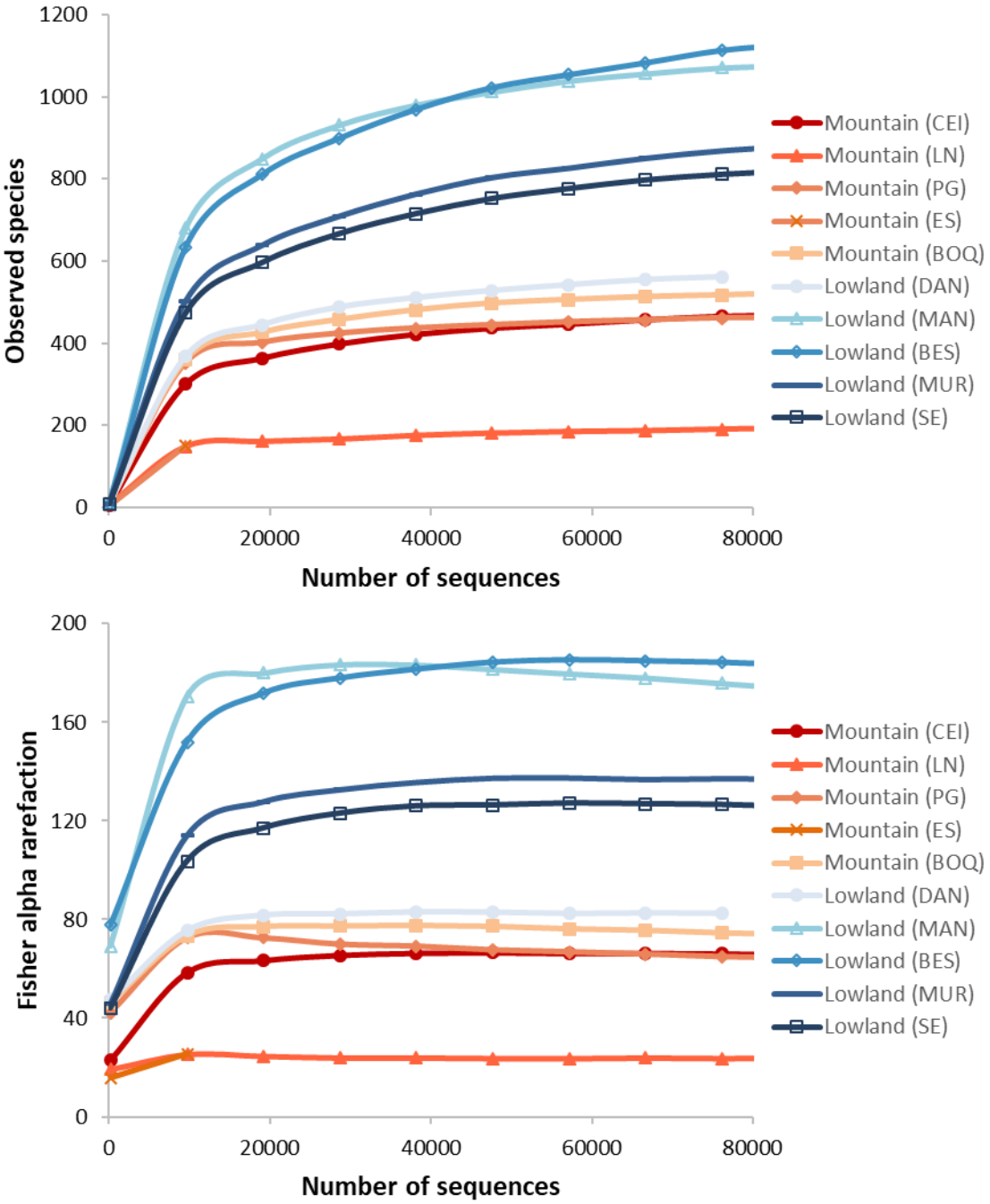


**Figure 4.S11.** Rarefaction curves for the fungal communities in the lateritic soils overall the locations sampled in the Santa Elena Peninsula per observed species (top) and Fisher Alpha (bottom) after sequencing the ITS2 region of nuclear ribosomal DNA.

# Chapter 5. Microbially-mediated iron and magnesium cycling in lateritic soils and their relationship with carbonate biomineralisation and methanogenesis

---

Agustín F. Solano-Arguedas[a*], Laura Newsome[ab], Christopher Boothman[a] and Jonathan R. Lloyd[a]

[a] Williamson Research Centre, School of Earth and Environmental Sciences, University of Manchester, Manchester, M13 9PL, United Kingdom

[b] Camborne School of Mines and Environment and Sustainability Institute, University of Exeter, Penryn, Cornwall, TR10 9FE, United Kingdom

[*] Corresponding author: agustin.solanoarguedas@postgrad.manchester.ac.uk

## 5.1 Abstract

The natural biogeochemical cycling of Fe and Mg as major elements in lateritic soils is integral to the serpentine ecosystems associated. The Santa Elena Ophiolite in the Pacific coast of Costa Rica has been proposed as a model area to study the natural geomicrobiology of lateritic soils as it is a protected ecological area that is subjected to active tropical lateritic soil formation from serpentinized peridotites. The aim of this study was to analyse the biogeochemical cycling of Fe and Mg in three different lateritic soils types from Santa Elena Ophiolite area, identified previously based on their geographical/ geochemical characterisation as mountain soils, inner ophiolite lowland soils and north lowland soils (Chapter 4). Biogeochemical cycling was stimulated in anoxic sediment microcosms using glucose and acetate-lactate as electron donors to promote reducing conditions, and subsequently the soils were oxidised in air to represent a full redox cycle. Results showed that intense microbial activity led to maximal release of Fe, Mn, Ni and Co from the mountain soils stimulated with glucose when compared to the two types of lowland soils, most likely linked to microbial reduction and dissolution of Fe(III) oxides. Mg was concurrently released

most likely during alteration of clay minerals. XRD of the post-reduction microcosm soils showed that Fe(II) had been re-precipitated as ferroan magnesite [$(Mg,Fe)CO_3$] and siderite ($FeCO_3$). The development of Fe(III)-reducing conditions caused a decrease in prokaryotic diversity and a shift towards a Firmicutes dominated prokaryotic community. Additionally, methanogenesis diminished potentially due to competition for reducing equivalents with Fe(III)-reduction coupled to anaerobic carbon metabolism as it was not developed in the lateritic mountain soils; while in both lowland soils, with less Fe content than the mountain soils, methane production was heavily enriched and a major relative abundance of methanogenic prokaryotes was found. When oxidising conditions were imposed, Fe(II) was re-oxidised, carbonate minerals decreased and some key microbial groups recovered (e.g. Acidobacteria and Proteobacteria), although anoxic conditions persisted for some time due to redox buffering. Overall these results showed that Fe, Mg and trace elements can be mobilised from lateritic soils of the mountains in Santa Elena Peninsula during periods of anerobiosis imposed by soil waterlogging in the rainy seasons, and carbon inputs including indigenous plant matter. Additionally, the fixation/mobilisation of carbon via carbonate biomineralisation and methane production provided evidence of the importance of the lateritic soils for carbon fluxes, that at a global scale should be considered in climate modelling. This research sets the basis for future work to better understand the role of microorganisms in diverse biogeochemical cycles potentially occurring in lateritic soils and serpentine ecosystems.

**Keywords:** Bioweathering, Santa Elena Ophiolite, geomicrobiology, serpentine soils, laterite.

**Highlights:**

Glucose anaerobic metabolism induced Fe and Mg mobilisation and bioweathering of minerals.

Mn, Ni and Co were mobilised with Fe in mountain lateritic soils via microbial Fe-redox cycling.

Fe-Mg carbonate biomineralisation occurred because of microbial Fe(III)-reduction coupled to anaerobic glucose metabolism.

Microbial Fe(III)-reduction coupled to anaerobic carbon metabolism outcompeted methanogenesis in certain lateritic soils.

Lateritic soils are important for climate modelling both by fixing and mobilising carbon.

## 5.2 Introduction

The biogeochemical cycling of Fe has been studied extensively with its redox activity coupled to a range processes Fe(II) can act as an electron donor and Fe(III) as a terminal electron acceptor for many microbially-mediated processes by a wide range of physiologically and phylogenetically diverse microorganisms, found in natural and engineered environments (Kappler et al., 2016). Nickel laterites are Fe and Mg-rich regoliths from serpentinized ultramafic rocks intensively weathered in humid tropical areas (Butt and Cluzel, 2013). Microbially-mediated Fe reactions have been investigated previously in Ni-laterites using model microorganisms including acidophilic Fe(III)- reducing bacteria, aiming to extract Ni and Co associated with Fe minerals from low-grade deposits or waste materials from mining operations (Hallberg et al., 2011; Johnson and du Plessis, 2015; Marrero et al., 2017). Natural microbial communities in Ni/Co lateritic sediments collected worldwide were recently described, and the anaerobic redox cycling of those metals was studied in some of them (Newsome *et al.*, in revision, Appendix 1), but the role of the indigenous microorganisms in the natural cycling of Fe and Mg in superficial lateritic soils remains relatively unexplored. Moreover, these studies have only focussed on anoxic (metal-reducing) conditions, and the behaviour of Fe and Mg under fluctuating redox conditions that are typically encountered in biogeochemically-active systems is poorly defined.

The Santa Elena Ophiolite is part of the oceanic complexes found in the Pacific coast of Costa Rica, specifically in the Santa Elena Peninsula, and is principally comprised of serpentinized peridotites (lherzolites, harzburgites and dunites) and associated lithologies including gabbros, diabases and basalts (Denyer and Gazel, 2009; Madrigal et al., 2015; Schwarzenbach et al., 2016; Whattam et al., 2016). The area is subjected to active lateritic soil formation as a consequence of the tropical climatic conditions of temperature and precipitation that prevail in the Peninsula, and because of its protected status, anthropogenic intervention has been absent for nearly 50 years, making it a unique place to study the natural processes associated with serpentine soils (Janzen and Hallwachs, 2016; Jiménez M. et al., 2016; Thorne et al., 2012).

The Santa Elena lateritic soils have been categorised into three different types based on their geography, geochemistry and microbial composition (Chapter 4). The first group are the soils of the *mountains* that govern the landscape in the Santa Elena Peninsula and these are rich in Fe

and associated trace metals including Ni, Mn or Co, with a mineralogy dominated by Fe(III) oxides and lizardite [$Mg_3Si_2O_5(OH)_4$]. The other two groups are the soils of the *inner ophiolite lowland* areas, as those in Potrero Grande basin and mangrove, that have mineralogy, geochemical composition and microbial communities similar to those from the surrounding mountains; and the soils of the *north lowlands of the ophiolite* area that have lower values of Fe and associated metals. The extant microbiology of these lateritic soils (and associations with soil geochemistry) has been studied recently highlighting the higher relative abundance of Fe-redox cycling bacteria in the *mountain* areas, and Mn-oxidising bacteria in the lowlands especially in the mangrove area of Potrero Grande (Chapter 4).

The aim of this study was to build on this earlier work and characterise the impact of biogeochemical redox cycling on iron and magnesium in the lateritic soils of the Santa Elena Peninsula. The main hypothesis is that microbially-mediated anaerobic/aerobic processes participate in the cycling of Fe and Mg in the lateritic soils through the weathering of Fe minerals, and that microbial influence over the biogeochemical cycles will be more evident in the mountain soils richer in Fe. Soils were selected from three different geographical locations associated with the area of the Santa Elena Ophiolite that differed in their geochemistry and microbiology. Fluctuating redox conditions were simulated in soil microcosm experiments, with organic substrates added to stimulate the development of reducing conditions, and aeration simulating oxidising conditions. Changes in aqueous geochemistry, soil mineralogy and microbial community composition were assessed to develop a better understanding of the biogeochemistry of these important tropical lateritic soil systems.

## 5.3 Material and methods

### 5.3.1 Sampling and location characterisation

Samples were collected in the Santa Elena Peninsula, Costa Rica, within the National Park Santa Rosa of the Area de Conservación Guanacaste (ACG), during the dry season of 2017 (April). Three locations along the Peninsula were chosen according to the geochemical/geographical classification (Figure 4.13, Chapter 4): one *mountain* location (CEI), one *inner ophiolite lowland*

location, specifically from the mangrove of Potrero Grande and named ‘lowland mangrove’ (MAN), and one *north lowland of the ophiolite* area, named here as ‘north lowland’ (BES) (Figure 5.1, Table 5.1). In each site, a sampling area of 5x5 m was traced wherein 3 different replicates were taken; surface soil was removed and 1 – 1.5 kg of soil collected from a depth of 10 - 15 cm. Large rocks and large roots were separated from the samples, which were stored into a re-sealable plastic bag at 4 °C before shipping to the University of Manchester.

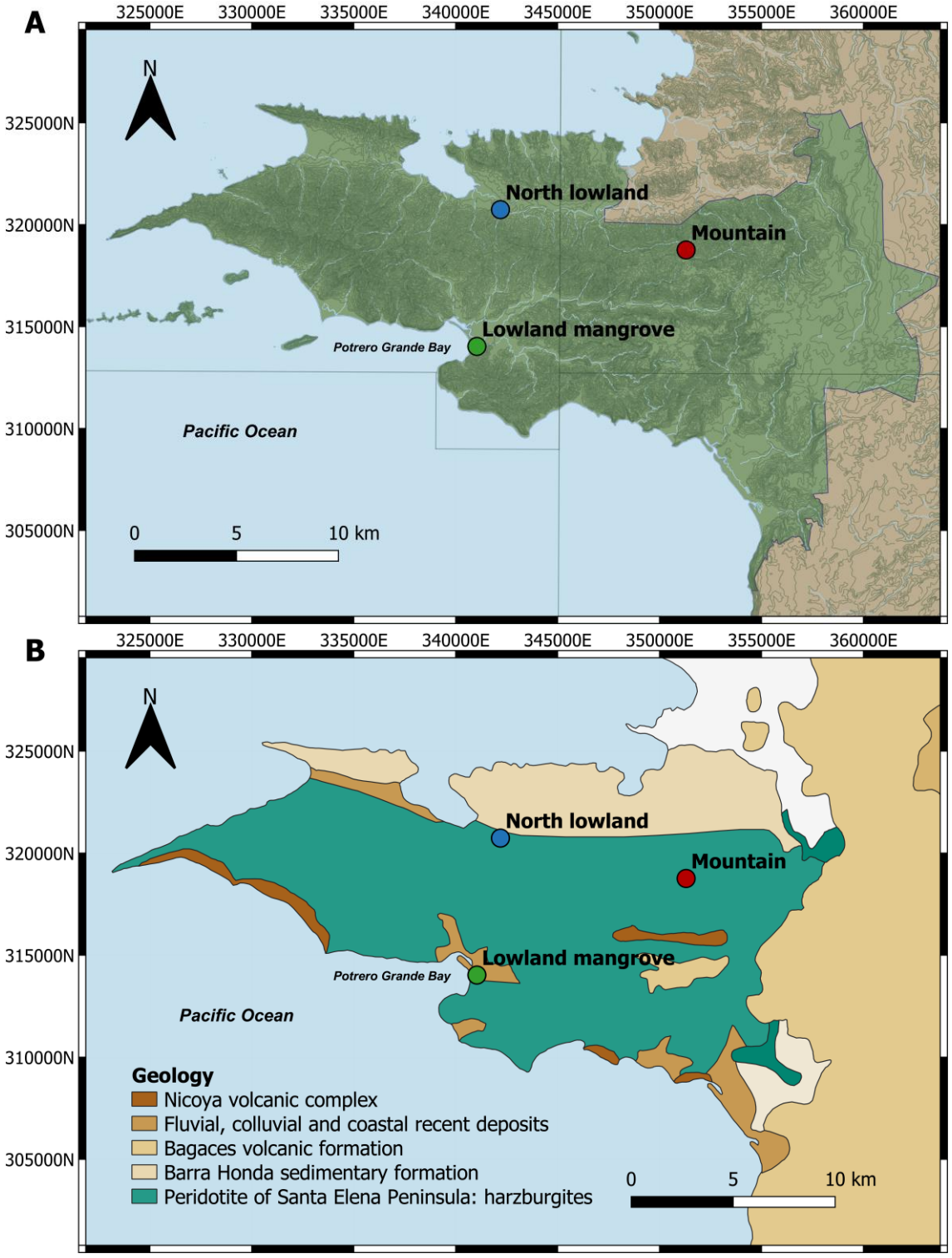


**Figure 5.1.** (A) Geographical distribution of the three locations sampled within the Santa Elena Peninsula. The coloured area is the National Park Santa Rosa. (B) Map of the geology in the Santa Elena Peninsula. Only the relevant colours have been labelled. Adapted from Medina (1999c).

**Table 5.1.** Summary of the locations sampled within the Santa Elena Peninsula and their main characteristics. Geochemical/geographical classification (GGC) is based in cluster analysis reported in Chapter 4 (Figure 4.13). A picture of each location is shown in Figure 5.2.

| Location | Coord. | Alt. | GGC | Vegetation* | Soil type* | Geology* | Topography |
|---|---|---|---|---|---|---|---|
| Mountain (CEI) | N10° 53.198' W85° 41.490' | 495 m | Mountain | Grass only but scarce, with patches of exposed soils | Entisol (Lithic ustorthent) | Ophiolite | Near the top of a hill (Cerro el Inglés) |
| Lowland mangrove (MAN) | N10° 50.606' W85° 47.110' | -4 m | Inner ophiolite lowland | Seasonal evergreen forest of lowlands, no grass present | Inceptisol (Fluventic ustropept) | Sedi-mentary deposits | Flat area between the base of a hill and the Potrero Grande mangrove flooded area |
| North lowland (BES) | N10° 54.249' W85° 46.493' | 18 m | North lowland of the ophiolite | Seasonal evergreen forest of lowlands no grass present | Inceptisol (Ustic dystropept) | Ophiolite (close to ophiolite northern margin) | Flat area on a river valley, between a river and El Silencio road |

* The vegetation, soil type and geology are geographically based on vegetation, soils, and geology maps of ACG (Medina, 2014). All the sampling points were plotted within every map in Figure 5.1 and 5.S1. / Coord: Coordinates; Alt: Altitude.


**Figure 5.2.** Detail of the three locations sampled within the Santa Elena Peninsula. (A) The mountain location CEI, (B) the lowland mangrove in the inner ophiolite lowland area (MAN) and (C) the north lowland location towards the northern boundary of the ophiolite (BES).

The soils in those three locations are Ni-rich laterites, with large amounts of Fe and Mg, as previously reported in Chapter 4 (Table 5.2). The mineralogy in all the locations is dominated by serpentine, Fe oxide and clay silicate minerals (Figure 4.9).

**Table 5.2.** Geochemical composition of the lateritic soils from the three locations of the Santa Elena Peninsula, adapted from Table 4.2 and 4.S2 (Chapter 4).

| Site | $Fe_2O_3$ (%) | MgO (%) | MnO (%) | Ni (%) | Co (ppm) | Water (wt%) | Total C (wt%) | pH |
|---|---|---|---|---|---|---|---|---|
| Mountain (CEI) | 41.6 ± 9.5 | 9.0 ± 6.4 | 0.51 ± 0.11 | 1.26 ± 0.14 | 359 ± 42 | 27.1 ± 3.7 | 12.1 ± 1.3 | 6.94 ± 0.18 |
| Lowland mangrove (MAN) | 18.4 ± 0.4 | 15.3 ± 0.5 | 0.48 ± 0.06 | 0.55 ± 0.01 | 250 ± 22 | 15.4 ± 2.3 | 10.2 ± 0.5 | 7.49 ± 0.19 |
| North lowland (BES) | 24.9 ± 0.5 | 4.4 ± 1.4 | 0.46 ± 0.01 | 0.38 ± 0.05 | 197 ± 4 | 17.2 ± 0.5 | 12.8 ± 0.2 | 6.47 ± 0.14 |

### 5.3.2 Redox cycling microcosm experiments

Redox cycling experiments were set up using 120 mL serum bottles. From each replicate location sampled, 10 g of each soil sample was added to the serum bottles, followed by 100 mL of the 10 mM electron donor solution prepared in artificial groundwater (AGW) (Wilkins et al., 2007). To stimulate the development of microbially-reducing conditions, two electron donor solutions were tested, 10 mM glucose and a mixture of 5 mM acetate and 5 mM lactate, while a third batch with only AGW was set up as a no-donor control. The headspace volume of the bottles was degassed with a mixture of 80:20 $N_2$ and $CO_2$, respectively, and the bottles were sealed with rubber caps afterwards. The bottles were incubated anoxically at 30 °C in the dark. After 10 months, oxic conditions were generated by decapping the serum bottles in a laminar flow chamber, replacing the rubber bung with a sterilised foam bung and foil cap, and incubating on a shaking incubator at 30 °C and 100 *g* for 5 months. Shaking was done only during oxic conditions.

The serum bottles were sampled periodically both during the anoxic and oxic stages using sterile syringes and needles, which were flushed with nitrogen when sampling during the anoxic stage. Briefly 0.6 mL of the sediment slurry was extracted from each microcosm bottle, of which 100 µL of the slurry was added to 4.9 mL of 0.5 M HCl and subsequently digested with hydroxylamine hydrochloride to quantify any bioavailable Fe(II) and the total Fe content, respectively, using a ferrozine assay (Lovley and Phillips, 1987, 1986). The rest of the slurry was centrifuged at 14800 *g*, and 100 µL of the supernatant was added to 0.9 mL of deionised water and other 100 µL of the

supernatant to 9.9 mL 2% $HNO_3$ to analyse the aqueous organic and inorganic geochemistry by ion chromatography and inducted coupled plasma spectroscopy, respectively. The remaining sample was used to measure the pH and the redox potential ($E_h$) using calibrated electrodes.

#### 5.3.2.1 Inductively coupled plasma atomic emission spectroscopy (ICP-AES) and mass spectroscopy (ICP-MS)

Supernatant slurry samples from the microcosm were acidified with $HNO_3$ 2% and analysed by ICP-AES to measure the content of Mg and Fe. Measurements were carried out on a Perkin-Elmer Optima 5300DV spectrometer, equipped with a concentric glass nebulizer system fitted to a cyclonic spray chamber, and based on an echelle polychromator with a segmented-array charge-coupled-device detector. Mn, Co and Ni concentrations in solution were analysed by ICP-MS using an Agilent Technologies 7700x spectrometer, equipped with a concentric MicroMist nebuliser, a quartz Peltier-cooled Scott-type double pass spray chamber, a 3rd generation Octopole Reaction System (ORS3) and an electron multiplier detector.

#### 5.3.2.2 Ion Chromatography (IC)

Supernatant slurry aliquots prepared in deionised water from the microcosm samples were analysed by ion chromatography to quantify both inorganic and organic anions, or volatile fatty acids (VFAs). Measurements were carried out on an ICS5000 dual channel ion chromatographer equipped with a conductivity detector. One channel incorporated a microbore Dionex AS18 column to determine inorganic anions including chloride, nitrate and sulphate; the other channel was equipped with a IonPac AS11-HC Hydroxide-Selective Anion-Exchange capillary column to determine VFAs as gluconate, lactate, acetate, formate, propionate, iso- and n-butyrate, iso- and n-valerate.

#### 5.3.2.3 Gas Chromatography (GC-TCD)

Headspace gas produced in the microcosm serum bottles was collected using sterile 50 mL syringes and sterile needles, by puncturing the septum and allowing the pressure of the incoming gas to move the piston of the syringe. The gas was transferred to an argon filled vial, leaving the sampling gas to replace the argon in the vial. Gas samples were analysed in an Agilent 7890 Gas Chromatography system equipped with a 7890 Thermal Conductivity Detector (TCD) and a HP

Molesieve column 30 m long and 0.53 mm diameter, for the detection of hydrogen, oxygen, nitrogen and methane.

#### 5.3.2.4 X-ray diffraction spectroscopy (XRD)

For every location, a representative replicate was chosen for mineralogy analysis at the start of the incubation and at the end of the anoxic and the oxic stages. Before analysis, the samples were dried using an anaerobic cabinet for the anaerobic samples and placed in airtight specimen holders with X-ray transparent caps for further analysis. Measurements were carried out on a Bruker D8 Advance diffractometer, equipped with a Göbel Mirror a Lynxeye detector and a copper X-ray tube, providing $CuK_{\alpha 1}$ X-rays with a wavelength of 1.5406 Å. Samples were scanned from 5-70$^{o}$ 2θ, with a step size of 0.02 $^{o}$ and a count time of 0.2 s per step. The resultant patterns were evaluated using EVA version 4, which compares experimental data to standards from the ICDD (International Centre for Diffraction Data) Database.

### 5.3.3 Microbial community analysis

#### 5.3.3.1 DNA extraction

To investigate changes in the microbial community during redox cycling, DNA was extracted from one replicate from each location at the start of the experiment, and at the end of both the anoxic and the oxic stages. DNA was extracted from 200 µl of sediment slurry using a DNeasy PowerLyzer PowerSoil Kit (Qiagen, Manchester, U.K). The 16S rRNA gene was amplified via PCR (polymerase chain reaction) using 8F (5'-AGAGTTTGATCCTGGCTCAG-3'), and 1492R (5'-TACGGYTACCTTGTTACGACTT-3') primers (Lane, 1991). Following amplification via PCR, the DNA was stained with SYBR Safe DNA Gel Stain (Thermo Fisher Scientific) before placement in an agarose gel, where it was subsequently separated using electrophoresis. The stained DNA was viewed under UV light, and target ~1500 base pair products were identified by comparison to a ladder of DNA fragments of varying lengths.

#### 5.3.3.2 Prokaryotic community analysis

The PCR amplicons from 16S rRNA gene amplification were sequenced using the Illumina MiSeq platform (Illumina, San Diego, CA, USA) targeting the V4 hyper variable region (forward primer, 515F, 5′-GTGYCAGCMGCCGCGGTAA-3′; reverse primer, 806R, 5′-

GGACTACHVGGGTWTCTAAT-3′) for 2 × 250-bp paired-end sequencing (Illumina) (Caporaso et al., 2012, 2011). PCR amplification was performed using the Roche FastStart High Fidelity PCR System (Roche Diagnostics Ltd, Burgess Hill, UK) in 50µl reactions under the following conditions: initial denaturation at 95°C for 2 min, followed by 36 cycles of 95 °C for 30 s, 55 °C for 30 s, 72 °C for 1 min, and a final extension step of 5 min at 72 °C. The PCR products were purified and normalised to ~20 ng each using the SequalPrep Normalization Kit (Fisher Scientific, Loughborough, UK). The PCR amplicons from all samples were pooled in equimolar ratios. The run was performed using a 4 pM sample library spiked with 4 pM PhiX to a final concentration of 10% following the method of Schloss and Kozich (Kozich et al., 2013).

Raw sequences for prokaryotes were divided into samples by barcodes (up to one mismatch was permitted) using a sequencing pipeline. Quality control and trimming was performed using Cutadapt (Martin, 2011), FastQC (Babraham Bioinformatics, n.d.), and Sickle (Joshi and Fass, 2011). MiSeq error correction was performed using SPADes (Nurk et al., 2013). Forward and reverse reads were incorporated into full-length sequences with Pandaseq (Masella et al., 2012). Chimeras were removed using ChimeraSlayer (Haas et al., 2011), and operational taxonomic units (OTUs) were generated with UPARSE (Edgar, 2013). OTUs were classified by Usearch (Edgar, 2010) at the 97% similarity level, and singletons were removed. Rarefaction analysis was conducted using the original detected OTUs in Qiime (Caporaso et al., 2010). The taxonomic assignment was performed by the RDP classifier (Wang et al., 2007).

### 5.3.4 Map plotting

The processing of map data was done using QGIS 3.10.0 A Coruña software (QGIS Development Team, 2019). GIS layers were taken from the ACG GIS-maps database (Medina, 2014) and Costa Rica Lambert Norte was used as the coordinate reference system.

## 5.4 Results and Discussion

### 5.4.1 Redox cycling microcosm experiments

Soils from three different locations in the Santa Elena Ophiolite were stimulated with glucose and acetate-lactate to study microbially-mediated cycling of Fe and Mg in lateritic soils. After

incubation under anoxic conditions, changes in the colours and textures of the soils were evident, when compared with the starting material, regardless of the location of origin (Figure 5.3 and 5.S2). Microcosms amended with the organic electron donors darkened in colour, most likely due to the microbial formation of Fe(II) and/or sulphide minerals. After the microcosm experiments were aerated, the original colour of the soils was recovered, likely due to the oxidation of reduced Fe mineral phases, to form ferric oxides or oxydroxydes (Figure 5.3).

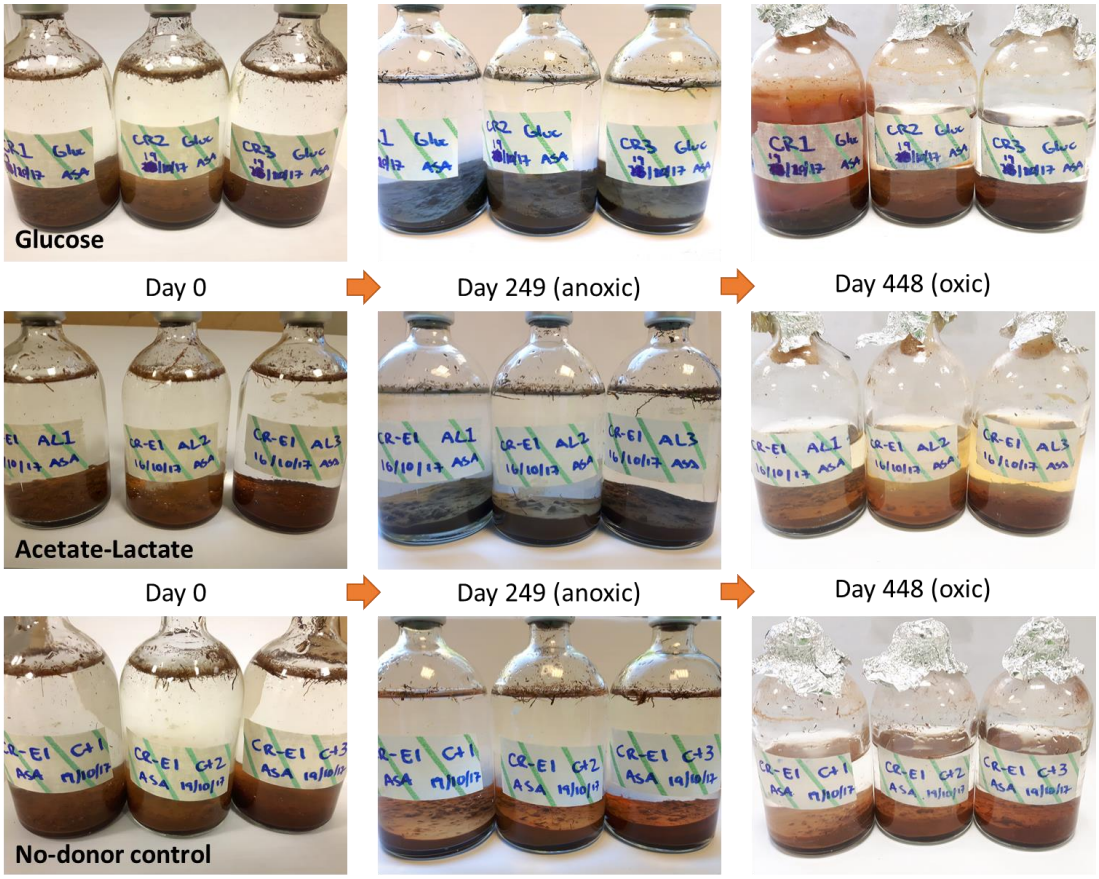


**Figure 5.3.** Microcosm serum bottle incubations for the three replicates of mountain location soils biostimulated with glucose, acetate-lactate and a no-donor control at the beginning of the redox cycling microcosm experiment (day 0), after 8 months of anoxic incubation (day 249 overall) and after 5 months of subsequent oxic incubation (day 448 overall). The other two sample locations are shown in Figure 5.S2.

### 5.4.2 Effects of redox cycling on aqueous geochemistry within lateritic soils

Following biostimulation with the organic substrates under anoxic conditions, the pH of the no-donor and acetate/lactate amended microcosms remained around 8 in all soils (Figure 5.4A, C, E). The pH of the glucose-amended lowland soil microcosms initially decreased to around 6.5

and slowly rebounded to 7.5 (Figure 5.4C, E), while the mountain soils decreased to pH 6 and remained low for over 6 months, before rebounding to pH 7 (Figure 5.4A). This decrease was likely due to metabolism of glucose generating a range of organic acid fermentation products and carbon dioxide (Lovley and Phillips, 1988). Under oxic conditions, the pH remained broadly circumneutral, with the acetate/lactate-stimulated microcosms constant at around pH 8, the no-donor controls showing a slight decrease to pH 7, and the glucose microcosms increasing slightly to 7.5. The redox potentials of all the microcosm experiments decreased during the anoxic phase of the experiment (Figure 5.4B, D, E). Those amended with glucose reached the lowest redox potential values (-400 mV). More moderate (approximately -200 mV) decreases in the no-donor controls were likely due to the metabolism of natural organic matter. The redox potential increased in all microcosms during subsequent aeration, reaching values close to 0 mV by the end of the oxic phase, confirming redox cycling.

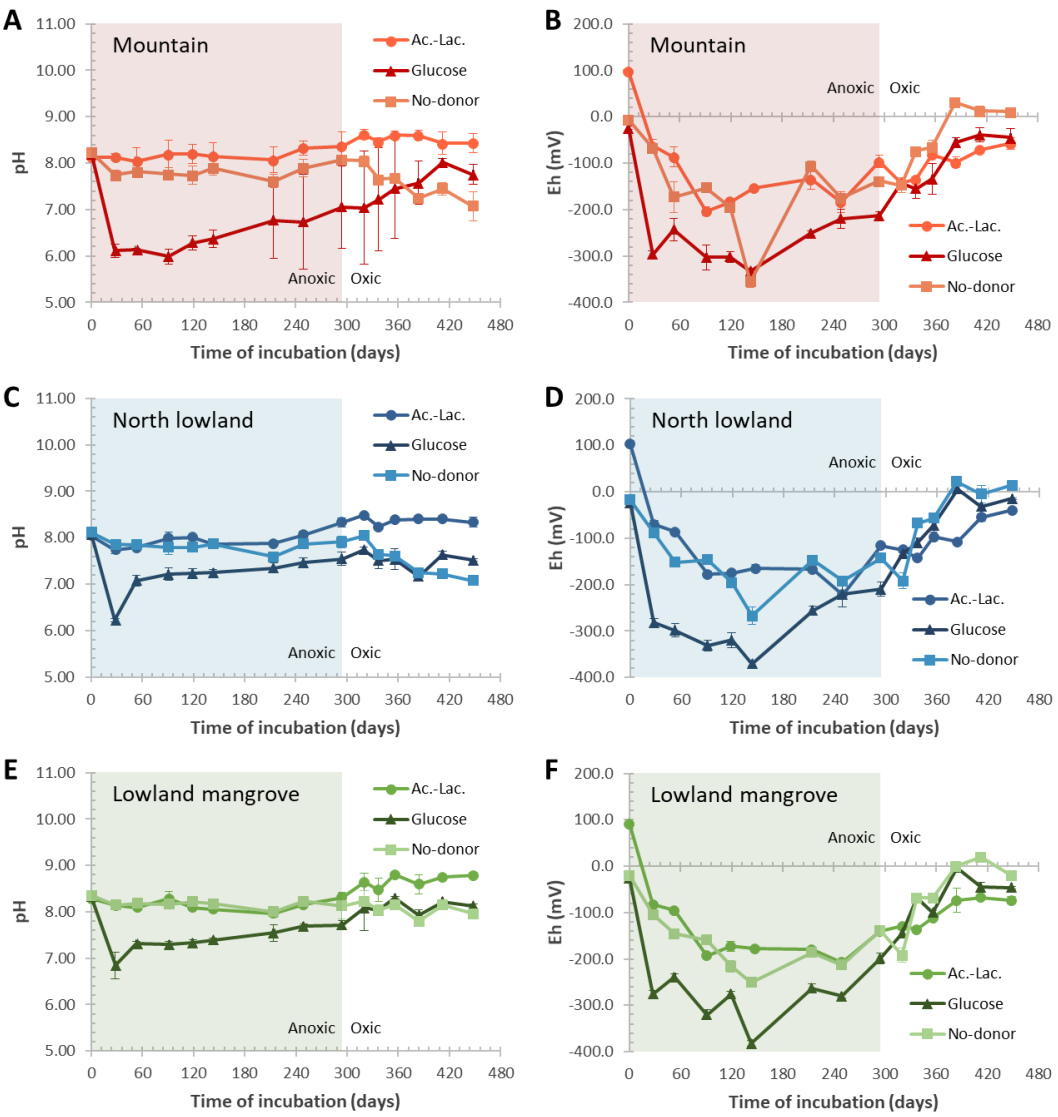


**Figure 5.4.** pH (A, C, E) and redox potential ($E_h$) (B, D, F) measured in the redox cycling microcosm experiments during both the anoxic (coloured area) and the oxic (clear area) phases for soils collected from the three locations sampled: mountain, north lowland and lowland mangrove. Results are shown as an average of the 3 replicates and their respective standard deviation.

The concentration of Fe(II) in soil slurry increased in all the samples during the anoxic period as a result of the microbially-mediated Fe(III) reduction (Figure 5.5A, C, E). Glucose was the more effective electron donor, generating more Fe(II) in all three soils than acetate-lactate, highlighting the potential dual importance of glucose fermentation and dissimilatory Fe(III) reduction in reductive transformations of the lateritic soil system. Fermentation can be linked to metal

reduction directly (using high oxidation metals such as Fe(III) for co-factor regeneration), while also generating fermentation end products such as organic acids, which can act as electron donors for metal reduction (Lloyd, 2003; Lovley and Phillips, 1986). The mountain sample generated the highest relative amounts of bioavailable Fe(II) (Figure 5.5A) followed by the north lowland sample (Figure 5.5C), which is in accordance with the relative content of Fe in the original samples (Table 5.2). During the anoxic phase, all of the Fe detected in the microcosm corresponded to bio-available Fe(II) irrespective of the location or the electron donor used (Figure 5.5B, D, F). It should be noted that no-donor controls in both lowland samples also generated significant levels of Fe(II) under anoxic conditions (Figure 5.5C, E), suggesting that either these soils also contained other natural carbon sources or electron donors that were not present in the mountain soils, or that geochemical differences between mountain and lowland serpentine soils could be present due to topographical factors. For example, in volcanic soils from Puerto Rico was reported that within a topographical gradient, soil oxygen concentrations decreased from ridge to slope to valley (Silver et al., 1999). Following aeration, the bioavailable Fe(II) decreased in all the samples, but for the mountain sample treated with glucose, bioavailable Fe(II) was still detected during the first two months of the aerobicoxic stage. This result together with pH and the redox potential (Figure 5.4) indicated that anoxic conditions likely persisted, most likely due to either (i) the stimulation of higher levels of biomass with the added glucose, and subsequent oxygen limitation in the oxic treatments at higher cell loadings, (ii) redox buffering provided by residual products of glucose (Newsome et al., 2017) or (iii) the presence of microsites with anoxic conditions as seen in other tropical soils (Coward et al., 2018; Ginn et al., 2017)..

Sulphate and nitrate decreased in the experimental solutions under anoxic conditions, suggesting their reduction; and as it also occurred in the no-donor controls (Figure 5.S3), then the presence of other natural organic matter able to be used in those processes was reinforced. The only exception was the no-donor control of the mountain location, where the sulphate concentration remained constant during the anoxic stage, further confirming that the mountain soils lacked other carbon sources or electron donors that were present in the lowland soils.

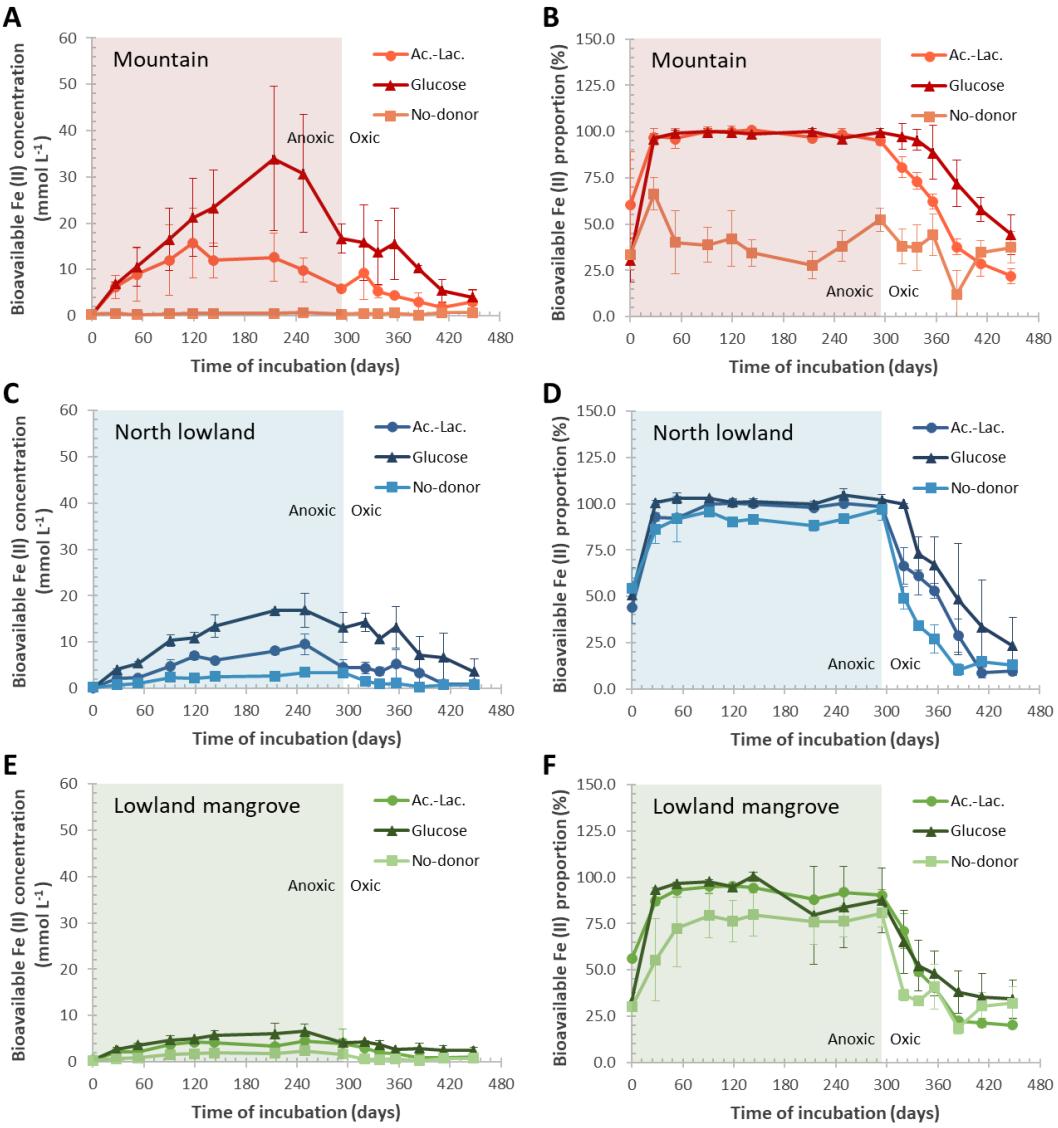


**Figure 5.5.** Bioavailable Fe(II) in the redox cycling microcosm experiments measured by ferrozine assay of soil slurry during both the anoxic (coloured area) and the oxic (clear area) phases for soils collected from the three locations sampled: mountain (A, B), north lowland (C, D) and lowland mangrove (E,F). Results are shown as an average of the 3 replicates and their respective standard deviation.

The influence of redox cycling on the behaviour of Fe and Mg within the soils tested was assessed (Figure 5.6). Iron was largely mobilised into the aqueous phase at the beginning of the anoxic stage, especially when biostimulated with glucose, with the highest concentration in soils from the mountain location. However, after two months of anoxic incubation, the concentration of aqueous Fe decreased substantially, with no Fe remaining in solution after aeration. This suggests that precipitation of Fe minerals was likely occurring under both anoxic and oxic conditions (see

Section 5.4.3 below), as seen in other upland tropical soils where periodic dynamic redox conditions influenced the formation of rapid reducible Fe(II) phases and re-oxidation of Fe(III) oxides (Ginn et al., 2017; Thompson et al., 2011). Also, it has been demonstrated that Fe(III) reduction could occur in tropical soils either with simple organic compounds or with complex mixtures such as leaf litter, and also without strict anoxic conditions in unsaturated soils and in superficial soils with high bulk $O_2$ (Hall et al., 2016; Liptzin and Silver, 2009). Magnesium was released into the aqueous phase of all microcosm experiments, regardless of the location or the treatment tested, indicating it was soluble under all experimental conditions. The highest Mg concentrations were observed in the glucose-biostimulated microcosms from the mountain and the mangrove locations, while acetate-lactate additions did not affect Mg concentration, when compared with the no-donor controls. This suggests that Mg mineral bioweathering in the lateritic soils occurs via a different mechanism than does iron mineral bioweathering. It is noteworthy that unlike Fe, the concentration of Mg was sustained during the anoxic phase both in the mountain and in the mangrove samples, decreasing later during the oxic conditions. This suggests that Mg remained soluble under anoxic conditions, and Mg minerals were likely precipitated exclusively under oxic conditions, in contrast to Fe mineralisation.

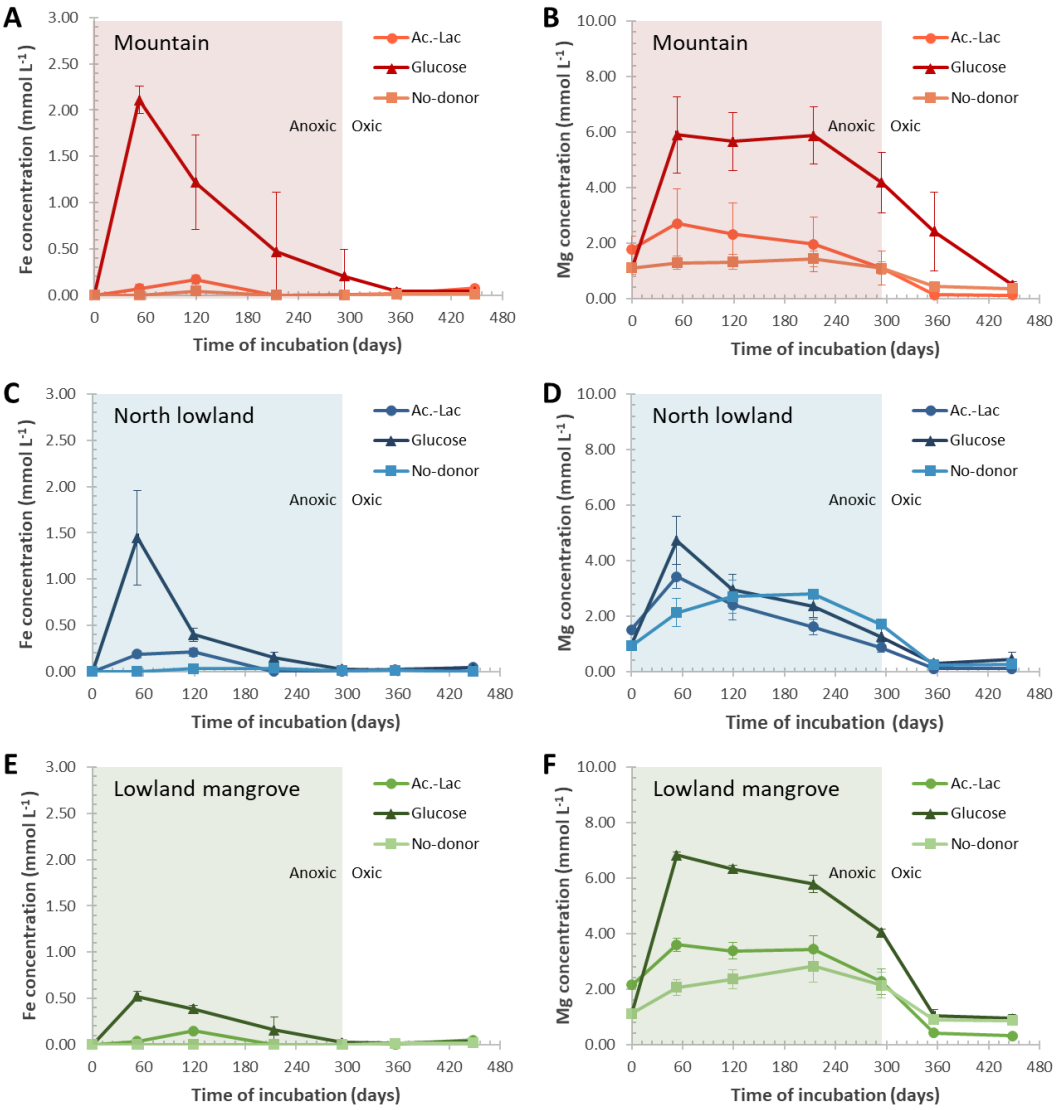


**Figure 5.6.** Iron (A, C, E) and magnesium (B, D, E) aqueous concentration in the redox cycling microcosm experiments after biostimulation with glucose and acetate-lactate during both anoxic (coloured area) and oxic (clear area) conditions for soils collected from the three locations sampled: mountain, north lowland and lowland mangrove. Results are shown as an average of the 3 replicates and their respective standard deviation.

The mobilisation of Mn, Ni and Co was similar to Fe only in the mountain soils biostimulated with glucose (Figure 5.7). Glucose was previously observed to be more effective in stimulating the development of microbial metal-reducing conditions that mobilised Ni and Co from Brazilian laterites compared to acetate-lactate (Newsome *et al.*, in revision, Appendix 1). In contrast, in the lowland soils, Mn, Ni and Co were not substantially released to solution, despite having similar relative amounts as the mountain soils (Table 5.2), and Fe(II) being released to solution (Figure

5.5). In opposition to these results, mangroves associated with an ultramafic watershed in New Caledonia, showed metal cycling of Fe, Ni and Mn from iron oxides and/or oxy-hydroxides related to bacterial-mediated organic matter decomposition, thus resulting in high aqueous concentrations of those metals (Marchand et al., 2012; Noël et al., 2015). In this study, the absence of metal mobilisation on mangrove serpentine soils could be associated with a different composition of the microbial communities. Moreover, metal cycling could have been indirectly inhibited perhaps because Mn was not bioavailable for reduction on the mineral phases found in the mangrove soils of Santa Elena Peninsula thus affecting the mobilisation of other Mn-related metals, such as cobalt, which cycling was observed to be mediated by manganese biogeochemical cycling in other laterites of the world (Newsome *et al.*, in revision, Appendix 1).

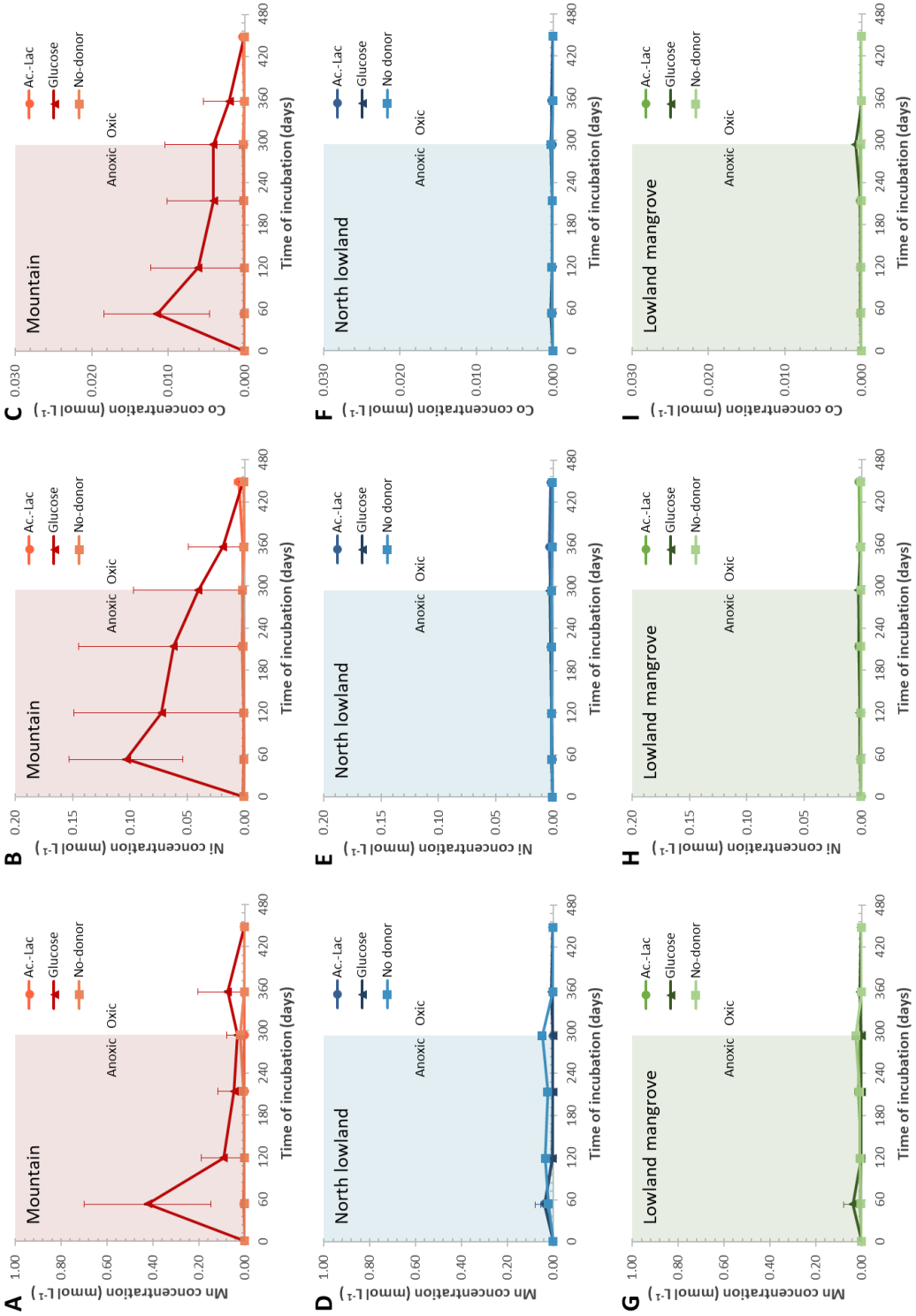


**Figure 5.7.** Manganese (A, D, G), cobalt (B, E, H) and nickel (C, F, I) aqueous concentration in the redox cycling microcosm experiments after biostimulation with glucose and acetate/lactate during both anoxic (coloured area) and oxic (clear area) conditions for soils collected from the three locations sampled: mountain, north lowland and lowland mangrove. Results are shown as an average of the 3 replicates and their respective standard deviation.

Volatile fatty acids (VFAs) and methane were measured as a proxy for breakdown of the electron donor amendments (Figure 5.8). VFAs are common fermentation products when Fe(II) bacteria metabolises substrates such as glucose (Lovley and Phillips, 1986). During the anoxic incubations, the glucose-amended mountain soils released VFA fermentation products to solution (Figure 5.8A), predominantly acetate, peaking after two months of anoxic incubation, alongside maximum aqueous concentration of Fe (Figure 5.6A). After being re-aerated, the acetate was further metabolised, supporting aerobic metabolism. In contrast to the mountain soils, the glucose-amended lowland soil microcosms (Figure 4.8C, E) did not accumulate significant levels of VFAs, with only a transient peak at 60 days detected in the North lowland microcosms. In all three soils with acetate-lactate electron donors, after 60 days there was a considerable decrease in the total VFAs content as a result of the oxidation of all the lactate present, but a residual concentration of acetate remained constant in the mountain soil until oxic conditions were imposed. In the lowland samples, complete degradation of all VFAs was noted during the anoxic incubations alongside the production of methane (Figure 5.8D, F) (which was not noted in the mountain soil microcosms; Figure 5.8B), suggesting the presence of acetoclastic methanogenesis in the lowland lateritic soils where no acetate was generated (Figure 5.8C, E), and hydrogen was not detected. However, despite the absence of hydrogen, hydrogenotrophic methanogenesis cannot be discarded as the $H_2$ could be consumed *in situ* given the excess of $CO_2$ present from the anaerobic carbon metabolism (Fenchel et al., 2012) (Figure 5.8B). Regardless of the mechanism, the latter suggests that methanogenesis dominated in the lowland soils rather than Fe(III)-reduction, and that could be due to either the relatively higher Fe content originally present in the mountain soil (Table 5.2), or to the possibility that both mechanisms compete for the carbon sources of the microcosm. Methanogens are abundant in environments with absence of $O_2$ but also with limited electron acceptors such as nitrate, Fe(III) and sulphate (Whitman et al., 2014). In all of these microcosm experiments, nitrate or sulphate decreased quickly (Figure 5.S3), suggesting that Fe(III) could be an important electron acceptor inhibiting methanogenesis in the mountain soils. No methane was produced in the no-donor controls, indicating that even though these samples contained sufficient organic matter to allow for nitrate and sulphate reduction (Figure 5.S3), there was not enough remaining for methanogenesis.

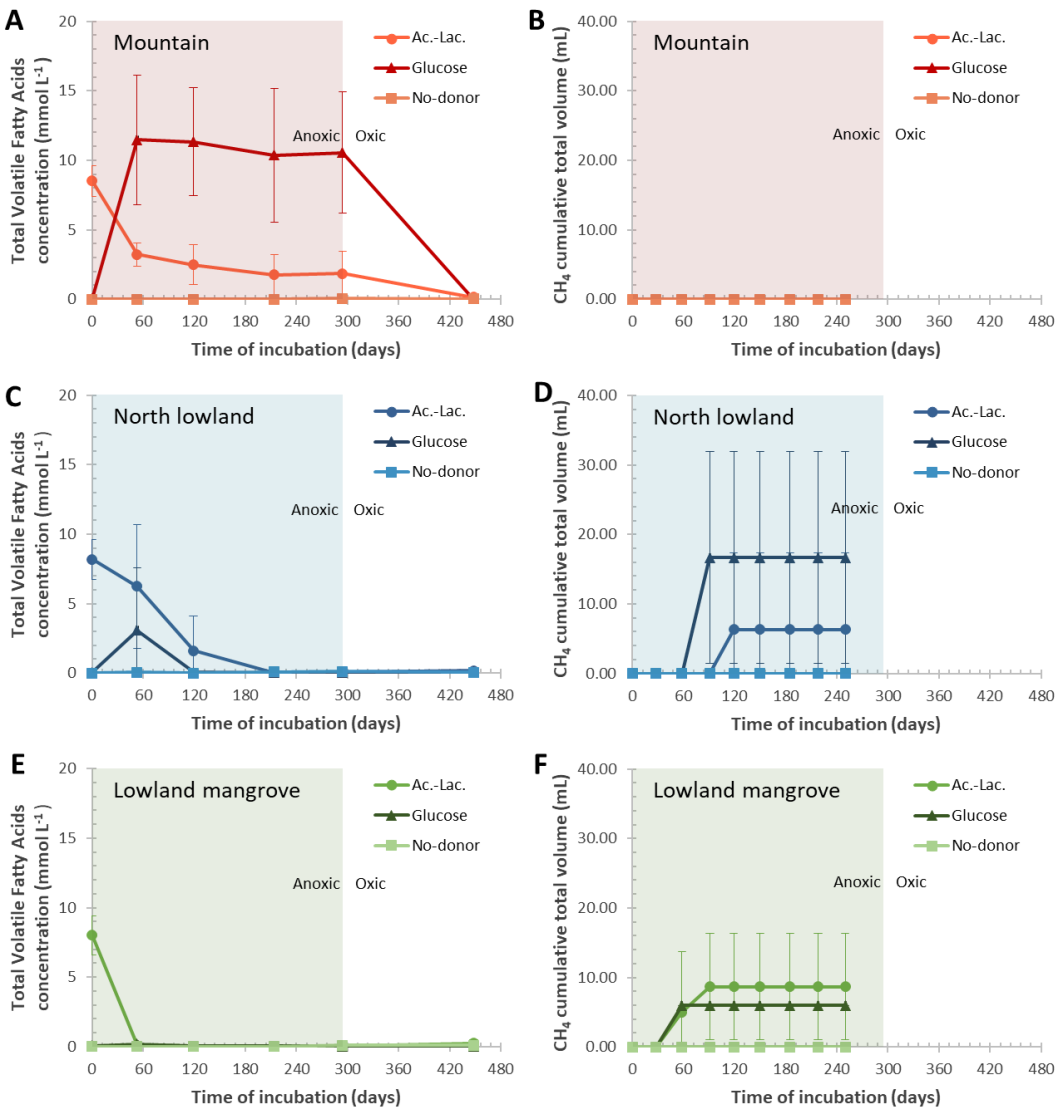


**Figure 5.8.** Aqueous total volatile fatty acids concentration (A, C, E) and approximate methane cumulative total volume (B, D, F) in the redox cycling microcosm experiments after biostimulation with glucose and acetate/lactate during both anoxic (coloured area) and oxic (clear area) conditions, for soils collected from the three locations sampled: mountain, north lowland and lowland mangrove. Results are shown as an average of the 3 replicates and their respective standard deviation. Methane was only sampled during the anoxic stage.

In summary, in the lateritic soils of Santa Elena Peninsula, microbially-mediated Fe(III) reduction was coupled to anaerobic carbon metabolism in the mountain soil microcosms, resulting in Fe mobilisation to the aqueous phase, as well as Mn, Ni and Co. Re-precipitation of Fe was observed mostly under anoxic conditions. In contrast, in the lowland soils Fe was less influenced by those mechanisms, resulting in the no mobilisation of Mn, Ni and Co; while other microbial biochemical

processes such as methanogenesis were detected. These differences between mountain and lowland soils may be attributed to the variations both in mineralogy and elemental composition, especially in the proportion of Fe oxides. Magnesium was also mobilised to the aqueous phase, but unlike Fe was not re-precipitated under anoxic conditions. A similar trend was observed in the lowland mangrove and the mountain soils suggesting that Mg behaviour was controlled by a different bioweathering processes. Thus, the soils from the *inner ophiolite lowland* areas, as the mangrove soil tested here, evidenced biogeochemical features during Fe and Mg cycling ranging between the mountain soils and the north lowland soils, just as with the geochemical separation previously reported (Figure 4.13, Chapter 4).

### 5.4.3 Effects of redox cycling on lateritic soil mineralogy

The mineralogy of the lateritic soils was characterised by XRD at the start of the experiment, and at the end of the anoxic and oxic incubations to investigate changes induced by redox cycling (Figure 5.9, 5.S4). Changes in mineralogy were particularly pronounced in the anaerobic mountain soil microcosms biostimulated with glucose. Depending on the location, there were variations in the Fe oxides detected in the soil samples, while new carbonate minerals were formed, evidencing biomineralisation processes (Figure 5.9). In the soils from the mountain locations, in the presence of glucose, hematite (α-$Fe_2O_3$) was no longer present in the sample at the end of the anoxic phase, and maghemite (γ-$Fe_2O_3$) also decreased probably as a result of the microbially-mediated Fe(III) reduction (Figure 5.5A, B). However, goethite (α-$Fe^{3+}OOH$) seemed not to have been affected. This may indicate that hematite and maghemite were susceptible to microbial Fe(III)-reduction in these samples. Similarly, in other laterites subjected to microbial reducing conditions, hematite was also reported to be affected by bioweathering processes while goethite remained unaltered. However, maghemite had the opposite behaviour as it was not present in the original sediments tested and was later recovered (Newsome *et al.*, in revision, Appendix 1). Additionally, on fluctuating redox experiments using different types of tropical soils but, under different experimental conditions than those used in this study, reductive dissolution of Fe(III) oxides and re-crystallisation of iron oxides and oxy-hydroxides have been widely reported (Ginn et al., 2017; Thompson et al., 2011, 2006; Tishchenko et al., 2015; Winkler et al., 2018). Moreover, the dissolution of those iron minerals could also determine the cycling of other metals within the superficial serpentine soils and in deeper layers of the regolith, as demonstrated with

trace elements that were susceptible to variations in the redox conditions within a humid tropical regolith profile (Chapela Lara et al., 2018).

Magnesite ($MgCO_3$) also formed during the anoxic stage in all the serpentine soils when biostimulated with glucose (Figure 5.9, 5.S4), and as Fe was no longer in solution at this point and large amounts of Mg remain solubilised (Figure 5.6A, B), it is possible that substitution of $Fe^{2+}$ could have contributed to the formation of ferroan magnesite [$(Mg,Fe)CO_3$] or siderite ($FeCO_3$). Siderite was also present in the mountain and north lowland soils to a lesser extent when bio-stimulated with acetate-lactate, while no evidence of carbonates was found in the no-donor control, confirming that their origin resulted from an excess of $CO_2$ produced from the microbial metabolism of glucose or lactate. After oxic conditions were imposed, hematite was recovered while the siderite disappeared in the acetate-lactate microcosm and in the glucose microcosm, Mg-Fe carbonate mineral decreased, both as a result of iron re-oxidation. In the aqueous geochemistry of the mountain soils, Mn, Ni and Co behaved similarly to Fe increasing their concentration towards the beginning of the anoxic stage, followed by a continuous decrease after two months of incubation (Figure 5.7A, B, C), possibly ending as minor cations in the carbonate minerals. In New Caledonian mangroves associated with ultramafic soils, with high concentrations of Fe, Ni and Cr, Mn-Fe carbonate minerals precipitated under anoxic conditions mediated by organic enrichments from the mangrove sediments (Marchand et al., 2012). Magnesium on the other hand, could have been solubilised from the clinochlore [$Mg_5Al(Si,Al)_4O_{10}(OH)_8$] as it was not detected after anoxic incubation but was further observed in the oxic phase; the other possible Mg source, lizardite [$Mg_3Si_2O_5(OH)_4$], seemed not to be affected by any of the biostimulation conditions tested although changes in this mineral cannot be entirely discounted.

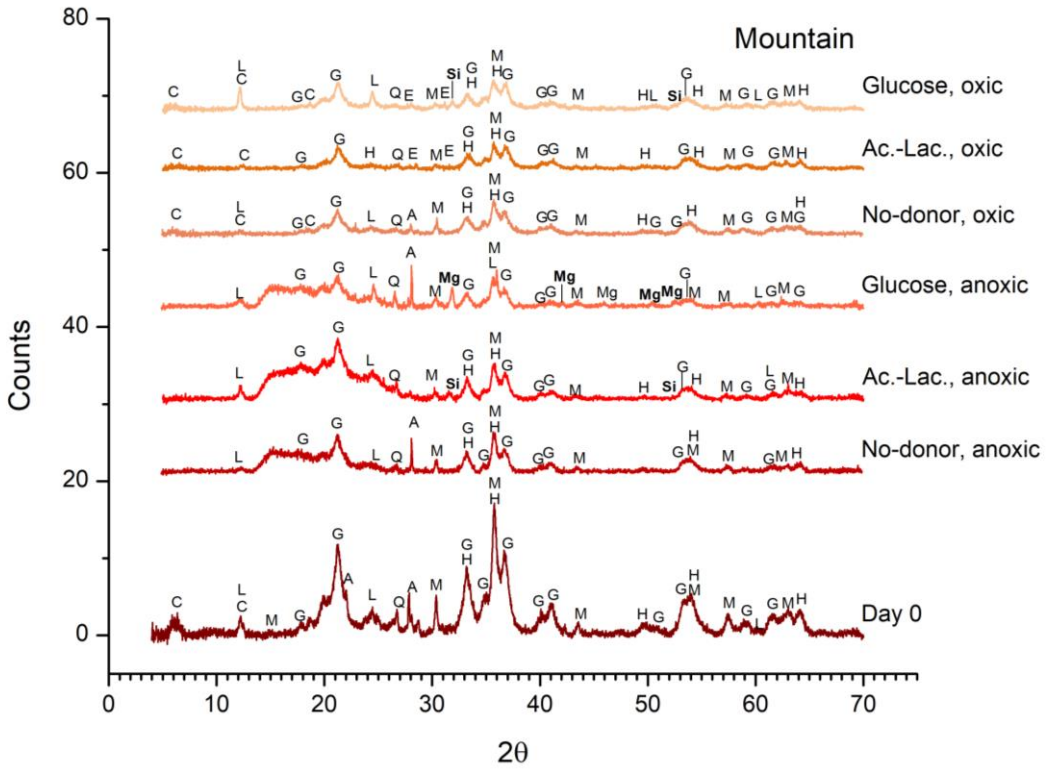


**Figure 5.9.** Mineralogy of the mountain lateritic soil at the start of the redox cycling microcosm experiment, and at the end of the anoxic and oxic incubations after biostimulation with glucose and acetate/lactate. Main minerals found with XRD were: goethite (G), hematite (H), maghemite (M), lizardite (L), siderite (Si), magnesite (Mg), enstatite (E), clinochlore (C), albite (A) and quartz (Q).

The formation of carbonate minerals observed under anoxic conditions in the lateritic soils may have implications for carbon fluxes and climate change. Under natural conditions, serpentinite and peridotite carbonation can occur during serpentinization or abiotic-biotic weathering processes of the serpentinites, and has been proposed as a mechanism to sequester carbon dioxide on a global scale (Lacinska et al., 2017). Mg carbonate precipitation resulting from biotic serpentine weathering can also occur as hydrated magnesium carbonate minerals as hydromagnesite [$Mg_5(CO_3)_4(OH)_2 \cdot 4H_2O$], dypingite [$Mg_5(CO_3)_4(OH)_2 \cdot 5H_2O$] and nesquehonite [$MgCO_3 \cdot 3H_2O$] (Power et al., 2013). Magnesite deposits have been reported for the Santa Elena Ophiolite as veins in the serpentinized peridotite together with calcite or as crusts covering the areas of alkaline springs, but the carbon source has been proposed to be $CO_2$ from meteoric waters and primary mantle carbon, while the sedimentary rocks underlying the Santa Elena

Nappe and in-situ microbial activity were suggested solely as minor possible causes of the carbonates in those rocks (Schwarzenbach et al., 2016). However, biogenic Mg-Fe carbonate minerals in the lateritic soils had not been reported previously for the Santa Elena Ophiolite (Figure 4.9, Chapter 4), and were not observed in the mineralogy of the starting soils (Figure 5.9), but their biomineralisation under anoxic conditions and further breakdown in the oxic stage suggests that microorganisms may have an essential role in the cycling of Fe, Mg and trace metals as Mn, Co and Ni in the lateritic soils of the Santa Elena Peninsula.

In lowland samples, the changes in the mineralogy were less evident (Figure 5.S4). In the North lowland sample, hematite decreased as a result of Fe(III) reduction, and as explained before, ferroan magnesite was also formed when anaerobically biostimulated with glucose. Siderite was still present after oxic conditions were imposed, but in lower proportions when compared with the anaerobic sample. In the mangrove soil microcosms, the presence of carbonate was detected only after anoxic incubation with glucose (but to a lesser extent). The large increase in Mg concentrations in the aqueous phase, could have been the result of changes in the chemical composition of the chlorite-group minerals or smectite-group minerals varying between stevensite [$Ca_{0.2}Mg_{2.9}Si_4O_{10}(OH)_2 \cdot 4H_2O$] and nontronite [$Na_{0.3}Fe_2Si_4O_{10}(OH)_2 \cdot 4H_2O$].

In summary, the mountain lateritic soils of the Santa Elena Peninsula were subject to bioweathering processes particularly when the development of anoxic conditions was stimulated with glucose, which led to the biogeochemical cycling of Fe and Mg minerals. Iron and associated metals (Mn, Ni and Co) were solubilised from the iron oxides of the lateritic soils into the aqueous phase to be further re-precipitated as carbonates, resulting in the biomineralisation of Fe-rich magnesite and siderite minerals. Magnesium was initially predominantly present in clay minerals and was released into solution in all the locations tested regardless of organic carbon amendment, although its aqueous concentration increased most as a result of glucose-stimulated bioweathering. Mg-Fe carbonates were not found in the starting soils, but their formation during anoxic conditions and further decrease in the oxic phase suggested the importance of the microbial activity in the cycling of Fe, Mg and trace metals as Mn, Co and Ni in the lateritic soils of the Santa Elena Peninsula.

### 5.4.4 Effects of redox cycling on the microbial communities of the serpentine soils

The changes in the prokaryotic communities of the lateritic soils of the Santa Elena Peninsula during the redox cycling microcosm experiments were also studied by sequencing the V4 variable region of 16S rRNA at the start of the experiment, at the end of the anoxic phase and at the end of the subsequent oxic stage. Compared to the starting soil, the Shannon diversity decreased in all locations when anaerobically biostimulated (Figure 5.10), with lower values obtained for glucose compared to acetate-lactate. After aeration, the Shannon diversity increased in both lowland locations recovering to values closer to those with no-donor; but in the mountain soils it remained lower, suggesting a strong ecological selection in this type of lateritic soil as a result of the microbial biostimulation during the previous anoxic stage.

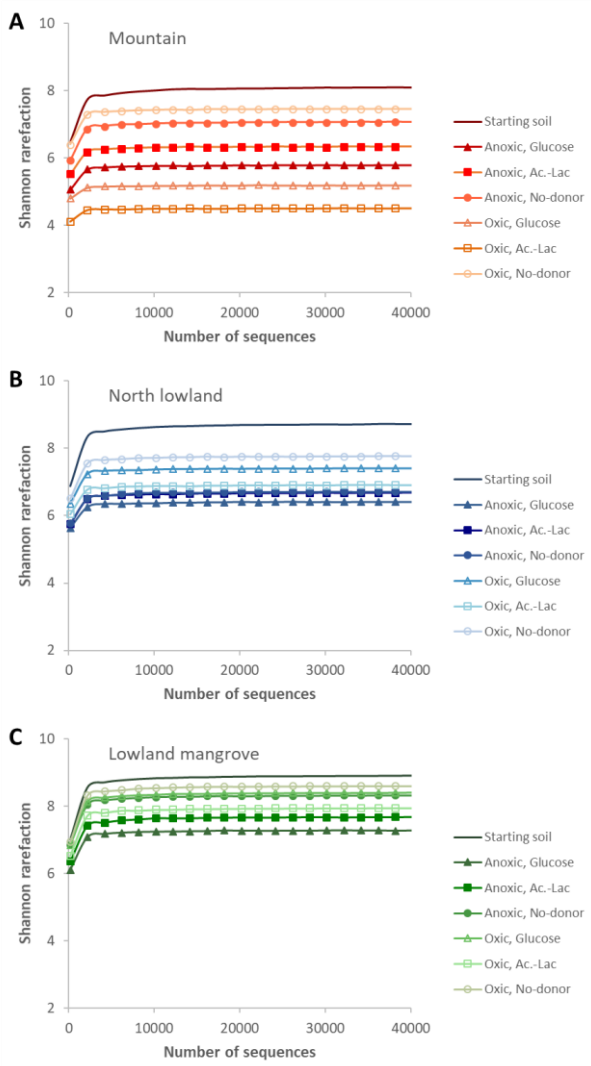


**Figure 5.10.** Shannon rarefaction curves obtained from the sequencing of the V4 region of 16S rRNA of redox cycling microcosm experiments after biostimulation with glucose, acetate-lactate

and no-donor controls under both oxic and anoxic conditions for the lateritic soils from the mountain (A), lowland North (B) and lowland mangrove (C) locations of the Santa Elena Peninsula. In every location the starting soil before biostimulation is also shown.

The impact of redox cycling was accompanied by changes in the composition of the microbial communities, especially with respect to the Firmicutes and methanogens (Figure 5.11). After anoxic incubation major changes were observed when glucose was tested as the electron donor, especially in the mountain soils where Firmicutes emerged as the dominant prokaryotic phylum, increasing from 0.1 - 0.3 % of the soil at the start of the experiment to 19 – 57% with the highest proportion in the mountain soil. Firmicutes are a Gram-positive group of eubacteria, that are not normally considered relatively abundant in soils when compared with other clades (Delgado-Baquerizo et al., 2018; Martin and Hine, n.d.); in the lateritic soils of the Santa Elena Peninsula the group constituted less than 0.1% of the prokaryotic relative abundance that was largely dominated by Actinobacteria, Proteobacteria and Acidobacteria (Section 4.4.4.1, Chapter 4), while in other ultramafic soils from New Caledonia, Firmicutes represented 5.17% of the bacterial relative abundance (Gourmelon et al., 2016). Additionally, after anaerobic biostimulation the clade was largely dominated by Clostridia phylogenetic class regardless of location or treatment (Figure 5.S5). The exception was the mountain soil stimulated with glucose, where the Firmicutes had a more balanced composition comprising Clostridia (23% of total abundance), Negativicutes (21%) and Bacilli (13%), all of them represented by anaerobic bacteria groups as *Clostridiaceae*, *Peptococcaceae*, *Heliobacteriaceae or Lachnospiraceae* (Sattley and Madigan, 2014; Stackebrandt, 2014a, 2014b, 2014c). Members of family *Veillonellaceae,* such as the Negativicutes found in the present study, have been reported to grow under anoxic atmosphere and able to ferment carbohydrates to lactate (Marchandin and Jumas-Bilak, 2014). The organism most closely affiliated with the Negativicutes group found in the mountain soils biostimulated with glucose was most closely related to *Sporomusa* sp. (12% of total abundance), and several *Sporomusa* species have been reported to produce acetate from the reduction of $CO_2$ (Aryal et al., 2017), which could have contributed to the accumulation of acetate in the total VFAs of this biostimulation experiment (Figure 5.8A). Therefore, Firmicutes found in the lateritic soils are likely to have an important role in the anaerobic cycling of Fe and Mg acting as indirect agents of bioweathering processes, where the microbially-mediated fermentation of glucose is coupled to

VFA formation and Fe(III) reduction as noted previously. These coupled processes induced both the mobilisation of Fe and Mg and associated metals such as Co, Ni and Mn, and the biomineralisation of Mg-Fe carbonates.

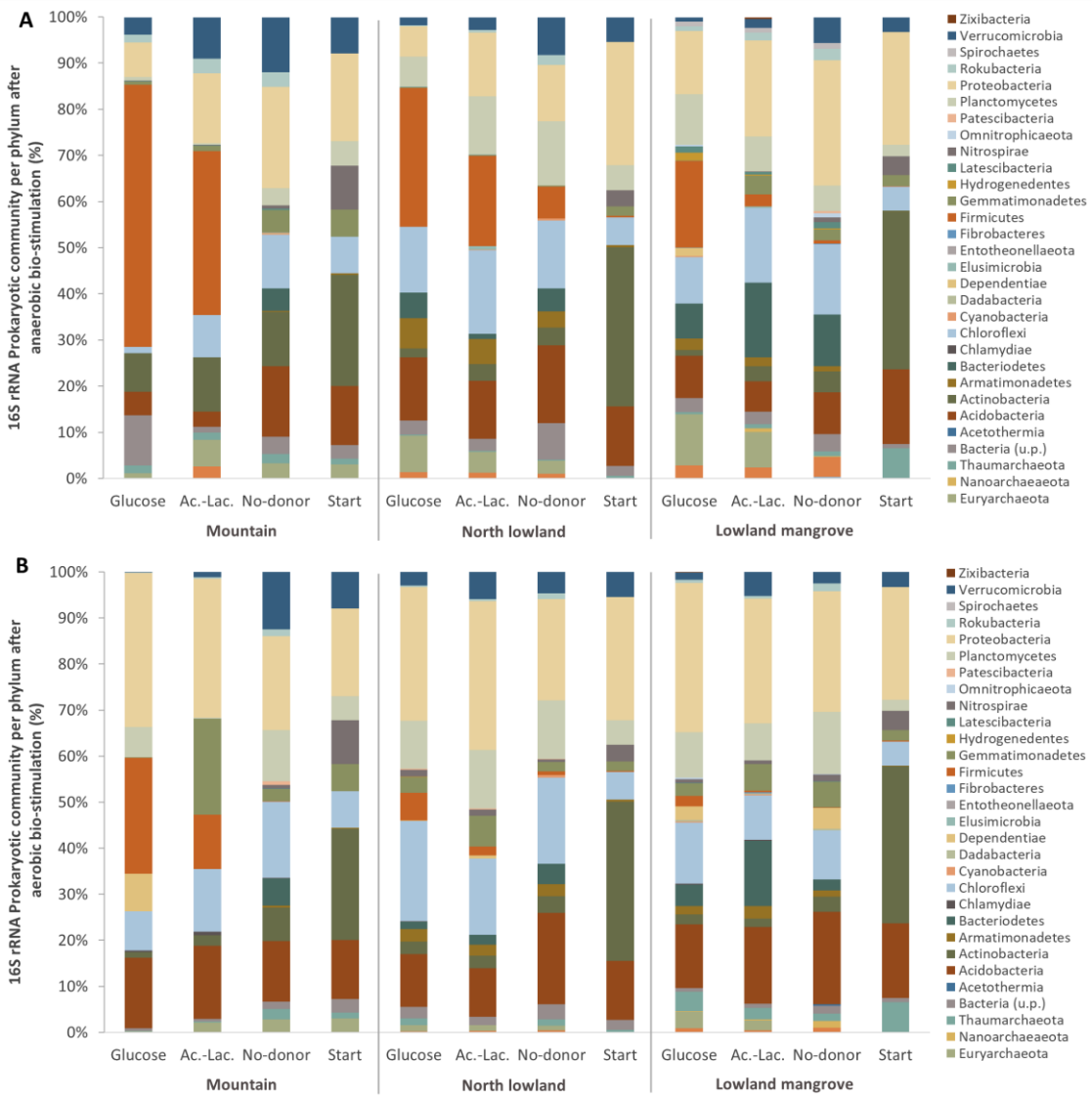


**Figure 5.11.** Prokaryotic communities in the lateritic soils of the Santa Elena Peninsula obtained by the sequencing of the V4 region of 16S rRNA from redox cycling microcosm experiments after biostimulation with glucose, acetate-lactate and no-donor controls. Relative abundance of all the sequences obtained per phylum (A) at the end of anoxic incubation and (B) at the end of subsequent oxic incubation. In every location the starting soil before biostimulation is also shown; 'u.p.': unclassified phylum. Prokaryotic communities per phylogenetic class of all the experiments are shown in Figure 5.S5 (anoxic conditions) and Figure 5.S6 (oxic conditions).

In both lowland lateritic soils, Firmicutes increased when subjected to redox cycling experiments, but to a lesser extent than in the mountain soil microcosms (Figure 5.11A, S6). Organisms affiliated with the Euryarcheota also increased substantially from < 0.1 % to 8 - 11% of total abundance. Euryarchaeota comprises several strict anaerobic methanogenic archaeal lineages (Huber, 2006) that are favoured when an electron donor is present, particularly glucose. Amongst these, *Methanosaeta* sp. and *Methanosarcina* sp. constituted between 38 – 84 % of methanogen abundance in both lowland soils when anaerobiosis was stimulated. The presence of microorganisms affiliated with both genres suggested that acetoclastic methanogenesis is an important mechanism in the formation of methane in the two types of lowland lateritic soils investigated here (Schlesinger and Bernhardt, 2013). However, hydrogenotrophic methanogenesis could also occur as other methanogens that use $H_2$ as electron donor were detected like *Methanobacterium* sp. (30% of methanogens abundance in the mangrove soils) (Oren, 2014) and members of the family *Methanocellaceae* (5 - 14% of methanogens in both lowland soils) (Sakai et al., 2014). Interestingly, this clade was relatively scarce in the mountain sample bio-stimulated with glucose (1%), also explaining the lack of methane production observed in this sample (Figure 5.8B). The latter suggests that when the geochemical characteristics of the lateritic soils of the Santa Elena Peninsula favoured microbial Fe(III) reduction coupled to glucose fermentation, then this mechanism outcompeted the methanogenesis for reduced substrates (Whitman et al., 2014). Methanogens have been previously reported in samples from the Santa Elena Ophiolite area but the investigations were restricted to hyperalkaline springs (Crespo-Medina et al., 2017; Sánchez-Murillo et al., 2014), and here it is demonstrated that methanogens are also present in lateritic ophiolite soils and, when the anoxic conditions are adequate (such as via an influx of organic carbon), are able to generate methane. This has implications for climate change and global carbon budgets, as the lateritic soils and the serpentine ecosystems in general, could be considered as carbon sinks not only by the fixation of carbon via Mg-Fe carbonates, but also by the inhibition of methane formation. As laterites are widely distributed around the world, they may play a crucial role in the carbon fluxes at a global scale.

In contrast to the rise of Firmicutes, the major prokaryotic groups originally present in the lateritic soils of Santa Elena Peninsula, Acidobacteria, Actinobacteria and Proteobacteria (Figure 4.14,

Chapter 4), decreased in their relative abundance after the development of anoxic conditions. In both lowland locations, Actinobacteria decreased from 34% to 1 – 4%, but likely as the result of the natural carbon sources found in the soils that were enough to develop anoxic conditions, and not because of the glucose or acetate-lactate stimulation as those percentages were like the no-donor controls. Proteobacteria was also affected by the anaerobic redox cycling experiments, as the major class in the starting soils, Alphaproteobacteria, decreased from 7 - 21% of relative abundance to 1- 5%. Deltaproteobacteria was also detected ranging from 2% of relative abundance to 18 % although lower values were presented in the glucose-amended microcosms. Among the deltaproteobacteria organisms found, iron reducing bacteria such as *Anaeromyxobacter* sp. or *Geobacter* sp. were present after the experiments were developed (Figure 5.S5) (Treude et al., 2003; Wilkins et al., 2007), although they only represented less than 3% of relative abundance in each microcosm soil.

When the microcosm experiments were subjected to oxic conditions, prokaryotic communities tended to return to similar compositions to the original soils (Figure 5.11B). Acidobacteria and Proteobacteria returned to their original relative abundancies, although this was not the case for the Actinobacteria, suggesting that the conditions imposed were not favourable for their metabolism. The phylogenetic class composition within the Proteobacteria was again largely dominated by Alphaproteobacteria (Figure 5.S6), including organisms related to iron-oxidising bacteria such as *Bradyrhizobium* sp. In contrast, the proportion of Firmicutes decreased substantially in almost all the microcosm experiments, (e.g. from 57% of total abundance at the end of the anoxic phase to 25% at the end of the oxic phase in the mountain soil initially treated with glucose). Within the Firmicutes, the three phylogenetic classes observed in the mountain soils were still present, Clostridia (11% of total abundance), Negativicutes (6%) and Bacilli (8%). The presence of the anaerobic Firmicutes clades and some remnants of strictly anaerobic Euryarcheota suggested the presence and coexistence of anoxic micro-environments in the lateritic soils within the oxic atmosphere of the microcosm experiments although their presence solely as DNA remnants cannot be ruled out.

In summary, redox cycling in lateritic soils of the Santa Elena Peninsula drove changes in microbial community structure both in terms of diversity and phylogenetic composition. Microcosms prepared from the mountain soils treated with glucose exhibited the most dramatic

changes, with the lowest prokaryotic diversity dominated by Firmicutes bacteria; differences that were consistent with the distinct geochemical features observed in these soils. Additionally, methanogens were found in both lowland locations stimulated by glucose, that could be linked to the absence of VFAs and the generation of methane (Figure 5.8) in those microcosm experiments. Together with the relatively low levels of Fe(III) reduction and metal release to the aqueous phase found in the lowland soils, suggest that when the adequate geochemical conditions are present in the lateritic soils of Santa Elena Peninsula, methanogenesis is outcompeted by microbially-mediated Fe(III) reduction for carbon sources.

### 5.5 Conclusions

Microbially-mediated iron cycling in the lateritic soils of Santa Elena Peninsula occurred in microcosms constructed from mountain soils when coupled to anaerobic glucose metabolism, inducing Fe mobilisation as Fe(II) to the aqueous phase. Magnesium was also mobilised under anoxic conditions regardless of the soil or the conditions tested. Fe and associated metals (Mn, Ni and Co) were solubilised from the iron oxides of the lateritic soils into the aqueous phase, and later bio-mineralised as carbonate minerals such as Fe-rich magnesite and siderite. Magnesium was also mobilised from the clay minerals into solution favoured by glucose-stimulated bioweathering.

The diversity and phylogenetic composition of the native microbial communities of these lateritic soils were also modified when biostimulated with electron donors. The lowest prokaryotic diversity was observed in the mountain soils treated with glucose, largely dominated by Firmicutes bacteria. These were the soils with the most active Fe and Mg cycling, suggesting a crucial role of this clade in the cycling of both elements that must be further studied. Additionally, iron reducing bacteria like *Anaeromyxobacter* sp. or *Geobacter* sp. were also detected, and both could be involved in using VFAs from fermentation for Fe(III) reduction.

Methanogens and methane production were noted in soils from both lowland locations. The evolution of methane was the result of both acetoclastic and hydrogenotrophic methanogenesis but preceded by anaerobic glucose metabolism in both cases. Moreover, these lowland sites had

lower contents of iron and metals associated and showed poor Fe(III) reduction and no metal release to the aqueous phase. Consequently, in the lateritic soils of Santa Elena Peninsula, microbially-mediated Fe(III) reduction outcompetes methanogenesis for carbon sources.

In conclusion, the mountain lateritic soils associated with the Santa Elena Ophiolite are subject to bioweathering and biomineralisation processes as a consequence of the cycling of both Fe and Mg coupled to anaerobic carbon metabolism, evidencing the essential part of the native microbial communities in the biogeochemical cycling of metals in the Santa Elena Peninsula and lateritic/serpentine ecosystems. Moreover, in a climate change context, it is important to quantify the role of lateritic soils in global carbon budgets, as they can fix carbon via carbonate biomieralisation and also inhibit methane generation via microbially-mediated Fe(III) reduction. This study has proven the potential of the Santa Elena Peninsula for study of the natural relationships between the native microbial communities of serpentine soils and the geochemistry of the lateritic soils and will serve as a basis for future research to better understand the role of microorganisms in the biogeochemical cycles occurring in serpentine ecosystems, and also their implications for carbon fluxes and climate change, even at a global scale.

### 5.6 Funding

This research was developed and funded by the scholarship for the PhD of AFSA granted by the Ministerio de Ciencia, Tecnología y Telecomunicaciones (MICITT) of the Government of Costa Rica and the Universidad de Costa Rica (UCR). MICITT funded the fieldwork, while the $CoG^3$ Consortium Project (CoG3 NE/M011518/1), funded by the Natural Environment Research Council (NERC), partially supported this investigation through several analyses.

### 5.7 Acknowledgements

We want to thank to María Marta Chavarría Diaz and Róger Blanco Segura from the Research Programme of the ACG for giving the permissions to develop this research in the Santa Rosa National Park and for their support and advice with the sampling logistics during the field campaigns. We are also very grateful to Daniel Arguedas Quesada for his hard work, transport and logistics support, and general assistance to AFSA in all the field campaigns. We want to thank

to Paul Lythgoe, Alastair Bewsher and John Waters (University of Manchester) for analytical support with ICP-AES, ICP-MS, IC and XRD. We also extend our gratitude to Dr. Richard A.D. Pattrick for mineralogical comments, and to Dr. Heather Buss and Dr. Vicky Coker for useful inputs to the final version of this paper. Finally, we want to thank the Unidad de Recursos Forestales (ReForesta-UCR) for allowing AFSA to use their research laboratories while in Costa Rica. The authors declared that all the biological samples were collected under the authorised permission given to AFSA from the Comisión Nacional para la Gestión de la Biodiversidad Costa Rica (CONAGEBIO) to access the DNA of the samples collected.

### 5.8 References

Aryal, N., Tremblay, P.-L., Lizak, D.M., Zhang, T., 2017. Performance of different Sporomusa species for the microbial electrosynthesis of acetate from carbon dioxide. Bioresour. Technol. 233, 184–190. https://doi.org/10.1016/j.biortech.2017.02.128

Babraham Bioinformatics, n.d. FastQC.

Butt, C.R.M., Cluzel, D., 2013. Nickel Laterite Ore Deposits: Weathered Serpentinites. Elements 9, 123–128. https://doi.org/10.2113/gselements.9.2.123

Caporaso, J.G., Kuczynski, J., Stombaugh, J., Bittinger, K., Bushman, F.D., Costello, E.K., Fierer, N., Peña, A.G., Goodrich, J.K., Gordon, J.I., Huttley, G.A., Kelley, S.T., Knights, D., Koenig, J.E., Ley, R.E., Lozupone, C.A., McDonald, D., Muegge, B.D., Pirrung, M., Reeder, J., Sevinsky, J.R., Turnbaugh, P.J., Walters, W.A., Widmann, J., Yatsunenko, T., Zaneveld, J., Knight, R., 2010. QIIME allows analysis of high-throughput community sequencing data. Nat. Methods 7, 335–336. https://doi.org/10.1038/nmeth.f.303

Caporaso, J.G., Lauber, C.L., Walters, W.A., Berg-Lyons, D., Huntley, J., Fierer, N., Owens, S.M., Betley, J., Fraser, L., Bauer, M., Gormley, N., Gilbert, J.A., Smith, G., Knight, R., 2012. Ultra-high-throughput microbial community analysis on the Illumina HiSeq and MiSeq platforms. Isme J. 6, 1621. https://doi.org/10.1038/ismej.2012.8

Caporaso, J.G., Lauber, C.L., Walters, W.A., Berg-Lyons, D., Lozupone, C.A., Turnbaugh, P.J., Fierer, N., Knight, R., 2011. Global patterns of 16S rRNA diversity at a depth of millions of sequences per sample. Proc. Natl. Acad. Sci. 108, 4516–4522. https://doi.org/10.1073/PNAS.1000080107

Chapela Lara, M., Buss, H.L., Pett-Ridge, J.C., 2018. The effects of lithology on trace element and REE behavior during tropical weathering. Chem. Geol. 500, 88–102. https://doi.org/10.1016/j.chemgeo.2018.09.024

Coward, E.K., Thompson, A., Plante, A.F., 2018. Contrasting Fe speciation in two humid forest soils: Insight into organomineral associations in redox-active environments. Geochim. Cosmochim. Acta 238, 68–84. https://doi.org/10.1016/j.gca.2018.07.007

Crespo-Medina, M., Twing, K.I., Sánchez-Murillo, R., Brazelton, W.J., McCollom, T.M., Schrenk, M.O., 2017. Methane Dynamics in a Tropical Serpentinizing Environment: The Santa Elena Ophiolite, Costa Rica. Front. Microbiol. 8, 916. https://doi.org/10.3389/fmicb.2017.00916

Delgado-Baquerizo, M., Oliverio, A.M., Brewer, T.E., Benavent-González, A., Eldridge, D.J.,

Bardgett, R.D., Maestre, F.T., Singh, B.K., Fierer, N., 2018. A global atlas of the dominant bacteria found in soil. Science (80-. ). 359, 320–325. https://doi.org/10.1126/science.aap9516

Denyer, P., Gazel, E., 2009. The Costa Rican Jurassic to Miocene oceanic complexes: Origin, tectonics and relations. J. South Am. Earth Sci. 28, 429–442. https://doi.org/10.1016/j.jsames.2009.04.010

Edgar, R.C., 2013. UPARSE: highly accurate OTU sequences from microbial amplicon reads. Nat. Methods 10, 996–998. https://doi.org/10.1038/nmeth.2604

Edgar, R.C., 2010. Search and clustering orders of magnitude faster than BLAST. Bioinformatics 26, 2460–2461. https://doi.org/10.1093/bioinformatics/btq461

Fenchel, T., King, G.M., Blackburn, T.H., 2012. Chapter 1 - Bacterial Metabolism, in: Fenchel, T., King, G.M., Blackburn, T.H.B.T.-B.B. (Third E. (Eds.), . Academic Press, Boston, pp. 1–34. https://doi.org/10.1016/B978-0-12-415836-8.00001-3

Ginn, B., Meile, C., Wilmoth, J., Tang, Y., Thompson, A., 2017. Rapid Iron Reduction Rates Are Stimulated by High-Amplitude Redox Fluctuations in a Tropical Forest Soil. Environ. Sci. Technol. 51, 3250–3259. https://doi.org/10.1021/acs.est.6b05709

Gourmelon, V., Maggia, L., Powell, J.R., Gigante, S., Hortal, S., Gueunier, C., Letellier, K., Carriconde, F., 2016. Environmental and Geographical Factors Structure Soil Microbial Diversity in New Caledonian Ultramafic Substrates: A Metagenomic Approach. PLoS One 11, 1–25. https://doi.org/10.1371/journal.pone.0167405

Haas, B.J., Gevers, D., Earl, A.M., Feldgarden, M., Ward, D. V, Giannoukos, G., Ciulla, D., Tabbaa, D., Highlander, S.K., Sodergren, E., Methé, B., DeSantis, T.Z., Human Microbiome Consortium, T.H.M., Petrosino, J.F., Knight, R., Birren, B.W., 2011. Chimeric 16S rRNA sequence formation and detection in Sanger and 454-pyrosequenced PCR amplicons. Genome Res. 21, 494–504. https://doi.org/10.1101/gr.112730.110

Hall, S.J., Liptzin, D., Buss, H.L., DeAngelis, K., Silver, W.L., 2016. Drivers and patterns of iron redox cycling from surface to bedrock in a deep tropical forest soil: a new conceptual model. Biogeochemistry 130, 177–190. https://doi.org/10.1007/s10533-016-0251-3

Hallberg, K.B., Grail, B.M., Plessis, C.A. du, Johnson, D.B., 2011. Reductive dissolution of ferric iron minerals: A new approach for bio-processing nickel laterites. Miner. Eng. 24, 620–624. https://doi.org/10.1016/j.mineng.2010.09.005

Huber, H., 2006. Euryarchaeota, in: eLS. American Cancer Society. https://doi.org/10.1038/npg.els.0004243

Janzen, D.H., Hallwachs, W., 2016. Biodiversity Conservation History and Future in Costa Rica: The Case of Área de Conservación Guanacaste (ACG), in: Kappelle, M. (Ed.), Costa Rican Ecosystems. The University of Chicago Press, p. 744.

Jiménez M., Q., Carrillo J., E., Kappelle, M., 2016. The Northern Pacific Lowland Seasonal Dry Forest of Ganacaste and the Nicoya Peninsula, in: Kappelle, M. (Ed.), Costa Rican Ecosystems. The University of Chicago Press, p. 744.

Johnson, D.B., du Plessis, C.A., 2015. Biomining in reverse gear: Using bacteria to extract metals from oxidised ores. Miner. Eng. 75, 2–5. https://doi.org/10.1016/j.mineng.2014.09.024

Joshi, N., Fass, J., 2011. Sickle: A sliding-window, adaptive, quality-based trimming tool for FastQ files.

Kappler, A., Emerson, D., Gralnick, J.A., Roden, E.E., Muehe, E.M., 2016. Geomicrobiology of Iron, in: Ehrlich, H.L., Newman, D.K., Kappler, A. (Eds.), Ehrlich's Geomicrobiology. CRC Press, pp. 343–399.

Kozich, J.J., Westcott, S.L., Baxter, N.T., Highlander, S.K., Schloss, P.D., 2013. Development of a dual-index sequencing strategy and curation pipeline for analyzing amplicon sequence data on the MiSeq Illumina sequencing platform. Appl. Environ. Microbiol. 79, 5112–5120. https://doi.org/10.1128/AEM.01043-13

Lacinska, A.M., Styles, M.T., Bateman, K., Hall, M., Brown, P.D., 2017. An Experimental Study of the Carbonation of Serpentinite and Partially Serpentinised Peridotites. Front. Earth Sci. 5, 37. https://doi.org/10.3389/feart.2017.00037

Lane, D.J., 1991. 16S/23S rRNA Sequencing, in: Stackebrandt, E., Goodfellow, M. (Eds.), Nucleic AcidTechniques in Bacterial Systematics. Wiley, New York, pp. 115–147.

Liptzin, D., Silver, W.L., 2009. Effects of carbon additions on iron reduction and phosphorus availability in a humid tropical forest soil. Soil Biol. Biochem. 41, 1696–1702. https://doi.org/https://doi.org/10.1016/j.soilbio.2009.05.013

Lloyd, J.R., 2003. Microbial reduction of metals and radionuclides. FEMS Microbiol. Rev. 27, 411–425. https://doi.org/10.1016/S0168-6445(03)00044-5

Lovley, D.R., Phillips, E.J.P., 1988. Novel Mode of Microbial Energy Metabolism: Organic Carbon Oxidation Coupled to Dissimilatory Reduction of Iron or Manganese. Appl. Envir. Microbiol. 54, 1472–1480.

Lovley, D.R., Phillips, E.J.P., 1987. Rapid Assay for Microbially Reducible Ferric Iron in Aquatic Sediments. Appl. Envir. Microbiol. 53, 1536–1540.

Lovley, D.R., Phillips, E.J.P., 1986. Organic Matter Mineralization with Reduction of Ferric Iron in Anaerobic Sediments. Appl. Envir. Microbiol. 51, 683–689.

Madrigal, P., Gazel, E., Denyer, P., Smith, I., Jicha, B., Flores, K.E., Coleman, D., Snow, J., 2015. A melt-focusing zone in the lithospheric mantle preserved in the Santa Elena Ophiolite, Costa Rica. Lithos 230, 189–205. https://doi.org/10.1016/j.lithos.2015.04.015

Marchand, C., Fernandez, J.-M., Moreton, B., Landi, L., Lallier-Vergès, E., Baltzer, F., 2012. The partitioning of transitional metals (Fe, Mn, Ni, Cr) in mangrove sediments downstream of a ferralitized ultramafic watershed (New Caledonia). Chem. Geol. 300–301, 70–80. https://doi.org/10.1016/j.chemgeo.2012.01.018

Marchandin, H., Jumas-Bilak, E., 2014. The Family Veillonellaceae, in: Rosenberg, E., DeLong, E.F., Lory, S., Stackebrandt, E., Thompson, F. (Eds.), The Prokaryotes: Firmicutes and Tenericutes. Springer Berlin Heidelberg, Berlin, Heidelberg, pp. 433–453. https://doi.org/10.1007/978-3-642-30120-9_361

Marrero, J., Coto, O., Schippers, A., 2017. Anaerobic and aerobic reductive dissolutions of iron-rich nickel laterite overburden by Acidithiobacillus. Hydrometallurgy 168, 49–55. https://doi.org/10.1016/J.HYDROMET.2016.08.012

Martin, E., Hine, R., n.d. Firmicutes. https://doi.org/10.1093/acref/9780198714378.013.6611

Martin, M., 2011. Cutadapt removes adapter sequences from high-throughput sequencing reads. EMBnet.journal 17, 10–12. https://doi.org/10.14806/ej.17.1.200

Masella, A.P., Bartram, A.K., Truszkowski, J.M., Brown, D.G., Neufeld, J.D., 2012. PANDAseq: paired-end assembler for Illumina sequences. BMC Bioinformatics 13, 31. https://doi.org/10.1186/1471-2105-13-31

Medina, W., 2014. Capas SIG - Área de Conservación Guanacaste [WWW Document]. URL https://www.acguanacaste.ac.cr/biodesarrollo/sistemas-de-informacion-geografica/capas-sig (accessed 2.19.19).

Medina, W., 1999a. Geología: Hoja Liberia - Area de Conservación Guanacaste [WWW Document]. Sist. Inf. Geográfica - Área Conserv. Guanacaste. URL

http://www.investigadoresacg.org/IMAGES/MAPFILES/maps/physical_biological/geologia_acg.jpg (accessed 12.11.16).

Medina, W., 1999b. Tipos de vegetación: Hoja Liberia - Area de Conservación Guanacaste [WWW Document]. Sist. Inf. Geográfica - Área Conserv. Guanacaste. URL http://www.investigadoresacg.org/IMAGES/MAPFILES/maps/physical_biological/vegetacion_acg.jpg (accessed 12.11.16).

Medina, W., 1999c. Suelos: Hoja Liberia - Area de Conservación Guanacaste [WWW Document]. Sist. Inf. Geográfica - Área Conserv. Guanacaste. URL http://www.investigadoresacg.org/IMAGES/MAPFILES/maps/physical_biological/suelos_acg.jpg (accessed 12.11.16).

Newsome, L., Cleary, A., Morris, K., Lloyd, J.R., 2017. Long-Term Immobilization of Technetium via Bioremediation with Slow-Release Substrates. Environ. Sci. Technol. 51, 1595–1604. https://doi.org/10.1021/acs.est.6b04876

Noël, V., Morin, G., Juillot, F., Marchand, C., Brest, J., Bargar, J.R., Muñoz, M., Marakovic, G., Ardo, S., Brown, G.E., 2015. Ni cycling in mangrove sediments from New Caledonia. Geochim. Cosmochim. Acta 169, 82–98. https://doi.org/10.1016/j.gca.2015.07.024

Nurk, S., Bankevich, A., Antipov, D., Gurevich, A.A., Korobeynikov, A., Lapidus, A., Prjibelski, A.D., Pyshkin, A., Sirotkin, A., Sirotkin, Y., Stepanauskas, R., Clingenpeel, S.R., Woyke, T., Mclean, J.S., Lasken, R., Tesler, G., Alekseyev, M.A., Pevzner, P.A., 2013. Assembling single-cell genomes and mini-metagenomes from chimeric MDA products. J. Comput. Biol. 20, 714–737. https://doi.org/10.1089/cmb.2013.0084

Oren, A., 2014. The Family Methanobacteriaceae, in: Rosenberg, E., DeLong, E.F., Lory, S., Stackebrandt, E., Thompson, F. (Eds.), The Prokaryotes: Other Major Lineages of Bacteria and The Archaea. Springer Berlin Heidelberg, Berlin, Heidelberg, pp. 165–193. https://doi.org/10.1007/978-3-642-38954-2_411

Power, I.M., Wilson, S.A., Dipple, G.M., 2013. Serpentinite Carbonation for CO2 Sequestration. Elements 9, 115–121. https://doi.org/10.2113/gselements.9.2.115

QGIS Development Team, 2019. QGIS Geographic Information System.

Sakai, S., Conrad, R., Imachi, H., 2014. The Family Methanocellaceae, in: Rosenberg, E., DeLong, E.F., Lory, S., Stackebrandt, E., Thompson, F. (Eds.), The Prokaryotes: Other Major Lineages of Bacteria and The Archaea. Springer Berlin Heidelberg, Berlin, Heidelberg, pp. 209–214. https://doi.org/10.1007/978-3-642-38954-2_318

Sánchez-Murillo, R., Gazel, E., Schwarzenbach, E.M., Crespo-Medina, M., Schrenk, M.O., Boll, J., Gill, B.C., 2014. Geochemical evidence for active tropical serpentinization in the Santa Elena Ophiolite, Costa Rica: An analog of a humid early Earth? Geochemistry, Geophys. Geosystems 15, 1783–1800. https://doi.org/10.1002/2013GC005213

Sattley, W.M., Madigan, M.T., 2014. The Family Heliobacteriaceae, in: Rosenberg, E., DeLong, E.F., Lory, S., Stackebrandt, E., Thompson, F. (Eds.), The Prokaryotes: Firmicutes and Tenericutes. Springer Berlin Heidelberg, Berlin, Heidelberg, pp. 185–196. https://doi.org/10.1007/978-3-642-30120-9_362

Schlesinger, W.H., Bernhardt, E.S., 2013. Chapter 7 - Wetland Ecosystems, in: Schlesinger, W.H., Bernhardt, E.S.B.T.-B. (Third E. (Eds.), . Academic Press, Boston, pp. 233–274. https://doi.org/10.1016/B978-0-12-385874-0.00007-8

Schwarzenbach, E.M., Gill, B.C., Gazel, E., Madrigal, P., 2016. Sulfur and carbon geochemistry of the Santa Elena peridotites: Comparing oceanic and continental processes during peridotite alteration. Lithos 252, 92–108. https://doi.org/10.1016/j.lithos.2016.02.017

Silver, W.L., Lugo, A.E., Keller, M., 1999. Soil oxygen availability and biogeochemistry along rainfall and topographic gradients in upland wet tropical forest soils. Biogeochemistry 44,

301–328. https://doi.org/10.1007/BF00996995

Stackebrandt, E., 2014a. The Emended Family Peptococcaceae and Description of the Families Desulfitobacteriaceae, Desulfotomaculaceae, and Thermincolaceae, in: Rosenberg, E., DeLong, E.F., Lory, S., Stackebrandt, E., Thompson, F. (Eds.), The Prokaryotes: Firmicutes and Tenericutes. Springer Berlin Heidelberg, Berlin, Heidelberg, pp. 285–290. https://doi.org/10.1007/978-3-642-30120-9_364

Stackebrandt, E., 2014b. The Family Lachnospiraceae, in: Rosenberg, E., DeLong, E.F., Lory, S., Stackebrandt, E., Thompson, F. (Eds.), The Prokaryotes: Firmicutes and Tenericutes. Springer Berlin Heidelberg, Berlin, Heidelberg, pp. 197–201. https://doi.org/10.1007/978-3-642-30120-9_363

Stackebrandt, E., 2014c. The Family Clostridiaceae, Other Genera, in: Rosenberg, E., DeLong, E.F., Lory, S., Stackebrandt, E., Thompson, F. (Eds.), The Prokaryotes: Firmicutes and Tenericutes. Springer Berlin Heidelberg, Berlin, Heidelberg, pp. 67–73. https://doi.org/10.1007/978-3-642-30120-9_214

Thompson, A., Chadwick, O.A., Rancourt, D.G., Chorover, J., 2006. Iron-oxide crystallinity increases during soil redox oscillations. Geochim. Cosmochim. Acta 70, 1710–1727. https://doi.org/0.1016/j.gca.2005.12.005

Thompson, A., Rancourt, D.G., Chadwick, O.A., Chorover, J., 2011. Iron solid-phase differentiation along a redox gradient in basaltic soils. Geochim. Cosmochim. Acta 75, 119–133. https://doi.org/10.1016/j.gca.2010.10.005

Thorne, R.L., Roberts, S., Herrington, R., 2012. Climate change and the formation of nickel laterite deposits. Geology 40, 331–334. https://doi.org/10.1130/G32549.1

Tishchenko, V., Meile, C., Scherer, M.M., Pasakarnis, T.S., Thompson, A., 2015. Fe2+ catalyzed iron atom exchange and re-crystallization in a tropical soil. Geochim. Cosmochim. Acta 148, 191–202. https://doi.org/10.1016/j.gca.2014.09.018

Treude, N., Rosencrantz, D., Liesack, W., Schnell, S., 2003. Strain FAc12, a dissimilatory iron-reducing member of the Anaeromyxobacter subgroup of Myxococcales. FEMS Microbiol. Ecol. 44, 261–269. https://doi.org/10.1016/S0168-6496(03)00048-5

Wang, Q., Garrity, G.M., Tiedje, J.M., Cole, J.R., 2007. Naive Bayesian classifier for rapid assignment of rRNA sequences into the new bacterial taxonomy. Appl. Environ. Microbiol. 73, 5261–5267. https://doi.org/10.1128/AEM.00062-07

Whattam, S.A., Gazel, E., Yi, K., Denyer, P., 2016. Origin of plagiogranites in oceanic complexes: A case study of the Nicoya and Santa Elena terranes, Costa Rica. Lithos 262, 75–87. https://doi.org/10.1016/j.lithos.2016.06.017

Whitman, W.B., Bowen, T.L., Boone, D.R., 2014. The Methanogenic Bacteria, in: Rosenberg, E., DeLong, E.F., Lory, S., Stackebrandt, E., Thompson, F. (Eds.), The Prokaryotes: Other Major Lineages of Bacteria and The Archaea. Springer Berlin Heidelberg, Berlin, Heidelberg, pp. 123–163. https://doi.org/10.1007/978-3-642-38954-2_407

Wilkins, M.J., Livens, F.R., Vaughan, D.J., Beadle, I., Lloyd, J.R., 2007. The influence of microbial redox cycling on radionuclide mobility in the subsurface at a low-level radioactive waste storage site. Geobiology 5, 293–301. https://doi.org/10.1111/j.1472-4669.2007.00101.x

Winkler, P., Kaiser, K., Thompson, A., Kalbitz, K., Fiedler, S., Jahn, R., 2018. Contrasting evolution of iron phase composition in soils exposed to redox fluctuations. Geochim. Cosmochim. Acta 235, 89–102. https://doi.org/10.1016/j.gca.2018.05.019

### 5.9 Supplementary figures

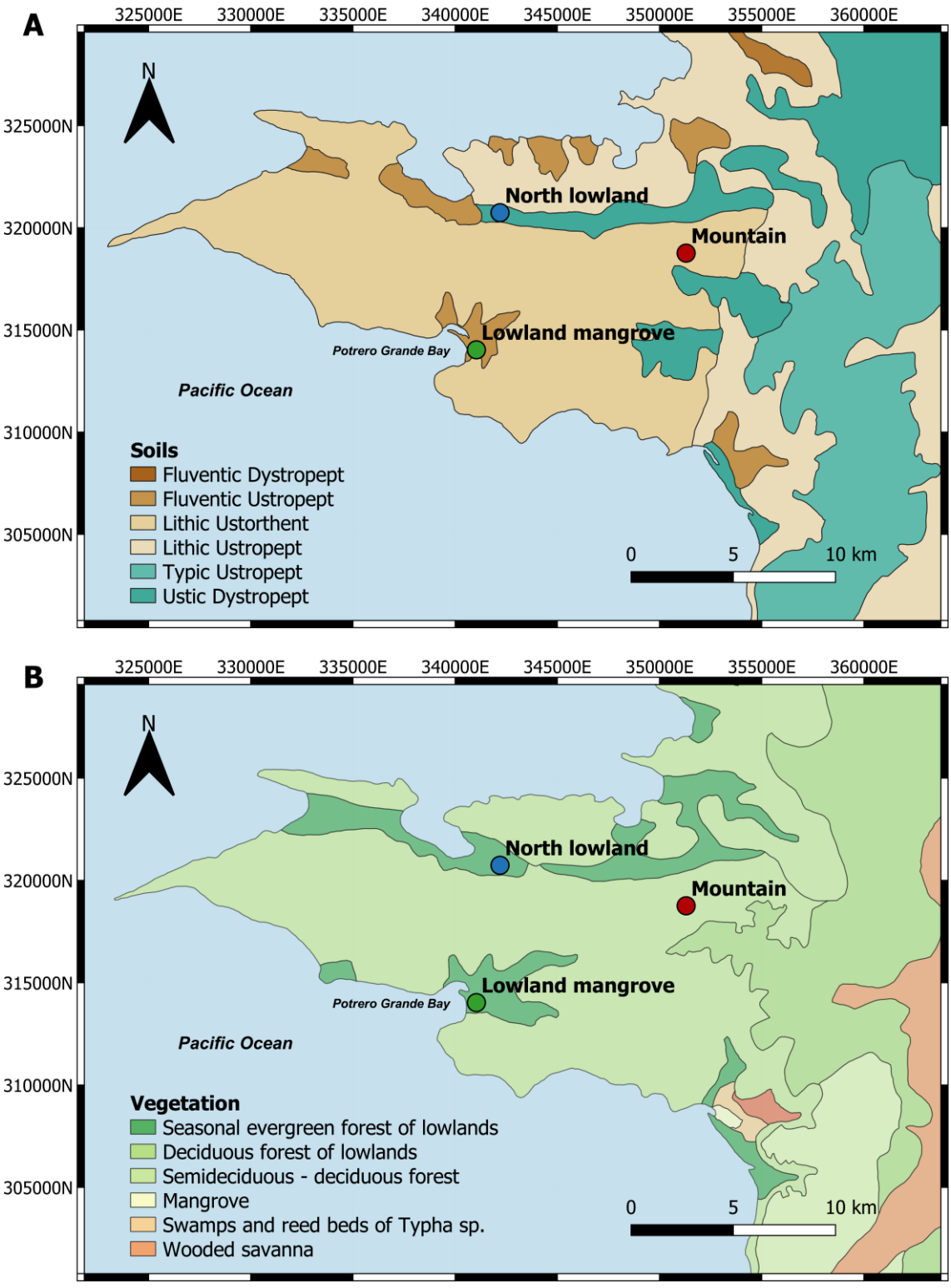


**Figure 5.S1.** (A) Geographical distribution of the three locations sampled within the maps of the soils and (B) vegetation of the Santa Elena Peninsula. Maps adapted from Medina (1999a, 1999b), only relevant colours have been labelled.

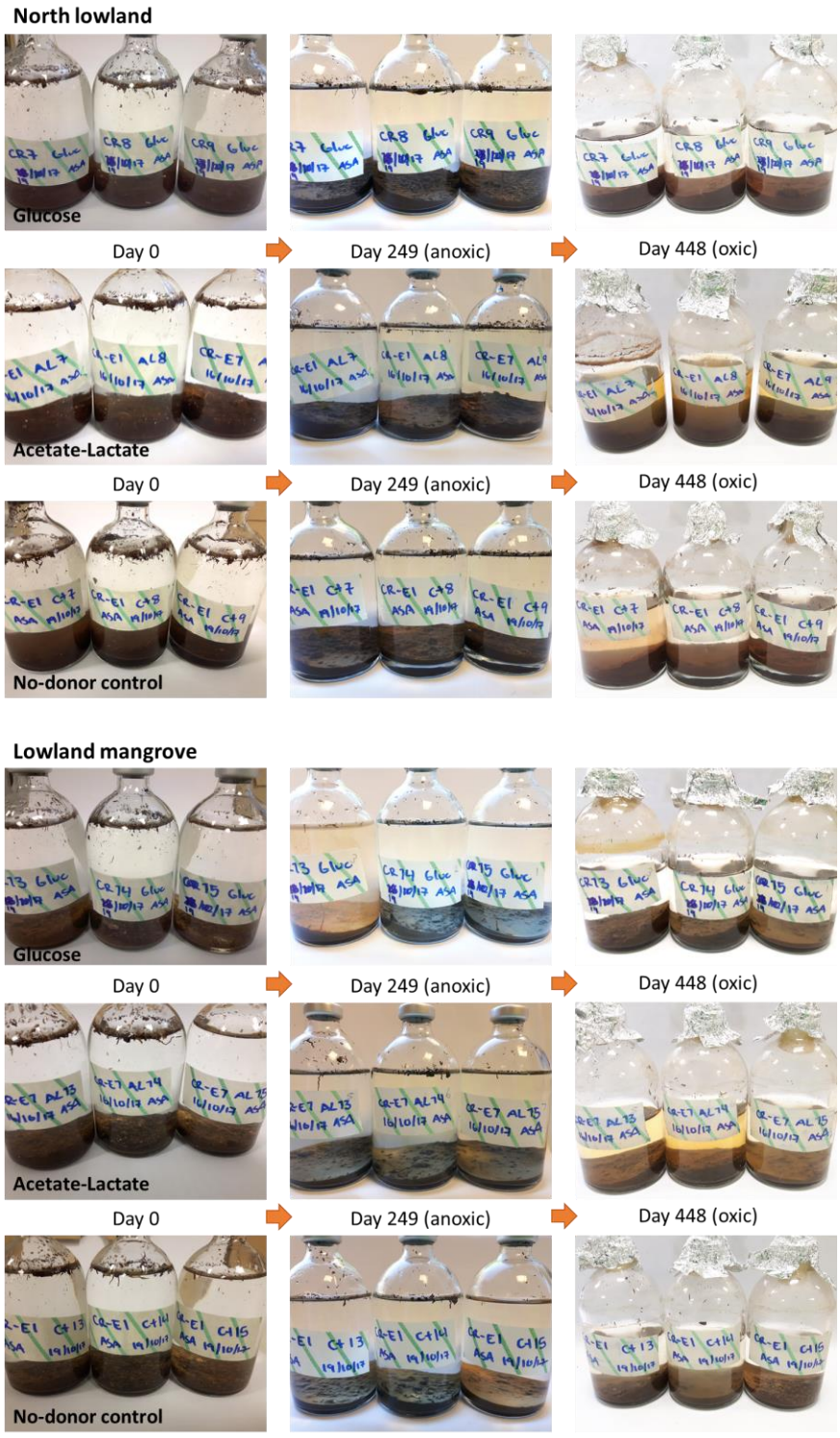


**Figure 5.S2.** Microcosm serum bottle incubations for the three replicates of the north lowland and lowland mangrove location soils biostimulated with glucose, acetate-lactate and a no-donor control at the beginning of the redox cycling microcosm experiment (day 0), after 8 months of anoxic incubation (day 249 overall) and after 5 months of subsequent oxic incubation (day 448 overall).

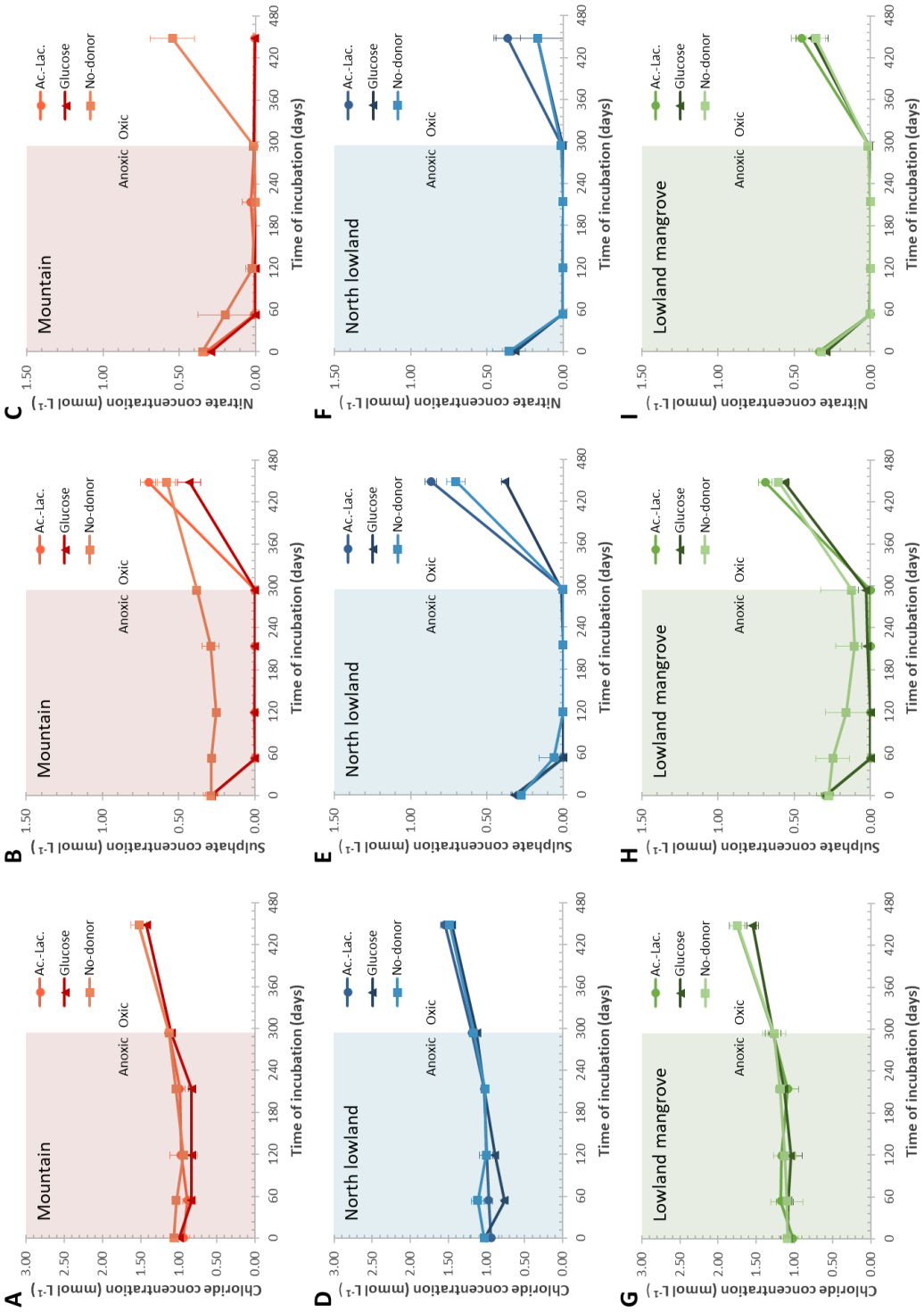


**Figure 5.S3.** Chloride (A, D, G), sulphate (B, E, H) and nitrate (C, F, I) aqueous concentration in the redox cycling microcosm experiments after biostimulation with glucose and acetate/lactate during both anoxic (coloured area) and oxic (clear area) conditions for the soils collected from three locations sampled: mountain, north lowland and lowland mangrove. Results are shown as an average of the 3 replicates and their respective standard deviation.

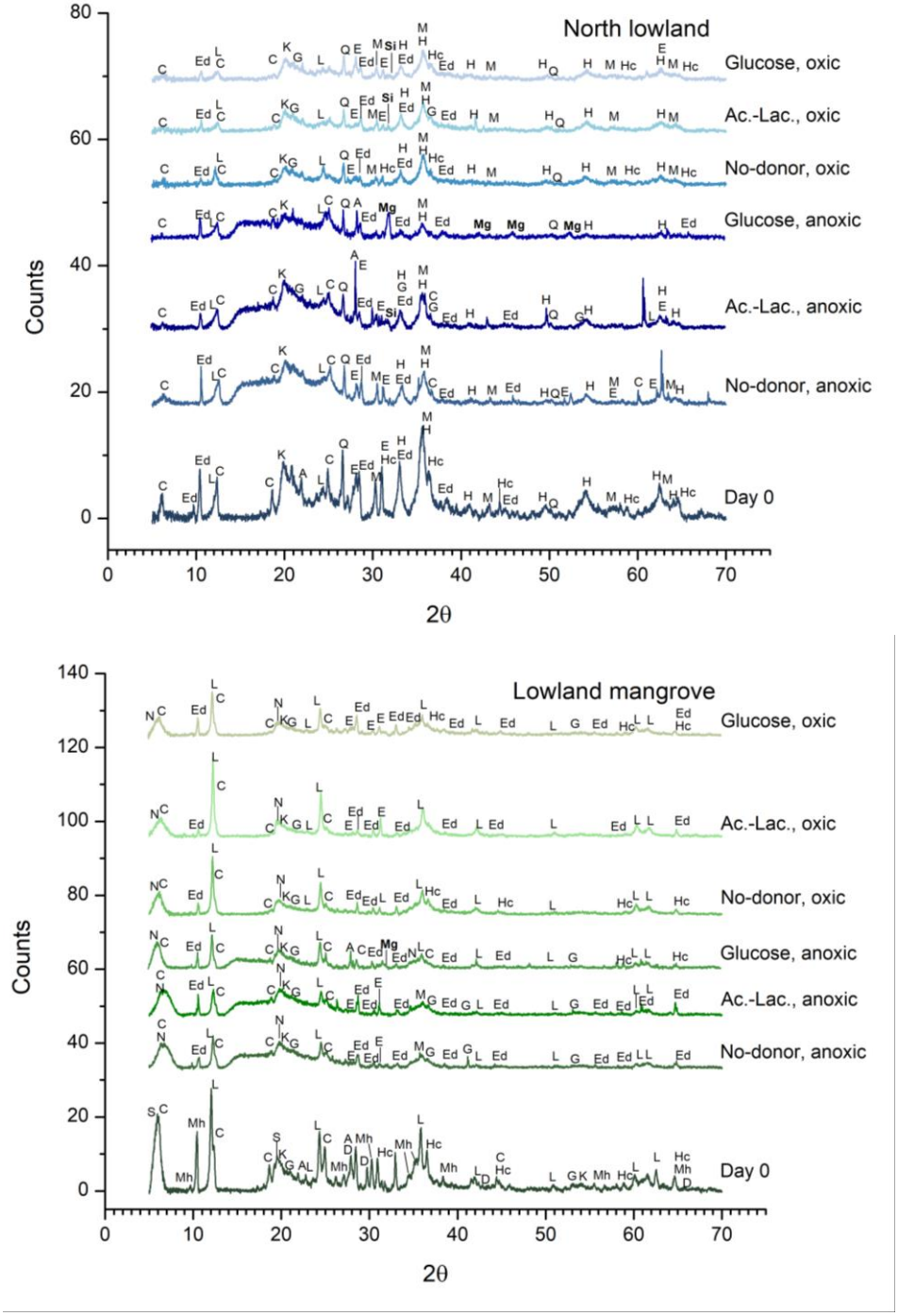


**Figure 5.S4.** Mineralogy of the lateritic soils from the north lowland (top) and the lowland mangrove (bottom) at the start of the redox cycling microcosm experiment, and at the end of the anoxic and oxic incubations, after biostimulation with glucose and acetate/lactate. Main minerals found with XRD were: goethite (G), hematite (H), maghemite (M), lizardite (L), siderite (Si), magnesite (Mg), enstatite (E), diopside (D), clinochlore (C), nontronite (N), stevensite (S), spinel (Sp), hercynite (Hc), magnesio-hornblende (Mh), edenite (Ed), kaolinite (K), albite (A) and quartz (Q).

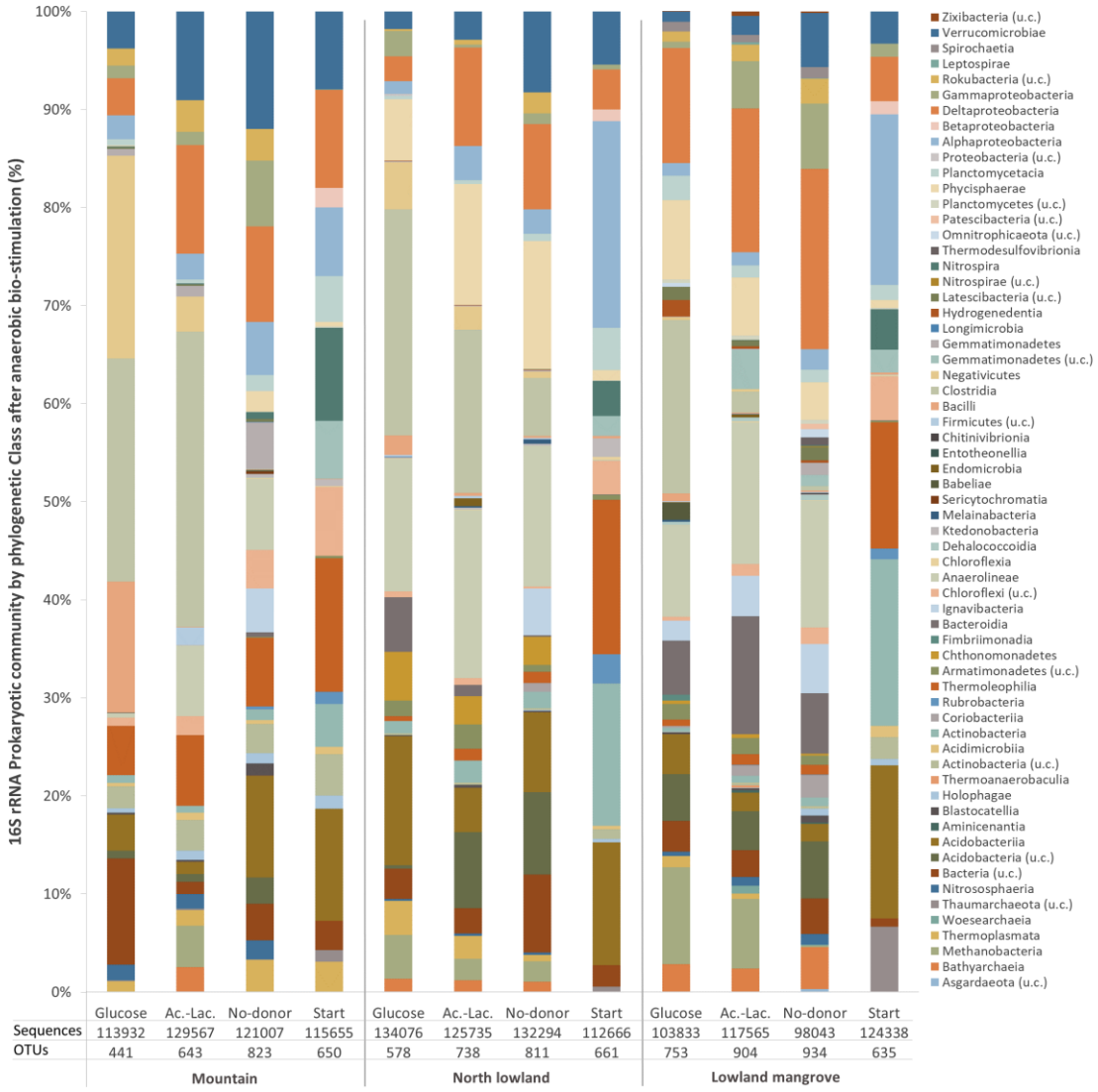


**Figure 5.S5.** Prokaryotic communities per phylogenetic class in the lateritic soils of the Santa Elena Peninsula obtained by the sequencing of the V4 region of 16S rRNA after anoxic biostimulation experiments with glucose, acetate-lactate and no-donor controls; these microcosm experiments were followed by subsequent oxic biostimulation experiments (Figure 5.S6). In every location the starting soil before redox cycling microcosm experiment is also shown; 'u.c.': unclassified class.

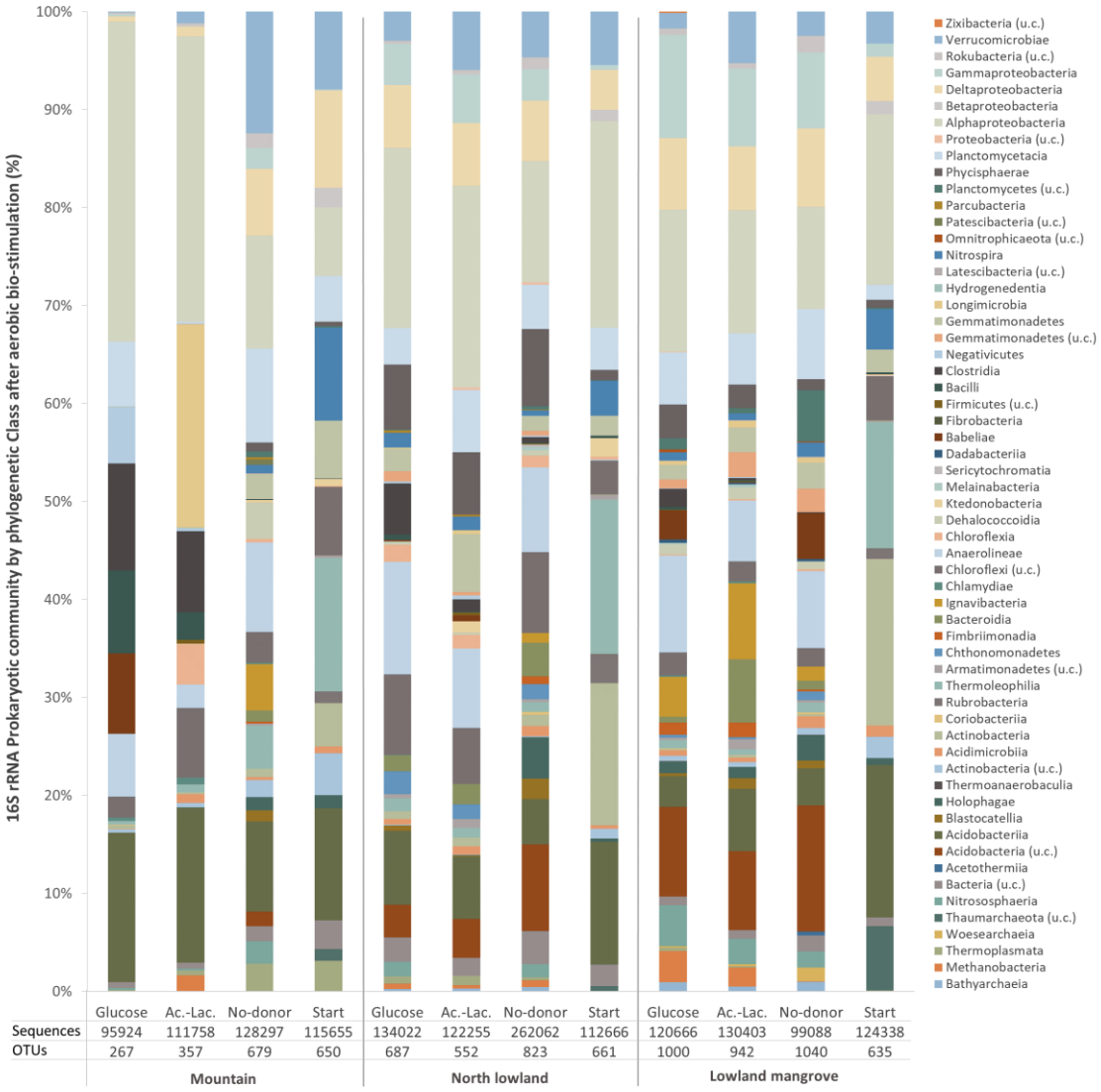


**Figure 5.S6.** Prokaryotic communities per phylogenetic class in the lateritic soils of the Santa Elena Peninsula obtained by the sequencing of the V4 region of 16S rRNA after oxic conditions followed previous anoxic biostimulation (Figure 5.S6) with glucose, acetate-lactate and no-donor controls. In every location the starting soil before redox cycling microcosm experiment is also shown; 'u.c.': unclassified class.

# Chapter 6. Cobalt, nickel and manganese cycling coupled to microbial cellulose degradation in lateritic soils under seasonal variations

---

Agustín F. Solano-Arguedas[a*], Laura Newsome[ab], Christopher Boothman[a], and Jonathan R. Lloyd[a]

[a] Williamson Research Centre, School of Earth and Environmental Sciences, University of Manchester, Manchester, M13 9PL, United Kingdom

[b] Camborne School of Mines and Environment and Sustainability Institute, University of Exeter, Penryn, Cornwall, TR10 9FE, United Kingdom

[*] Corresponding author: agustin.solanoarguedas@postgrad.manchester.ac.uk

## 6.1 Abstract

Serpentine soils are rich in metals such as Co, Ni and Mn, due to their origin from laterites developed from the weathering of ultramafic lithologies; and understanding their biogeochemical cycles have earned attention to secure the supply of cobalt as a critical metal. Recently, the biogeochemistry of cobalt in laterites worldwide was studied by using glucose to biostimulate anoxic conditions able to mobilise Co as part of a bioprocessing strategy to improve its recovery from Ni-rich laterites. In Santa Elena Peninsula in Costa Rica, laterites are actively formed in the Santa Elena Ophiolite area due to the local tropical climate with a strong dry-wet seasonality, resulting in the development of lateritic soils and serpentine ecosystems. Additionally, rainfall patterns can generate redox fluctuations in the soils, potentially affecting microbially-mediated processes. In chapter 5, fluctuating redox conditions were tested to biostimulate Fe, Mg and Co cycling. However, the role of other natural carbon sources, such as cellulose from plant matter, in the natural biogeochemical cycling of Co is still unexplored, and the impact of seasonal precipitation on the biogeochemical cycles of metals have not been tested for tropical serpentine soils. The aim of this study was to continue previous work and characterise the natural biogeochemical cycling of Co, Ni and Mn in the lateritic soils of the Santa Elena Peninsula,

considering the influence of cellulose and seasonal rainfall. Fluctuating redox cycling microcosm experiments were used to simulate biogochemical cycling using two geochemically different soils described in chapter 4 (mountain and north lowland) collected during both the dry and wet season. Results showed that Co, Ni and Mn were released to the aqueous phase during microbial cellulose degradation. In anoxic conditions this was linked to microbial Fe(III) reduction of iron oxides, and under oxic environments to the bioweathering of Mg minerals. DNA sequencing of the samples after biostimulation with cellulose showed that the Firmicutes clades dominated the cellulose-stimulated microcosms and could have a key role in the natural cycling of Co, Ni and Mn in lateritic soils in the presence of cellulose, likely by performing the depolymerisation of cellulose into smaller molecules bioavailable for other microbial processes such as Fe(III) redox cycling. Moreover, cellulose biostimulation generated concentrations of Co, Ni and Mn three to four times higher than biostimulation with glucose likely due to the additional bioweathering of Mg-minerals (not only Fe oxides) and probably also by metal chelating effects likely from the products of microbial aerobic cellulose degradation. Finally, seasonal rainfall variations affected, to a different extent the serpentine soils depending on their topographical characteristics. In the mountain soils precipitation induced faster rates of anaerobic microbially-mediated processes such as Fe(III) reduction and methanogenesis during the wet season. In the lowland soils, variations of metal cycling between seasons were more evident, reflecting the mobilisation of Co, Ni, Mn, Fe occurring in the mountain soils but only during the wet season, while in dry season metal mobilisation did not occur and methanogenesis was favoured instead. That difference was potentially related to more Fe(III) available in the lowland soils during wet season due to Fe(III) influxes from the surrounding mountains to the lowlands originated by rainfall erosive processes. Thus, local seasonal variations are key to understand the natural conditions supporting Co, Ni and Mn cycling in serpentine soils, together with the likely inputs of plant matter as cellulose, shown here to stimulate the release of metals to the aqueous phase, during both anoxic and oxic conditions.

**Keywords:** serpentine soils, Santa Elena Ophiolite, iron redox cycling, bioweathering, geomicrobiology, Firmicutes.

**Highlights:**

Co, Ni and Mn mobilisation in serpentine soils is enhanced due to microbial cellulose degradation.

Metal cycling under anoxic conditions was caused by microbial Fe(III) reduction coupled to cellulose degradation.

Oxic conditions in presence of cellulose favoured metal cycling bioweathering of Mg-minerals.

Firmicutes played a key role in the cycling of Co, Ni and Mn likely by mediating initial cellulose breakdown.

Seasonal precipitation had distinct topographical repercussions in the biogeochemical cycling of Co, Ni, Mn and Fe in serpentine soils.

## 6.2 Introduction

Cobalt is a critic metal for modern society and its demand is likely to increase exponentially in the next decade due to the expansion of electric transportation, as it is an essential component for batteries, and other high technology industries (Alves Dias et al., 2018). One of the ores for cobalt supply are nickel laterites that are formed from serpentinized ultramafic rocks exposed to intensive weathering in humid tropical areas under present or past climates, developing reserves of Ni and Co that comprise about 70% of global Ni resource (Butt and Cluzel, 2013). However, laterites represent only 40% of world nickel production, and the recovery of Co in those deposits (with concentrations around 0.025-0.18%) is mostly as a by-product from Ni mining (Roberts and Gunn, 2014). These Ni deposits can be separated according to their mineralogy: hydrous-silicate deposits including serpentine and chlorite minerals, clay silicate deposits dominated by smectites and oxide deposits largely comprised of iron-oxyhydroxides (Butt and Cluzel, 2013; Roberts and Gunn, 2014).

Laterite formation is largely driven by local climate conditions but is also controlled by several geological variables, as most Ni-Co laterites are developed from the weathering of ophiolites. The Santa Elena Ophiolite in the Santa Elena Peninsula is one of the oceanic complexes found on the Pacific coast of Costa Rica, with serpentinized peridotites (lherzolites, harzburgites and

dunites) as the main lithologies, but gabbros, diabases and associate basalts are also present (Denyer and Gazel, 2009; Madrigal et al., 2015; Schwarzenbach et al., 2016; Whattam et al., 2016). In the tropical and sub-tropical zones, nickel laterites are formed in areas of ultramafic rocks exposed to over 1000 mm of annual precipitation and seasonal temperatures ranges between 15-33°C (Thorne et al., 2012). Such tropical climatic conditions are present in the Santa Elena Peninsula, where the average annual temperature during the day is 33°C and 22°C at night, and the average annual precipitation is 1528 mm. The climate is mostly dry to sub-humid and only 5% of the precipitation occurs during the dry season (December-mid May) resulting in an evident dry-wet seasonality through the year (Herrera, 2016; Instituto Meteorológico Nacional, n.d.; Jiménez M. et al., 2016). Therefore, the Santa Elena Peninsula is an active area of lateritic soil formation, and based on their geography, geochemistry and microbial composition, the lateritic soils of the Santa Elena Peninsula have been categorised into three different types. The main soils in the area are those from the *mountains* that are predominantly rich in Fe, Ni, Mn and Co, dominated by Fe(III) oxides and lizardite [$Mg_3Si_2O_5(OH)_4$] mineralogies. The other two groups of soils are in the lowland areas of the peninsula, one being the *north lowlands* soils of the ophiolite area which have lower values of Fe, Ni, Mn and Co. The third group, the *inner ophiolite lowland* soils*,* are geochemically and microbially more similar to the *mountain* soils as they are surrounded by mountains (Chapter 4).

Biomining of Ni-laterites with model microorganisms has been investigated to improve the extraction of Ni and Co laterites from low-grade deposits or waste materials from mining operations (Hallberg et al., 2011; Johnson and du Plessis, 2015; Marrero et al., 2017, 2015; Smith et al., 2017), leading to the necessity to better understand natural Co and Ni biogeochemistry. Redox cycling of Co was recently studied in laterites from four different ores worldwide, and was found that the natural behaviour of Co was controlled by microbially-mediated manganese cycling under anoxic conditions when biostimulated with glucose as carbon source (Newsome *et al.*, in revision, Appendix 1). In superficial lateritic soils of Santa Elena Peninsula, the natural redox cycling of Fe and Mg was also studied using glucose as electron donor but using fluctuating redox conditions (Chapter 5). In that study, Co, Ni and Mn mobilisation occurred closely associated with microbial redox iron cycling, but only under anoxic conditions (Figure 5.6, 5.7, Chapter 5). Moreover, these studies have only focused on redox cycling conditions biostimulated with small

carbohydrates but the behaviour of other carbon sources widely present in natural environments, such as cellulose from plant matter, are still unexplored. Additionally, seasonal variations in the soils have not previously being investigated, despite being of particular interest in the Santa Elena Peninsula due to the major fluxes of water into the system during the wet season, which can enhance physical weathering and cause soil waterlogging and thus anaerobiosis. The sensitivity of tropical humid ecosystems to climatic variations in precipitation has been reported, impacting on soil $O_2$ and generating anoxic conditions regardless of how well aerated are the soils (Silver et al., 1999). Additionally, the Peninsula of Santa Elena emerges as a unique place to study those natural processes associated with the serpentine soils, not only because of the adequate natural climatic conditions that generate a serpentine ecosystem with active lateritic soil formation, but also because no anthropogenic intervention has occurred in the area for nearly 50 years (Janzen and Hallwachs, 2016).

The aim of this study was to build on previous work to characterise the natural biogeochemical cycling of cobalt, nickel and manganese in the lateritic soils of the Santa Elena Peninsula, considering also the impact of seasonal rainfall. Soils were selected from two topographically related locations within the area of the Santa Elena Ophiolite, but with different geochemical composition. Annual fluctuating redox conditions in the soils were simulated in long term microcosm experiments, using cellulose as an 'environmental' organic substrate to stimulate the development of 'natural' reducing conditions that might occur during the rainy season and when plant matter enters the soil environment more in general. Aeration experiments were used to simulate oxidising conditions that are likely to occur during periods with less water saturation. Also, soil samples were collected during both the dry and wet seasons to see if climate conditions prime the microbial structure and geochemistry of soils. Thus, this study explores the hypothesis of differences in the dominancy of anaerobic or aerobic microbially-mediated processes, depending on the seasonality, that could determine the presence of oxic/anoxic local environments and also impact the biogeochemical cycling of metals such as Co, Ni and Mn.

## 6.3 Material and methods

### 6.3.1 Sampling and location characterisation

Samples were collected in the Santa Elena Peninsula, Costa Rica, within the National Park Santa Rosa of the Area de Conservación Guanacaste (ACG). Two locations along the Peninsula were chosen according to the geochemical/geographical classification (Figure 4.13, Chapter 4): one *mountain* location (ES) and one from the *north lowland of the ophiolite* area (BES), named as 'north lowland' (Figure 6.1, Table 6.1). Samples were collected from both locations during the wet season (September 2016) and the dry season (April-May 2017). In each site, a sampling area of 5 x 5 m was traced and from which 3 different replicates were taken. Surface soil was removed and 1 - 1.5 kg of soil was collected from a depth of 10 - 15 cm. Large rocks or large roots were separated from the samples, which were stored into a re-sealable plastic bag at 4 °C before shipping to the University of Manchester.

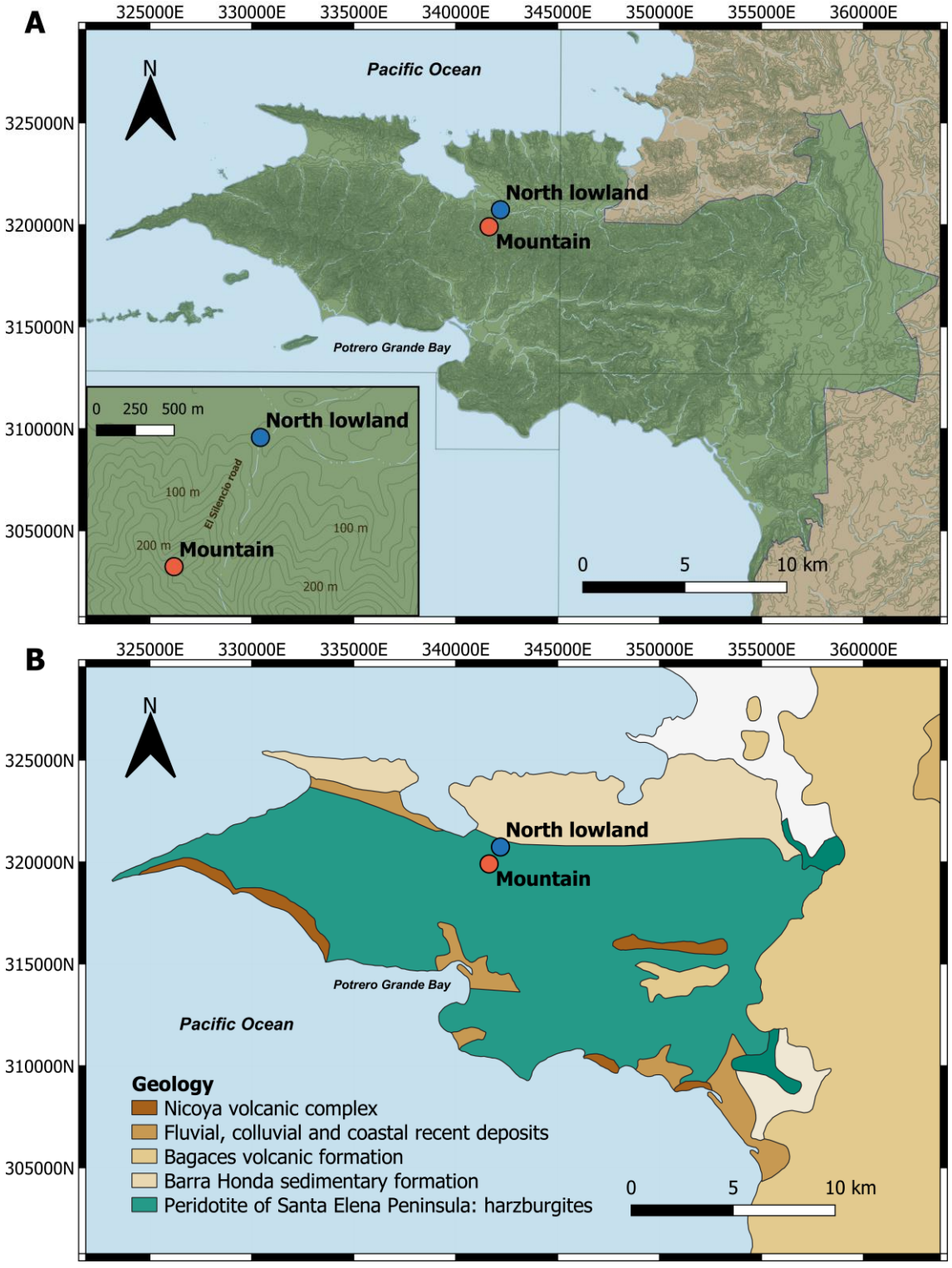


**Figure 6.1.** (A) Geographical distribution of the two locations sampled within the Santa Elena Peninsula (A). The coloured area is the National Park Santa Rosa. Inset is the sampling area in detail. (B) Map of the geology in the Santa Elena Peninsula. Only the relevant colours have been labelled. Adapted from Medina (1999c).

**Table 6.1.** Summary of the locations sampled within the Santa Elena Peninsula. Geochemical/geographical classification (GGC) is based in cluster analysis reported in Chapter 4 (Figure 4.13). A picture of each location is shown in Figure 6.2.

| Location | Coord. | Alt. | GGC | Vegetation* | Soil type* | Geology* | Topography |
|---|---|---|---|---|---|---|---|
| Mountain (ES) | N10° 53.797' W85° 46.796' | 197 m | Mountain | Grass dominated, Semi-deciduous/ deciduous forest | Entisol (Lithic ustorthent) | Ophiolite | Top of a mountain uphill BES location (over El Silencio road) |
| North lowland (BES) | N10° 54.249' W85° 46.493' | 18m | North lowland of the ophiolite | Seasonal evergreen forest of lowlands no grass present | Inceptisol (Ustic dystropept) | Ophiolite (close to ophiolite northern margin) | Flat area on a river valley, between a river and El Silencio road, downhill of ES mountain |

* The vegetation, soil type and geology are geographically based on vegetation, soils, and geology maps of ACG (Medina, 2014). All the sampling points were plotted within every map in Figure 6.1 and 6.S1. / Coord: coordinates, Alt: altitude

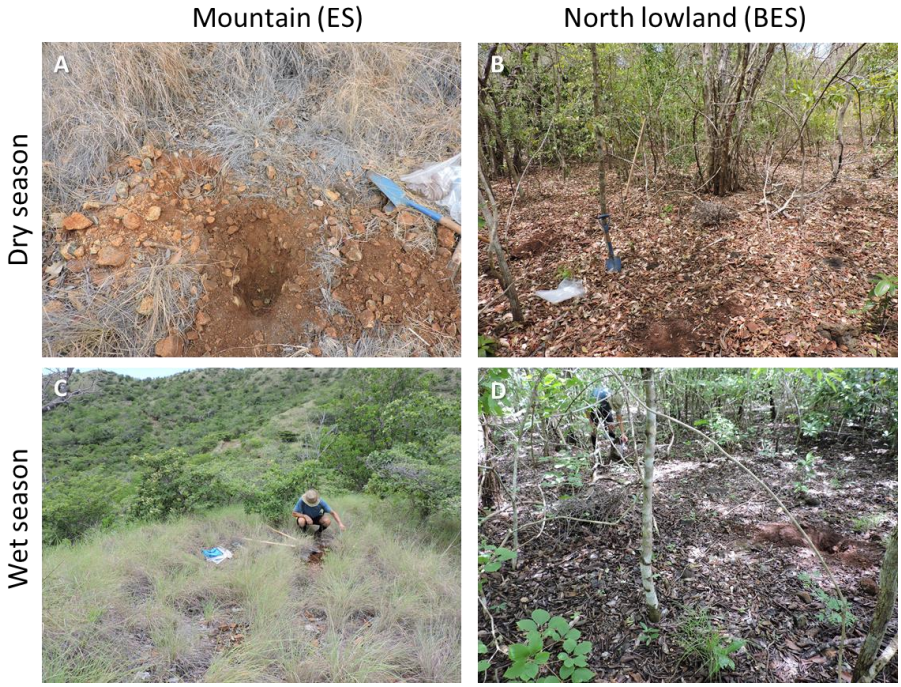


**Figure 6.2.** Detail of the two locations sampled within the Santa Elena Peninsula. (A, C) The mountain location ES and (B, D) the north lowland location of the ophiolite (BES); showing the

variation in the vegetation coverage between dry and wet seasons, the latter with greener and more copious grasses in the mountain and more leaf litter over soil surface in the lowland.

The soils in those two locations are nickel-rich laterites, with large amounts of iron and magnesium, as previously reported in Chapter 4 (Table 6.2). The mineralogy in both the locations is dominated by serpentine, iron oxide and clay silicate minerals (Figure 4.9, Chapter 4).

**Table 6.2.** Geochemical composition of the lateritic soils from the two locations of the Santa Elena Peninsula, adapted from Table 4.1 an 4.S2 (Chapter 4).

| Site | $Fe_2O_3$ (%) | MgO (%) | MnO (%) | Ni (%) | Co (ppm) | Water (wt%) | Total C (wt%) | pH |
|---|---|---|---|---|---|---|---|---|
| Mountain (ES) | 27.0 ± 2.0 | 14.8 ± 1.9 | 0.32 ± 0.05 | 0.84 ± 0.11 | 253 ± 31 | 26.3 ± 0.9 | 12.4 ± 0.1 | 7.15 ± 0.03 |
| North lowland (BES) | 24.9 ± 0.5 | 4.4 ± 1.4 | 0.46 ± 0.01 | 0.38 ± 0.05 | 197 ± 4 | 17.2 ± 0.5 | 12.8 ± 0.2 | 6.47 ± 0.14 |

### 6.3.2 Redox cycling microcosm experiments

Redox cycling experiments were set up using 120 mL serum bottles. From each replicate location, 10 g of each soil sample was added to the serum bottles, followed by 1 g of nanocrystalline cellulose to stimulate the development of microbially-reducing conditions, and then 100 mL of artificial ground water (AGW) (Wilkins et al., 2007). A second batch with no added cellulose was set up as a no-donor control. The headspace volume of the bottles was degassed with a mixture of 80:20 $N_2$ and $CO_2$, and the bottles were sealed with rubber caps. The bottles were incubated anoxically at 30 °C in the dark. After 10 months, oxic conditions were generated by decapping the serum bottles in a laminar flow chamber, replacing the rubber bung with a sterilised foam bung and foil cap, and incubating on a stirring incubator at 30 °C and 100 *g* for 5 months.

The serum bottles were sampled periodically both during the anoxic and oxic stages using sterile syringes and needles, which were flushed with nitrogen when sampling during the anoxic stage. Briefly 0.6 mL of the sediment slurry was extracted from each microcosm bottle, of which 100 µL of the slurry was added to 4.9 mL of 0.5M HCl and subsequently digested with hydroxylamine hydrochloride to quantify any bioavailable Fe(II) and the total Fe content, respectively, using a

ferrozine assay (Lovley and Phillips, 1987, 1986). The rest of the slurry was centrifuged at 14800 *g*, and 100 µL of the supernatant was added to 0.9 mL of deionised water and other 100 µL of the supernatant to 9.9 mL 2% $HNO_3$ to analyse the aqueous organic and inorganic geochemistry by ion chromatography and inductively coupled plasma-atomic emission spectroscopy, respectively. The remaining sample was used to measure the pH and the redox potential ($E_h$) using calibrated electrodes.

#### 6.3.2.1 Inductively coupled plasma mass spectroscopy (ICP-MS) and atomic emission spectroscopy (ICP-AES)

Supernatant samples were diluted in 2% $HNO_3$ and analysed by ICP-MS to measure the content of Co, Ni and Mn. Measurements were carried out on an Agilent Technologies 7700x spectrometer, equipped with a concentric MicroMist nebuliser, a quartz Peltier-cooled Scott-type double pass spray chamber, a 3rd generation Octopole Reaction System (ORS3) and an electron multiplier detector. Fe and Mg concentrations in solution were analysed by ICP-AES using a Perkin-Elmer Optima 5300DV spectrometer, equipped with a concentric glass nebulizer system fitted to a cyclonic spray chamber, and based on an echelle polychromator with a segmented-array charge-coupled-device detector.

#### 6.3.2.2 Ion Chromatography (IC)

Aliquots of supernatant aliquots were diluted in deionised water and analysed by ion chromatography to quantify both inorganic and organic anions, and volatile fatty acids (VFAs). Measurements were carried out on an ICS5000 dual channel ion chromatographer equipped with a conductivity detector. One channel incorporated a microbore Dionex AS18 column to determine inorganic anions including chloride, nitrate and sulphate; the other channel was equipped with a IonPac AS11-HC Hydroxide-Selective Anion-Exchange capillary column to determine VFAs including gluconate, lactate, acetate, formate, propionate, iso- and n-butyrate, iso- and n-valerate.

#### 6.3.2.3 Gas Chromatography (GC-TCD)

Headspace gas produced in the microcosm serum bottles was collected using sterile 50 mL syringes and sterile needles, by puncturing the septum and allowing the pressure of the incoming gas to move the piston of the syringe. The gas was transferred to an argon filled vial, leaving the

sampling gas to replace the argon in the vial. Gas samples were analysed in an Agilent 7890 Gas Chromatography system equipped with a 7890 Thermal Conductivity Detector (TCD) and a HP Molesieve column 30 m long and 0.53 mm diameter, for the detection of hydrogen, oxygen, nitrogen and methane.

#### 6.3.2.4 X-ray diffraction spectroscopy (XRD)

For every location, a representative replicate was chosen for mineralogical characterisation by XRD at the start of the incubation and at the end of the anoxic and the oxic stages. Before analysis, the samples were dried using an anaerobic cabinet for the anaerobic samples, and placed in Coy anaerobic dome specimen holders with X-ray transparent caps. Measurements were carried out on a Bruker D8 Advance diffractometer, equipped with a Göbel Mirror a Lynxeye detector and a copper X-ray tube, providing $CuK_{\alpha 1}$ X-rays with a wavelength of 1.5406 Å. Samples were scanned from 5-70$^{o}$ 2θ, with a step size of 0.02 $^{o}$ and a count time of 0.2 s per step. The resultant patterns were evaluated using EVA version 4, which compares experimental data to standards from the ICDD (International Centre for Diffraction Data) Database.

### 6.3.3 Microbial community analysis

#### 6.3.3.1 DNA extraction

To investigate changes in the microbial community during redox cycling, DNA was extracted from one replicate from each location and season at the start of the experiment, and at the end of both the anoxic and the oxic stages. DNA was extracted from 200 µl of sediment slurry using a DNeasy PowerLyzer PowerSoil Kit (Qiagen, Manchester, U.K). The 16S rRNA gene was amplified via PCR (polymerase chain reaction) using 8F (5'-AGAGTTTGATCCTGGCTCAG-3'), and 1492R (5'-TACGGYTACCTTGTTACGACTT-3') primers (Lane, 1991). Following amplification via PCR, the DNA was stained with SYBR Safe DNA Gel Stain (Thermo Fisher Scientific) before placement in an agarose gel, where it was subsequently separated using electrophoresis. The stained DNA was viewed under UV light, and target ~1500 base pair products were identified by comparison to a ladder of DNA fragments of varying lengths.

#### 6.3.3.2 Prokaryotic community analysis

The PCR amplicons from 16S rRNA gene amplification were sequenced using the Illumina MiSeq platform (Illumina, San Diego, CA, USA) targeting the V4 hyper variable region (forward primer, 515F, 5′-GTGYCAGCMGCCGCGGTAA-3′; reverse primer, 806R, 5′-GGACTACHVGGGTWTCTAAT-3′) for 2 × 250-bp paired-end sequencing (Illumina) (Caporaso et al., 2012, 2011). PCR amplification was performed using the Roche FastStart High Fidelity PCR System (Roche Diagnostics Ltd, Burgess Hill, UK) in 50µl reactions under the following conditions: initial denaturation at 95°C for 2 min, followed by 36 cycles of 95 °C for 30 s, 55 °C for 30 s, 72 °C for 1 min, and a final extension step of 5 min at 72 °C. The PCR products were purified and normalised to ~20 ng each using the SequalPrep Normalization Kit (Fisher Scientific, Loughborough, UK). The PCR amplicons from all samples were pooled in equimolar ratios. The run was performed using a 4 pM sample library spiked with 4 pM PhiX to a final concentration of 10% following the method of Schloss and Kozich (Kozich et al., 2013).

Raw sequences for prokaryotes were divided into samples by barcodes (up to one mismatch was permitted) using a sequencing pipeline. Quality control and trimming was performed using Cutadapt (Martin, 2011), FastQC (Babraham Bioinformatics, n.d.), and Sickle (Joshi and Fass, 2011). MiSeq error correction was performed using SPADes (Nurk et al., 2013). Forward and reverse reads were incorporated into full-length sequences with Pandaseq (Masella et al., 2012). Chimeras were removed using ChimeraSlayer (Haas et al., 2011), and operational taxonomic units (OTUs) were generated with UPARSE (Edgar, 2013). OTUs were classified by Usearch (Edgar, 2010) at the 97% similarity level, and singletons were removed. Rarefaction analysis was conducted using the original detected OTUs in Qiime (Caporaso et al., 2010). The taxonomic assignment was performed by the RDP classifier (Wang et al., 2007).

### 6.3.4 Map plotting

The processing of map data was done using QGIS 3.10.0 A Coruña software (QGIS Development Team, 2019). GIS layers were taken from the ACG GIS-maps database (Medina, 2014) and Costa Rica Lambert Norte was used as the coordinate reference system.

## 6.4 Results and Discussion

### 6.4.1 Microbial processes on cellulose-amended redox cycling microcosm experiments

Lateritic soil samples from the Santa Elena Ophiolite were collected from two different locations in the wet and dry seasons and then biostimulated with cellulose to study the cycling of Co, Ni and Mn. While few visible changes were observed in the no added electron donor controls, the presence of cellulose led to changes in both colouration and texture after 10 months of anoxic incubation and subsequent oxic incubation for 5 months (Figure 6.3 and 6.S2). This was more evident in the mountain soil samples, and a similar response was observed for the samples from the wet and the dry seasons. Darkening of the soils in the presence of cellulose indicated anoxic conditions, likely due to the microbially-mediated reduction of Fe(III) and/or sulphate into ferrous and sulphide minerals.

As well as this colour change, gas was generated in all of the serum bottles treated with cellulose, more vigorously in the lowland soil samples and for a longer period in the dry season soils compared to the wet season samples. Gas production occurred throughout the period of anoxic incubation in the dry season lowland microcosms (Figure 6.S2A).

After 10 months of anoxic incubation, each microcosm experiment was subjected to aeration. The colour of those originally treated with cellulose slowly changed from black to orange/brown after 20 days of oxic incubation, and after 5 months of aeration the samples had returned to their original colour. No colour changes were observed in the no-donor controls during anoxic or aerobic incubation. A similar trend was observed in lateritic soils from the Santa Elena Peninsula after biostimulation with glucose, but interestingly only with mountain soils, not the lowland soils (Figure 5.3, 5.S2, Chapter 5). This suggests that the microbial communities in the mountain and lowland soils both responded differently to biostimulation with glucose or cellulose. Also, the walls of the bottles containing both mountain soil samples amended with cellulose were covered with an orange thin film. In the lowland soils, those changes only occurred in the wet season samples, but one of the replicates behaved differently than the other two, reflecting the natural heterogeneity of the soils (Figure 6.S2B). Both the recovering of the original colouration and the formation of thin orange films suggested the presence of Fe(III) oxides. Finally, during both anoxic

and oxic stages, and regardless of season or location, unconsumed cellulose remained present in the microcosms, visible as a white sediment.


**Figure 6.3.** Microcosm serum bottles for the three replicates of the mountain lateritic soil from both dry (A) and wet season (B) biostimulated with cellulose and a no-donor control at the beginning of the redox cycling microcosm experiment (day 0), after 8 months of anoxic incubation (day 249 overall) and after 5 months of subsequent oxic incubation (day 448 overall). The samples from the north lowland location during both seasons are shown in Figure 6.S2.

During anaerobic biostimulation with cellulose, the pH of each microcosm decreased from pH 8 to pH 6 and remained stable, while the no-donor controls remained close to pH 8 (Figure 6.4A, B). This difference was likely due to microbial cellulose metabolism under anoxic conditions

involving the production of $CO_2$ and organic acids into the aqueous phase, both contributing to the acidification of the media (Béguin and Aubert, 1994). Upon aeration, the pH of the cellulose-stimulated mountain soils decreased further to 4.5 (Figure 6.4A) suggesting that oxygen ingress destabilised the equilibrium by either increasing the rate of cellulose degradation or inducing a second mechanism of cellulose degradation. The response of the lowland soils differed depending on the seasonal origin, especially during the oxic phase (Figure 6.5B). Under oxic conditions, the lowland sample from the wet season had low pH values like the mountain soils while the dry season samples behaved similarly to those biostimulated with glucose previously reported, that showed a stable pH slightly above 7 (Figure 5.4C, Chapter 5).

Fluctuating redox cycling conditions were observed in all the microcosm experiments (Figure 6.4C, D), confirming the effectiveness of this methodology in simulating environmental redox cycling, as described beforehand (Chapter 5). Similar to previous work with glucose (Figure 5.4), cellulose biostimulation led to the redox potential stabilising at around -400 mV during anoxic conditions regardless of location (Figure 6.4). However, the rate to reach the minimum redox potential differed in the mountain soil samples; it was faster in the wet season (60 days) compared to the dry season (90 days) (Figure 6.4C), suggesting that precipitation could be important to induce redox processes in the serpentine soils by facilitating the development of anoxic conditions in those soils. In upland tropical soils from Hawaii was observed that rainfall increased the potential for Fe reduction, favouring redox processes in microsites of predominantly oxic soils (Hodges et al., 2018); and in tropical soils from Puerto Rico, rainfall generated short redox fluctuations that lead to more rapid iron reduction rates (Barcellos et al., 2018a). The redox potential also decreased in all of the no-donor controls, likely due to the metabolism of natural organic matter present in the soils by the indigenous microbial community. After aeration all of the samples similarly increased their redox potential to values close to 0 mV, though the mountain sample from the wet season reached close to 100 mV by the end of the experiment.

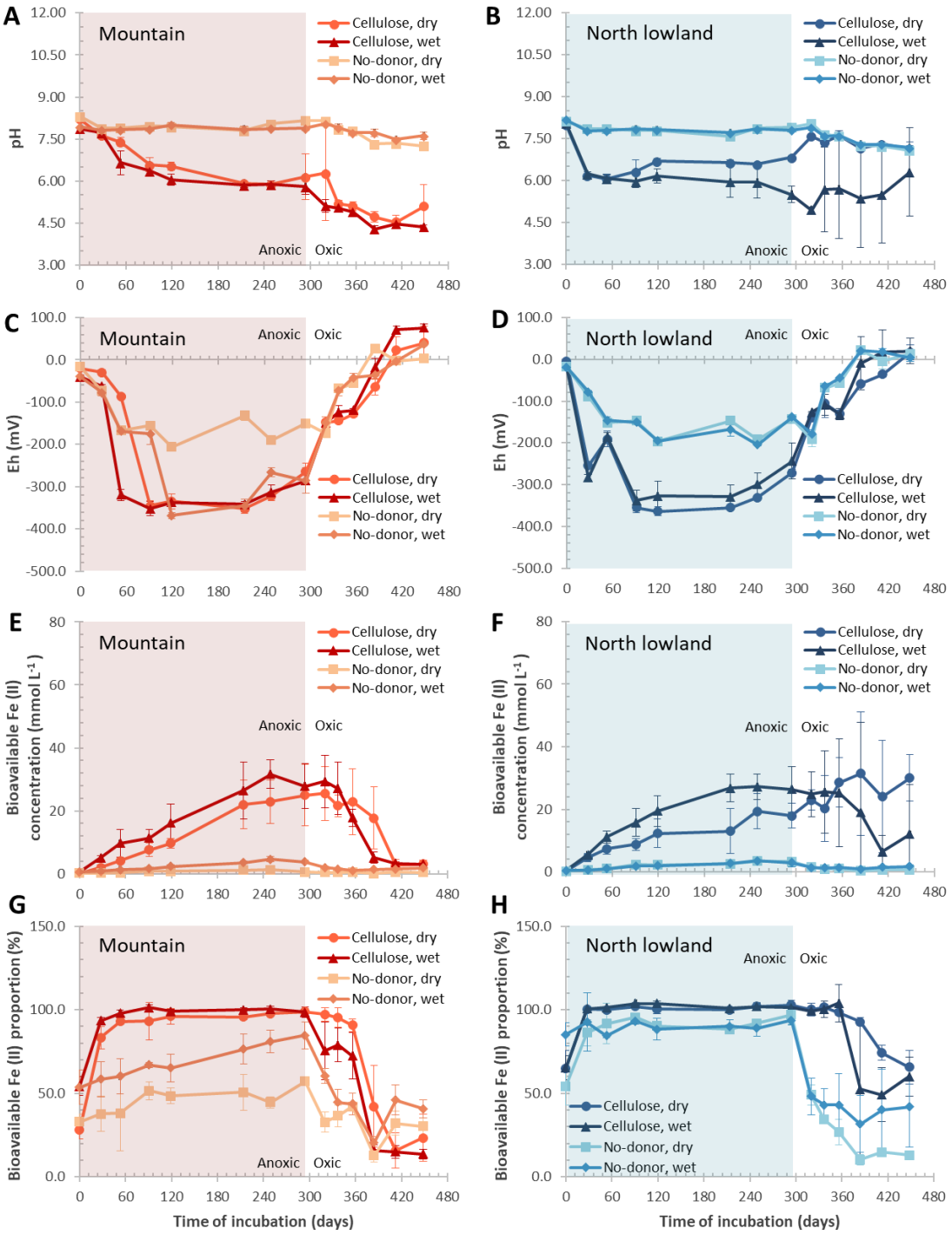


**Figure 6.4.** (A, B) pH, (C, D) redox potential (Eh) and (E-H) bio-available Fe(II) after biostimulation with cellulose during the anoxic (coloured area) and the oxic (clear area) phases of the redox cycling microcosm experiments, for both locations and seasons sampled. Results are shown as an average of the 3 replicates tested and their respective standard deviation.

The concentration of Fe(II) increased during anaerobic cellulose degradation in each experiment regardless of location or season, likely due to microbial Fe(III) reduction (Figure 6.4E, F). Higher

concentrations of Fe(II) were observed in samples collected during the wet season from both locations during the anoxic phase, just like reported in tropical basaltic soils from Hawaii (Thompson et al., 2011). Following aeration, Fe(II) remained present in solution at a stable concentration for the first two months, likely due to an incomplete oxidising environment by the presence of microsites of anoxic conditions (Ginn et al., 2017; Silver et al., 1999) or because of redox buffering by excess cellulose (Newsome et al., 2017). After two months, the wet season mountain soil samples became susceptible to Fe(II) re-oxidation, followed by the dry season samples 30 days later (Figure 6.4E, G). Similar trends were observed in the lowland samples, but which were more recalcitrant to re-oxidation than the mountain soils (Figure 6.4F, H), which could be associated with their topographical context (Barcellos et al., 2018; Silver et al., 1999). The presence of Fe(II) in the no-donor was again likely due to the occurrence of natural organic matter in the soils. In unsaturated upland tropical soils of humid environments was demonstrated that Fe(III) reduction could occur with complex mixtures of organic compounds such as leaf litter, and even without strict anaerobic conditions (Liptzin and Silver, 2009). Additionally, the characteristics of redox fluctuation *per se*, such as the rate of transition between oxic/anoxic conditions and the length of time of every stage, can influence the cycling of iron and organic matter in soils; as seen in tropical soils from Puerto Rico of volcanic nature (Barcellos et al., 2018a). Thus, this study could be the basis for further work considering more redox cycles or varying the length of the anoxic conditions, to better understand the impact of the seasonal precipitation on the redox cycling processes occurring on serpentine soils.

Nitrate aqueous concentration decreased at the beginning of the anoxic conditions in all of the microcosm experiments regardless of location or season and including the no added electron donor controls (Figure 6.S3E, F), suggesting that nitrate reduction occurred, and also, the presence of natural carbon sources in the soils. Sulphate reduction occurred in each microcosm stimulated with cellulose (Figure 6.S3C, D), but not in the mountain soil controls. This suggests the amount of natural organic matter was insufficient to allow the development of sulphate reducing conditions.

Volatile fatty acids (VFAs) and methane generation were measured as a proxy for cellulose degradation in the redox cycling microcosm experiments (Figure 6.5). Cellulose is transformed into methane and carbon dioxide mediated by anaerobic cellulolytic organisms, via fermentation

of glucose derived from the cellulose into $H_2$, $CO_2$ and organic molecules such as acids and alcohols, that can be later transformed into acetate and $CO_2$ in a second step (Béguin and Aubert, 1994). In this study, cellulose biostimulation under anoxic conditions influenced the microbial production of VFAs, mostly as acetate, likely due to Fe(III) reduction after cellulose was microbially depolymerised into shorter units (Killham and Prosser, 2015; Lovley et al., 2004). However, its accumulation was different between locations; in mountain lateritic soils it constantly increased as a result of the excess cellulose constantly supplying carbon for microbial iron reduction (Figure 6.5A). Meanwhile, in the lowland soils (Figure 6.5B), build-up of VFAs occurred only in samples from the wet season although VFAs concentration stabilised after 60 days of anoxic incubation, the same time point when the VFAs in the dry season samples started to decrease.

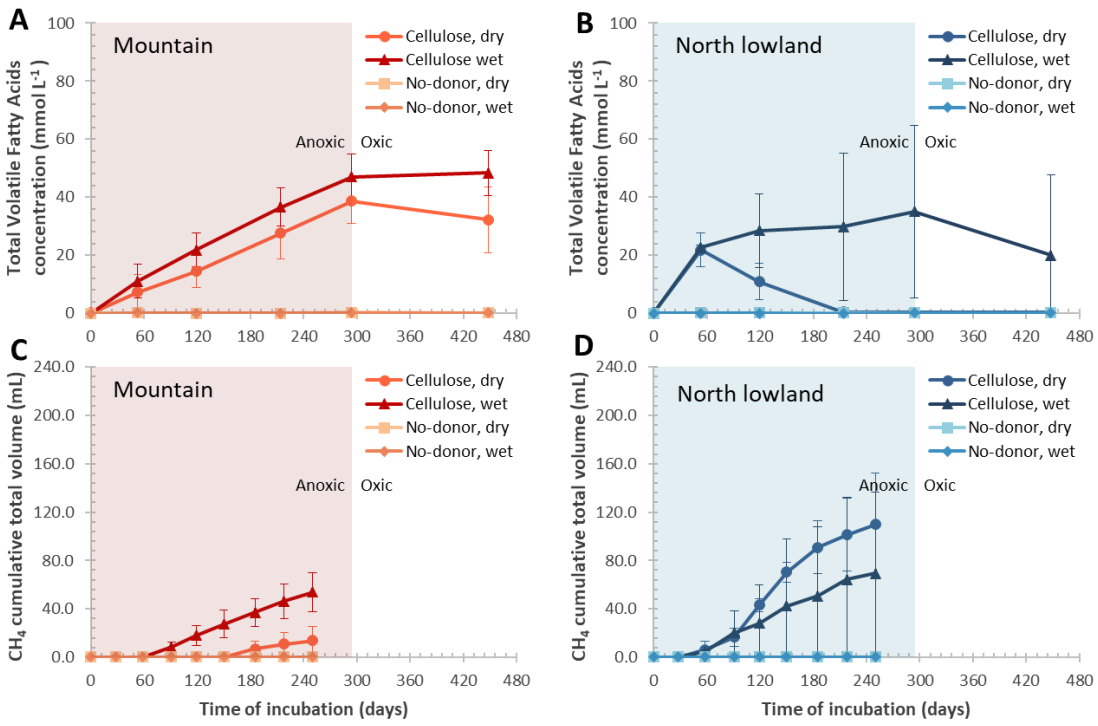


**Figure 6.5.** (A, B) Aqueous total volatile fatty acids concentration and (C, D) approximate methane cumulative total volume in the redox cycling microcosm experiments after biostimulation with cellulose during the anoxic (coloured area) and the oxic (clear area) phases, for both locations and seasons sampled. Results are shown as an average of the 3 replicates tested and their respective standard deviation.

Methanogenesis occurred in all of the samples treated with cellulose regardless of the season collected and with an increasing rate of production measured in all soils tested, although lower volumes of methane were generated in the mountain soils (Figure 6.5C, D). Previous work in Santa Elena Peninsula lateritic soils did not reveal methanogenesis occurring in mountain soils when biostimulated with glucose (Figure 5.8B, Chapter 5), though those samples were collected from the dry season and here it was the soils from wet season that produced the highest volumes of methane. Similarly in upland tropical forests soils from Puerto Rico, methane concentration was reported to be sensitive to changes in rainfall, resulting in dynamic soil systems in terms of methane cycling, where microorganisms can respond fast to microsite variations (Silver et al., 1999). In the lowland soil from the wet season, methane evolution commenced when the VFAs started to stabilise (60 days) (Figure 6.5B, D), similar to when VFAs decreased in the lowland soils from the dry season. That was the same time point when measurable methane occurred in the 'north lowland' soils biostimulated with glucose in a previous study (Figure 5.8D, Chapter 5). The different behaviour of VFAs and methane production depending on the seasonality suggests that in the lowland lateritic soils from the Santa Elena Peninsula, microbial Fe(III)-reduction coupled to anaerobic carbon metabolism competes with methanogenesis for reducing equivalents from the carbon sources naturally found in the soils, especially during the dry season. In general, methanogens are abundant not only in the absence of $O_2$ but also where electron acceptors including nitrate, Fe(III) and sulphate are limited (Whitman et al., 2014). In these microcosm experiments, nitrate or sulphate behaved similarly in both seasons (Figure 6.S3) thus not representing a major impact on methanogenesis rates, and therefore suggesting that Fe(III) could be a key electron acceptor during wet season. Fe(III) could be more abundant in the lowland soils during wet season than in the dry season due to Fe(III) influxes from the surrounding mountains, which soils are rich in Fe(III) minerals and Fe content in general (Figure 4.9 and Table 4.S2, Chapter 4), to the lowlands. The intense seasonal rains increase the rate of erosive processes in the overexposed soils of the mountains (Section 4.4.3, Chapter 4) and also facilitate mobilisation of rocks, minerals and solved cations, ultimately depositing all of them in the lowland soils. In other tropical soils but of volcanic nature was also reported that the degree of weathering increased with altitude, reflecting local climatic conditions, and in particular, precipitation (Taboada et al., 2016). This higher Fe(III) content could also explain the higher bioavailability of

Fe(II) observed during anoxic biostimulation in the lowland soils from the wet season (Figure 6.4F). Following aeration, the concentration of VFAs stabilised likely due to the disappearance of microbial Fe(III) reduction processes; but the VFAs concentration did not decrease either, suggesting that microbial carbon metabolism continued but favouring the production of acetate.

### 6.4.2 Effects of cellulose biostimulation on Co, Ni and Mn cycling under reducing conditions

Natural microbial redox cycling of Co, Ni and Mn in the lateritic soils of the Santa Elena Peninsula was enhanced when inducing cellulose biostimulation under fluctuating redox conditions (Figure 6.6). In mountain soils, the mobilisation of Co, Ni and Mn was favoured when cellulose was present (Figure 6A, C, E) and following a similar behaviour to iron during anoxic conditions (Figure 6.6G). The latter association with iron was also observed in other laterites when biostimulated with glucose (Newsome *et al.*, in revision, Appendix 1), and in previous work in this type of soils from the Santa Elena Peninsula (Section 5.4.2, Chapter 5), but here several differences were observed. First, the maximum concentration of Co, Ni, Mn, Fe and even Mg was reached after 210 days of anoxic incubation with cellulose (Figure 6.6A, C, E, G, I) while with glucose it only took 60 days. That difference of time could be related to the breakdown of cellulose as a limiting step for subsequent microbial assimilation of the resulting glucose (Killham and Prosser, 2015), making the metabolism of glucose slower and so too the associated microbial Fe(III) reduction as well as the mobilisation of Co, Ni and Mn. Second, the maximum concentrations of metals in solution under anoxic conditions with cellulose were stable during the total anoxic stage and considerably higher when compared with glucose. For example, Co and Ni were four times more concentrated, Mn three times; and aqueous concentrations of the major elements Fe and Mg were seven and two times higher (respectively) with no evidence of precipitation (Figure 5.6 and 5.7, Chapter 5). Higher concentrations of metals in the aqueous phase could be just an effect of the excess of cellulose in the medium continuously supplying carbon to the system while glucose was quickly assimilated and consumed in previous work. However, the fact that the increase was not homogeneous for all the metals, and was considerably higher for Fe than for Mg, suggests that cellulose anaerobic metabolism favoured the bioweathering of Fe minerals over Mg minerals. This enhanced microbial Fe(III) reduction led to more Co, Ni and Mn being mobilised, particularly from the mountain lateritic soils.

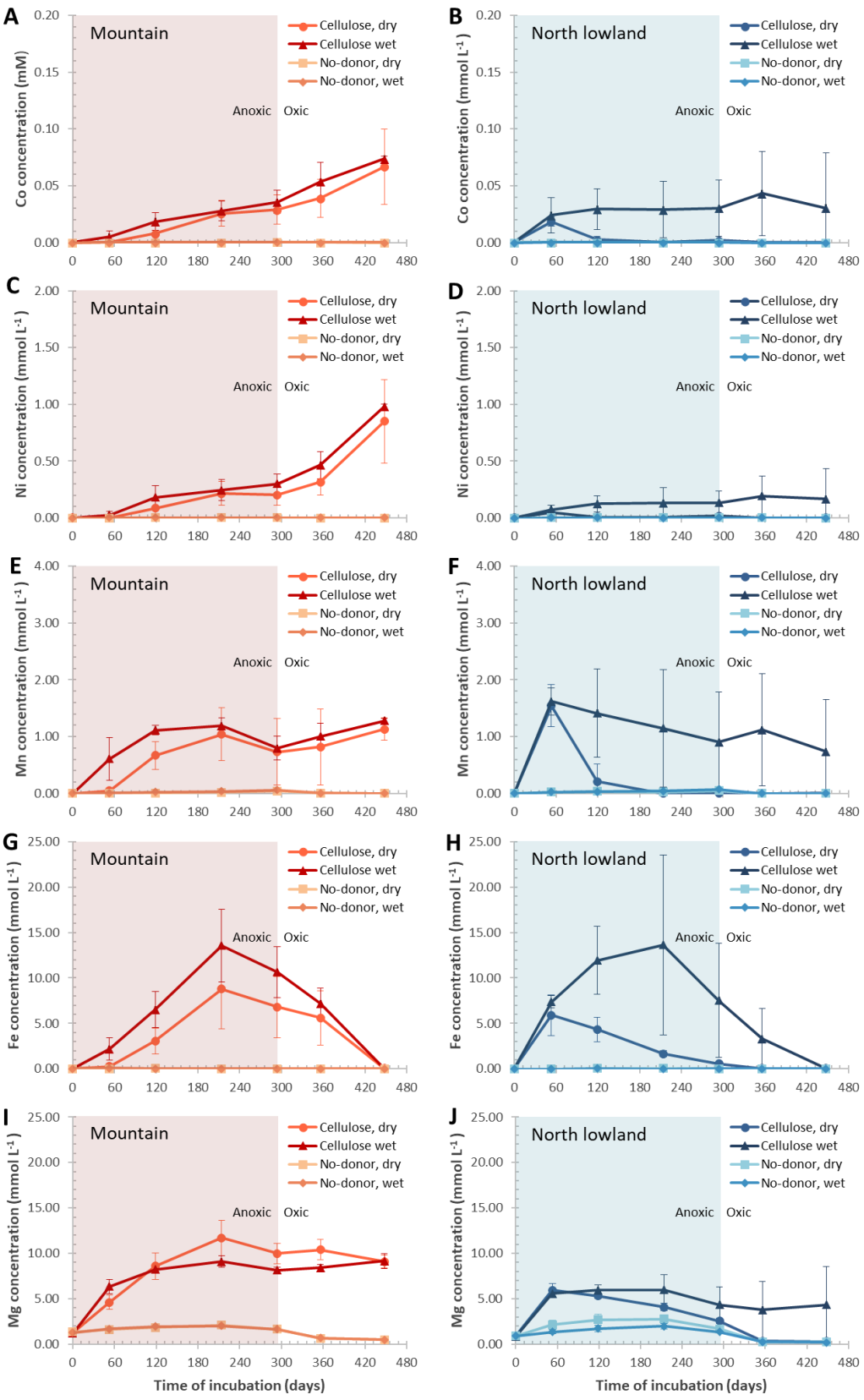


**Figure 6.6.** Aqueous concentration of Co (A, B), Ni (C, D), Mn (E, F), Fe (G, H) and Mg (I, J) after biostimulation with cellulose during the anoxic (coloured area) and the oxic (clear area) phases

of the redox cycling microcosm experiments, for both locations and seasons sampled. Results are shown as an average of the 3 replicates tested and their respective standard deviation.

The season of collection of the mountain soils, did not significantly affect the response of these soils in the experiments, with similar trends and concentrations observed for most biogeochemical parameters (Figure 6.4, 6.5, 6.6). However, the cellulose-stimulated wet season sample from the mountain produced more methane than the dry season sample (Figure 6.5C), and the wet season no-donor control generated more reducing conditions and produced some Fe(II) (Figure 6.4C, E). These results suggest that, under natural conditions, the impact of seasonal rains on the mountain serpentine soils could be a trigger to stimulate the development of anaerobic microbially-mediated processes such as Fe(III) reduction or even methanogenesis. A similar trend has been reported in other types of upland tropical soils such as in andesite volcanoclastic soils from Puerto Rico where methane concentration in soils was highly sensible to rainfall changes (Silver et al., 1999); or basaltic soils from Hawaii where aqueous Fe(II) removal was enhanced by high water-throughput and anoxia conditions (Thompson et al., 2011). In contrast to the mountain samples, differences on metal cycling between the wet and dry season samples were clearly apparent in the lowland samples when anaerobically biostimulated with cellulose. The wet season samples generated higher concentrations of aqueous metals, which remained in solution throughout the anoxic phase of the experiment (Figure 6.6B, D, F, G, I), and also had lower pH (Figure 6.4B) and more Fe(II) (Figure 6.4F). These results suggest that the wet season lowland soils are richer in Fe(III), resembling the general geochemical composition of the mountain soils in the entire Santa Elena Peninsula described in previous work (Figure 4.9 and Table 4.S2, Chapter 4); and indeed behave more geochemically similar to the wet and dry season mountain soils. As explained in section 6.4.2, a higher content of Fe(III) could be a temporal *in situ* condition of the lowland soils during wet season; an increase that could be supported by elevated rates of erosive processes occurring uphill in the mountains due to the intense precipitation, resulting on higher influxes of minerals and cations from the mountains to the lowlands. Unlike the mountain soils, the no-donor controls for the wet and dry season lowland soils showed a similar response with few indicators of biogeochemical activity, except for nitrate reduction (Figure 6.S3). Therefore, during the wet season, cellulose degradation is a key process to stimulate metal cycling in the serpentine soils of lowlands. This is the time of the year when more plant litter could be available in the soils (from

the more abundant vegetation due to the precipitation) and thus degradation rates could be more intense (likely including high fungal cellulolytic activity too). As cellulose degradation is enhanced, then other microbial processes like Fe(III) reduction are boosted, which seems not to occur during the dry season and in the absence of cellulose.

### 6.4.3 Effects of cellulose biostimulation on Co, Ni and Mn cycling under oxidising conditions

Following aeration in the microcosm experiments, the concentrations of aqueous Co and Ni continued to increase in the cellulose biostimulated mountain soils (Figure 6.6A, C), Mg and Mn remained constant (Figure 6.6E, I), while concentrations of aqueous Fe decreased rapidly (Figure 6.6G), likely due to the precipitation of Fe(III) oxide (Ginn et al., 2017; Thompson et al., 2011). These results suggest that in the presence of cellulose and under oxic conditions, the fate of Co, Ni and Mn to a lesser extent, is no longer associated with Fe biogeochemical cycling in these lateritic soils, but are still microbially mediated and linked to cellulose metabolism. However, the concentration of VFAs in the aqueous phase did not increase during the oxic phase (Figure 6.5A) as it did the concentration of Co and Ni. This suggests that other organic products from a different microbial cellulose degradation metabolic pathway could have occurred resulting in the chelation of those metals, and thus an increase of their aqueous concentrations (Gadd, 2007; Horwath, 2015). Similar behaviour was again observed for the wet and dry season mountain soil samples suggesting that the biogeochemical response did not vary depending on the season. This was not the case for the lowland samples (Figure 6.6B, D, F, H, J), where upon aeration, concentrations of Co, Ni, Mg and Mn remained constant in the wet season samples while Fe decreased substantially (indeed again behaving similarly to the mountain soil samples). The dry season lowland samples maintained low concentrations of aqueous metals throughout the aeration phase. When those soils were anaerobically biostimulated with glucose, none of those metals were present by the end of the oxic phase (Figure 5.6, 5.7, Chapter 5). Therefore, aerobic cellulose degradation emerges as an important mechanism in the natural biogeochemical cycling of Co, Ni and Mn when oxic conditions are present in the lateritic soils of Santa Elena Peninsula. This is likely due to the aerobic bioweathering of Mg minerals that contain these elements such as hydrous Mg silicates or Mg-rich clay smectites naturally present in both locations (Figure 4.9, Chapter 4).

### 6.4.4 Effects of cellulose biostimulation on seasonal serpentine soil mineralogy

The mineralogy of the lateritic soils was characterised by XRD at the start of the redox cycling microcosm experiment and at the end of the anoxic and oxic incubations. At the start of the experiment, the mountain soil mineralogy comprised iron oxides as hematite ($\alpha$-$Fe_2O_3$), Mg-silicates and smectite minerals, similar mineralogy than previously reported for this type of soil (Figure 6.7) (Figure 4.9, Chapter 4). After anoxic incubation with cellulose, hematite disappeared in both the wet and dry season samples, likely as a result of microbially-mediated Fe(III) reduction, as seen previously in these soils when biostimulated with glucose (Section 5.4.3, Chapter 5) and in other laterites with the same electron donor (Newsome *et al.*, in revision, Appendix 1), and thus resulting in the increase of associated metals such as Co, Ni and Mn. An analogous metal cycling was also reported in mangroves associated with an ultramafic watershed, where metals present in iron oxides and/or oxy-hydroxides were dissolved when coupled to bacterial-mediated organic matter decomposition resulting in high aqueous concentrations of metals such as Fe, Ni and Mn (Marchand et al., 2012). Following aeration, Fe(III) minerals were observed to have formed in the mountain soils as hematite and goethite ($\alpha$-$Fe^{3+}OOH$). Indeed, these were visible as precipitates on the glass surfaces of all the microcosm serum bottles with mountain soils and amended with cellulose (Figure 6.3). Similar behaviour was observed for both lowland soils, with hematite absent from the anaerobic samples (Figure 6.S4). However, goethite was only formed on the glass surfaces of the microcosm bottles from the wet season lowland soil samples (Figure 6.S2), again confirming their similar biogeochemistry with mountain soils. Re-crystallisation of iron oxides and oxy-hydroxides after reductive dissolution of Fe oxides have been widely reported on fluctuating redox experiments using different types of soils from different tropical regions of the world (Ginn et al., 2017; Thompson et al., 2006; Tishchenko et al., 2015; Winkler et al., 2018); but, under different experimental conditions (e.g. using reactors, without carbon electron donors, short length incubations), and were not specifically focused in targeting the biostimulation of microbial communities.

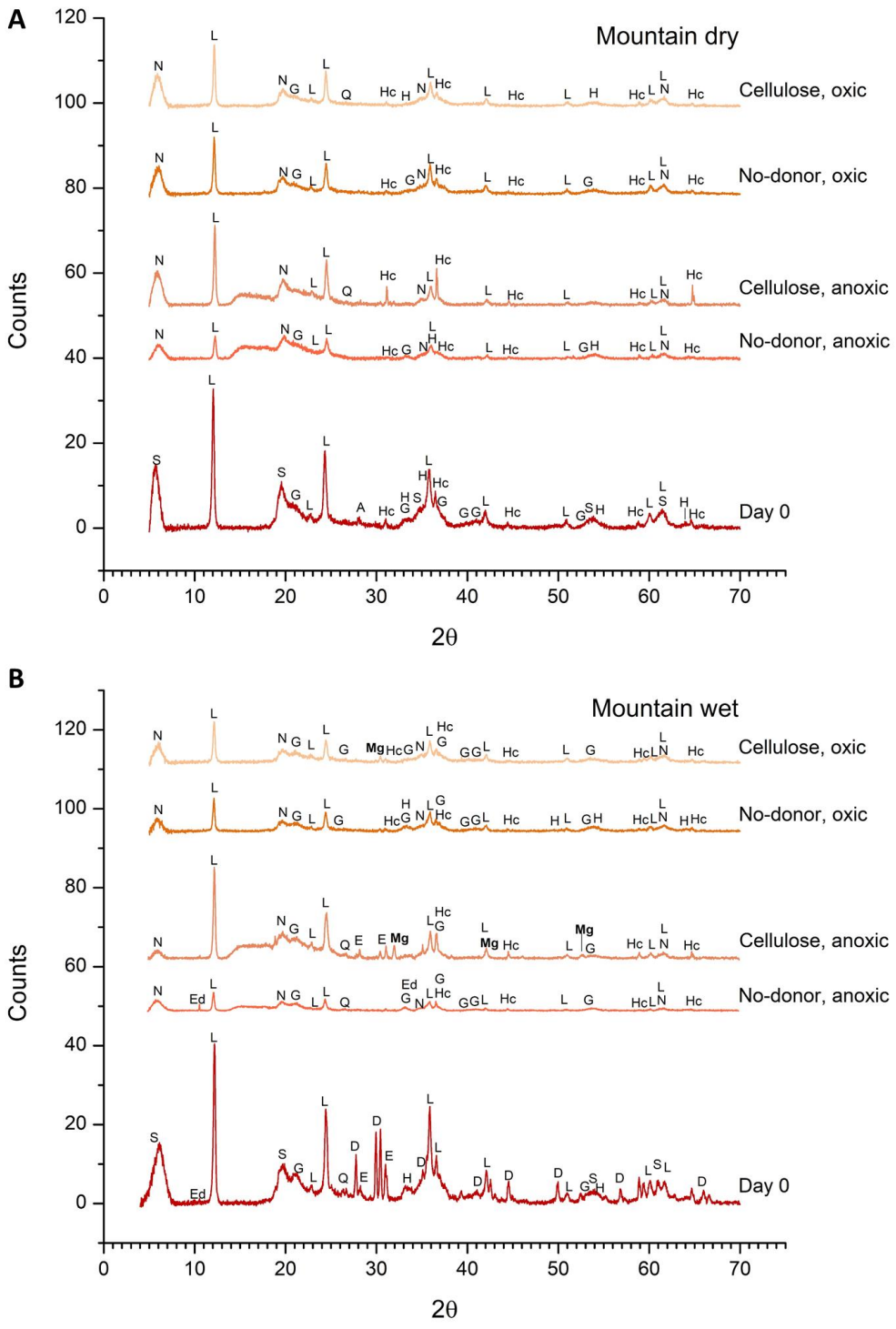


**Figure 6.7.** Mineralogy of the mountain lateritic soil at the start of the redox cycling microcosm experiment, and at the end of the anoxic and aerobic incubations after biostimulation with cellulose, for soils from dry (A) and wet (B) seasons. Main minerals found with XRD were: goethite (G), hematite (H), maghemite (M), lizardite (L), siderite (Si), magnesite (Mg), enstatite (E), diopside (D), clinochlore (C), hercynite (Hc), albite (A) and quartz (Q). North lowland samples are in Figure 6.S4.

The Mg mobilisation seen in the redox cycling microcosm experiments (Figure 6.6) could have occurred from the bioweathering of hydrous Mg silicates such as lizardite [$Mg_3Si_2O_5(OH)_4$], present in all of the samples, or as clinochlore [$Mg_5Al(Si,Al)_4O_{10}(OH)_8$] in the lowland soils (Figure 6.7 and 6.S4). The other Mg source were the smectite clays that were present in mountain soils with a chemical composition between stevensite [$Ca_{0.2}Mg_{2.9}Si_4O_{10}(OH)_2 \cdot 4H_2O$] and nontronite [$Na_{0.3}Fe_2Si_4O_{10}(OH)_2 \cdot 4H_2O$]. All of these minerals are also possible sources of both Ni and Co (Butt and Cluzel, 2013; Roberts and Gunn, 2014). As the mineralogy of the soils after biostimulation was similar to the original samples (Figure 6.7), the mobilisation of Co, Ni and Mn may have occurred via cation substitutions with Fe or Mg, without affecting the general mineralogical structure.

When the soils were biostimulated with cellulose under anoxic conditions, biomineralisation of magnesite ($MgCO_3$) happened in all samples except the mountain dry season soil. Magnesite was not present in any of the no-donor controls suggesting an excess of $CO_2$ in solution produced from the anaerobic microbial metabolism of cellulose in those soils that led to the indirect precipitation of carbonate minerals. Similar Mg-Fe carbonate biomineralisation was previously reported in the lateritic soils of Santa Elena Peninsula but when biostimulated with glucose (Section 5.4.3, Chapter 5). Also, in mangroves related to ultramafic soils from New Caledonia, Mn-Fe carbonate minerals precipitated under anoxic conditions (Marchand et al., 2012). It is likely that a large substitution of $Fe^{2+}$ towards a ferroan magnesite [$(Mg,Fe)CO_3$] or siderite ($FeCO_3$) must have occurred given the elevated production of Fe(II) when cellulose was present (Figure 6.4E, F) and the Fe mobilisation to aqueous media (Figure 6.6G, H). However, XRD was unable to distinguish between these substituted mineral forms due to the complex nature of these environmental soil samples (Zhou et al., 2018). Therefore Fe-Mg carbonate minerals can be formed in lateritic soils in the presence of natural carbon sources as cellulose, and during the wet and dry seasons, highlighting the importance of these microbial processes to the carbon fluxes throughout the year in serpentine soils of Santa Elena Peninsula and in other serpentine ecosystems overall (Power et al., 2013).

In summary, the presence of cellulose induced bioweathering processes in lateritic soils of the Santa Elena Peninsula. Anoxic environments led to the removal of hematite due to microbially-mediated Fe(III) reduction coupled to anaerobic carbon metabolism, while oxic conditions

favoured the formation of Fe(III) minerals like hematite and goethite. Mg mobilisation occurred throughout the entire microcosm redox experiment, due to the bioweathering Mg minerals, namely lizardite, chlorite or smectite. Given the similar geochemical behaviour observed for Mg, Co, Ni and Mn, it is likely that these Mg minerals were the source of the Co and Ni mobilisation during aerobic biostimulation with cellulose. Finally, Mg-Fe carbonate minerals were biomineralised stressing the importance of these biogeochemical cycles in the carbon budgets of these lateritic/serpentine soils.

### 6.4.5 Biogeochemical redox cycling of metals in serpentine soils coupled to cellulose degradation

In summary, in the lateritic soils of Santa Elena Peninsula, microbial degradation of cellulose induced the mobilisation of Co, Ni and Mn by stimulating the bioweathering of Fe and Mg minerals. However, the microbial mechanisms that facilitated the cycling of Co, Ni and Mn in the presence of cellulose differed depending on the dominant environmental redox conditions. In anoxic conditions, microbial heterotrophic Fe(III) reduction coupled to carbon fermentation drove the solubilisation of those metals, preceded by microbial cellulose depolymerisation into smaller molecules. Under oxic conditions, potential microbial cellulose degradation further improved the mobilisation of Co and Ni, presumably from Mg-rich minerals such as hydrous Mg silicates and clay smectites. Understanding better Co and Ni mobilisation from laterites under oxic conditions could be of interest for biomining purposes, as a bioprocessing proceeding to extract Co from laterites was recently proposed but focused only on anoxic biostimulation (Newsome *et al.*, in revision, Appendix 1).

Few differences were observed between the wet and dry seasons in mountain soils, but the lowland soils behaved very differently depending on their season of origin. During wet season and when biostimulated with cellulose, the lowland soils had an active cycling of metals such as Co, Ni, Mn and Fe, just like the mountain soils biogeochemical behaviour. During the dry season, redox cycling of those metals was inhibited, favouring the developing of methanogenesis, potentially outcompeted by Fe(III) reduction during the wet season. In volcanic felsic soils from Puerto Rico was demonstrated that when a soil is exposed to frequent shifts in redox conditions, as happens in the Santa Elena Peninsula with the seasonal precipitation, then the soil can be

primed for rapid Fe-reduction (Ginn et al., 2017). Thus, the results of this study suggest that in serpentine soils, microbial degradation of cellulose is a key ecological process for the biogeochemical cycling of Mg, Fe and metals associated such as Co, Ni and Mn, both under oxic and anoxic conditions, with seasonal precipitation acting as a driving force stimulating the activation and/or intensity of those cycles.

### 6.4.6 Effects of cellulose biostimulation on microbial communities from seasonal serpentine soils

The prokaryotic communities of the lateritic soils of the Santa Elena Peninsula were studied during redox cycling microcosm experiments by sequencing the V4 variable region of 16S rRNA at the start of the experiment, at the end of the anoxic phase and at the end of the subsequent oxic stage, for both the cellulose biostimulated experiments and the no-donor controls. Compared to the starting soils (Figure 6.8A), the development of anoxic conditions in the presence of cellulose caused a large decrease in Shannon diversity for both mountain and lowland soils, regardless of the seasonal origin (Figure 6.8B). Following aeration, the Shannon diversity increased only in the samples collected in the dry season but they did not reach the original values (Figure 6.8C). This suggests that by the end of the dry season (when these samples were taken), microbial communities could be more resilient to changes in the redox environment of lateritic soils, easily adaptable to fluctuating conditions of sudden waterlogging of soils from the first rains; analogous to tropical Puerto Rican soils where was proposed that variations in redox conditions due to frequent precipitation could prepare a soil for quick Fe-reduction (Ginn et al., 2017). In contrast, under anoxic incubation only a small decrease in the Shannon diversity of the no-donor controls was observed, and it remained broadly constant following aeration. Interestingly, the no-donor control samples collected from the dry season showed slightly lower Shannon diversity values compared to the wet season (especially the mountain soils). Together these results confirmed that cellulose metabolism was a driving force shaping the composition of microbial communities in the laterite sediment microcosms. In New Caledonia tropical rainforests with ultramafic soils, microbial richness, composition and abundance were related to plant cover type and dominant plant species; and the association was explained due to host preference, litter quality or root exudates (Bordez et al., 2016; Gourmelon et al., 2016).

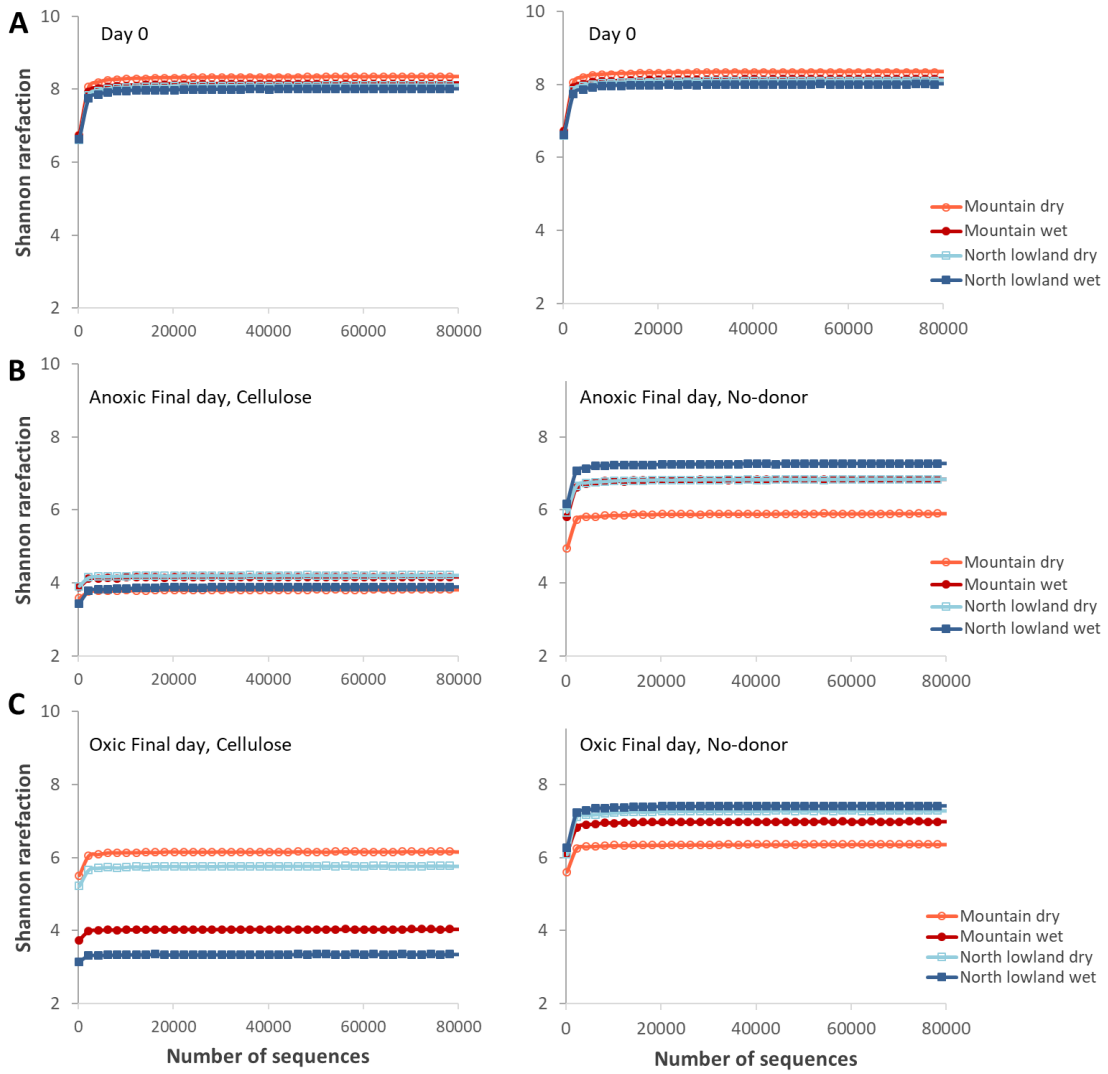


**Figure 6.8.** Shannon rarefaction curves in the lateritic soils of the Santa Elena Peninsula from both dry and wet seasons, obtained by the sequencing of the V4 region of 16S rRNA. Soil slurry samples were analysed from the redox cycling microcosm experiments at the start (A), and after anoxic (B) and oxic (C) conditions during biostimulation with cellulose (left) and no-donor control (right).

The composition of the prokaryotic communities in the lateritic soils of Santa Elena Peninsula changed during redox cycling associated with anaerobic and aerobic cellulose metabolism (Figure 6.9). The Day 0 samples resembled the typical prokaryotic structure of the lateritic soils from Santa Elena Peninsula described in previous work, that was largely dominated by Acidobacteria, Actinobacteria and Proteobacteria (27, 18 and 17 % of relative abundance) (Section 4.4.4.1, Chapter 4). However, there were some differences compared to other tropical

ultramafic soils from New Caledonia rainforests, where bacterial communities were dominated by Proteobacteria (31% of relative abundance), followed by Planctomycetes (19%), Acidobacteria (12%) and Actinobacteria (9%) (Gourmelon et al., 2016). And more generally, Proteobacteria tends to be the dominant group of bacteria in soils across the world, seconded by Acidobacteria and Actinobacteria (Delgado-Baquerizo et al., 2018). Also, in each location there was not significant differences in the prokaryotic community between seasons even at a phylogenetic class level (Figure 6.S5). The no-donor samples broadly resembled the Day 0 samples at the phylum level both at the end of the anoxic and oxic incubations. Cellulose biostimulation led to significant shifts in the prokaryotic community composition. In particular, some of the major groups initially present, such as Actinobacteria and Proteobacteria, decreased during anoxic incubation, while anaerobes such as methanogens were favoured, only to be reconfigured after oxic conditions (Figure 6.9).

Anoxic conditions provoked a substantial decrease in the relative abundance of Actinobacteria regardless of soil sample or season, ranging from 27 - 38% at the start of the experiment to <1 - 2% at the end of the anoxic phase. This decrease was not strictly related to cellulose degradation as it also occurred in the no-donor controls but to a lesser extent (4 - 12% of relative abundance after oxic phase). Proteobacteria also diminished from 10 - 23% of relative abundance at the beginning of the experiment to 1 - 4% at the end of the anoxic conditions, but unlike Actinobacteria, this decrease was likely linked to cellulose microbial degradation as in no-donor controls the relative abundance of this clade even increased in some samples (13 - 29%). The third group of importance in the original soils, Acidobacteria, increased only in the dry season samples ranging from 14 – 17 % to 30 – 31 % of relative abundance when anaerobically stimulated with cellulose. Acidobacteria have been reported to be associated with carbon metabolism in organic matter rich soils, and are able to breakdown polysaccharides as in the degradation of lignocellulosic plant biomass (Rawat et al., 2012).

However, regardless of location or seasonal origin, the major clade present under these anoxic conditions with cellulose was Firmicutes (Figure 9), which increased in relative abundance from 0.1 – 0.9 % in the starting soils to 38 - 67 %. The anaerobic structure of Firmicutes was largely represented by Clostridia comprising anaerobic bacteria groups as *Clostridiaceae*, *Peptococcaceae*, *Heliobacteriaceae, Lachnospiraceae* or *Ruminococcaceae* (Figure 6.S5)

(Huang et al., 2019; Liu et al., 2014; Sattley and Madigan, 2014; Stackebrandt, 2014a, 2014b, 2014c). Similar dominancy was found in lateritic soils of Santa Elena Peninsula anaerobically biostimulated with glucose although other phylogenetic classes from Firmicutes were also present in the mountain lateritic soils (Section 5.4.4, Chapter 5). The presence of cellulolytic groups, such as in Clostridia, able to breakdown of cellulose into smaller molecules that are easier to be assimilated by microorganisms, such as glucose, is a crucial step in the development of other microbial processes as microbial Fe(III) reduction (Horwath, 2015; Killham and Prosser, 2015).

As well as Clostridia, biostimulation with cellulose led to an increase in the proportion of the strictly methanogenic archaea Euryarchaeota, from < 0.1 – 1.9 % to 6 – 21 % of relative abundance. This reflects the geochemical data, which showed large volumes of methane were produced (Figure 6.5C, D). Sequences closely related to *Methanobacterium* sp. dominated the methanogenic community in the mountain soils during dry season (99 % of methanogens) and in both season lowland samples (dry 95 %, and wet 98 %). The exception was the mountain soil from the wet season, that had the smaller relative abundance of methanogens (6 %) despite the larger volumes of methane generated if compared with dry season soils (Figure 5). Here, *Methanocellaceae* was the most abundant methanogenic group (71 %). Both *Methanobacterium sp. and Methanocellaceae* are hydrogenotrophic methanogens (Oren, 2014; Sakai et al., 2014), and $H_2$ was not detected by GCTCD, suggesting a rapid consumption of hydrogen as fast as it was produced, and thus indicating this is the main methanogenic process under anaerobic biostimulation with cellulose in lateritic soils of Santa Elena Peninsula. Remarkably, in previous work using lowland lateritic soils of Santa Elena Peninsula, but with glucose as the electron donor, the relative high abundance of *Methanosaeta* sp. and *Methanosarcina* sp. suggested that large proportion of methane production was driven by acetoclastic methanogenesis (Section 5.4.4, Chapter 5) (Schlesinger and Bernhardt, 2013). However, it appears that cellulose metabolism did not favour this metabolic pathway despite the large amounts of acetate in solution, presumably due to the differences between glucose and cellulose metabolism and/or the heterogeneity in the soils (Figure 6.5). Lastly, the occurrence of a large proportion of unclassified Bacteria in the mountain soils from the wet season after anoxic incubation with cellulose (30 % of relative prokaryotic abundance) (Figure 6.9A) and in the other samples to a lesser extent, confirmed the

potential of the Santa Elena Peninsula to develop endemism to adapt to the particular biogeochemical characteristics of those serpentine soils (Section 4.4.4, Chapter 4).

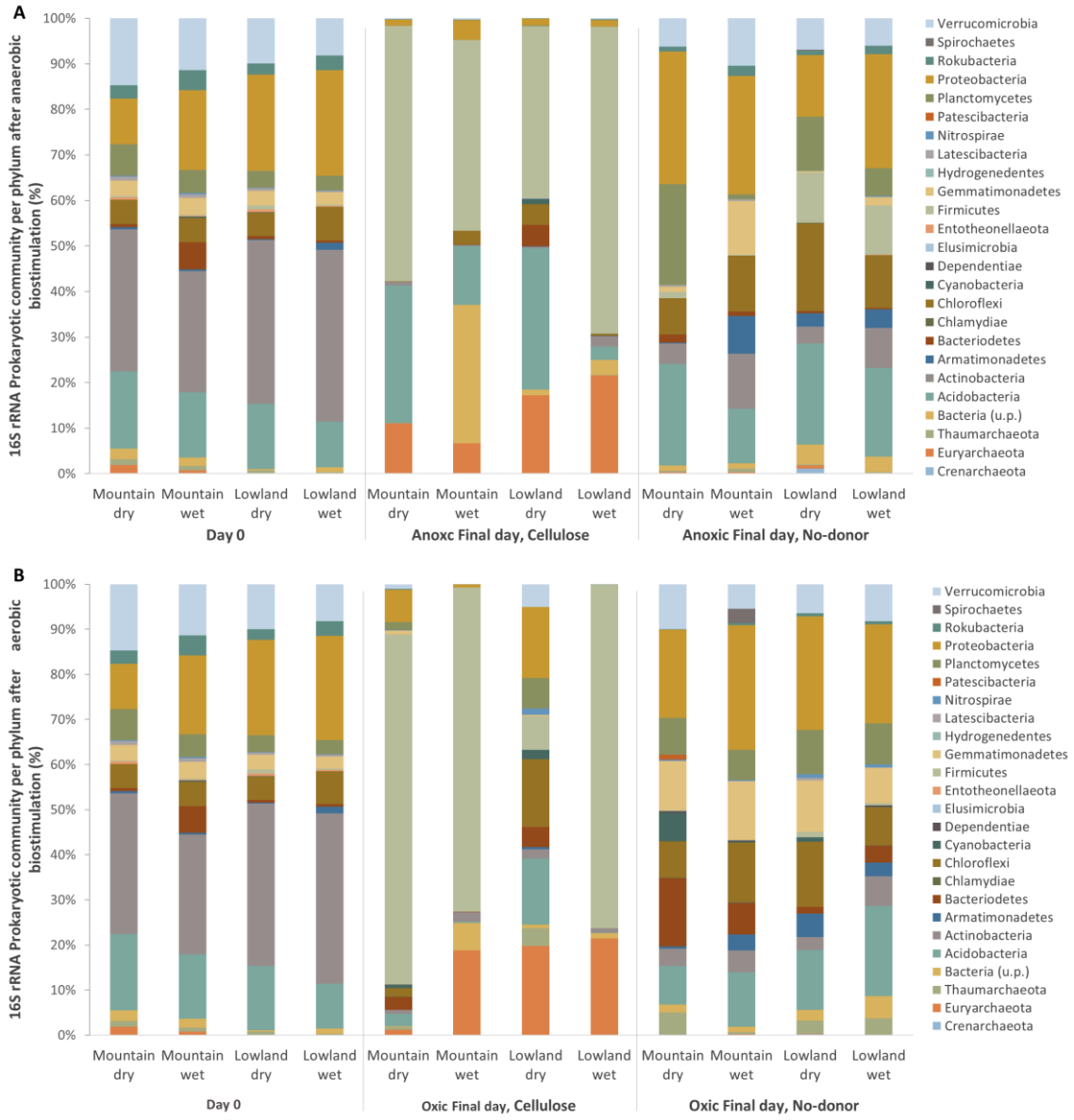


**Figure 6.9.** Prokaryotic communities in the lateritic soils of the Santa Elena Peninsula from both dry and wet seasons obtained by the sequencing of the V4 region of 16S rRNA after redox cycling microcosm experiments biostimulated with cellulose and no-donor controls. Relative abundance of all the sequences obtained per phylum at the end of anoxic incubation (A) and at the end of subsequent oxic incubation (B). In every stage, the starting soil before biostimulation is also shown for ease, but the anoxic stage directly preceded the oxic phase in the experiment; 'u.p': unclassified phylum. Prokaryotic communities per phylogenetic class of all the experiments are shown in Figure 6.S5 (anoxic conditions) and Figure 6.S6 (oxic conditions).

Following aeration, the composition of the prokaryotic at the phylum level more closely resembled the anaerobic community compared to the initial Day 0 community (Figure 6.9B). Both mountain soil samples and the samples from the lowland soils collected during the wet season, where cycling of Co and Ni was boosted after oxic conditions (Figure 6.6A, C), had an increase of Firmicutes relative abundance (mountain dry 78 %, mountain wet 72 % and lowland wet 76 %), and were still dominated by Clostridia in both mountain soils, while the lowland wet soil contained similar proportions of Bacilli and Clostridia (Figure 6.S6). The presence of Bacilli suggests the coexistence of both aerobic and anaerobic degradation of cellulose in the lowland soils from the wet season, as members represented in this group are common aerobic soil bacteria able to depolymerise the cellulose (Horwath, 2015). The lowland dry season sample was the only one where Firmicutes did not dominate after oxic incubation. Indeed, the prokaryotic community composition at the end of the oxic stage was more alike to the no-donor control, similar to the aqueous geochemistry where no further cycling of Co, Ni, Mn, Fe and Mg was observed (Figure 6.6). In three of the microcosms amended with cellulose (both lowland samples and mountain from the wet season), methanogens were still present at the end of the oxic incubations (Figure 6.9B) and comprised 19 – 21 % of the prokaryotic relative abundance and with *Methanobacterium* as the sole major genus. This was surprising given that methanogens are obligate anaerobes, but in the bulk soil environment it has been demonstrated that methane and $O_2$ can coexist in tropical soils exposed to high rainfall conditions (Silver et al., 1999).

The presence of the anaerobic Firmicutes clades and Euryarcheota suggested that anoxic conditions may have been maintained in the microcosm experiments despite aeration and the $E_h$ values reached (Figure 6.4C, D), and like explained for Fe(II) in Section 6.4.1, it could be possibly due to redox buffering constantly supplied by the excess of cellulose in the media (Newsome et al., 2017) or to the presence of anoxic microenvironments (Ginn et al., 2017; Silver et al., 1999). However, it cannot be discounted that their identification solely occurred as a result of residual DNA from the anoxic phase. In addition, aerobic cellulose metabolism can be present, and was likely in the lowland lateritic soil samples from the wet season. In the mountain dry soils, the methanogens were observed to decrease from 11 % after anoxic conditions to 1 % at the end of the oxic conditions, and that could indicate that during dry season methanogens are more sensible to redox changes in the mountain soils, likely due to faster rates of re-crystallisation of

Fe(III) minerals during re-oxidation (Barcellos et al., 2018a). Because anoxic conditions were potentially restricted to microsites during the oxic stage of the microcosm experiment, methanogenesis could have not been favoured in the mountain soils due to a sudden increase in the content of Fe(III), and also of sulphate, that only increased in the dry season sample (Figure 6.S3), both associated with microbial anaerobic processes that outcompete methanogenesis for reducing equivalents (Whitman et al., 2014). These results also highlight that methanogenesis and anaerobic microbial processes in general, can be sustained on serpentine soils during the entire year, regardless of seasonality or topography, just as seen in other types of soils (Barcellos et al., 2018a, 2018b; Silver et al., 1999), but given the relative higher amounts of Fe in serpentine soils, those processes could be more relevant when considering large scale carbon effluxes or influxes from serpentine ecosystems overall.

In summary, the Firmicutes appeared to be a crucial group in the cycling of Co, Ni and Mn in lateritic soils by either facilitating the reduction of Fe or by aiding Mg mobilisation, both coupled to cellulose degradation and further carbon metabolism. Clostridia was the major clade of Firmicutes present in both the anoxic and oxic phases when cellulose was present, acting as indirect agents of different bioweathering processes depending on the environmental conditions. In anoxic conditions, Fe minerals were solubilised due to Fe (III) reduction while during oxic conditions - despite Fe re-oxidation – potential aerobic cellulose metabolism continued to stimulate the bioweathering of Mg minerals, while anaerobic microbial processes were still sustained in microsites with anoxic conditions. Methanogenesis occurred in each of these lateritic soils regardless of soil type or seasonal origin when adequate geochemical anoxic conditions were present, stimulated by cellulose metabolism. Methane generated in lateritic soils was previously described in these soils (Chapter 5), but its contribution to the overall carbon inputs of this ecosystem could be more important given its ease to progress as far as cellulosic matter is available and *in situ* anoxic conditions are developed, and occurring all along the year regardless of the seasonality of the site.

## 6.5 Conclusions

Redox cycling experiments were successfully performed in the lateritic soils of Santa Elena Peninsula using cellulose as a natural source of carbon for microbial biostimulation. Microbial cellulose degradation induced the mobilisation of Co, Ni and Mn to aqueous solution from different minerals although the mineral phase affected differed depending on the dominant redox conditions. Under anoxic environments, cellulose degradation led to microbial Fe(III)-reduction, causing the solubilisation of ferric minerals and releasing Co, Ni and Mn to solution. In oxic conditions, iron(II) was re-oxidised and precipitated as Fe(III) minerals like hematite and goethite, while the mobilisation of Co and Ni (and Mn to a lesser extent) continued. In addition, in oxic conditions, microbial degradation of cellulose and its subsequent metabolism induced the leaching of Co, Ni and Mn from Mg minerals present as hydrous silicates (lizardite or chlorite) or clays (smectite), favoured by either (i) aerobic microbial processes, (ii) redox buffering produced from the cellulosic microbial metabolism or (iii) by the presence of anaerobic processes occurring at anoxic microsites. When compared to the results of glucose biostimulation previously reported, cellulose biostimulation caused greater concentrations of Co, Ni and Mn to be mobilised from the soils (three to four times more). These results could be of interest for biomining purposes, as here was demonstrated that bioprocessing of laterites to extract Co and Ni can be enhanced by using cellulose to biostimulate microbial processes both under anoxic and oxic conditions.

Microbial communities of the lateritic soils of Santa Elena Peninsula were strongly selected during anoxic conditions biostimulated with cellulose, largely favouring the presence of Firmicutes (entirely as Clostridia clades), methanogenic archaea and Acidobacteria (only in dry season samples). The presence of prokaryotic groups that are able to perform cellulose depolymerisation aerobic or anaerobically is vital for the bioavailability of smaller carbon molecules that can be used in other microbial processes as Fe(III) redox cycling. Firmicutes clades are well known to degrade cellulose either aerobic as anaerobically, and therefore have emerged as a crucial group of prokaryotes for the biogeochemical cycling of Co, Ni and Mn coupled to the degradation of cellulose in serpentine soils. Additionally, the presence of methanogens regardless of soil type, seasonality or redox condition, also highlighted that methanogenesis and anaerobic microbial

processes in general, can be sustained on serpentine soils during the entire year, regardless of seasonality or topography, just as seen in other types of soils (Barcellos et al., 2018a, 2018b; Silver et al., 1999), but that given the relative high amounts of Fe in serpentine soils, those processes could be more relevant when considering large scale carbon effluxes or influxes from serpentine ecosystems overall.

Seasonal variation of precipitation in the Santa Elena Peninsula affected the lateritic soils differently depending on the geographical/geochemical origin. In general terms, and as expected, precipitation was pivotal to induce redox processes in the serpentine soils by facilitating the development of anoxic conditions, either in the bulk soil system or in microsites. In the mountain soils the impact was weak, as the biogeochemical cycle of Co, Ni and Mn associated with cellulose degradation and the microbial communities behaved similarly in both seasons, with the sole differences of anoxic conditions developing at a faster rate and more methane generated in the wet season. Thus, in mountain serpentine soils, the development of anaerobic microbially-mediated processes such as Fe(III) reduction or methanogenesis, can be triggered and stimulated by the seasonal rains. But in the north lowland soils, differences between seasonal origin were more evident when the soil samples were biostimulated with cellulose. During anoxic conditions, the wet season samples had a similar biogeochemical behaviour to the mountain soils, especially with analogous mobilisation of Fe, Co, Ni and Mn. In contrast, the samples from the dry season did not lead to the same cycling of metals nor the same changes in microbial community composition while more methane was generated. This difference could be associated with more Fe(III) available in the lowland soils during the wet season due to Fe(III) influxes from the surrounding mountains to the lowlands as a consequence of the mayor rates of erosion and of mobilisation of minerals/solved cations mediated by the heavy intense precipitation, thus favouring microbial Fe(III)-reduction coupled to anaerobic carbon metabolism over methanogenesis. Additionally, when fluctuating redox conditions are intermittent, like in the transition months between dry and wet season, the microbial communities of serpentine soils seem to be more resilient to changes in the redox environment, easily adaptable to fluctuating anoxic conditions of sudden waterlogging of soils and developing anaerobic microbially-mediated processes such as Fe(III)-reduction.

Therefore, considering local seasonal variations is essential to better understand the natural conditions underpinning Co, Ni and Mn cycling in lateritic soils, especially those located in tropical regions. Fe and Mg microbially mediated cycling and methanogenesis are also affected by seasonal traits in serpentine soils, even with repercussions on the serpentine ecosystem carbon fluxes on a larger scale. These results demonstrated that microbial degradation of cellulose (i.e. natural plant matter) is a key ecological process to understand other microbially-mediated processes naturally occurring in serpentine soils, such as the biogeochemical cycling of Co, Ni and Mn, both under oxic and anoxic conditions. The development of those conditions can be largely determined by the seasonal precipitation, by stimulating the initiation and/or driving the intensity of those cycles. Finally, this work has set the basis to better understand the impact of seasonal rainfall on the biogeochemical cycling of metals on serpentine soils, and the Santa Elena Peninsula represents a model experimental site to develop further work not only about precipitation effects, but also to study other natural biotic/abiotic relationships underpinning serpentine ecosystems.

### 6.6 Funding

This research was developed and funded by the scholarship for the PhD of AFSA granted by the Ministerio de Ciencia, Tecnología y Telecomunicaciones (MICITT) of the Government of Costa Rica and the Universidad de Costa Rica (UCR). MICITT funded the fieldwork, while the CoG$^3$ Consortium Project (CoG3 NE/M011518/1), funded by the Natural Environment Research Council (NERC), partially supported this investigation through several analyses.

### 6.7 Acknowledgements

We want to thank to María Marta Chavarría Diaz and Róger Blanco Segura from the Research Programme of the ACG for giving the permissions to develop this research in the Santa Rosa National Park and for their support and advice with the sampling logistics during the field campaigns. We are also very grateful to Daniel Arguedas Quesada for his hard work, transport and logistics support, and general assistance to AFSA in all the field campaigns. We want to thank

to Paul Lythgoe, Alastair Bewsher and John Waters (University of Manchester) for analytical support with ICP-AES, ICP-MS, IC and XRD. We also thank to Dr. Heather Buss and Dr. Vicky Coker for the valuable input to improve this paper. Finally, we want to thank the Unidad de Recursos Forestales at the Universidad de Costa Rica (ReForesta-UCR) for allowing AFSA to use their research laboratories while in Costa Rica. The authors declared that all the biological samples were collected under the authorised permission given to AFSA from the Comisión Nacional para la Gestión de la Biodiversidad Costa Rica (CONAGEBIO) to access the DNA of the samples collected.

### 6.8 References

Alves Dias, P., Blagoeva, D., Pavel, C., Arvanitidis, N., 2018. Cobalt: demand-supply balances in the transition to electric mobility. Publications Office of the European Union, Luxembourg. https://doi.org/10.2760/97710

Babraham Bioinformatics, n.d. FastQC.

Barcellos, D., Cyle, K.T., Thompson, A., 2018a. Faster redox fluctuations can lead to higher iron reduction rates in humid forest soils. Biogeochemistry 137, 367–378. https://doi.org/10.1007/s10533-018-0427-0

Barcellos, D., O'Connell, C., Silver, W., Meile, C., Thompson, A., 2018b. Hot Spots and Hot Moments of Soil Moisture Explain Fluctuations in Iron and Carbon Cycling in a Humid Tropical Forest Soil. Soil Syst. 2, 59. https://doi.org/10.3390/soilsystems2040059

Béguin, P., Aubert, J.-P., 1994. The biological degradation of cellulose. FEMS Microbiol. Rev. 13, 25–58. https://doi.org/10.1111/j.1574-6976.1994.tb00033.x

Bordez, L., Jourand, P., Ducousso, M., Carriconde, F., Cavaloc, Y., Santini, S., Claverie, J.M., Wantiez, L., Leveau, A., Amir, H., 2016. Distribution patterns of microbial communities in ultramafic landscape: a metagenetic approach highlights the strong relationships between diversity and environmental traits. Mol. Ecol. 25, 2258–2272. https://doi.org/10.1111/mec.13621

Butt, C.R.M., Cluzel, D., 2013. Nickel Laterite Ore Deposits: Weathered Serpentinites. Elements 9, 123–128. https://doi.org/10.2113/gselements.9.2.123

Caporaso, J.G., Kuczynski, J., Stombaugh, J., Bittinger, K., Bushman, F.D., Costello, E.K., Fierer, N., Peña, A.G., Goodrich, J.K., Gordon, J.I., Huttley, G.A., Kelley, S.T., Knights, D., Koenig, J.E., Ley, R.E., Lozupone, C.A., McDonald, D., Muegge, B.D., Pirrung, M., Reeder, J., Sevinsky, J.R., Turnbaugh, P.J., Walters, W.A., Widmann, J., Yatsunenko, T., Zaneveld, J., Knight, R., 2010. QIIME allows analysis of high-throughput community sequencing data. Nat. Methods 7, 335–336. https://doi.org/10.1038/nmeth.f.303

Caporaso, J.G., Lauber, C.L., Walters, W.A., Berg-Lyons, D., Huntley, J., Fierer, N., Owens, S.M., Betley, J., Fraser, L., Bauer, M., Gormley, N., Gilbert, J.A., Smith, G., Knight, R., 2012. Ultra-high-throughput microbial community analysis on the Illumina HiSeq and MiSeq platforms. Isme J. 6, 1621. https://doi.org/10.1038/ismej.2012.8

Caporaso, J.G., Lauber, C.L., Walters, W.A., Berg-Lyons, D., Lozupone, C.A., Turnbaugh, P.J.,

Fierer, N., Knight, R., 2011. Global patterns of 16S rRNA diversity at a depth of millions of sequences per sample. Proc. Natl. Acad. Sci. 108, 4516–4522. https://doi.org/10.1073/PNAS.1000080107

Delgado-Baquerizo, M., Oliverio, A.M., Brewer, T.E., Benavent-González, A., Eldridge, D.J., Bardgett, R.D., Maestre, F.T., Singh, B.K., Fierer, N., 2018. A global atlas of the dominant bacteria found in soil. Science (80-. ). 359, 320–325. https://doi.org/10.1126/science.aap9516

Denyer, P., Gazel, E., 2009. The Costa Rican Jurassic to Miocene oceanic complexes: Origin, tectonics and relations. J. South Am. Earth Sci. 28, 429–442. https://doi.org/10.1016/j.jsames.2009.04.010

Edgar, R.C., 2013. UPARSE: highly accurate OTU sequences from microbial amplicon reads. Nat. Methods 10, 996–998. https://doi.org/10.1038/nmeth.2604

Edgar, R.C., 2010. Search and clustering orders of magnitude faster than BLAST. Bioinformatics 26, 2460–2461. https://doi.org/10.1093/bioinformatics/btq461

Gadd, G.M., 2007. Geomycology: biogeochemical transformations of rocks, minerals, metals and radionuclides by fungi, bioweathering and bioremediation. Mycol. Res. 111, 3–49. https://doi.org/10.1016/j.mycres.2006.12.001

Ginn, B., Meile, C., Wilmoth, J., Tang, Y., Thompson, A., 2017. Rapid Iron Reduction Rates Are Stimulated by High-Amplitude Redox Fluctuations in a Tropical Forest Soil. Environ. Sci. Technol. 51, 3250–3259. https://doi.org/10.1021/acs.est.6b05709

Gourmelon, V., Maggia, L., Powell, J.R., Gigante, S., Hortal, S., Gueunier, C., Letellier, K., Carriconde, F., 2016. Environmental and Geographical Factors Structure Soil Microbial Diversity in New Caledonian Ultramafic Substrates: A Metagenomic Approach. PLoS One 11, 1–25. https://doi.org/10.1371/journal.pone.0167405

Haas, B.J., Gevers, D., Earl, A.M., Feldgarden, M., Ward, D. V, Giannoukos, G., Ciulla, D., Tabbaa, D., Highlander, S.K., Sodergren, E., Methé, B., DeSantis, T.Z., Human Microbiome Consortium, T.H.M., Petrosino, J.F., Knight, R., Birren, B.W., 2011. Chimeric 16S rRNA sequence formation and detection in Sanger and 454-pyrosequenced PCR amplicons. Genome Res. 21, 494–504. https://doi.org/10.1101/gr.112730.110

Hallberg, K.B., Grail, B.M., Plessis, C.A. du, Johnson, D.B., 2011. Reductive dissolution of ferric iron minerals: A new approach for bio-processing nickel laterites. Miner. Eng. 24, 620–624. https://doi.org/10.1016/j.mineng.2010.09.005

Herrera, W., 2016. Climate of Costa Rica, in: Kappelle, M. (Ed.), Costa Rican Ecosystems. The University of Chicago Press, p. 744.

Hodges, C., King, E., Pett-Ridge, J., Thompson, A., 2018. Potential for Iron Reduction Increases with Rainfall in Montane Basaltic Soils of Hawaii. Soil Sci. Soc. Am. J. 82, 176–185. https://doi.org/10.2136/sssaj2017.06.0193

Horwath, W., 2015. Carbon Cycling: The Dynamics and Formation of Organic Matter, in: Paul, E.A. (Ed.), Soil Microbiology, Ecology and Biochemistry. Academic Press, Boston, pp. 339–382. https://doi.org/10.1016/B978-0-12-415955-6.00012-8

Huang, X., Liu, L., Zhao, J., Zhang, J., Cai, Z., 2019. The families Ruminococcaceae, Lachnospiraceae, and Clostridiaceae are the dominant bacterial groups during reductive soil disinfestation with incorporated plant residues. Appl. Soil Ecol. 135, 65–72. https://doi.org/10.1016/J.APSOIL.2018.11.011

Instituto Meteorológico Nacional, n.d. Clima en Costa Rica-Pacífico Norte [WWW Document]. URL https://www.imn.ac.cr/documents/10179/31165/PacificoNorte.pdf/4a0e8960-8c51-4390-8a8d-73d9d825d59b (accessed 1.24.17).

Janzen, D.H., Hallwachs, W., 2016. Biodiversity Conservation History and Future in Costa Rica: The Case of Área de Conservación Guanacaste (ACG), in: Kappelle, M. (Ed.), Costa Rican Ecosystems. The University of Chicago Press, p. 744.

Jiménez M., Q., Carrillo J., E., Kappelle, M., 2016. The Northern Pacific Lowland Seasonal Dry Forest of Ganacaste and the Nicoya Peninsula, in: Kappelle, M. (Ed.), Costa Rican Ecosystems. The University of Chicago Press, p. 744.

Johnson, D.B., du Plessis, C.A., 2015. Biomining in reverse gear: Using bacteria to extract metals from oxidised ores. Miner. Eng. 75, 2–5. https://doi.org/10.1016/j.mineng.2014.09.024

Joshi, N., Fass, J., 2011. Sickle: A sliding-window, adaptive, quality-based trimming tool for FastQ files.

Killham, K., Prosser, J.I., 2015. The Bacteria and Archaea, in: Paul, E.A. (Ed.), Soil Microbiology, Ecology, and Biochemistry. Academic Press, Boston, p. 582. https://doi.org/10.1016/B978-0-12-415955-6.00003-7

Kozich, J.J., Westcott, S.L., Baxter, N.T., Highlander, S.K., Schloss, P.D., 2013. Development of a dual-index sequencing strategy and curation pipeline for analyzing amplicon sequence data on the MiSeq Illumina sequencing platform. Appl. Environ. Microbiol. 79, 5112–5120. https://doi.org/10.1128/AEM.01043-13

Lane, D.J., 1991. 16S/23S rRNA Sequencing, in: Stackebrandt, E., Goodfellow, M. (Eds.), Nucleic AcidTechniques in Bacterial Systematics. Wiley, New York, pp. 115–147.

Liptzin, D., Silver, W.L., 2009. Effects of carbon additions on iron reduction and phosphorus availability in a humid tropical forest soil. Soil Biol. Biochem. 41, 1696–1702. https://doi.org/https://doi.org/10.1016/j.soilbio.2009.05.013

Liu, Y., Qiao, J.-T., Yuan, X.-Z., Guo, R.-B., Qiu, Y.-L., 2014. Hydrogenispora ethanolica gen. nov., sp. nov., an anaerobic carbohydrate-fermenting bacterium from anaerobic sludge. Int. J. Syst. Evol. Microbiol. 64, 1756–1762. https://doi.org/10.1099/ijs.0.060186-0

Lovley, D.R., Holmes, D.E., Nevin, K.P., 2004. Dissimilatory Fe(III) and Mn(IV) Reduction. Adv. Microb. Physiol. 49, 219–286. https://doi.org/10.1016/S0065-2911(04)49005-5

Lovley, D.R., Phillips, E.J.P., 1987. Rapid Assay for Microbially Reducible Ferric Iron in Aquatic Sediments. Appl. Envir. Microbiol. 53, 1536–1540.

Lovley, D.R., Phillips, E.J.P., 1986. Organic Matter Mineralization with Reduction of Ferric Iron in Anaerobic Sediments. Appl. Envir. Microbiol. 51, 683–689.

Madrigal, P., Gazel, E., Denyer, P., Smith, I., Jicha, B., Flores, K.E., Coleman, D., Snow, J., 2015. A melt-focusing zone in the lithospheric mantle preserved in the Santa Elena Ophiolite, Costa Rica. Lithos 230, 189–205. https://doi.org/10.1016/j.lithos.2015.04.015

Marchand, C., Fernandez, J.-M., Moreton, B., Landi, L., Lallier-Vergès, E., Baltzer, F., 2012. The partitioning of transitional metals (Fe, Mn, Ni, Cr) in mangrove sediments downstream of a ferralitized ultramafic watershed (New Caledonia). Chem. Geol. 300–301, 70–80. https://doi.org/10.1016/j.chemgeo.2012.01.018

Marrero, J., Coto, O., Goldmann, S., Graupner, T., Schippers, A., 2015. Recovery of Nickel and Cobalt from Laterite Tailings by Reductive Dissolution under Aerobic Conditions Using Acidithiobacillus Species. Environ. Sci. Technol. 49, 6674–6682. https://doi.org/10.1021/acs.est.5b00944

Marrero, J., Coto, O., Schippers, A., 2017. Anaerobic and aerobic reductive dissolutions of iron-rich nickel laterite overburden by Acidithiobacillus. Hydrometallurgy 168, 49–55. https://doi.org/10.1016/J.HYDROMET.2016.08.012

Martin, M., 2011. Cutadapt removes adapter sequences from high-throughput sequencing reads.

EMBnet.journal 17, 10–12. https://doi.org/10.14806/ej.17.1.200

Masella, A.P., Bartram, A.K., Truszkowski, J.M., Brown, D.G., Neufeld, J.D., 2012. PANDAseq: paired-end assembler for Illumina sequences. BMC Bioinformatics 13, 31. https://doi.org/10.1186/1471-2105-13-31

Medina, W., 2014. Capas SIG - Área de Conservación Guanacaste [WWW Document]. URL https://www.acguanacaste.ac.cr/biodesarrollo/sistemas-de-informacion-geografica/capas-sig (accessed 2.19.19).

Medina, W., 1999a. Geología: Hoja Liberia - Area de Conservación Guanacaste [WWW Document]. Sist. Inf. Geográfica - Área Conserv. Guanacaste. URL http://www.investigadoresacg.org/IMAGES/MAPFILES/maps/physical_biological/geologia_acg.jpg (accessed 12.11.16).

Medina, W., 1999b. Tipos de vegetación: Hoja Liberia - Area de Conservación Guanacaste [WWW Document]. Sist. Inf. Geográfica - Área Conserv. Guanacaste. URL http://www.investigadoresacg.org/IMAGES/MAPFILES/maps/physical_biological/vegetacion_acg.jpg (accessed 12.11.16).

Medina, W., 1999c. Suelos: Hoja Liberia - Area de Conservación Guanacaste [WWW Document]. Sist. Inf. Geográfica - Área Conserv. Guanacaste. URL http://www.investigadoresacg.org/IMAGES/MAPFILES/maps/physical_biological/suelos_acg.jpg (accessed 12.11.16).

Newsome, L., Cleary, A., Morris, K., Lloyd, J.R., 2017. Long-Term Immobilization of Technetium via Bioremediation with Slow-Release Substrates. Environ. Sci. Technol. 51, 1595–1604. https://doi.org/10.1021/acs.est.6b04876

Noël, V., Morin, G., Juillot, F., Marchand, C., Brest, J., Bargar, J.R., Muñoz, M., Marakovic, G., Ardo, S., Brown, G.E., 2015. Ni cycling in mangrove sediments from New Caledonia. Geochim. Cosmochim. Acta 169, 82–98. https://doi.org/10.1016/j.gca.2015.07.024

Nurk, S., Bankevich, A., Antipov, D., Gurevich, A.A., Korobeynikov, A., Lapidus, A., Prjibelski, A.D., Pyshkin, A., Sirotkin, A., Sirotkin, Y., Stepanauskas, R., Clingenpeel, S.R., Woyke, T., Mclean, J.S., Lasken, R., Tesler, G., Alekseyev, M.A., Pevzner, P.A., 2013. Assembling single-cell genomes and mini-metagenomes from chimeric MDA products. J. Comput. Biol. 20, 714–737. https://doi.org/10.1089/cmb.2013.0084

Oren, A., 2014. The Family Methanobacteriaceae, in: Rosenberg, E., DeLong, E.F., Lory, S., Stackebrandt, E., Thompson, F. (Eds.), The Prokaryotes: Other Major Lineages of Bacteria and The Archaea. Springer Berlin Heidelberg, Berlin, Heidelberg, pp. 165–193. https://doi.org/10.1007/978-3-642-38954-2_411

Power, I.M., Wilson, S.A., Dipple, G.M., 2013. Serpentinite Carbonation for CO2 Sequestration. Elements 9, 115–121. https://doi.org/10.2113/gselements.9.2.115

QGIS Development Team, 2019. QGIS Geographic Information System.

Rawat, S.R., Männistö, M.K., Bromberg, Y., Häggblom, M.M., 2012. Comparative genomic and physiological analysis provides insights into the role of Acidobacteria in organic carbon utilization in Arctic tundra soils. FEMS Microbiol. Ecol. 82, 341–355. https://doi.org/10.1111/j.1574-6941.2012.01381.x

Roberts, S., Gunn, G., 2014. Cobalt, in: Gunn, G. (Ed.), Critical Metals Handbook. John Wiley & Sons, Oxford, pp. 122–149. https://doi.org/10.1002/9781118755341.ch6

Sakai, S., Conrad, R., Imachi, H., 2014. The Family Methanocellaceae, in: Rosenberg, E., DeLong, E.F., Lory, S., Stackebrandt, E., Thompson, F. (Eds.), The Prokaryotes: Other Major Lineages of Bacteria and The Archaea. Springer Berlin Heidelberg, Berlin, Heidelberg, pp. 209–214. https://doi.org/10.1007/978-3-642-38954-2_318

Sattley, W.M., Madigan, M.T., 2014. The Family Heliobacteriaceae, in: Rosenberg, E., DeLong, E.F., Lory, S., Stackebrandt, E., Thompson, F. (Eds.), The Prokaryotes: Firmicutes and Tenericutes. Springer Berlin Heidelberg, Berlin, Heidelberg, pp. 185–196. https://doi.org/10.1007/978-3-642-30120-9_362

Schlesinger, W.H., Bernhardt, E.S., 2013. Chapter 7 - Wetland Ecosystems, in: Schlesinger, W.H., Bernhardt, E.S.B.T.-B. (Third E. (Eds.), . Academic Press, Boston, pp. 233–274. https://doi.org/10.1016/B978-0-12-385874-0.00007-8

Schwarzenbach, E.M., Gill, B.C., Gazel, E., Madrigal, P., 2016. Sulfur and carbon geochemistry of the Santa Elena peridotites: Comparing oceanic and continental processes during peridotite alteration. Lithos 252, 92–108. https://doi.org/10.1016/j.lithos.2016.02.017

Silver, W.L., Lugo, A.E., Keller, M., 1999. Soil oxygen availability and biogeochemistry along rainfall and topographic gradients in upland wet tropical forest soils. Biogeochemistry 44, 301–328. https://doi.org/10.1007/BF00996995

Smith, S.L., Grail, B.M., Johnson, D.B., 2017. Reductive bioprocessing of cobalt-bearing limonitic laterites. Miner. Eng. 106, 86–90. https://doi.org/10.1016/j.mineng.2016.09.009

Stackebrandt, E., 2014a. The Emended Family Peptococcaceae and Description of the Families Desulfitobacteriaceae, Desulfotomaculaceae, and Thermincolaceae, in: Rosenberg, E., DeLong, E.F., Lory, S., Stackebrandt, E., Thompson, F. (Eds.), The Prokaryotes: Firmicutes and Tenericutes. Springer Berlin Heidelberg, Berlin, Heidelberg, pp. 285–290. https://doi.org/10.1007/978-3-642-30120-9_364

Stackebrandt, E., 2014b. The Family Lachnospiraceae, in: Rosenberg, E., DeLong, E.F., Lory, S., Stackebrandt, E., Thompson, F. (Eds.), The Prokaryotes: Firmicutes and Tenericutes. Springer Berlin Heidelberg, Berlin, Heidelberg, pp. 197–201. https://doi.org/10.1007/978-3-642-30120-9_363

Stackebrandt, E., 2014c. The Family Clostridiaceae, Other Genera, in: Rosenberg, E., DeLong, E.F., Lory, S., Stackebrandt, E., Thompson, F. (Eds.), The Prokaryotes: Firmicutes and Tenericutes. Springer Berlin Heidelberg, Berlin, Heidelberg, pp. 67–73. https://doi.org/10.1007/978-3-642-30120-9_214

Taboada, T., Rodríguez-Lado, L., Ferro-Vázquez, C., Stoops, G., Martínez Cortizas, A., 2016. Chemical weathering in the volcanic soils of Isla Santa Cruz (Galápagos Islands, Ecuador). Geoderma 261, 160–168. https://doi.org/10.1016/j.geoderma.2015.07.019

Thompson, A., Chadwick, O.A., Rancourt, D.G., Chorover, J., 2006. Iron-oxide crystallinity increases during soil redox oscillations. Geochim. Cosmochim. Acta 70, 1710–1727. https://doi.org/0.1016/j.gca.2005.12.005

Thompson, A., Rancourt, D.G., Chadwick, O.A., Chorover, J., 2011. Iron solid-phase differentiation along a redox gradient in basaltic soils. Geochim. Cosmochim. Acta 75, 119–133. https://doi.org/10.1016/j.gca.2010.10.005

Thorne, R.L., Roberts, S., Herrington, R., 2012. Climate change and the formation of nickel laterite deposits. Geology 40, 331–334. https://doi.org/10.1130/G32549.1

Tishchenko, V., Meile, C., Scherer, M.M., Pasakarnis, T.S., Thompson, A., 2015. Fe2+ catalyzed iron atom exchange and re-crystallization in a tropical soil. Geochim. Cosmochim. Acta 148, 191–202. https://doi.org/10.1016/j.gca.2014.09.018

Wang, Q., Garrity, G.M., Tiedje, J.M., Cole, J.R., 2007. Naive Bayesian classifier for rapid assignment of rRNA sequences into the new bacterial taxonomy. Appl. Environ. Microbiol. 73, 5261–5267. https://doi.org/10.1128/AEM.00062-07

Whattam, S.A., Gazel, E., Yi, K., Denyer, P., 2016. Origin of plagiogranites in oceanic complexes: A case study of the Nicoya and Santa Elena terranes, Costa Rica. Lithos 262, 75–87. https://doi.org/10.1016/j.lithos.2016.06.017

Whitman, W.B., Bowen, T.L., Boone, D.R., 2014. The Methanogenic Bacteria, in: Rosenberg, E., DeLong, E.F., Lory, S., Stackebrandt, E., Thompson, F. (Eds.), The Prokaryotes: Other Major Lineages of Bacteria and The Archaea. Springer Berlin Heidelberg, Berlin, Heidelberg, pp. 123–163. https://doi.org/10.1007/978-3-642-38954-2_407

Wilkins, M.J., Livens, F.R., Vaughan, D.J., Beadle, I., Lloyd, J.R., 2007. The influence of microbial redox cycling on radionuclide mobility in the subsurface at a low-level radioactive waste storage site. Geobiology 5, 293–301. https://doi.org/10.1111/j.1472-4669.2007.00101.x

Winkler, P., Kaiser, K., Thompson, A., Kalbitz, K., Fiedler, S., Jahn, R., 2018. Contrasting evolution of iron phase composition in soils exposed to redox fluctuations. Geochim. Cosmochim. Acta 235, 89–102. https://doi.org/10.1016/j.gca.2018.05.019

Zhou, X., Liu, D., Bu, H., Deng, L., Liu, H., Yuan, P., Du, P., Song, H., 2018. XRD-based quantitative analysis of clay minerals using reference intensity ratios, mineral intensity factors, Rietveld, and full pattern summation methods: A critical review. Solid Earth Sci. 3, 16–29. https://doi.org/10.1016/J.SESCI.2017.12.002

### 6.9 Supplementary figures

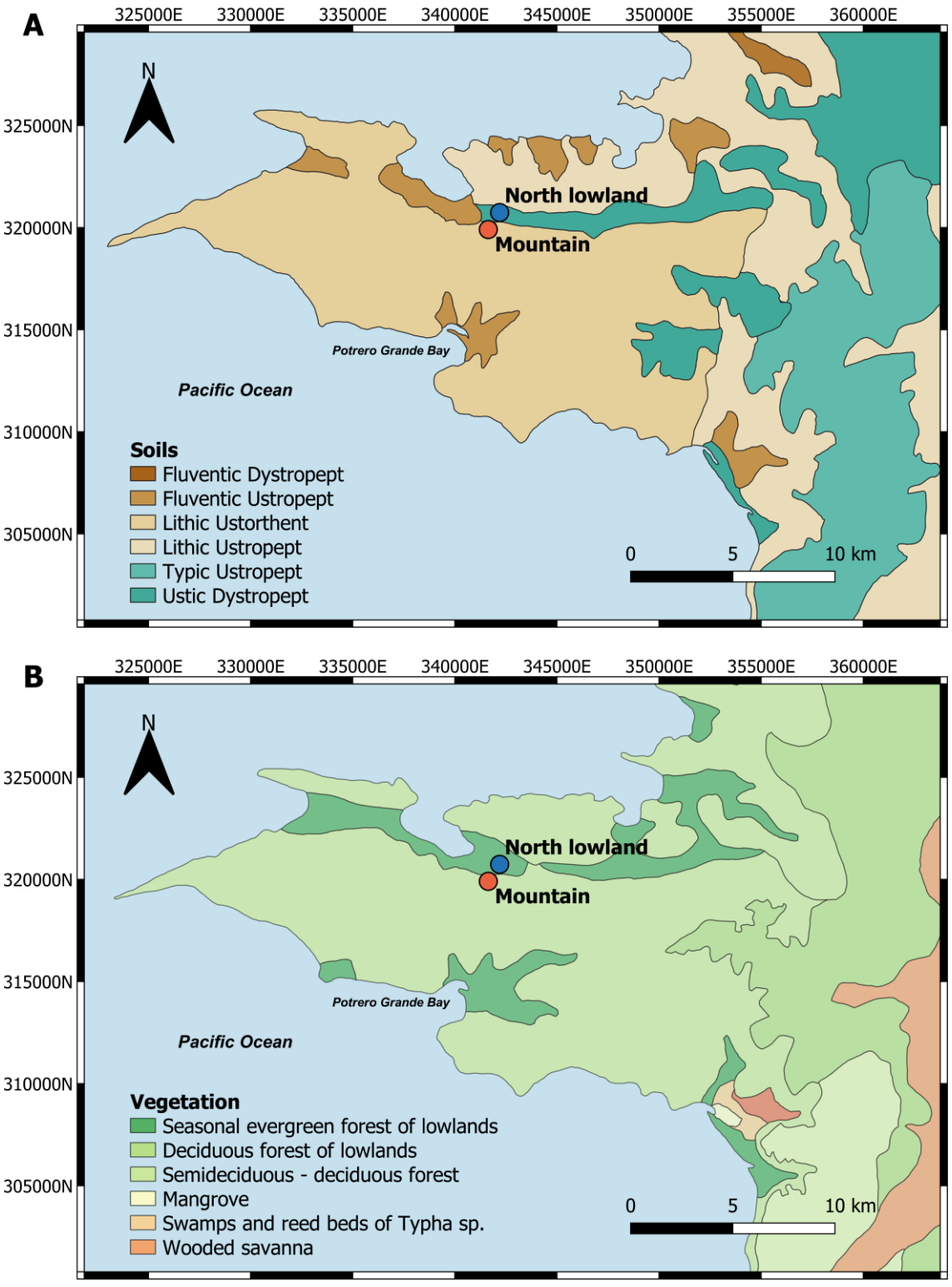


**Figure 6.S1.** (A) Geographical distribution of both locations sampled within the maps of the soils and (B) vegetation of the Santa Elena Peninsula. Maps adapted from Medina (1999a, 1999b), only relevant colours have been labelled.

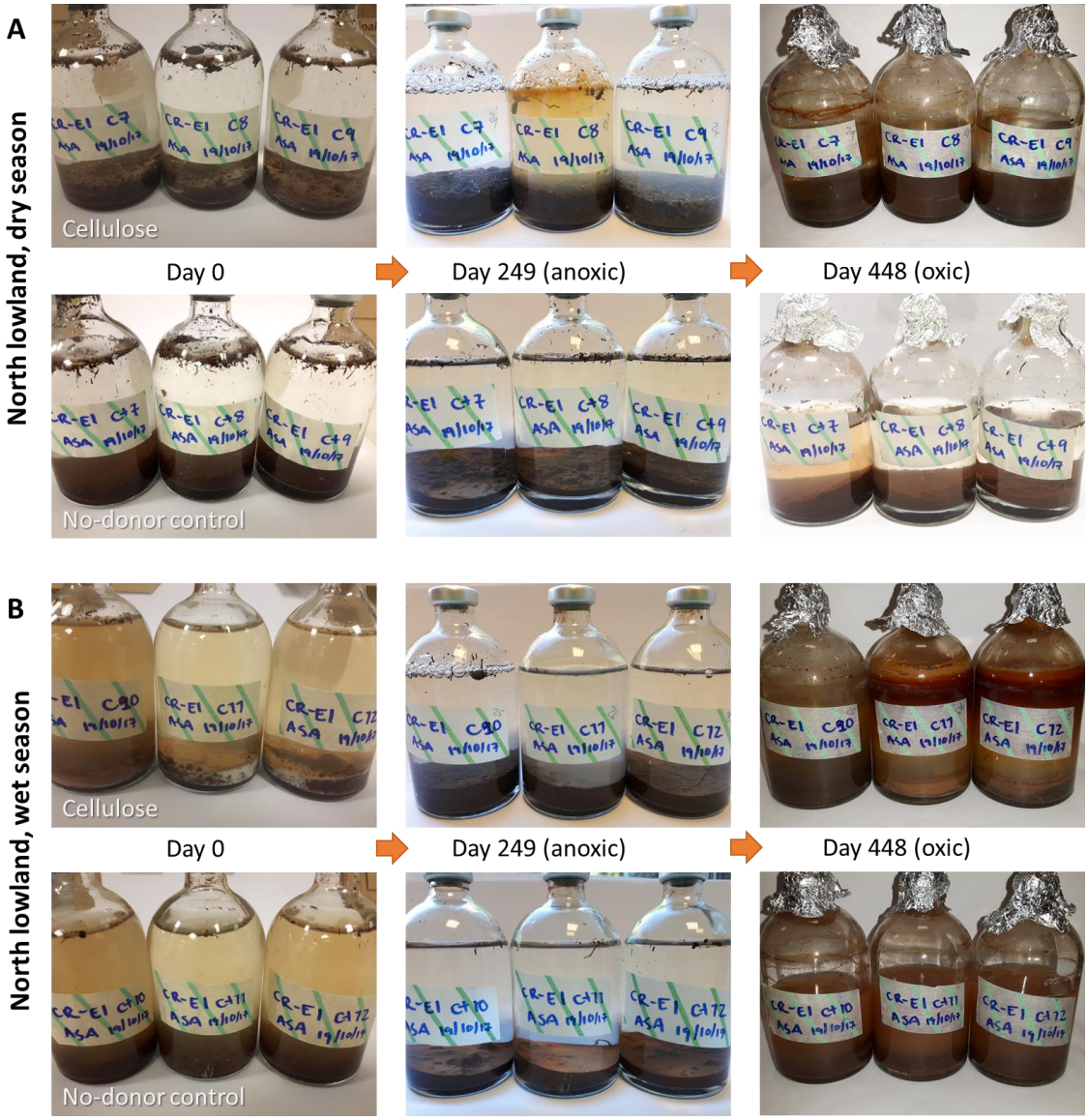


**Figure 6.S2.** Microcosm serum bottles for the three replicates of the north lowland lateritic soil from both dry (A) and wet (B) season biostimulated with cellulose and a no-donor control at the beginning of the redox cycling microcosm experiment (day 0), after 8 months of anoxic incubation (day 249 overall) and after 5 months of subsequent oxic incubation (day 448 overall).

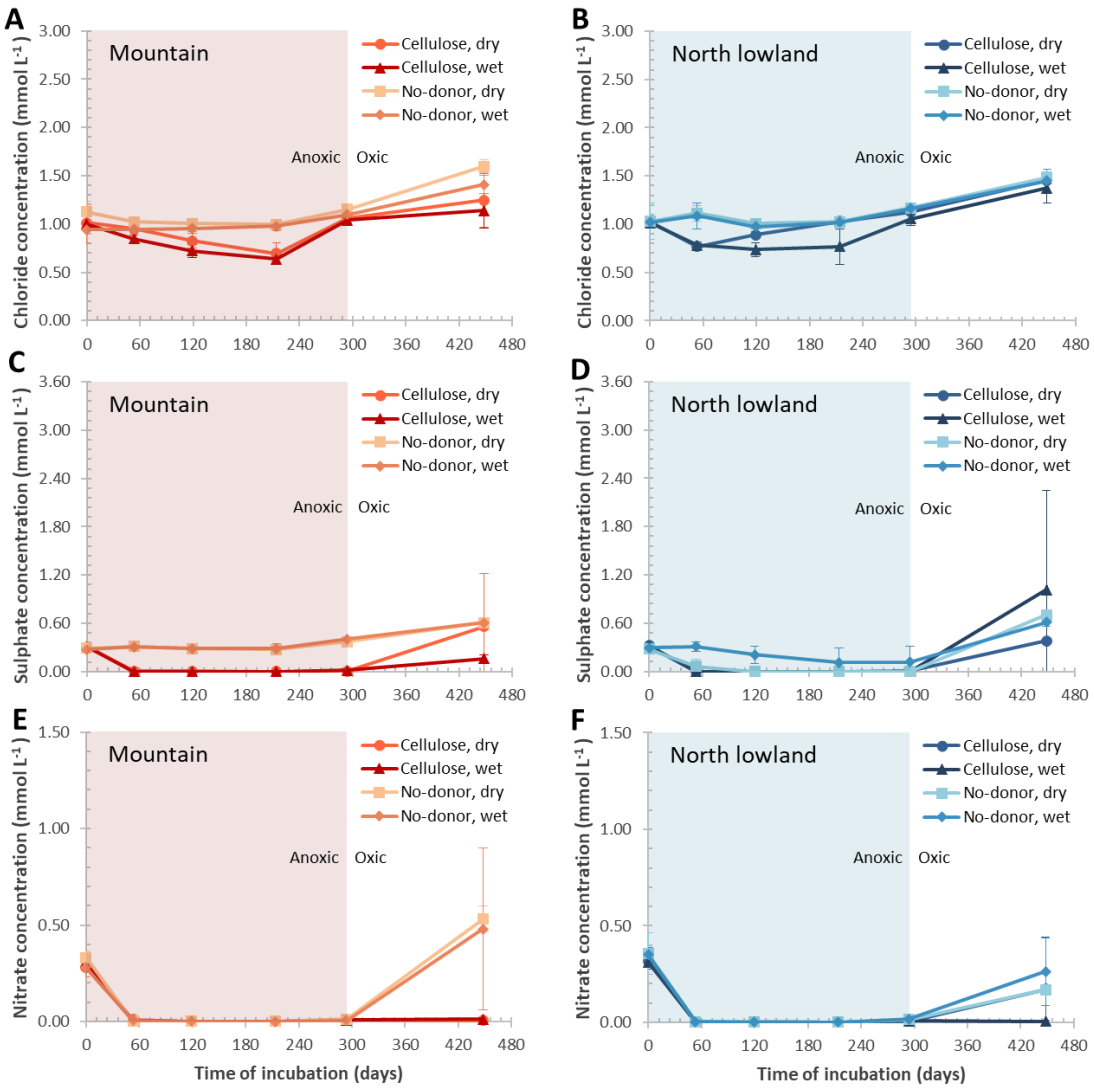


**Figure 6.S3.** Chloride (A, B), sulphate (C, D) and nitrate (E, F) aqueous concentration in the redox cycling microcosm experiments after biostimulation with glucose and acetate/lactate during both anoxic (coloured area) and oxic (clear area) conditions for both locations and seasons sampled. Results are shown as an average of the 3 replicates tested and their respective standard deviation.

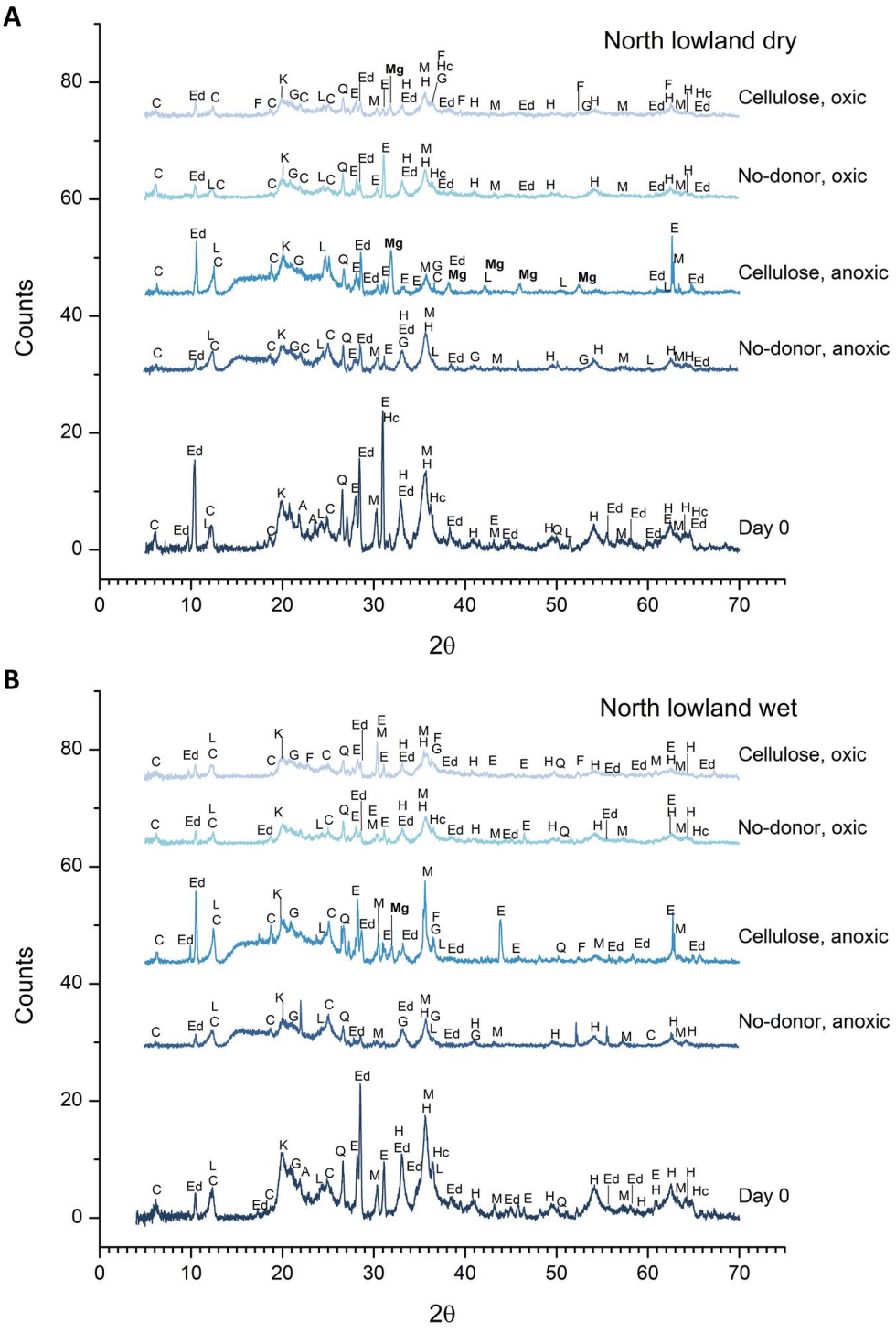


**Figure 6.S4.** Mineralogy of the lateritic soils from the North lowland at the start of the redox cycling microcosm experiment, and at the end of the anoxic and oxic incubations, after biostimulation with cellulose for soils from dry (A) and wet (B) seasons. Main minerals found with XRD were: goethite (G), hematite (H), maghemite (M), lizardite (L), siderite (Si), magnesite (Mg), enstatite (E), clinochlore (C), nontronite (N), stevensite (S), hercynite (Hc), edenite (Ed), kaolinite (K), albite (A) and quartz (Q).

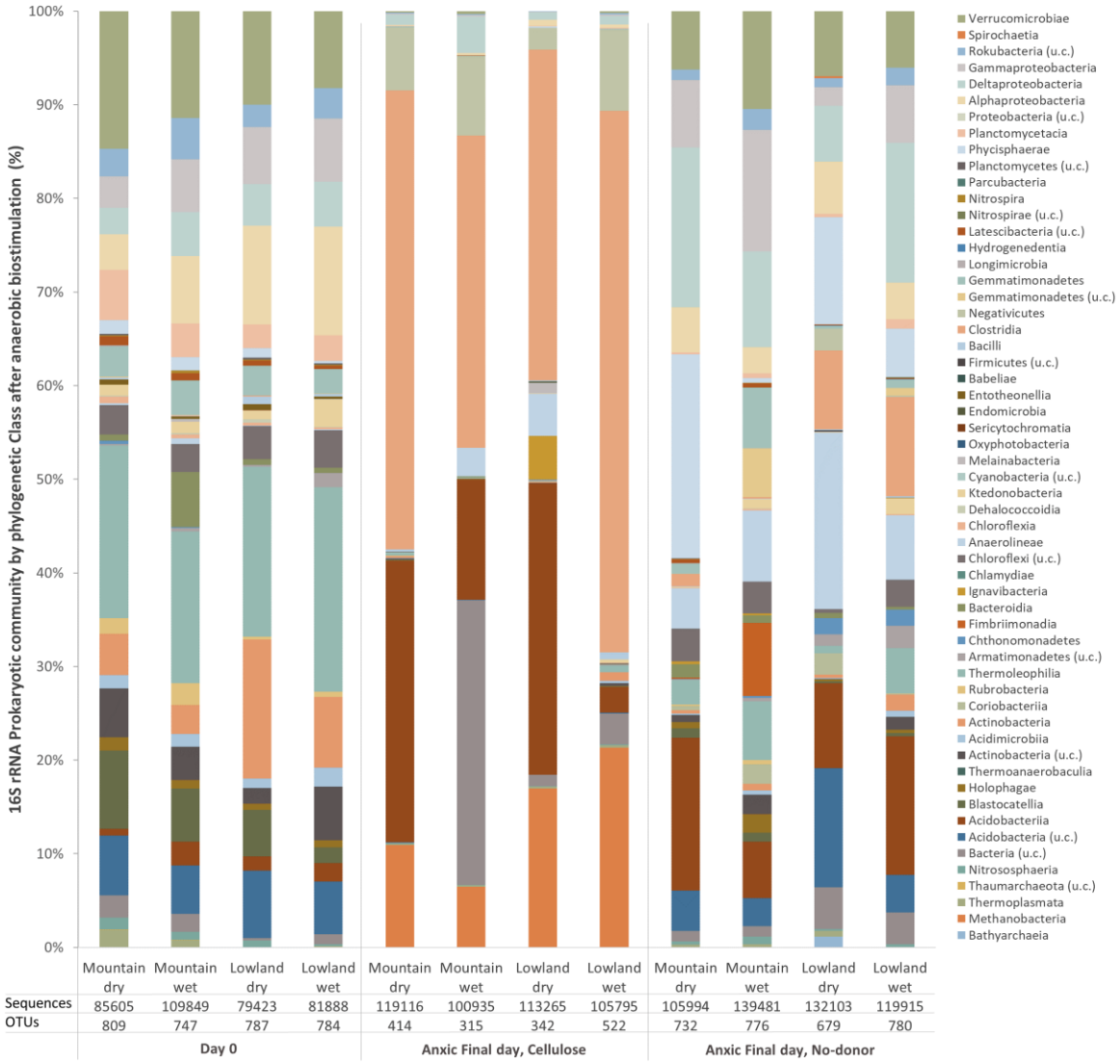


**Figure 6.S5.** Prokaryotic communities per phylogenetic class in the lateritic soils of the Santa Elena Peninsula from both wet and dry seasons obtained by the sequencing of the V4 region of 16S rRNA after anaerobic biostimulation experiments with cellulose and no-donor controls; these microcosm experiments were followed by subsequent aerobic biostimulation experiments (Figure 6.S6). In every stage the starting soil before redox cycling microcosm experiment is also shown; 'u.c.': unclassified class.

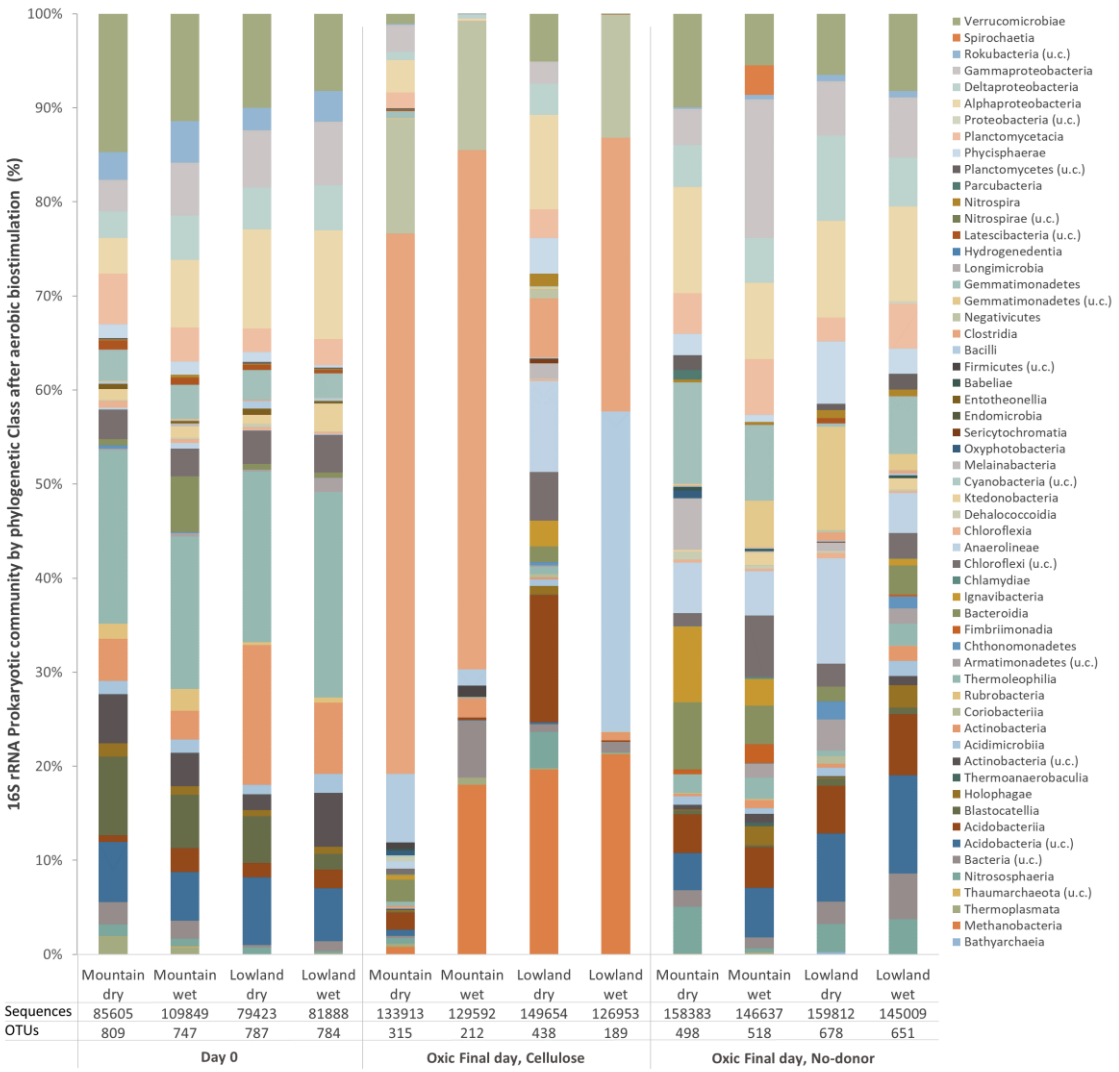


**Figure 6.S6.** Prokaryotic communities per phylogenetic class in the lateritic soils of the Santa Elena Peninsula obtained by the sequencing of the V4 region of 16S rRNA after oxic conditions followed previous anoxic biostimulation (Figure 6.S6) with cellulose and no-donor controls. In every location the starting soil before the entire redox cycling microcosm experiment is also shown; 'u.c.': unclassified class.

# Chapter 7. Conclusions and future directions

## 7.1 Conclusions

The biochemical cycling of Fe, Co, Ni and Mn in the lateritic soils from the Santa Elena Peninsula was studied in this thesis. This is a protected ecological area in Costa Rica including the Santa Elena Ophiolite, and a unique area to study the natural geomicrobiology of lateritic soils because it is subjected to active tropical lateritic soil formation from serpentinized peridotites due to the strong dry-wet seasonality of the site. Overall, a detailed geochemical and microbiological characterisation of the lateritic soils from the Santa Elena Peninsula was performed, considering weathering processes in serpentinized peridotites and using a landscape approach. The geological, biological and ecological repercussions in the natural context of Santa Elena Peninsula were assessed. The microorganisms present in the lateritic soils showed a determinant role in the mobilisation of those elements either through aerobic or anaerobic processes that influenced bioweathering of Fe and Mg minerals, biomineralisation of Fe/Mg carbonates and methanogenesis. Those microbially-mediated processes were also affected by the seasonal patterns of the site inducing variations in the biogeochemical cycling of Fe, Co, Ni and Mn.

In Chapter 4, the geochemistry and microbiology of the lateritic soils from the Santa Elena Peninsula were characterised considering a landscape geographical approach. The soils were confirmed as Ni-rich laterites (Section 4.4.2), but with geochemical variations depending on their geographical position within the ophiolite area (4.4.3), resulting in three different lateritic soil types identified: *mountain* soils, *inner ophiolite lowland* soils and *North lowland* soils (Figure 4.13). The mountain soils were rich in Fe, Co, Ni and Mn and dominated by lizardite and iron oxide minerals, and their microbial communities were characterised by a relative high abundance of Fe-redox cycling bacteria and fungal groups restricted to these areas (Section 4.4.4). The lowland soils, despite sharing similar landscapes, showed variations in their geochemistry, separating those inside the ophiolite area, that were geochemically and microbiologically more similar to the

mountain soils, from the soils at the northern boundaries of the ophiolite that have a more complex geochemical composition although still ophiolite influenced. Also, in the lowlands, Mn-oxidising bacteria were more abundant, with the highest relative abundance in the mangrove areas. Other geographical differences were found; within the mountain soils the influence of altitude-associated characteristics (Section 4.4.3), as the minor degree of vegetation coverage and more direct climate exposure, favoured the concentration of Co and Ni. Altitude has been demonstrated to be a relevant factor for weathering, associated with erosive processes in non-tropical serpentine soils (D'Amico et al., 2015), and in other non-serpentine soils (Taboada et al., 2019, 2016). However, on tropical serpentine soils this association has not been properly tested, and this study supposes one of the first efforts to demonstrate it; and evidenced the necessity to further study the influence of the altitude-associated characteristics such as vegetation coverage and climate exposure on weathering processes. Both variables are highly relevant in tropical serpentine soils, climate variations are frequent, for example with heavy climatic conditions of precipitation when a tropical storm is present. Vegetation on the other hand can influence the composition, richness and abundance of microorganisms in soils, and that has been demonstrated in other serpentine tropical areas (Bordez et al., 2016; Carriconde et al., 2019; Gourmelon et al., 2016) and non-tropical regions (Branco and Ree, 2010; Touceda-González et al., 2018). Moreover, high diversity patterns in the tropics are well known, and together with the plant endemism observed on other serpentine ecosystems (Anacker, 2011; Kay et al., 2011; Kazakou et al., 2008), evidenced the large range of interesting ecological studies that can be developed on a serpentine ecosystem as the one from Santa Elena Peninsula.

In the inner ophiolite lowlands, concentrations of trace metals were higher downstream within the same riparian basin, evidencing the mangrove locations as metal-sink areas and supporting their unique microbial community composition (Section 4.4.2 and 4.4.3). The metal-sink behaviour of mangroves occurs worldwide, and the metal source could be of natural origin as from ultramafic/serpentine deposits (Marchand et al., 2012; Noël et al., 2015) or from anthropogenic sources such as reported in Australia (Holloway et al., 2016; Nath et al., 2013), Senegal (Bodin et al., 2013), Singapore (Cuong et al., 2005) or Brazil (Fonseca et al., 2013; Machado et al., 2002). However, the relationships between the high content of metals such as Co, Ni, Mn, Fe or Cr, and the microbial communities inhabiting the ultramafic-derived sediments of mangroves is

still poorly understood. Thus, this research has provided evidence that mangroves associated with serpentine ecosystems could be relevant as model systems to understand the biogeochemical cycling of metals in those complex ecological environments; and also the microbial communities can have a crucial role in those cycles.

Microbial communities from Santa Elena Peninsula were relatively homogeneous along the Santa Elena Peninsula, and similar to other tropical serpentine soils (Gourmelon et al., 2016) and soils in general (Delgado-Baquerizo et al., 2018). However, the results of this research evidenced how microbial communities in serpentine soils can be affected by variations of biotic factors like vegetation type and coverage, and abiotic factors such as the geochemistry of the soils or the altitude, even within a small geographical area.

This chapter also highlighted that, when studying the soils of the Santa Elena Peninsula, not only the taxonomic soil classification should be taken in account, but also the geochemical composition of the soils according to their geographical location within the ophiolite area must be considered, especially in inner ophiolite lowland areas or the top of the mountains. Also, this was the first detailed description of the mineralogy and the geochemistry of these soils, and the first report of the microbial communities (both prokaryotic and fungal) in the lateritic soils from the Santa Elena Peninsula. On a broader context, this research evidenced the importance of landscape characteristics such as topography, vegetation, and climate, in the development of weathering processes such as serpentinization and lateritization under tropical conditions. However, not only abiotic factors or vegetation should be considered to understand those geochemical processes, microbial communities (both fungal and prokaryotic) are of great relevance, and those microscopic organisms can contribute to shape the serpentine ecosystem and the landscape associated, as demonstrated in this research.

In Chapter 5, the natural biogeochemical cycling of Fe and Mg in the lateritic soils from the Santa Elena Peninsula was studied following the geographical/geochemical classification of those soils reported in Chapter 4. The results of fluctuating redox cycling microcosm experiments evidenced differences in the biogeochemical cycling of those soils depending on the soil origin within that classification (Section 5.4.1). Intense microbial activity induced the release of Fe, Mn, Ni and Co from the mountain soils stimulated under anoxic conditions with glucose, as a result of microbial

reduction and dissolution of iron(III) oxides (Section 5.4.2). At the same time, Mg was released from the bioweathering of clay minerals. Biomineralisation also occurred after reductive conditions were tested in the microcosm experiments as Fe(II) was re-precipitated as Fe/Mg carbonate minerals (Section 5.4.3). Also, those conditions caused a decrease in prokaryotic diversity of the mountain soils and a prokaryotic community dominated by Firmicutes (Section 5.4.4). In contrast, methanogenesis was observed in the lowland soils that had lower contents of iron, less Fe(III) reduction and no metal release to the aqueous phase; suggesting that methanogenesis was diminished in the mountain soils potentially due to competition for reducing equivalents with Fe(III)-reduction coupled to anaerobic carbon metabolism (section 5.4.2). When the oxic conditions were reinstated in the microcosms then Fe(II) was re-oxidised, carbonate minerals decreased and prokaryotic groups such as Acidobacteria and Proteobacteria were recovered especially in those with mountain soils amended with glucose. Reductive dissolution of Fe(III) oxides and re-crystallisation of iron oxides and oxy-hydroxides have been widely reported when stimulating tropical soils using fluctuating redox experiments (Ginn et al., 2017; Thompson et al., 2011, 2006; Tishchenko et al., 2015; Winkler et al., 2018), however the focus of those studies was more mineralogical/geochemical and the experiments were not targeting directly the stimulation of microbial communities. Here was demonstrated that fluctuating redox experiments can be developed using long-term microcosm experiments focused on biostimulation of microbial communities. Thus, the microcosm technique could be used for further studies involving more redox cycles or different conditions, although it can be still improved for example by optimising the length of the experiments. This chapter confirmed that the geographical/geochemical differences of the lateritic soils found in Chapter 4 were also reflected in the biogeochemical cycles occurring in those soils, especially for Fe and Mg that can be mobilised from lateritic soils of the mountains in Santa Elena Peninsula during periods of anaerobiosis. It also highlighted that the fixation/mobilisation of carbon via carbonate biomineralisation and methane production provide evidence of the importance of the lateritic soils for carbon fluxes.

In Chapter 6, the biogeochemical cycling of Co, Ni and Mn in the lateritic soil from Santa Elena Peninsula was assessed following the fluctuating redox cycling microcosm methodology successfully tested in Chapter 5. However, for a better simulation of the natural environments found in the lateritic soils, cellulose was used as an electron donor to emulate the natural carbon

source from plant matter, and soils collected from both dry and wet seasons were tested to cover different seasonal environments (Section 6.4.1). Microbial cellulose degradation was closely associated with Co, Ni and Mn cycling in these lateritic soils. Under anoxic environments (Section 6.4.2), cellulose degradation was coupled to microbial Fe(III) reduction, resulting in the bioweathering of Fe-oxides and releasing Co, Ni and Mn present in those minerals. After subsequent oxic conditions were induced, Fe was re-oxidised and precipitated as Fe(III) minerals such as hematite or goethite. Mobilisation of Co, Ni and Mn continued to a lesser extent associated with the bioweathering of Mg minerals including hydrous silicates (lizardite or chlorite) or clays (smectite) (Section 6.4.4), and favoured either by (i) redox buffering produced from the same cellulosic microbial metabolism, by (ii) the presence of anoxic microsites, and/or by (iii) aerobic cellulose degradation as suggested by the presence of Bacilli in wet season lowland soils. During cellulose biostimulation, the Firmicutes clades had a critical role in the natural cycling of Co, Ni and Mn in these lateritic soils, likely performing the depolymerisation of cellulose into smaller molecules bioavailable for other microbial processes such as Fe(III) redox cycling (Section 6.4.6). Additionally, cellulose biostimulation showed greater concentrations of Co, Ni and Mn mobilised than compared to glucose biostimulation reported in Chapter 5. Finally, seasonal variations in the lateritic soils have different biogeochemical outputs depending on the topographical origin of the soil, where precipitation could be pivotal to induce redox processes in the serpentine soils by facilitating the development of anoxic conditions in those soils, as seen in other upland tropical soils from Hawaii or Puerto Rico, where rainfall generated short redox fluctuations that lead to more rapid iron reduction rates or the presence of anoxic microsites (Barcellos et al., 2018b, 2018a; Ginn et al., 2017; Hodges et al., 2018; Silver et al., 1999; Thompson et al., 2011). In mountain soils, precipitation induced faster rates of anaerobic microbially-mediated processes such as Fe(III) reduction and methanogenesis that affected how fast the biogeochemical cycling of metals started (faster in the wet season). During the wet season the lowland soils had analogous trends of Fe, Co, Ni and Mn mobilisation than the mountain soils, and similar changes in the microbial composition, potentially related to more Fe(III) available in the lowland soils during wet season due to Fe(III) influxes from the surrounding mountains to the lowlands originated by rainfall erosive processes. Methanogenesis was also seasonally affected; it was more intense in soils collected during the wet season in the mountain soils but in the lowland

soils was stronger in soils collected in the dry season, also associated with the Fe(III) available, as in dry season metal mobilisation did not occur to the lowlands and methanogenesis was favoured instead (Section 6.4.5).

This chapter highlighted that Fe, Mg and trace elements as Co, Ni and Mn, can be naturally mobilised from lateritic soils in Santa Elena Peninsula using carbon inputs including indigenous plant matter, but also showed the importance of considering the seasonality of the site, as it can impact those cycles by increasing anaerobiosis periods imposed by soil waterlogging in the rainy season, especially in lowland locations via erosive processes occurring in the surrounding mountains Thus, the results of this study suggests that in serpentine soils, microbial degradation of cellulose is a key ecological process for the biogeochemical cycling of Mg, Fe and metals associated such as Co, Ni and Mn, both under oxic and anoxic conditions, with seasonal precipitation acting as a driving force stimulating the activation and/or intensity of those cycles.

In summary, the lateritic soils from Santa Elena Peninsula had geographical-geochemical differences that separated the lateritic soils into three groups: *mountain* soils, *inner ophiolite lowland* soils and *north lowland* soils. Microbially-mediated processes involving carbon metabolism, including Fe-redox cycling, carbonate biomineralisation and methanogenesis, affected the biogeochemical cycling of Fe, Mg, Co, Ni and Mn in these lateritic soils due to the direct and/or indirect bioweathering of Fe and Mg minerals; although those processes differed depending on the soil type and of the seasonality. Amongst the microbial communities detected in the lateritic soils of Santa Elena Peninsula, the Firmicutes clades emerged as a crucial group of prokaryotes for the biogeochemical cycling of those metals when coupled to the degradation of cellulose and other carbon substrates including glucose.

More in general, the results of this thesis demonstrated that microbial degradation of cellulose (i.e. natural plant matter) is a key ecological process to understand other microbially-mediated processes naturally occurring in serpentine soils, such as the biogeochemical cycling of Co, Ni and Mn, both under oxic and anoxic conditions. Also, the development of those conditions can be largely determined by the seasonal precipitation, by stimulating the initiation and/or driving the intensity of those cycles. Additionally, methanogenesis and anaerobic microbial processes in general, can be sustained on serpentine soils during the entire year, regardless of seasonality or

topography, highlighting how relevant these microbial processes could be in large scale carbon effluxes or influxes from serpentine ecosystems overall, especially considering the large amount of iron in the serpentine soils. Thus, this thesis has contributed to better understand the geomicrobiological process occurring on serpentine ecosystems, and the impact of abiotic factors such as the seasonal rainfall on the biogeochemical cycling of metals on serpentine soils.

This thesis has also demonstrated the potential of the Santa Elena Peninsula as a useful site to study the natural geomicrobiology of lateritic soils under tropical conditions. The ophiolite nature, an environment that is under active lateritic formation processes due to its variable tropical climate, different topographies and vegetation types, its potential as a hotspot for serpentinization endemism and the absence of anthropogenic intervention for nearly 50 years due to its protected status, make this area of Costa Rica a very interesting place and a model experimental site to develop further work not only about geomicrobiological studies, but also to study other natural biotic/abiotic relationships underpinning serpentine ecosystems. This study will serve as a basis for future research to better understand the role of microorganisms not only in the biogeochemical cycles occurring in those serpentine soils, but also in the carbon fluxes and their implications to climate change, even at a global scale.

### 7.2 Further work

Following the results obtained in this thesis, several lines of investigation could be further assessed in the lateritic soils and serpentine ecosystems of Santa Elena Peninsula. In this research, three different soil types were found according to their geographical location and geochemical composition, also influencing the biogeochemical cycling of the Fe and metals associated. More specifically, some interesting trends were observed as the increase of Fe, Co, Ni and Mn with the altitude of the mountains or the increasing concentration of metals downstream a riparian basin accumulating in the mangroves at the end (Section 4.4.2 and 4.4.3). This leads to the study of those biogeochemical cycles not only in the serpentine soils of the Santa Elena Peninsula, but in other serpentine soils (tropical and non-tropical) to compare with other soil types from different ecological contexts or geological origins, as it has been reported before (D'Amico et al., 2015; Taboada et al., 2019, 2016). The study could be done using the fluctuating redox

cycling microcosm experiments successfully performed in this thesis, but considering an altitude transect or a riparian basin to understand better how the geochemistry and the microbial composition change in those gradients. As said before, accumulation of Ni has been reported in mangrove sediments downstream ultramafic deposits from New Caledonia (Marchand et al., 2012; Noël et al., 2015), but was studied in an intertidal context and not in a riparian transect.

Another interesting area to analyse would be a depth gradient within lateritic soils. Some exploratory work was done in this thesis considering samples at 30cm depth in some of the locations tested, but the geochemistry and the microbial communities did not differ substantially. However, deeper soil samples could have greater variations, especially when close to the bedrock/saprolite limit (that is relatively shallow in some of the lateritic soils in Santa Elena Peninsula). In a different regolith, was proposed that bacterial growth is dominated by Fe(II) electron donor flux in the bedrock/saprolite limit, and Fe-oxidising bacteria could contribute to saprolite formation (Buss et al., 2005). Moreover it has been demonstrated that the dissolution of iron minerals could also determine the fate of metals both within the superficial serpentine soils and in deeper layers of the regolith, as demonstrated with trace elements that were susceptible to variations in the redox conditions within a humid tropical regolith profile (Chapela Lara et al., 2018). In this study was demonstrated that Co, Ni and Mn can be mobilised in superficial serpentine soils mediated by microbial processes, but further work should focus in understanding deeper profiles to better understand the bioweathering processes occurring near the bedrock of ultramafic lithologies. Understanding better Co and Ni mobilisation from laterites under fluctuating redox conditions like those studied in this thesis could be of interest for biomining purposes, as a bioprocessing proceeding to extract Co from laterites was recently proposed but focused only on anoxic biostimulation (Newsome *et al.*, in revision, Appendix 1). The laterite profile of Santa Elena Peninsula could be of great relevance to asses those questions about metal cycling in lateritic profiles, given the high concentrations of iron found in the soils and the active microbially-mediated Fe cycling demonstrated in this thesis. Also, *in situ* measurements or a constant monitoring of pH and redox potential of the soils within this depth profile or during an entire year would help to understand better the influence of seasonal rainfall in the waterlogging of serpentine soils and thus in the anoxic environments of the soils. An interesting approach to study those vertical variations can be done with column experiments (Lewis and Sjöstrom, 2010), trying to

emulate a natural vertical profile and following mineralogical, geochemical and microbiological changes at different depths and across time.

This thesis has also demonstrated the important role of microorganisms in the biogeochemical cycling of Fe, Mg, Co, Ni and Mn in serpentine soils, but many observations still need to be addressed. Here was shown how prokaryotic communities changed during fluctuating redox conditions stimulated with different carbon sources including cellulose (Sections 5.4.4 and 6.4.6). Fungal communities must be considered in future experiments involving these lateritic soils as their known cellulolytic activity (Baldrian and Valášková, 2008) could be a determinant step for microbial processes involving carbon metabolism that were demonstrated in this thesis. Fungi can also have a direct effect in the cycling of Fe, Mg, Co, Ni and Mn of lateritic soils as they can be important bioweathering agents (Gadd, 2007; Valix et al., 2001). Mineral-fungi stimulations could be proved useful to help understand those direct effects. All this together also highlights the necessity to understand the relationship prokaryote/fungi in the lateritic soils of Santa Elena Peninsula, for example considering the ratio prokaryote/fungi that could be delivered from quantitative-real time PCR (Bonk et al., 2018). Moreover, in this thesis large quantities of unknown prokaryotes and fungi were detected, highlighting the potential of the Santa Elena Peninsula for identification and/or isolation studies that can result in the discovering of new species with potential serpentine specialisation (Anacker, 2011).

Finally, this thesis can help underpin fundamental work for ecological research set on a larger scale within the Santa Elena Peninsula, for example considering how these biogeochemical cycles occur at the soil level can influence the diversity and/or distribution of vegetation in those soils (Moore and Elmendorf, 2011), as demonstrated in ultramafic soils of New Caledonia (Bordez et al., 2016; Gourmelon et al., 2016), the hyperaccumulation of Ni, Co and Mn in those plants as studied in serpentine flora in Cuba or previously explored in Santa Elena Peninsula (Reeves et al., 2007, 1999), or potential mycorrhizal relationships to support those plant-stressful conditions (Carriconde et al., 2019).

On the other hand, serpentinites and serpentine systems have been reported as key points for sequestration of $CO_2$ on a global scale (Power et al., 2013). Additionally, this study evidenced that methanogenesis and anaerobic microbial processes in general, can be sustained on

serpentine soils during the entire year, regardless of seasonality or topography, just as seen in other types of soils (Barcellos et al., 2018b; Silver et al., 1999), that together with the relative high amounts of Fe in serpentine soils, highlight how relevant these microbial processes could be in when considering large scale carbon effluxes or influxes from serpentine ecosystems overall. So, the other large scale set of experiments that could be assessed in the Santa Elena Peninsula are those based on the quantification of carbon fluxes within the serpentine ecosystem, considering carbon mobilisation/fixation via microbial processes as Fe-redox cycling, methanogenesis, bioweathering, biomineralisation, all demonstrated in this thesis and potentially associated with microbial carbon degradation. These studies could be enhanced considering the bioavailability in soils of cellulose or the organic matter pool in general, or the presence of black carbon from biomass burnt during natural fires commonly present in Santa Elena Peninsula during dry season (Lorenz et al., 2010). All this together will contribute to understand better how laterites and serpentine ecosystems contribute to global carbon budgets in a climate change context.

### 7.3 References


Anacker, B.L., 2011. Phylogenetic patterns of endemism and diversity, in: Harrison, S., Rajakaruna, N. (Eds.), Serpentine: The Evolution and Ecology of a Model System. University of California Press, Berkeley, p. 446.

Baldrian, P., Valášková, V., 2008. Degradation of cellulose by basidiomycetous fungi. FEMS Microbiol. Rev. 32, 501–521. https://doi.org/10.1111/j.1574-6976.2008.00106.x

Barcellos, D., Cyle, K.T., Thompson, A., 2018a. Faster redox fluctuations can lead to higher iron reduction rates in humid forest soils. Biogeochemistry 137, 367–378. https://doi.org/10.1007/s10533-018-0427-0

Barcellos, D., O'Connell, C., Silver, W., Meile, C., Thompson, A., 2018b. Hot Spots and Hot Moments of Soil Moisture Explain Fluctuations in Iron and Carbon Cycling in a Humid Tropical Forest Soil. Soil Syst. 2, 59. https://doi.org/10.3390/soilsystems2040059

Bodin, N., N'Gom-Kâ, R., Kâ, S., Thiaw, O.T., Tito de Morais, L., Le Loc'h, F., Rozuel-Chartier, E., Auger, D., Chiffoleau, J.-F., 2013. Assessment of trace metal contamination in mangrove ecosystems from Senegal, West Africa. Chemosphere 90, 150–157. https://doi.org/10.1016/j.chemosphere.2012.06.019

Bonk, F., Popp, D., Harms, H., Centler, F., 2018. PCR-based quantification of taxa-specific abundances in microbial communities: Quantifying and avoiding common pitfalls. J. Microbiol. Methods 153, 139–147. https://doi.org/https://doi.org/10.1016/j.mimet.2018.09.015

Bordez, L., Jourand, P., Ducousso, M., Carriconde, F., Cavaloc, Y., Santini, S., Claverie, J.M., Wantiez, L., Leveau, A., Amir, H., 2016. Distribution patterns of microbial communities in ultramafic landscape: a metagenetic approach highlights the strong relationships between diversity and environmental traits. Mol. Ecol. 25, 2258–2272.

https://doi.org/10.1111/mec.13621

Branco, S., Ree, R.H., 2010. Serpentine Soils Do Not Limit Mycorrhizal Fungal Diversity. PLoS One 5, e11757. https://doi.org/10.1371/journal.pone.0011757

Buss, H.L., Bruns, M.A., Schultz, M.J., Moore, J., Mathur, C.F., Brantley, S.L., 2005. The coupling of biological iron cycling and mineral weathering during saprolite formation, Luquillo Mountains, Puerto Rico. Geobiology 3, 247–260. https://doi.org/10.1111/j.1472-4669.2006.00058.x

Carriconde, F., Gardes, M., Bellanger, J.-M., Letellier, K., Gigante, S., Gourmelon, V., Ibanez, T., McCoy, S., Goxe, J., Read, J., Maggia, L., 2019. Host effects in high ectomycorrhizal diversity tropical rainforests on ultramafic soils in New Caledonia. Fungal Ecol. 39, 201–212. https://doi.org/10.1016/j.funeco.2019.02.006

Cuong, D.T., Bayen, S., Wurl, O., Subramanian, K., Shing Wong, K.K., Sivasothi, N., Obbard, J.P., 2005. Heavy metal contamination in mangrove habitats of Singapore. Mar. Pollut. Bull. 50, 1732–1738. https://doi.org/https://doi.org/10.1016/j.marpolbul.2005.09.008

D'Amico, M.E., Freppaz, M., Leonelli, G., Bonifacio, E., Zanini, E., 2015. Early stages of soil development on serpentinite: the proglacial area of the Verra Grande Glacier, Western Italian Alps. J. Soils Sediments 15, 1292–1310. https://doi.org/10.1007/s11368-014-0893-5

Delgado-Baquerizo, M., Oliverio, A.M., Brewer, T.E., Benavent-González, A., Eldridge, D.J., Bardgett, R.D., Maestre, F.T., Singh, B.K., Fierer, N., 2018. A global atlas of the dominant bacteria found in soil. Science (80-. ). 359, 320–325. https://doi.org/10.1126/science.aap9516

Fonseca, E.F., Baptista Neto, J.A., Silva, C.G., 2013. Heavy metal accumulation in mangrove sediments surrounding a large waste reservoir of a local metallurgical plant, Sepetiba Bay, SE, Brazil. Environ. Earth Sci. 70, 643–650. https://doi.org/10.1007/s12665-012-2148-3

Gadd, G.M., 2007. Geomycology: biogeochemical transformations of rocks, minerals, metals and radionuclides by fungi, bioweathering and bioremediation. Mycol. Res. 111, 3–49. https://doi.org/10.1016/j.mycres.2006.12.001

Ginn, B., Meile, C., Wilmoth, J., Tang, Y., Thompson, A., 2017. Rapid Iron Reduction Rates Are Stimulated by High-Amplitude Redox Fluctuations in a Tropical Forest Soil. Environ. Sci. Technol. 51, 3250–3259. https://doi.org/10.1021/acs.est.6b05709

Gourmelon, V., Maggia, L., Powell, J.R., Gigante, S., Hortal, S., Gueunier, C., Letellier, K., Carriconde, F., 2016. Environmental and Geographical Factors Structure Soil Microbial Diversity in New Caledonian Ultramafic Substrates: A Metagenomic Approach. PLoS One 11, 1–25. https://doi.org/10.1371/journal.pone.0167405

Hodges, C., King, E., Pett-Ridge, J., Thompson, A., 2018. Potential for Iron Reduction Increases with Rainfall in Montane Basaltic Soils of Hawaii. Soil Sci. Soc. Am. J. 82, 176–185. https://doi.org/10.2136/sssaj2017.06.0193

Holloway, C.J., Santos, I.R., Tait, D.R., Sanders, C.J., Rose, A.L., Schnetger, B., Brumsack, H.-J., Macklin, P.A., Sippo, J.Z., Maher, D.T., 2016. Manganese and iron release from mangrove porewaters: A significant component of oceanic budgets? Mar. Chem. 184, 43–52. https://doi.org/10.1016/j.marchem.2016.05.013

Kay, K.M., Ward, K.L., Watt, L.R., Schemske, D.W., 2011. Plant Speciation, in: Harrison, S., Rajakaruna, N. (Eds.), Serpentine: The Evolution and Ecology of a Model System. University of California Press, Berkeley, p. 446.

Kazakou, E., Dimitrakopoulos, P.G., Baker, A.J.M., Reeves, R.D., Troumbis, A.Y., 2008. Hypotheses, mechanisms and trade-offs of tolerance and adaptation to serpentine soils: from species to ecosystem level. Biol. Rev. 83, 495–508. https://doi.org/10.1111/j.1469-185X.2008.00051.x

Lewis, J., Sjöstrom, J., 2010. Optimizing the experimental design of soil columns in saturated and unsaturated transport experiments. J. Contam. Hydrol. 115, 1–13. https://doi.org/https://doi.org/10.1016/j.jconhyd.2010.04.001

Lorenz, K., Lal, R., Jiménez, J.J., 2010. Characterization of soil organic matter and black carbon in dry tropical forests of Costa Rica. Geoderma 158, 315–321. https://doi.org/10.1016/j.geoderma.2010.05.011

Machado, W., Silva-Filho, E. V, Oliveira, R.R., Lacerda, L.D., 2002. Trace metal retention in mangrove ecosystems in Guanabara Bay, SE Brazil. Mar. Pollut. Bull. 44, 1277–1280. https://doi.org/10.1016/S0025-326X(02)00232-1

Marchand, C., Fernandez, J.-M., Moreton, B., Landi, L., Lallier-Vergès, E., Baltzer, F., 2012. The partitioning of transitional metals (Fe, Mn, Ni, Cr) in mangrove sediments downstream of a ferralitized ultramafic watershed (New Caledonia). Chem. Geol. 300–301, 70–80. https://doi.org/10.1016/j.chemgeo.2012.01.018

Moore, K.A., Elmendorf, S.C., 2011. Plant competition and facilitation in systems with strong environmental gradients, in: Harrison, S., Rajakaruna, N. (Eds.), Serpentine: The Evolution and Ecology of a Model System. University of California Press, Berkeley, p. 446.

Nath, B., Birch, G., Chaudhuri, P., 2013. Trace metal biogeochemistry in mangrove ecosystems: A comparative assessment of acidified (by acid sulfate soils) and non-acidified sites. Sci. Total Environ. 463–464, 667–674. https://doi.org/10.1016/j.scitotenv.2013.06.024

Noël, V., Morin, G., Juillot, F., Marchand, C., Brest, J., Bargar, J.R., Muñoz, M., Marakovic, G., Ardo, S., Brown, G.E., 2015. Ni cycling in mangrove sediments from New Caledonia. Geochim. Cosmochim. Acta 169, 82–98. https://doi.org/10.1016/j.gca.2015.07.024

Power, I.M., Wilson, S.A., Dipple, G.M., 2013. Serpentinite Carbonation for CO2 Sequestration. Elements 9, 115–121. https://doi.org/10.2113/gselements.9.2.115

Reeves, R.D., Baker, A.J.M., Borhidi, A., Berazaín, R., 1999. Nickel Hyperaccumulation in the Serpentine Flora of Cuba. Ann. Bot. 83, 29–38. https://doi.org/10.1006/anbo.1998.0786

Reeves, R.D., Baker, A.J.M., Romero, R., 2007. The ultramafic flora of the Santa Elena peninsula, Costa Rica: A biogeochemical reconnaissance. J. Geochemical Explor. 93, 153–159. https://doi.org/10.1016/j.gexplo.2007.04.002

Silver, W.L., Lugo, A.E., Keller, M., 1999. Soil oxygen availability and biogeochemistry along rainfall and topographic gradients in upland wet tropical forest soils. Biogeochemistry 44, 301–328. https://doi.org/10.1007/BF00996995

Taboada, T., Ferro-Vázquez, C., Stoops, G., Martínez-Cortizas, A., Rodríguez-Flores, R., Rodríguez-Lado, L., 2019. Secondary aluminium, iron and silica phases across a volcanic soil climosequence, Galápagos Islands. Eur. J. Soil Sci. 70, 540–549. https://doi.org/10.1111/ejss.12788

Taboada, T., Rodríguez-Lado, L., Ferro-Vázquez, C., Stoops, G., Martínez Cortizas, A., 2016. Chemical weathering in the volcanic soils of Isla Santa Cruz (Galápagos Islands, Ecuador). Geoderma 261, 160–168. https://doi.org/10.1016/j.geoderma.2015.07.019

Thompson, A., Chadwick, O.A., Rancourt, D.G., Chorover, J., 2006. Iron-oxide crystallinity increases during soil redox oscillations. Geochim. Cosmochim. Acta 70, 1710–1727. https://doi.org/0.1016/j.gca.2005.12.005

Thompson, A., Rancourt, D.G., Chadwick, O.A., Chorover, J., 2011. Iron solid-phase differentiation along a redox gradient in basaltic soils. Geochim. Cosmochim. Acta 75, 119–133. https://doi.org/10.1016/j.gca.2010.10.005

Tishchenko, V., Meile, C., Scherer, M.M., Pasakarnis, T.S., Thompson, A., 2015. Fe2+ catalyzed iron atom exchange and re-crystallization in a tropical soil. Geochim. Cosmochim. Acta 148,

191–202. https://doi.org/10.1016/j.gca.2014.09.018

Touceda-González, M., Kidd, P.S., Smalla, K., Prieto-Fernández, A., 2018. Bacterial communities in the rhizosphere of different populations of the Ni-hyperaccumulator Alyssum serpyllifolium and the metal-excluder Dactylis glomerata growing in ultramafic soils. Plant Soil 431, 317–332. https://doi.org/10.1007/s11104-018-3767-6

Valix, M., Usai, F., Malik, R., 2001. Fungal bio-leaching of low grade laterite ores. Miner. Eng. 14, 197–203. https://doi.org/https://doi.org/10.1016/S0892-6875(00)00175-8

Winkler, P., Kaiser, K., Thompson, A., Kalbitz, K., Fiedler, S., Jahn, R., 2018. Contrasting evolution of iron phase composition in soils exposed to redox fluctuations. Geochim. Cosmochim. Acta 235, 89–102. https://doi.org/10.1016/j.gca.2018.05.019

# Appendix 1. Manganese and cobalt redox cycling in laterites; biogeochemical and bioprocessing implications

---

Laura Newsome[a1*], Agustín Solano Arguedas[a], Victoria S. Coker[a], Christopher Boothman[a] and Jonathan R. Lloyd[a]

[a] Williamson Research Centre, School of Earth and Environmental Sciences, University of Manchester, Manchester, M13 9PL, United Kingdom

[1] Present address: Camborne School of Mines and Environment and Sustainability Institute, University of Exeter, Penryn, Cornwall, TR10 9FE, United Kingdom

[*] Corresponding author: Laura Newsome, l.newsome@exeter.ac.uk, 01326 259018

## A1.1 Abstract

Cobalt is essential for the modern technology that underpins decarbonisation of our economies, but its supply is limited leading to its designation as a critical metal. Cobalt biogeochemistry is poorly understood, yet knowledge of how biogeochemical cycling impacts cobalt behaviour could assist the development of new techniques to recover cobalt from ores, and so improve the security of supply. Laterites are an important source of cobalt, they are primarily processed for nickel using energy or chemical intensive processes, with cobalt recovered as a by-product. Metal-reducing conditions were stimulated in laterite sediment microcosms by the addition of simple and cheaply available organic substrates (acetate or glucose). At the end of the experiment the amount of easily recoverable cobalt (aqueous or extractable with acetic acid) increased from < 1% to up to 64%, which closely mirrored the behaviour of manganese, while only a small proportion of iron was transformed into an easily recoverable phase. Sequencing of the microbial community showed that the addition of organic substrates stimulated the growth of indigenous prokaryotes closely related to known manganese(IV)/iron(III) reducers, particularly from the Clostridiales, and that fungi assigned to *Penicillium,* known to produce organic acids beneficial for leaching cobalt and nickel from laterites, were identified. Overall, the results indicate that the environmental

behaviour of cobalt in laterites (and sediments) is likely to be controlled by manganese biogeochemical cycling by microorganisms. These results are compelling given that similar behaviour was observed in four laterites (Acoje, Çaldağ, Piauí and Shevchenko) from different continents. A new bioprocessing strategy is proposed whereby laterites are treated with an organic substrate to generate metal-reducing conditions, then rinsed with acetic acid to remove the cobalt. Not only are organic substrates environmentally-friendly and potentially sourced from waste carbon substrates, a minimal amount of iron oxides was mobilised and consequently less waste generated.

**Keywords:** Biogeochemistry, bioreduction, cobalt, nickel, iron-reduction, manganese-reduction

### A1.2 Introduction

Cobalt is a critical metal essential for a sustainable modern world. It is increasingly in demand for use in rechargeable batteries for solar power and electric cars, permanent magnets in wind turbines, as well as in core applications such as superalloys to increase the strength and resistance of materials, electronics, catalysts, pigments and healthcare (The Cobalt Institute, 2019). Although Co is not rare in the Earth's crust, it is only found in economic quantities in a few countries, with 50 % of reserves in the Democratic Republic of Congo (US Geological Survey, 2018). This has led to Co being designated a critical raw material by the EU in 2011, to highlight the importance of securing a reliable and sustainable supply.

Laterites are an important source of cobalt. They are primarily mined for Ni and supply 40 % of the world's annual production (Yongue-Fouateu et al., 2006). Co is recovered as a side product and Ni-laterites supplied 48 % of the world's annual production in 2007 (British Geological Survey, 2009). Laterites are iron-rich deposits formed during intense long-lasting weathering of ultramafic bedrock in tropical climates, which leads to the enrichment of residual elements such as Ni and Co. The cobalt in laterites is typically associated with Mn-oxide enriched horizons (Elias et al., 1981; Yongue-Fouateu et al., 2006; Dublet et al., 2017), with a similar relationship observed in soil environments (Taylor and McKenzie, 1966; Uren, 2013). Currently Ni and Co are recovered from laterites using pressure acid leaching, heap leaching and/or solvent extraction (British

Geological Survey, 2009; Kursunoglu and Kaya, 2016; Oxley et al., 2016). A number of studies have demonstrated that Co and Ni can be recovered from laterite and sulfide ores by bioleaching, for example by inoculating the ore with acidophilic cultures such as *Acidothiobacillus* spp. (Johnson et al., 2013; Marrero et al., 2015; Chen et al., 2016; Smith et al., 2017), or fungi that generate organic acids (Tzeferis et al., 1994; Valix et al., 2001). Further research into bioleaching technologies, including field application is ongoing as part of the Natural Environment Research Council CoG3 project (http://www.nhm.ac.uk/our-science/our-work/sustainability/cog3-cobalt-project.html).

Over 30 years ago it was discovered that microorganisms are able to reduce Mn(IV) and Fe(III) coupled to the oxidation of organic carbon or hydrogen, and in doing so gain energy for growth (Lovley and Phillips, 1986; Myers and Nealson, 1988). Under near-neutral and alkaline environmental conditions this can solubilise Mn(IV)-oxide and Fe(III)-oxide minerals by forming aqueous Mn(II) and Fe(II). Microbial metal reduction has since been observed in a broad diversity of prokaryotes from many different environments (Lovley et al., 2004). Although microbial Mn(IV)/Fe(III) reducers have previously been observed in a Cuban laterite (Perez et al., 2013), their potential to liberate Co from oxide minerals during the development of metal-reducing conditions has not been explored.

In fact, the biogeochemistry of cobalt in terrestrial environments is surprisingly poorly understood. Cobalt most frequently occurs as Co(II) or Co(III), with Co(II) thermodynamically stable under most environmental conditions (Hem, 1985). An exception to this is where Co is associated with Mn-oxides; Mn-oxides are able to oxidise Co(II) to Co(III) which then sorbs to and becomes incorporated into the Mn-oxide crystal lattice (Murray and Dillard, 1979; Tanaka et al., 2013; Simanova and Peña, 2015). Microbes have been shown to reduce Co(III) to Co(II) under carefully controlled laboratory conditions, for example with Co(III) stabilised using a strong ligand such as EDTA (Gorby et al., 1998; Singh et al., 2015). It has been suggested that concomitant reduction of Mn oxides and Co(III) in soils is required to generate Mn(II) and Co(II) ions that are suitable for uptake by plants (Uren, 2013). In a study where lake sediments were incubated with *Shewanella putrefaciens*, a model Fe(III)-reducing bacterium, Co and Ni were released to the aqueous phase concurrent with the dissolution of reactive Mn minerals (Crowe et al., 2007). Another study subjected rice paddy soils to reduced conditions by degassing with $N_2/CO_2$ and observed a

correlation between lower Eh values and increased Co in the aqueous phase (Shaheen et al., 2014). Together this indicates that microbial metal cycling is likely to play an important role in controlling the mobility of Co in the environment.

The aim of this study was to characterise the biogeochemistry of Co in terrestrial sediment systems, and to use this new understanding to inform potentially new and sustainable ways to recover Co from laterites. Here we explored the impact of the adding organic electron donors (acetate or glucose) to biostimulate microbial metal reduction, on the fate of Co and Ni, using microcosms containing four different laterites (Acoje, Çaldağ, Piauí, Shevchenko). A multidisciplinary approach was used to dissect the system, including the use of next generation DNA sequencing to identify key indigenous microorganisms and X-ray absorption spectroscopy to characterise metal speciation. A simple two-step bioprocessing strategy was designed based on stimulating microbial metal reduction to transform Co from a 'reducible' phase extractable by hydroxylamine-hydrochloride to a more labile 'exchangeable' phase that could be extracted using a simple acetic acid wash.

## A1.3 Materials and methods

### A1.3.1 Sample characterisation and experimental set up

#### A1.3.1.1 Laterite characterisation

Three laterite samples were obtained from the collection of the Natural History Museum, London. These included an actively forming laterite "Acoje" from the Philippines and two laterites that are not currently subject to tropical weathering, "Çaldağ" from Turkey and "Shevchenko 11" from Kazakhstan. Samples were also collected from another laterite not currently subject to tropical weathering in April 2016; the Piauí deposit, Brazil. Two samples were used in these experiments "Piauí 23" and "Piauí 4". All were composite samples collected from heaps and represent a range of horizons throughout the deposits.

Samples of each laterite were dried overnight at 105 °C, powdered in a ball mill and analysed by X-ray diffraction (XRD, Bruker D8 Advance) for mineralogy and X-ray fluorescence (XRF) for chemical composition. Total organic carbon (TOC) measurements were analysed using a

Shimadzu SSM5000A. Leach tests were performed by adding 1 g of laterite (wet weight) to 10 ml of deionised water or 30 mM bicarbonate. After 33 days pH measurements were made and the aqueous phase monitored for Co, Fe, Mn and Ni content using inductively coupled plasma atomic emission spectroscopy (ICP-AES, Perkin-Elmer Optima 5300 DV).

#### A1.3.1.2 Biostimulated Natural History Museum laterite sediment microcosms

Sediment microcosms were set up to investigate whether acetate-biostimulation of indigenous microbial communities in the Natural History Museum (NHM) laterites would generate metal-reducing conditions in the Fe(III) and Mn(IV) containing deposits, and liberate Co and Ni. These contained 3 g of laterite (wet weight), 30 ml of an anaerobic modified freshwater minimal medium (after Lovley *et al.*, 1991) at pH 7 with 10 mM acetate as the electron donor. The headspace was degassed with an 80:20 $N_2$:$CO_2$ mix and the bottles incubated in the dark at 30 °C. Experiments were conducted in triplicate and compared to no added electron donor controls.

#### A1.3.1.3 Bioaugmented Natural History Museum laterite sediment microcosms

Parallel NHM laterite sediment microcosms were augmented with a model Fe(III)-reducing bacterium (*Geobacter sulfurreducens*) to generate strongly Fe(III)-reducing conditions. These comprised 3 g of laterite, 30 ml of 30 mM sodium bicarbonate, 10 mM acetate and a washed cell suspension of *G. sulfurreducens* at an optical density at 600 nm of 0.8. *G. sulfurreducens* was obtained from the University of Manchester Geomicrobiology Laboratory culture collection and grown at 30 °C in the dark in an anaerobic modified freshwater enrichment medium (after Lovley and Phillips, 1988) at pH 7, with 15 mM acetate as the electron donor and 40 mM fumarate as the electron acceptor. Cells were harvested at the late-logarithmic phase by centrifugation (5,000 *g*, 20 minutes), washed twice in anaerobic 30 mM bicarbonate buffer, before adding to the sediment microcosms. Experiments were conducted in triplicate and compared to no added electron donor controls.

#### A1.3.1.4 Biostimulated Piauí laterite sediment microcosms

To test the ability of different electron donors to stimulate metal-reducing conditions and consequently mobilise Co and Ni, sediment microcosms were set up with the Piauí laterite and biostimulated with two different electron donors. These contained 3 g of laterite, 30 ml of sterile

artificial groundwater (Wilkins et al., 2007), and either 5 mM acetate and 5 mM lactate or 10 mM glucose. The headspace was degassed with an 80:20 $N_2$:$CO_2$ mix and the bottles incubated in the dark at 30 °C. Subsequently glucose was selected as the more effective electron donor and the microcosms were repeated with 10 g laterite, 100 ml artificial groundwater and 10 mM glucose in triplicate and compared to no added electron donor controls. As significant heterogeneities were observed, these were repeated with duplicate glucose-biostimulated sediment microcosms and an additional no added electron donor control.

### A1.3.2 Aqueous geochemistry

Aliquots of sediment slurry were periodically removed from sediment microcosms using a sterile $N_2$ degassed needle and syringe, and monitored for geochemical changes. In brief, 0.1 ml of slurry was added to 4.9 ml 0.5 N HCl or 0.5 N hydroxylamine-hydrochloride and digested for 1 hour before analysis for Fe(II) and total bioavailable Fe by the ferrozine assay (Lovley and Phillips, 1986; Lovley and Phillips, 1987). Supernatant was obtained by centrifugation (16,200 *g*, 5 minutes). The supernatant was analysed for major anions and volatile fatty acids using ion chromatography (Dionex ICS 5000). pH and Eh were measured using calibrated electrodes. Glucose concentrations in supernatant from selected samples were monitored using a Glucose Oxidase (GO) Assay Kit (Sigma). An aliquot of the supernatant was diluted into 2 % $HNO_3$ and analysed for Co, Fe, Mn and Ni via ICP-AES.

### A1.3.3 Microbial community analysis

The prokaryotic and fungal communities were characterised for each of the laterites to identify the composition of the indigenous microbial communities, and the groups that responded to biostimulation. Samples were analysed at the start and the end of the biostimulation experiments, including the microcosms stimulated with electron donor and the no added electron donor controls. For the NHM laterites microbial community characterisation was performed on the Day 0 and Day 90 time points, and on Days 0, 28 and 76 for the Piauí laterite. DNA was extracted from 0.2 ml of sediment slurry using a PowerSoil DNA isolation kit (MO Bio).

#### A1.3.3.1 Prokaryotic community analysis

The prokaryotic DNA was amplified using the universal 16S rRNA amplicon primers 8F and 1492R (Lane, 1991) and the purity of the polymerase chain reaction (PCR) products was determined by visualisation under short-wave UV light after staining with Sybersafe® and separation by electrophoresis in Tris-acetate-EDTA gel. The PCR products were cleaned up, quantified and the 16S rRNA genes were sequenced using the Illumina MiSeq platform (Illumina, San Diego, CA, USA) targeting the V4 hyper variable region (forward primer, 515F, 5′-GTGYCAGCMGCCGCGGTAA-3′; reverse primer, 806R, 5′-GGACTACHVGGGTWTCTAAT-3′) for 2 × 250-bp paired-end sequencing (Illumina) (Caporaso et al., 2011; Caporaso et al., 2012). PCR amplification was performed using Roche FastStart High Fidelity PCR System (Roche Diagnostics Ltd, Burgess Hill, UK) in 50µl reactions under the following conditions: initial denaturation at 95°C for 2 min, followed by 36 cycles of 95°C for 30 s, 55°C for 30 s, 72°C for 1 min, and a final extension step of 5 min at 72°C. The PCR products were purified and normalised to ~20ng each using the SequalPrep Normalization Kit (Fisher Scientific, Loughborough, UK). The PCR amplicons from all samples were pooled in equimolar ratios. The run was performed using a 4 pM sample library spiked with 4 pM PhiX to a final concentration of 10% following the method of Schloss and Kozich (Kozich et al., 2013).

Raw sequences for prokaryotes were divided into samples by barcodes (up to one mismatch was permitted) using a sequencing pipeline. Quality control and trimming was performed using Cutadapt (Martin, 2011), FastQC (https://www.bioinformatics.babraham.ac.uk/projects/fastqc/), and Sickle (Joshi and Fass, 2011). MiSeq error correction was performed using SPADes (Nurk et al., 2013). Forward and reverse reads were incorporated into full-length sequences with Pandaseq (Masella et al., 2012). Chimeras were removed using ChimeraSlayer (Haas et al., 2011), and operational taxonomic units (OTUs) were generated with UPARSE (Edgar, 2013). OTUs were classified by Usearch (Edgar, 2010) at the 97% similarity level, and singletons were removed. Rarefaction analysis was conducted using the original detected OTUs in Qiime (Caporaso et al., 2010). The taxonomic assignment was performed by the RDP classifier (Wang et al., 2007) and Blastn was used to identify the closest GenBank matches (http://blast.ncbi.nlm.nih.gov).

#### A1.3.3.2 Fungal community analysis

The fungal DNA was amplified using the Internal Transcribed Spacer Region (ITS) primers ITS1F and ITS4 (Brown et al., 1993; Gardes and Bruns, 1993) and the purity of the polymerase chain reaction (PCR) products was determined by visualisation under short-wave UV light after staining with Sybersafe® and separation by electrophoresis in Tris-acetate-EDTA gel. Sequencing of PCR amplicons of the ITS2 region of nuclear ribosomal DNA was conducted with the Illumina MiSeq platform (Illumina, San Diego, CA, USA), targeting the ITS2 internal transcribed spacer region between the large subunit (LSU) and the 5.8S ribosomal genes (forward primer, ITS4F, 5′-AGCCTCCGCTTATTGATATGCTTAART -3′, reverse primer, 5.8SR, 5′-AACTTTYRRCAAYGGATCWCT -3′;) (Taylor et al., 2016) for 2 × 300-bp paired-end sequencing (Illumina) (Caporaso et al., 2011; Caporaso et al., 2012). PCR amplification was performed using Roche FastStart High Fidelity PCR System (Roche Diagnostics Ltd, Burgess Hill, UK) in 50µl reactions under the following conditions: initial denaturation at 95°C for 2 min, followed by 36 cycles of 95°C for 30 s, 56°C for 45 s, 72°C for 2 min, and a final extension step of 5 min at 72°C. The PCR products were purified and normalised to ~20 ng each using the SequalPrep Normalization Kit (Fisher Scientific, Loughborough, UK). The PCR amplicons from all samples were pooled in equimolar ratios. The run was performed using a 10 pM sample library spiked with 10 pM PhiX to a final concentration of 10% following the method of Schloss and Kozich (Kozich et al., 2013).

The ITS sequencing data produced by the Miseq platform was analysed using the PIPITS automated pipeline (Gweon et al., 2015). Chimeras were removed by reference based chimera detection using UCHIME (Edgar et al., 2011) in conjunction with the UNITE UCHIME reference data set. The taxonomic assignment was performed by the RDP classifier (Wang et al., 2007) using the UNITE fungal ITS reference data set.

#### A1.3.3.3 Microbial community abundances

The abundance of prokaryotic DNA was determined in selected samples using quantitative PCR (qPCR). A serial dilution series was performed using a gBlock double stranded DNA gene fragment (Integrated DNA Technologies, Leuven, Belgium) covering nucleotide positions 1-570 of the 16S rRNA gene from species *Telluria mixta DSM 4832*. The standard curve for the qPCR

reaction was created by plotting the $C_T$ (Cycle threshold) values of the dilution series against the log input of DNA template. Concentrations ranging from 8.4 x $10^{-2}$ fg $\mu l^{-1}$ to 8.4 x $10^{5}$ fg $\mu l^{-1}$ were used to generate the standard curve.

PCR amplification was performed using Brilliant II SYBR Green QPCR Master Mix (Agilent Technologies LDA UK Limited, Stockport, UK) in a 25 µl final volume containing 2 µl of sample DNA, 0.15 µM of each primer and 12.5 µl of qPCR SYBR Green Master Mix. All the amplifications were carried out in optical grade qPCR tubes on a MX3000P qPCR system with an initial step of 94 °C for 10 minutes followed by 30 cycles of 94 °C for 30 seconds, 50 °C for 30 seconds, 72 °C for 45 seconds and a dissociation curve was run between 94 °C and 50 °C to check primer specificity. Cycle threshold ($C_T$) was determined automatically by the instrument. All samples were analysed in triplicate and the $r^2$ value was 0.986.

### A1.3.4 Solid geochemistry and mineralogy

#### A1.3.4.1 Sequential extractions

The distribution of metals in the laterites before and after biostimulation (with the added carbon substrates) and bioaugmentation (with added cells of *G. sulfurreducens*) was assessed using sequential extractions, allowing changes in metal extractability to be determined. The modified BCR procedure was used (Rauret et al., 1999; Bacon and Davidson, 2008) with 0.5 g of dried sediment and comprised extraction steps of 0.11 M acetic acid for the “exchangeable” fraction, 0.5 M hydroxylamine hydrochloride for the “reducible” fraction, 8.8 M hydrogen peroxide and 1.0 M ammonium acetate for the “oxidisable” fraction, and aqua regia for the “residual” fraction. The first two steps were done under anaerobic conditions for the biostimulated sediment to avoid mobilisation by oxidation (Keith-Roach et al., 2003). Extracts were analysed for Co, Mn, Fe and Ni using ICP-AES.

#### A1.3.4.2 Mineralogy and microscopy of microbially-reduced laterite sediment

At the end of the experiments (33 days for the bioaugmented NHM sediment microcosms, 90 days for the acetate-biostimulated NHM laterite microcosms, 143 days for the glucose-biostimulated Piauí microcosms) the solid phase was separated from the aqueous phase by centrifugation (5,000 *g*, 20 minutes), the resulting sediment paste was dried anaerobically, and

powdered by hand in an anaerobic cabinet using a pestle and mortar. XRD (Bruker D8 Advance) was performed on the dried sediment using a Coy anaerobic dome to assess for changes in mineralogy.

Transmission electron microscopy (TEM) was used to look for changes in sediment texture that occurred after biostimulation in sediment microcosms. To prepare the samples a small amount of deionised water was added to powdered laterite sediment (prepared in the ball mill for the laterites as supplied, or powdered by hand in the anaerobic cabinet for the post-microcosm samples), the mixture was shaken and left to settle for a few seconds, and then approximately 5 µl of suspension was dropped onto a Cu grid and left to dry. The post-microcosm samples were prepared and stored in an anaerobic cabinet. Although the different grinding methods may have had some impact on the size of particles analysed, similar sized suspension particles should have been obtained from suspension. TEM was performed using a FEI TF30 FEG operating at 300 kV and images were collected using Gatan Digital Micrograph. Selected area electron diffraction (SAED) and energy dispersive spectroscopy (EDS) were used to look for changes in mineralogy and chemistry before and after reduction. EDS analysis was carried out using an Oxford Xmax detector and Oxford INCA analysis software.

#### A1.3.4.3 Metal speciation by XAS

To investigate changes in metal speciation, iron and nickel $L_{II}$ and $L_{III}$ edge X-ray absorption spectroscopy (XAS) was carried out on the laterites before and after biostimulation using the 6.3.1 beamline at the Advanced Light Source, Berkeley, CA in conjunction with X-ray magnetic circular dichroism (XMCD). Measurements were made on dry samples prepared and analysed under anaerobic conditions, using total electron yield (TEY) to achieve an effective probing depth of around 3-4 nm. Two XAS spectra were collected using opposing applied magnetic fields of ± 1 T parallel and antiparallel to the beam direction, normalised to the incident beam and subtracted from each other to give XMCD spectra (Pattrick et al., 2002; Coker et al., 2008). It was not possible to obtain *L*-edge spectra for Co and Mn on these beamlines due to the low concentrations of these elements in the laterites. *L*-edge XAS spectra were compared qualitatively to known standards for goethite, ferrihydrite and magnetite (Joshi et al., 2018) as well as a calculated spectrum for $Ni^{2+}$ in octahedral coordination (Laan and Kirkman, 1992; Coker et al., 2008).

High resolution X-ray absorption near edge spectra (HR-XANES) were obtained for the Co and Ni *K*-edges using the I20 beamline at the Diamond Light Source. *K*-edge EXAFS spectra were also obtained for Ni but Co concentrations were too low for EXAFS analyses. ATHENA (Ravel and Newville, 2005) was used to calibrate, background subtract and normalise XANES spectra, and to remove glitches in the data at around 8620, 8928 and 9013 eV. ARTEMIS (Ravel and Newville, 2005) was used to fit the Ni EXAFS spectra, with additional shells only included if they significantly improved the fitting parameters (Downward et al., 2007).

### A1.4 Results

#### A1.4.1 Laterite characterisation

Each laterite contained the common rock forming minerals quartz and Al and/or Mg silicates, as well as the Fe(III)-oxide goethite (Table A1.S1). The Acoje laterite contained the mixed Fe(II)/Fe(III) minerals maghemite and hornblende, which together with the higher water content may indicate a lower degree of weathering, and potentially reflect that this laterite is actively forming. The Mn, Fe, Co and Ni contents of the laterites are listed in Table A1.1, correlation plots showed Mn and Co were positively correlated, and a negative correlation between Fe and Si (Figure A1.S1). These metals were mostly insoluble; less than 0.01 mM Co, Mn and Ni, and less than 0.1 mM of Fe was released to solution from leaching of the laterites with deionised water or 30 mM bicarbonate (except for Piauí 4 which released 0.09 ± 0.01 mM Ni to solution after 33 days in deionised water) (Table A1.S1). The pH of the laterites in deionised water ranged from 6.3 to 8.7, TOC was between 0.05 and 0.23 % and the water were: Çaldağ 6.8 %, Acoje 26 %, Shevchenko 11 6.5 %, Piauí 4 28 % and Piauí 23 13 % (Table A1.S1).

**Table A1.1**– Metal content of the laterites.

| Composition by XRF (%) | Çaldağ | Acoje | Shevchenko 11 | Piauí 4 | Piauí 23 |
|---|---|---|---|---|---|
| Mn | 0.32 | 0.64 | 0.91 | 0.22 | 0.38 |
| Fe | 30.6 | 44.6 | 20.5 | 13.4 | 24.7 |
| Co | 0.05 | 0.05 | 0.13 | 0.03 | 0.07 |
| Ni | 0.14 | 0.16 | 0.17 | 0.27 | 0.21 |

### A1.4.2 Natural History Museum laterite microcosms

Samples of the Acoje, Çaldağ and Shevchenko laterites were biostimulated with acetate or bioaugmented with *Geobacter sulfurreducens* and acetate to stimulate the development of metal-reducing conditions, observe the impact on Co and Ni extractability, and to identify the indigenous prokaryotes likely responsible.

#### A1.4.2.1 Stimulated microbial metal reduction in the NHM laterite sediment microcosms

Aqueous geochemical monitoring showed that Fe(III)-reducing conditions rapidly developed in each of the microcosms augmented with *G. sulfurreducens* (results are shown in Figure A1.1 for the Acoje laterite, and for brevity the Çaldağ and Shevchenko laterites are in the supporting information, respectively as Figure A1.S2 and A1.S3). After just 24 hours of incubation, Fe(II) had been produced in the bioaugmented Çaldağ and Shevchenko laterites, while Fe(II) was first measured in the Acoje laterite on Day 7. After 33 days considerable quantities of Fe(II) had been generated in the Çaldağ (62 ± 44 mM) and Acoje (23 ± 8.8 mM) microcosms. The texture of the laterites had changed significantly in the bioaugmented microcosms (Figure A1.S4), with an absence of a visible finer grained fraction and significant clumping of the sediment meaning it very rapidly settled from solution after shaking. This was particularly pronounced in the Shevchenko laterite which meant it was not possible to obtain a representative sample using a needle and syringe, hence the low Fe(II) concentrations reported with relatively large errors (1.6 ± 0.8 mM). These physical changes were not observed in the no added electron donor controls. The results for each of the biostimulated NHM laterite microcosms were similar, with Fe(II) produced and reducing conditions developed, albeit at a slower rate.

Less than 0.1 mM of Fe, Mn, Ni or Co was measured in the aqueous phase in all biostimulated and bioaugmented laterite sediment microcosms (Figs. A1.1, A1.S2, A1.S3), indicating that any geochemical transformations involving these elements, such as the production of Mn(II) or Fe(II), must have been limited to the solid phase. Anions were monitored in the biostimulated sediment microcosms to investigate the development of reducing conditions; the results showed that acetate was used by the sediment microbial community and small quantities of nitrate and large quantities of sulphate were released to the aqueous phase (Figs. A1.1, A1.S2, A1.S3). The

sulphate concentrations then decreased over time in the Çaldağ and Acoje biostimulated microcosms, presumably by microbial sulphate reduction.

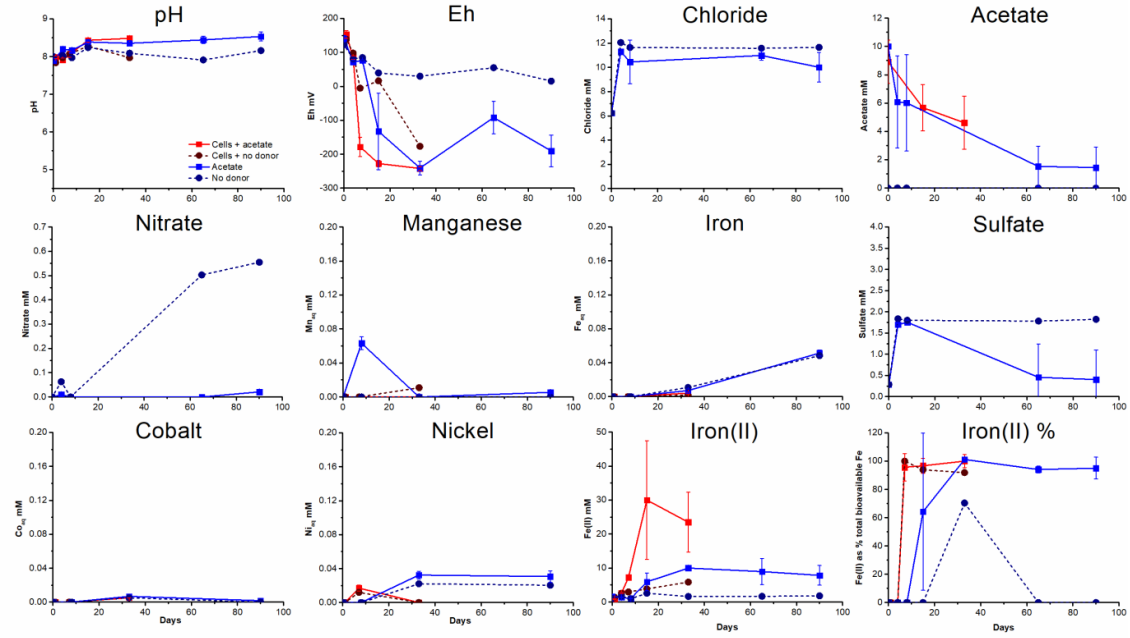


**Figure A1.1**– Geochemical monitoring of the biostimulated (blue) and bioaugmented (red) Acoje laterite sediment microcosms. Results are the average of three values; error bars ± 1 standard deviation (SD). ND refers to the single no added electron donor controls (dashed lines). The bioaugmented microcosms were stopped after 33 days. Very low concentrations of metals were released to the aqueous phase; just above the method reporting limit of 0.01 mM. Sediment clumping made it difficult to obtain a representative sample for Fe(II) measurement by the Ferrozine assay, generating relatively large SDs.

### A1.4.2.2 Sequential extractions to investigate metal fate in the NHM laterite sediment microcosms

Sequential extractions were performed to investigate the fate of metals in the solid phase. This included the laterite as supplied, and samples of the sediment microcosms 90 days after biostimulation with acetate, and 33 days after bioaugmentation with *G. sulfurreducens,* together with corresponding no added electron donor controls.

For each laterite, in the sediment as supplied (and the Day 90 no added electron control) most of the Co and Mn was associated with the 0.5 M hydroxylamine-extractable “reducible” phase, and most of the Ni and Fe associated with the aqua regia-extractable “residual” phase (Figs. A1.2,

A1.S5, A1.S6). In contrast, the biostimulated and bioaugmented laterites showed significantly more Co and Mn (and some Ni) were present in the acetic acid-extractable “exchangeable” phase. Therefore, although these metals were not released to the aqueous phase during microbial metal reduction (Figs. A1.1, A1.S2, A1.S3), they were instead transformed from a likely crystalline “reducible” phase into a loosely bound “exchangeable” or sorbed phase, and similar behaviour was observed in all three laterites.

The proportion of Co associated with easily recoverable phases in the laterites (that is, the aqueous content plus the acetic-acid extractable “exchangeable” fraction) after biostimulation or bioaugmentation increased from < 1 % to up to 45 % while Ni increased from < 1.5 % to up to 11 % (Table A1.2). Easily recoverable Mn also increased from < 1.5 % to up to 66 %, likely via microbial Mn(IV) reduction associated with the development of reducing conditions, while easily recoverable Fe increased from 0 % to 4.8 %.

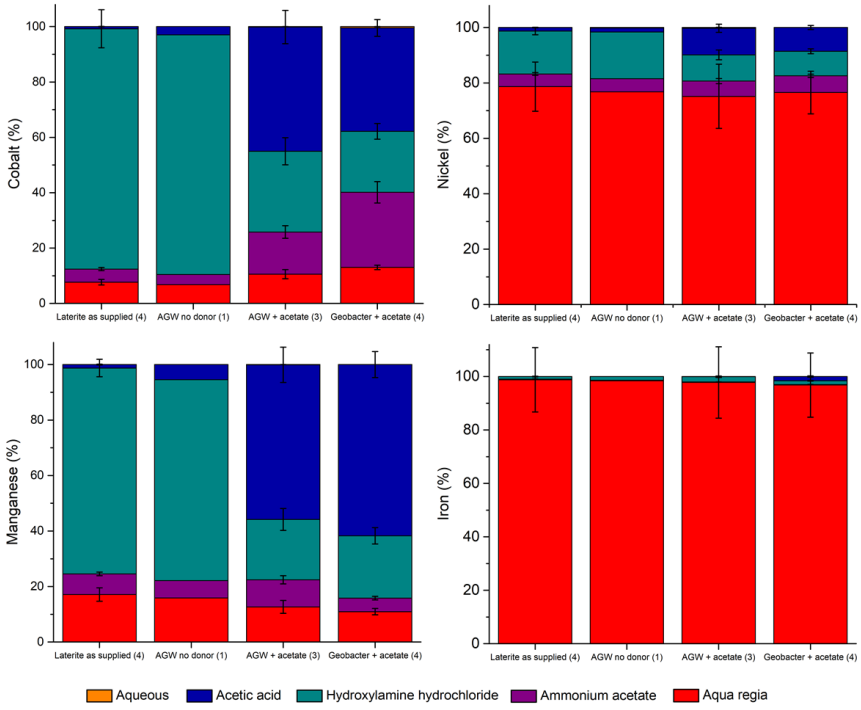


**Figure A1.2**– Analysis of metal distribution in the Acoje laterite using sequential extractions. The laterites as supplied and the no electron donor control (left hand columns) showed very little metals in the acetic-acid extractable “exchangeable” phase. Biostimulation and bioaugmentation (right hand columns) increased the proportion of Co, Mn and Ni associated with the “exchangeable” phase. Numbers in brackets represent the replicates used for the sequential extraction procedure.

**Table A1.2**– Easily recoverable metals in the Natural History Museum laterite samples (sum of aqueous and acetic-acid extractable fractions).

| | Acoje | Çaldağ | Shevchenko |
|---|---|---|---|
| **Cobalt %** | | | |
| Laterite as supplied | 0.78 ± 0.08 | 0.29 ± 0.09 | 0.07 ± 0.01 |
| No electron donor control | 2.99 | 10.98 | 0.63 |
| Biostimulated with acetate | 45.0 ± 6.03 | 29.3 ± 6.94 | 30.7 ± 2.41 |
| Bioaugmented with *G. sulfurreducens* + acetate | 37.8 ± 3.04 | 35.6 ± 4.55 | 29.8 ± 4.72 |
| **Nickel %** | | | |
| Laterite as supplied | 1.26 ± 0.11 | 1.31 ± 0.07 | 0.70 ± 0.05 |
| No electron donor control | 1.65 | 3.22 | 1.35 |
| Biostimulated with acetate | 9.87 ± 1.48 | 8.79 ± 1.13 | 11.1 ± 0.84 |
| Bioaugmented with *G. sulfurreducens* + acetate | 8.59 ± 0.72 | 8.56 ± 1.23 | 10.4 ± 0.96 |
| **Manganese %** | | | |
| Laterite as supplied | 0.51 ± 0.04 | 1.21 ± 0.21 | 1.25 ± 0.14 |
| No electron donor control | 2.38 | 18.61 | 5.48 |
| Biostimulated with acetate | 39.4 ± 3.75 | 68.4 ± 9.59 | 55.8 ± 6.37 |
| Bioaugmented with *G. sulfurreducens* + acetate | 43.1 ± 4.58 | 66.3 ± 8.50 | 61.7 ± 4.69 |
| **Iron %** | | | |
| Laterite as supplied | 0.00 ± 0.00 | 0.00 ± 0.00 | 0.00 ± 0.00 |
| No electron donor control | 0.03 | 0.03 | 0.02 |
| Biostimulated with acetate | 0.24 ± 0.07 | 5.95 ± 0.05 | 0.08 ± 0.01 |
| Bioaugmented with *G. sulfurreducens* + acetate | 1.69 ± 0.03 | 4.80 ± 0.47 | 1.58 ± 0.23 |

#### A1.4.2.3 Changes to the NHM laterite microbial communities during acetate biostimulation

The composition of the microbial community in the acetate-biostimulated sediment microcosms and associated no electron donor controls was characterised by Illumina sequencing for both prokaryotes (all laterites) and fungi (Acoje laterite). The most frequently detected prokaryotic sequences in the Day 0 microbial communities tended to be from the Acidobacteria, Actinobacteria, Bacteriodetes and Proteobacteria, reflecting typical soil environments (Figure A1.3). The abundance of 16S rRNA genes detected in the laterites at Day 0 was low (4.5 – 9.3 fg/g laterite) (Table A1.S2) and considerably lower than values previously reported from Cuban

laterites (Perez et al., 2013); reported in copy number per gram dry sample were in the order of 1 x $10^7$ - 1 x $10^8$, compared to 1.1 x $10^4$ – 2.2 x $10^4$ here.

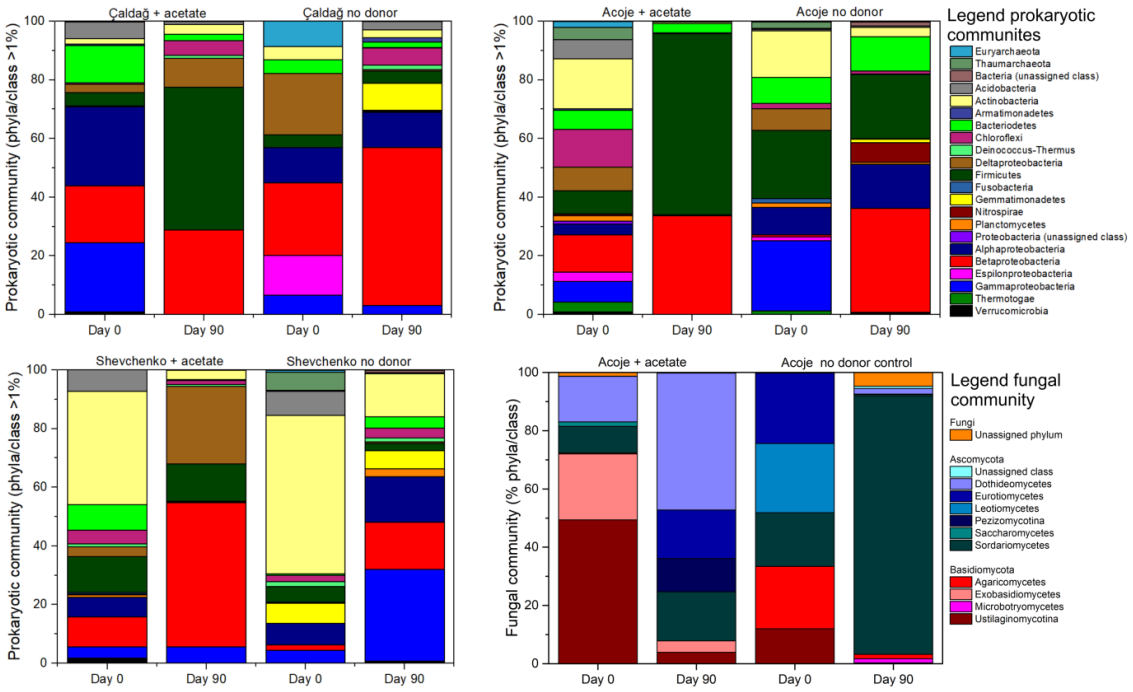


**Figure A1.3**– Microbial phylogenetic diversity of the Natural History Museum laterite sediment microcosms stimulated with acetate compared to the no added electron donor controls.

After 90 days incubation the diversity of the prokaryotic communities had decreased slightly in most microcosms, and was substantially lower in the acetate-amended Acoje and Shevchenko sediments (Table A1.S2), perhaps reflecting their becoming dominated by relatively few OTUs (Table A1.S2). Compared to the Day 0 results the number of OTUs was higher after 90 days incubation in the Acoje and Çaldağ samples, but similar in the Shevchenko sample, with similar trends observed for the acetate-amended samples and no electron donor controls (Figure A1.S7). The abundance of 16S rRNA genes was quantified for the Acoje laterite and increased over 90 days in both the acetate amended microcosms (from 9.3 to 384 fg/g) and the no electron donor control (from 4.5 to 155 fg/g) (Table A1.S2). This indicates that incubation of the sediment microcosms either enhanced prokaryotic growth regardless of electron donor addition, or broke down the laterite substrate to make it more amenable to DNA extraction. Over the course of the experiment the OTUs that had dominated the Day 0 samples had decreased substantially, in most cases to comprise less than 1 % of the corresponding Day 90 samples for both the acetate-

amended microcosms and no electron donor controls. This demonstrates that incubation in sediment microcosms has a significant effect on microbial community composition, which therefore needs to be taken into account when observing the impact of biostimulation by comparing the results against changes in the no electron donor controls (Table A1.S3).

Acetate biostimulation of laterite sediment microcosms caused the Day 90 microbial communities to become dominated by Firmicutes, Betaproteobacteria and Deltaproteobacteria (Figs. A1.3, A1.S9, Table A1.S3). The proportion of sequences closely related to known Mn(IV)/Fe(III)-reducers increased in each laterite (Figure A1.S8). The most frequently detected OTUs in the acetate-amended Acoje and Çaldağ laterites were from the Clostridiales, many of which are obligate anaerobes and spore formers (Vos et al., 2009); sequences assigned to the *Thermincola* genus and most closely related to uncultured bacteria from acetate biostimulation and Fe(III)-reducing environments comprised 40 % of the Acoje and 28 % of the Çaldağ prokaryotic communities. Other notable Fe(III) reducers included sequences most closely related to *Geosporobacter subterraneus* (also from the Clostridiales) which comprised 10 % of the Shevchenko community, and sequences assigned to the *Anaeromyxobacter* genus which comprised 10 % of the Çaldağ and 26 % of the Shevchenko communities.

Sulphate-reducing *Desulfurispora* formed 10 % of the Day 90 Çaldağ prokaryotic community, reflecting the geochemical data which showed that sulphate reduction occurred in this sample (Figure A1.1) but not in the Shevchenko microcosms (Figure A1.S3). In both the Çaldağ and Acoje samples the proportion of sequences assigned to the *Thermincola* genus increased substantially over the course of the experiment. *Thermincola* spp. have been shown to reduce thiosulphate but not sulphate (Zavarzina et al., 2007). The Day 90 Shevchenko prokaryotic community was dominated by sequences most closely related to *Azoarcus anaerobius (*48 %), a strict anaerobe that can respire nitrate (Reinhold-Hurek and Hurek, 2006). OTUs most closely related to the aforementioned Clostridiales groups, *Anaeromyxobacter, Desulfurispora, Thermincola* and *Azoarcus* spp. comprised less than 0.1 % of the Day 90 no added electron donor controls (Table A1.S3), suggesting that their growth was stimulated by the addition of acetate, and that they likely contributed to the reduction of terminal electron acceptors in the laterite sediment microcosms. Indeed, very few sequences closely related to known Fe(III) or sulfur-reducers were found in the Day 90 no added electron donor controls (Figure A1.S8),

demonstrating that acetate amendment was required to stimulate these groups in the laterite sediment microcosms.

Some of the most frequently detected sequences in the Day 90 acetate-amended microcosms were also observed to substantially increase in relative abundance in the no added electron donor controls (Figure A1.S9, Table A1.S3). All these sequences initially comprised less than 0.3 % of the Day 0 communities, indicating that they must have grown during the course of the 90 day experiment, whether or not acetate was added. In the Acoje and Çaldağ sediment microcosms these were primarily from the Burkholderiales and most closely related to *Herbaspirillum* spp., *Cupriavidus* spp. or assigned to the Comamonadaceae; these bacteria were previously found to be associated with sediments with redox boundaries and are known denitrifiers that can couple nitrate reduction to Fe(II) and Mn(II) oxidation. Interestingly, some species of *Herbaspirillum* and *Cupriavidus* spp. are facultative autotrophs (Ding and Yokota, 2004; Pohlmann et al., 2006) and some can fix nitrogen (Kirchhof et al., 2001; da Silva et al., 2012). The *Herbaspirillum* and *Cupriavidus* genera have been identified as a common contaminant of DNA extraction kit reagents and laboratory environments (Salter et al., 2014), but this is considered to be unlikely here due to the very low concentrations detected in the Day 0 samples (Table A1.S3). In the Shevchenko sediment microcosms sequences most closely related to *Pseudomonas stutzeri*, another known denitrifier, were present in both the acetate-amended and the no electron donor control microcosms. Given these increases in sequences closely related to known denitrifiers it is noteworthy that the anaerobic modified freshwater minimal medium used for these sediment microcosms did not contain any added nitrate. Aqueous nitrate was not detected in the Çaldağ or the Shevchenko microcosms (Figs. A1.S2, A1.S3), but it was observed in the Acoje no added electron donor microcosm (Figure A1). Together this suggests that incubation in sediment microcosms caused changes to the microbial community, particularly in groups associated with N cycling. Given that no source of organics was added, this might be linked to autotrophic growth or the metabolism of sediment organic carbon (Table A1.S1). Either way, it is important that this effect is taken into account when interpreting shifts in microbial community composition in future sediment microcosm experiments.

The fungal community was sequenced in the acetate amended microcosms and no electron donor controls for the Acoje laterite, to observe how the fungal community changes in sediment

microcosms, and the impact of anoxic conditions caused by acetate-biostimulation of sediment microbial communities. Relatively few fungal OTUs were present compared to prokaryotes (Table A1.S2). Like the prokaryotic community there were considerable differences between the day 0 microbial community in the acetate-amended microcosm and the no electron donor control (Figure A1.4) likely due to sediment heterogeneity. The five most frequently detected fungal OTUs were typically saprotrophs and/or plant pathogens, or had no close "Type Strain" relatives (Table A1.S4). Sequences most closely related to *Trichoderma, Alternaria, Penicillium* and *Staphylotrichum* species had increased substantially 90 days after acetate amendment, while *Purpureocillium, Pseudallescheria* and *Fusarium* species increased in the no electron donor control. These fungi are all commonly found in soil environments or associated with plants. Interestingly, *Penicillium* spp. have previously been shown to produce organic acids that could successfully bioleach Co and Ni from laterites (Tzeferis et al., 1994; Valix et al., 2001).

### A1.4.3 Piauí laterite microcosms

Samples of the Piauí laterite were biostimulated with glucose to develop metal-reducing conditions, observe the impact on Co and Ni extractability, and to identify the indigenous prokaryotes likely responsible.

A1.4.3.1 Stimulated microbial metal reduction in the Piauí laterite sediment microcosms
Given the lack of metal mobilisation to the aqueous phase observed in the acetate biostimulated NHM laterites, additional electron donors were selected to stimulate the development of metal-reducing conditions in the Piauí laterite. These included an acetate/lactate mix and glucose, chosen for their potential to chelate metals and glucose also to generate acidity during microbial metabolism. Results of initial tests showed that glucose was more effective in stimulating the indigenous microbial community to develop Mn(IV)- and Fe(III)-reducing conditions compared to a mix of acetate and lactate, and also liberated Co and Ni to the aqueous phase (Figure A1.S10). Therefore glucose was selected as the preferred electron donor for the Piauí laterite biostimulation experiments.

Results for sample 'Piauí 23' are shown in Figure A1.4, and similar results were obtained for Piauí 4 (Figure A1.S11). Fe(III) reduction as monitored by the Ferrozine assay only occurred in one of the three Piauí 23 replicates (causing large error bars in the average iron(II) % values Figure

A1.4), and two of the three Piauí 4 replicates, therefore additional microcosms were set up to repeat the analysis for the Piauí 23 laterite (Figure A1.S12). In total, Fe(II) was produced in two of the five Piauí 23 microcosms but not in the other three, demonstrating considerable heterogeneity in the ability of glucose fermentation to stimulate Fe(III) reduction within this laterite sample. The pH decreased from around 8.0 to 6.5 in Piauí 23 and 6.0 in Piauí 4, and the Eh decreased slightly compared to the no electron donor control in Piauí 4.

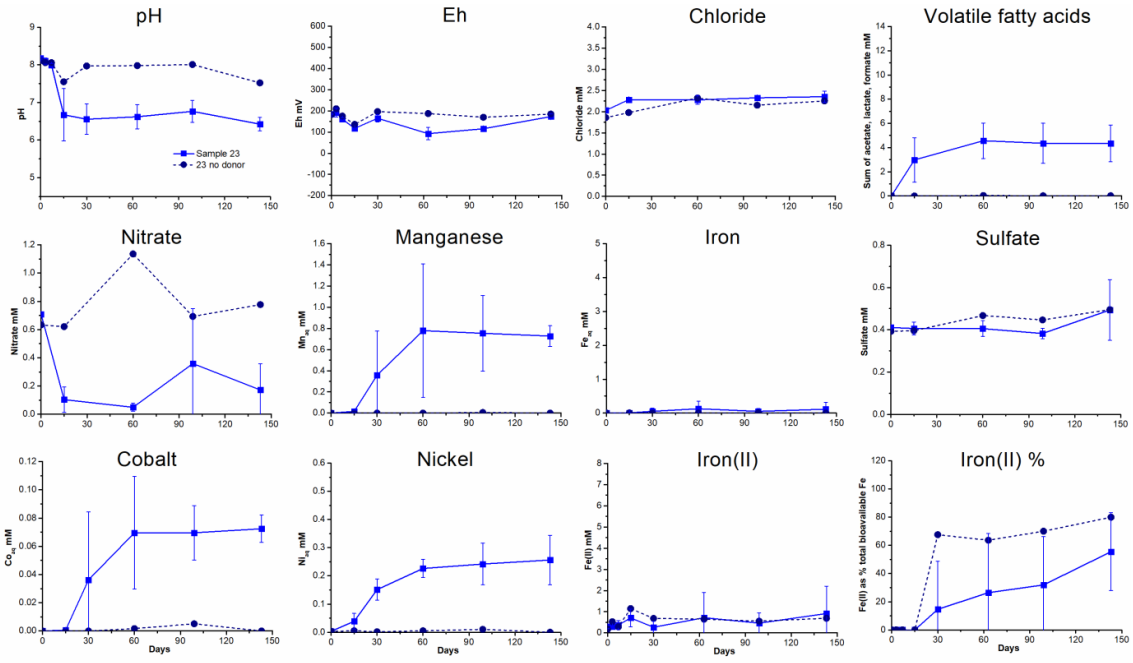


**Figure A1.4**– Geochemical monitoring of the Piauí '23' laterite sediment microcosm that was biostimulated with glucose. Results are the average of three values; error bars ± 1 standard deviation. ND refers to the single no added electron donor controls (dashed lines). Data for the replicate experiment is presented in Figure A1.S10.

Cobalt, manganese and nickel were released to solution in each of the glucose-biostimulated Piauí 4 and Piauí 23 microcosms but not in the no added electron donor controls, indicating that microbial processes were responsible for this metal solubilisation (Figs. A1.4, A1.S11). This is in contrast to the acetate-biostimulated NHM laterites, in which limited Co, Mn and Ni were released to the aqueous phase during microbial metal reduction (Figs. A1.1, A1.S2, A1.S3). A similarly close relationship between Co and Mn geochemistry was previously observed in a bioleaching study of laterites (Smith et al., 2017).

Approximately 0.4 mM nitrate was released to the aqueous phase from the sediment in the Piauí 23 microcosms, but not in the Piauí 4 microcosms where the initial concentrations of 0.3 mM were from the added artificial groundwater (Figs. A1.4, A1.S11). In both cases nitrate concentrations decreased over time likely due to microbial nitrate reduction. Unlike in the NHM laterites, no sulphate was released to the aqueous phase, and the concentration remained constant over the experiment (at ~ 0.4 mM which was added in the artificial groundwater), indicating that microbial sulphate reduction was not stimulated by glucose addition in these systems.

The microbial fermentation of glucose led to the production of volatile fatty acids (VFAs) lactate, acetate and formate. Interestingly the three Piauí 23 microcosms which did not produce Fe(II) had considerably higher VFA concentrations (5.1, 5.3, 7.6 mM), compared to the two in which Fe(II) was generated (2.6 and 3.6 mM). Given that Mn release occurred in all microcosms, likely as Mn(II) following microbial Mn(IV) reduction, it seems that in some cases the microbial community progressed through the classic terminal electron accepting processes of Fe(III) and then towards the start of sulphate reduction (observed in one replicate, Figure A1.S12), while in other cases the microbial community switched towards the breakdown of glucose to generate volatile fatty acids (via fermentation). This trend was not observed in Piauí 4, where the replicate with no Fe(III) reduction had 8.5 mM total VFAs compared to the two where Fe(II) was generated which had 8.8 and 13.2 mM total VFAs. It is likely that these differences are due to heterogeneities in particular aliquots of sediment, and also across the laterite deposit, which may have implications for resource processing. The replicate Piauí 23 samples were additionally monitored at Day 264, at this point no VFAs were detected.

#### A1.4.3.2 Sequential extractions to investigate metal fate in the Piauí laterite sediment microcosms

To investigate the distribution of metals in the solid phase, sequential extractions were performed on the laterite as supplied and on samples of the sediment microcosms 143 days after biostimulation with glucose. Similar results were obtained for both the Piauí samples (Figs. A1.5, A1.S13), showing that biostimulation of the sediment microbial communities with glucose transformed a significant proportion of metals into the acetic acid-extractable “exchangeable phase”, broadly comparable to the results for the NHM laterites.

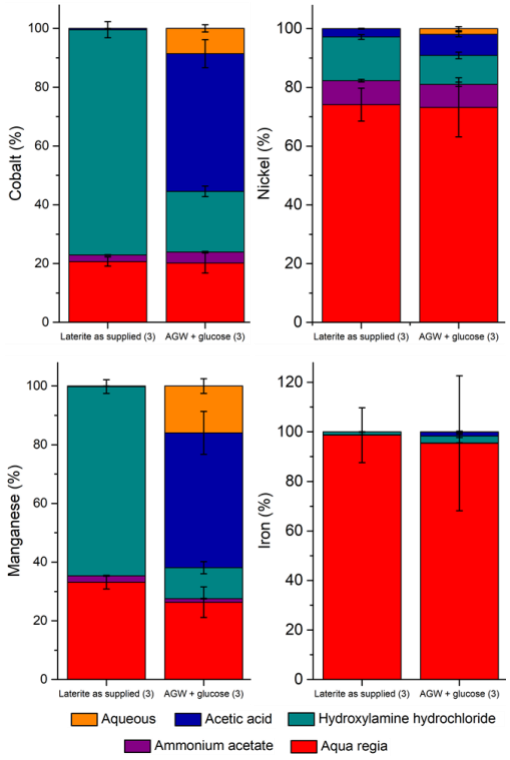


**Figure A1.5**– Analysis of metal distribution in the Piauí 23 laterite using sequential extractions. (a) cobalt. (b) manganese. (c) nickel. (d) iron. The laterite as supplied (left hand column) showed very little metals in the acetic-acid extractable “exchangeable” phase. Biostimulation of the sediment microbial community with glucose (right hand column) increased the proportion of Co, Mn and Ni associated with the acetic-acid extractable “exchangeable” phase. Numbers in brackets represent the number of replicates used for the sequential extraction procedure.

The proportion of Co associated with easily recoverable phases in the laterites (that is, the aqueous content plus the acetic-acid extractable “exchangeable” fraction) after biostimulation with glucose increased from < 0.5 % to up to 64 % while Ni increased from < 5 % to up to 12 % (Table A1.3). Easily recoverable Mn also increased from < 0.5 % to up to 72 %, while easily recoverable Fe increased from 0 % to up to 9 %. Around 9 % of the Fe was transformed into an easily recoverable phase in the Piauí 4 sample, but not in the Piauí 23 sample; additional data would be required to fully characterise this heterogeneity within the deposit prior to designing a laterite processing strategy.

**Table A1.3**– Easily recoverable metals in the Piauí laterites samples (sum of aqueous and acetic-acid extractable fractions).

| | Piauí 4 | Piauí 23 |
|---|---|---|
| **Cobalt %** | | |
| Laterite as supplied | 0.36 ± 0.02 | 0.43 ± 0.02 |
| Biostimulated with glucose | 63.5 ± 2.62 | 55.4 ± 4.94 |
| **Nickel %** | | |
| Laterite as supplied | 4.94 ± 0.40 | 2.83 ± 0.15 |
| Biostimulated with glucose | 11.5 ± 0.56 | 9.11 ± 1.06 |
| **Manganese %** | | |
| Laterite as supplied | 0.25 ± 0.03 | 0.19 ± 0.01 |
| Biostimulated with glucose | 71.6 ± 6.50 | 61.9 ± 7.73 |
| **Iron %** | | |
| Laterite as supplied | 0.00 ± 0.00 | 0.00 ± 0.00 |
| Biostimulated with glucose | 9.08 ± 1.71 | 1.66 ± 0.37 |

#### A1.4.3.3 Changes to the Piauí microbial community during glucose biostimulation

Given the heterogeneity in Fe(III) reduction observed in the geochemical data, the prokaryotic microbial community was characterised in two of the Piauí 23 glucose-stimulated sediment microcosms ('Sample A' where Fe(II) was generated and partial sulphate reduction observed, and 'Sample B' where no Fe(II) was generated) and an associated no electron donor control. It was not possible to successfully extract DNA from the original biostimulation experiment shown in Figure A1.4, but after optimising the DNA extraction protocols by increasing the amount of bead beating, sufficient DNA was extracted from the replicate biostimulation experiment shown in Figure A1.S12 at the 0, 28 and 76 day time points. Overall, relatively few prokaryotic OTUs were found in the Piauí laterite sediment microcosms (Table A1.S2, Figure A1.S14) and the Shannon diversities were lower than in the NHM laterites (Table A1.S2). This may reflect the difficulties in extracting DNA from these challenging iron oxide-rich samples. The abundance of 16S rRNA genes detected in the Day 0 samples was slightly higher than in the NHM laterites (32 – 49 fg/g sediment, Table A1.S2), but again considerably lower than the values previously reported for the Cuban laterites by Perez et al. (2013) (copy number per gram dry sample $6.6 \times 10^4$ - $1 \times 10^5$ here, compared to $1 \times 10^7$ - $1 \times 10^8$). Similar to the results for the Acoje laterite, the abundance of 16S rRNA genes detected increased over the course of the experiment in both the glucose biostimulated microcosm (from 49 to 2940 fg/g laterite), and in the no added electron donor control

(from 32 to 110 fg/g laterite), showing incubation in sediment microcosms increased the amount of DNA, and that glucose biostimulation caused significant growth of prokaryotes. At the phylum/class level the Day 0 communities in both of the glucose-stimulated microcosms were dominated by Firmicutes (Figure A1.6) in particular, sequences most closely related to *Paenibacillus* spp., as well as Actinobacteria, Cyanobacteria and Alphaproteobacteria. The no added electron donor control contained far fewer Firmicutes.

At the OTU level the response of the two glucose stimulated microcosms was somewhat different. The composition of the microbial community in Sample A was broadly similar at Day 28 and Day 76, and dominated by sequences most closely related to *Bacillus soli* and *Paenibacillus* spp., which together made up 83 % of the prokaryotic community at Day 76 (Table A1.S5). Both *Bacillus* and *Paenibacillus* spp. are Gram positive spore-forming facultative anaerobes typically associated with soils and the rhizosphere. *Paenibacillus* spp. are known Mn(IV) and Fe(III)-reducers (Petrie et al., 2003; Rowe et al., 2017), and the dominant OTU in Sample A was most closely related to an Fe(III)-reducing isolate from Brazilian and Cameroonian soil (Loyaux-Lawniczak et al., 2019) (Table A1.S5). *Bacillus soli* is a facultative anaerobic capable of nitrate reduction (Heyrman et al., 2004). Neither the *Paenibacillus* nor the *Bacillus* OTUs were present in the Day 76 no added electron donor control. Although some sulphate reduction appeared to occur in Sample A (Figure A1.S12), only a tiny amount of sequences closely related to known sulphate-reducers (0.01 % *Desulfitobacterium* spp.) were identified in the microbial community.

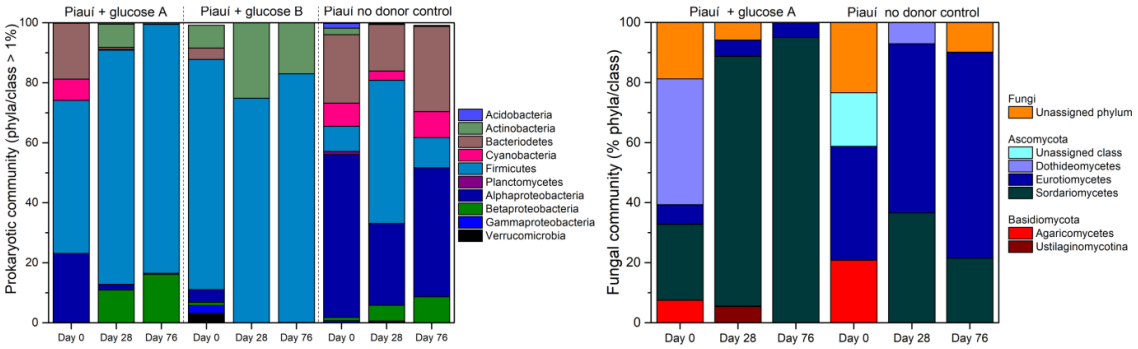


**Figure A1.6**– Microbial phylogenetic diversity of the Piauí laterite sediment microcosms stimulated with glucose compared to the no added electron donor controls, prokaryotic community (left), fungal community (right).

In contrast to Sample A, the Day 76 results for Sample B showed the proportion of sequences most closely related to *Bacillus* spp. decreased from 55 % to 18 % and *Paenibacillus* spp. from 19 % to 3 %, while those most closely related to *Desulfitobacterium* spp. increased from < 0.1% to 61 % (Table A1.S5). *Desulfitobacterium* spp. are strict anaerobes that can use a wide range of electron acceptors including nitrate, metals, humic acids and sulphate (Villemur et al., 2006; Zhang et al., 2016). The dominant OTU in Sample B was most closely related to *Desulfitobacterium metallireducens* which is known to reduce Mn(IV), Fe(III) and thiosulphate, as well as fermenting pyruvate, but it is not able to reduce nitrate or sulphate (Villemur et al., 2006). This is interesting given that limited iron(III) reduction and increased VFA production were observed in this sample, and suggests that *Desulfitobacterium* spp. may have primarily employed a fermentative metabolism in this sample. *Desulfitobacterium* spp. were not present in the Day 76 no added electron donor control.

Like for the NHM laterites, the Day 76 control microcosm contained some similar OTUs to the biostimulated microcosms, in this case most closely related to *Porphyrobacter*, *Flavobacterium*, and *Herbaspirillum* spp. from freshwater environments, the rhizosphere, and from studies of phototrophy and cyanobacteria associations (Table A1.S5). However, most of these were also present in the Day 0 Piauí microcosms, suggesting that they remained present throughout the course of the experiment rather than their growth being stimulated by incubation in sediment microcosms.

Relatively few fungal OTUs were detected during the Piauí 23 microcosm experiment (Table A1.S2). The five most frequently detected fungal OTUs were typically saprotrophs and/or plant pathogens, or had no close Type Strain relatives (Table A1.S6). It appeared that glucose biostimulation favoured the growth of fungi closely related to *Fusarium* spp., which made up more than 80 % of the day 28 and day 76 glucose-amended microcosms (Figure A1.6). Sequences most closely related to *Alternaria, Penicillium* and *Talaromyces* species increased over time in the no electron donor control. Interestingly, *Alternaria* and *Penicillium* species were found to be stimulated by acetate amendment in the Acoje laterite (Table A1.S4), but given the low quantity of total organic carbon (0.05 %) in the Piauí laterite their increase in proportion in the Piauí control is unexplained. Again, the potential for *Penicillium* spp. to bioleach Co and Ni from laterites has previously been demonstrated (Tzeferis et al., 1994; Valix et al., 2001).

### A1.4.4 Solid phase characterisation in the laterites before and after incubation in sediment microcosms

A range of different techniques were applied to characterise the laterites as supplied and after incubation in sediment microcosms, and to observe the impact of the development of microbially reducing conditions on the laterite mineralogy and metal speciation.

#### A1.4.4.1 XRD

Changes in mineralogy in the laterites before and after the development of reducing conditions were examined using XRD. Goethite was present in the XRD patterns of all the laterites at the start and end of the experiment. Mn oxides were not apparent in the XRD patterns, but this was expected given the Mn content of the laterites was < 1 %. For the most part where haematite, clinochlore and hornblende were identified in the XRD patterns in the laterites as supplied, they were absent from the corresponding biostimulated and bioaugmented sediment microcosms, suggesting the development of microbially reducing conditions caused them to decrease to less than 5 % by mass (Figure A1.S16). Maghemite was observed in all the biostimulated and bioaugmented samples, but its absence in the Acoje and Çaldağ laterites as supplied suggests it may have formed during the development of reducing conditions. Kaolinite was only observed in the biostimulated and bioaugmented Piauí 23 and Shevchenko sediment microcosms, and siderite was only observed in the bioaugmented Acoje sediment microcosm. Overall this indicates that the development of reducing conditions in sediment microcosms principally affected the Fe-bearing minerals haematite, clinochlore and hornblende. Maghemite, kaolinite and siderite appeared post-reduction, while goethite remained present throughout the experiment.

#### A1.4.4.2 TEM and SAED

On the macro scale, the laterites appeared visibly different after incubation in microbially active sediment microcosms (Figure A1.S4), with less fine grained Fe oxide present and marked clumping in sediment grains. Therefore selected laterites were examined using TEM and SAED to look for changes in sediment morphology and mineralogy occurring at the nanoscale after incubation in sediment microcosm experiments.

#### A1.4.4.2.1 Acoje

The Acoje laterite as supplied mostly contained angular, elongate lath-shaped particles (0.76 ± 0.38 µm in length, N = 9 measured), and some more spherical particles (0.82 ± 0.20 µm in diameter, N = 5). The SAED varied between broad rings from poorly crystalline/nanocrystalline material and individual spot patterns indicating the presence of larger single crystals (Figure A1.S17). The EDS spectra indicated the dominance of an Fe-oxide phase, with a relatively small Si peak.

After incubation in microbially-active sediment microcosms the images showed the laterite mostly comprised of slightly smaller more electron dense spherical particles (0.46 ± 0.18 µm in diameter, N = 19) with fewer, similarly sized needle/oblong shaped particles (0.66 ± 0.40 µm in length, N = 8). The smaller, more electron dense spherical particles were absent in the laterite as supplied, suggesting they were formed as a result of biostimulation. The microbially-reduced sediment was mostly nanocrystalline as indicated by the rings of spots present in the SAED. The d-spacings were calculated and compared to values for the minerals identified by XRD, but it was not possible to make any positive identifications. The EDS spectra showed the Fe peak was smaller than the O peak while the Si peak had increased in proportion substantially. Together this may indicate that microbial transformation of Fe minerals had occurred.

#### A1.4.4.2.2 Piauí

The Piauí laterite as supplied contained small particles (0.84 ± 0.33 µm in diameter, N = 8) and elongate laths (0.62 ± 0.35 µm in length, N = 12) that appeared similar to the characteristic shape of goethite (Cutting et al., 2009). The SAED was dominated by concentric rings made of spots and more diffuse rings indicating the presence of both nanocrystalline and poorly ordered material (Figure A1.17). The EDS suggested it comprised a mixture of Fe oxide and Mg silicate minerals.

After incubation in sediment microcosms the sediment appeared denser, with similarly sized elongate laths (0.69 ± 0.40 µm in length, N = 12) and spherical particles (0.86 ± 0.44 µm in diameter, N = 8). The grid pattern of spots in the SAED indicated diffraction from large single crystals and some concentric rings made of spots indicating nanocrystalline material. This suggests that in this sample biostimulation may have transformed some of the poorly ordered material into more crystalline phases. Again it was not possible to make any positive mineral

identifications from the measured d-spacings. The EDS showed the Fe peak appeared larger proportionally relative to the O peak post-reduction, with the Mg and Si peaks of slightly lower proportions.

#### A1.4.4.3 XAS

Samples were analysed by XAS to determine the speciation of Co, Ni, Fe and Mn before and after biostimulation. Fe and Ni concentrations were sufficiently high to obtain $L_{II}$ and $L_{III}$ edge XAS, while concentrations of Co and Mn were too low for this technique. Additional beam time allowed *K*-edge XAS to be collected for Co and Ni, with the concentrations of Ni sufficiently high to collect EXAFS data.

##### A1.4.4.3.1 Iron speciation

The iron $L_{II}$ and $L_{III}$ edge XAS were very similar for the laterites as supplied, and after incubation in biostimulated sediment microcosms (Figure A1.7). No significant XMCD signal was measurable from any of the samples. Comparing the spectra with the known Fe(III) standards ferrihydrite, goethite and hematite and the mixed Fe(II)/Fe(II) standard magnetite (Joshi et al., 2018) showed the samples had the same spectral shape as the pure Fe(III) standards, particularly at the diagnostic $L_3$ edge. In addition, the trough between the two positive peaks of the $L_3$ edge was greater in the samples than in the ferrihydrite standard and more similar in size to goethite (hematite was not considered to be as relevant as goethite was identified to be present by XRD).

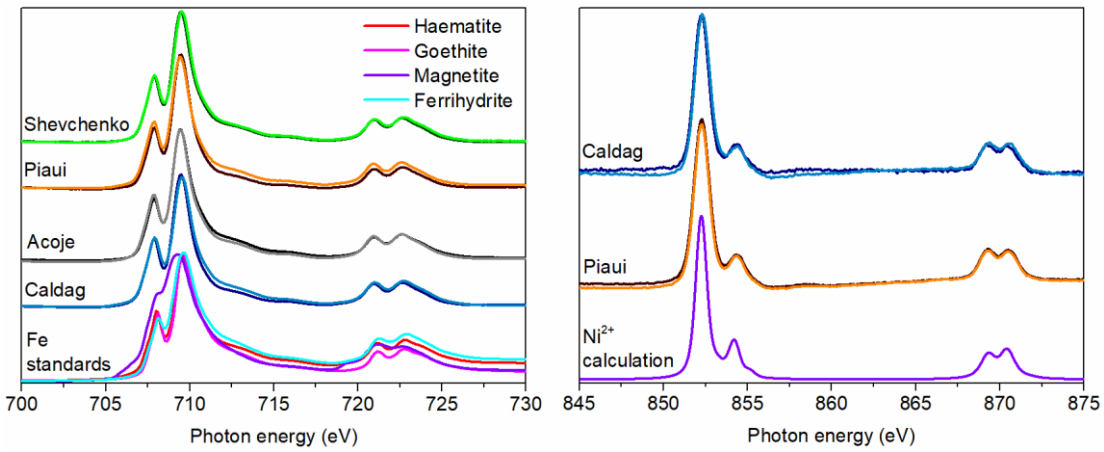


**Figure A1.7**– Fe (left) and Ni (right) $L_{II}$ and $L_{III}$ edge spectra for the laterites as supplied (darker colours) and at the end of the sediment microcosm study (lighter colours) compared to standards;

metal speciation appeared the same in the laterites as supplied and in the microbially reduced sediments.

#### A1.4.4.3.2 Nickel speciation

Nickel speciation was determined using both $L_{II}$ and $L_{III}$ edges and *K*-edge XAS. Nickel $L_{II}$ and $L_{III}$ edge spectra could only be obtained for the Çaldağ and the Piauí laterites, despite the Çaldağ laterite having the lowest Ni content. The spectra for both laterites closely resembled a known calculated standard for Ni(II) in octahedral coordination (Figure A1.7) (Laan and Kirkman, 1992; Coker et al., 2008). Ni *K*-edge XANES spectra were also similar for all samples, both before and after biostimulation (Figure A1.8) and indicative of Ni in octahedral coordination in goethite; the position of the main peak (~8349 eV) was close to published values for Ni in goethite (Landers et al., 2011), and the presence of a small pre-edge feature at 8333 eV indicated that Ni was in octahedral coordination with minimal distortion (Landers et al., 2011).

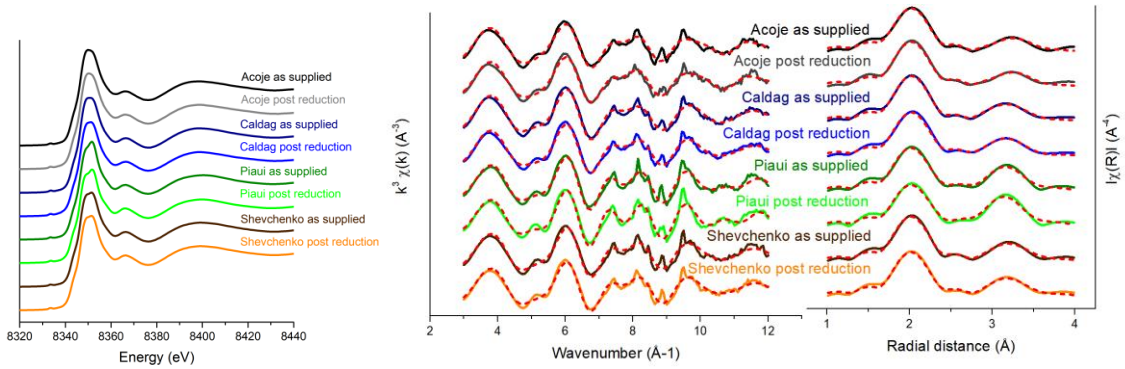


**Figure A1.8**– Ni K-edge XANES (left), EXAFS (centre) and Fourier transform of EXAFS (right) before and after microcosm experiments. Best fits for the EXAFS are shown as red dashed lines and were obtained for Ni substituted in goethite.

Three models were tested to fit the Ni *K*-edge EXAFS informed by the literature on Ni speciation in other laterites; Ni in Mg-phyllosilicates (Roqué-Rosell et al., 2017), Ni in goethite (Manceau et al., 2000; Landers et al., 2011) and Ni in Mn-oxides (Roqué-Rosell et al., 2010). The best fitting parameters were obtained for Ni in goethite (Figure A1.8, Table A1.S7), with 6 Ni-O at 2.05 Å, 2.6 – 3.9 Ni-Fe at 3.07 Å (edge-sharing) and 1.5 – 5.5 Ni-Fe at 3.49 Å (corner-sharing). These values closely reflected published values (Manceau et al., 2000; Landers et al., 2011) and Ni substituted in goethite corresponds with the high Fe contents measured by XRF, and the presence of goethite

in the XRD patterns (Table A1.S1). Differences in the coordination numbers fitted for Ni-Fe between the laterites suggests substitution of Ni into different positions in the goethite crystal lattice. Although reasonable fitting parameters were obtained for Ni in Mn-oxides, this model had 6 Mn atoms surrounding Ni which was not considered physically-realistic given the laterites contained 1.5 to 4.4 times more Ni than Mn. Ni in Mg-phyllosilicates had significantly worse fitting parameters.

#### A1.4.4.3.3 Cobalt speciation

The Co *K*-edge XANES spectra for the laterites as supplied mostly closely resembled the Co-doped $MnO_2$ standard (Figure A1.9), and the position of the main peak (7730 eV) was similar to reported values for Co(III)OOH (Dublet et al., 2017). Although under most environmental conditions Co(II) is thermodynamically favoured, in the presence of Mn(IV)-oxides it has been shown to sorb and be rapidly (within 12 hours) oxidised to Co(III) (Tanaka et al., 2013; Simanova and Peña, 2015). Cobalt(III) bearing Mn(III/IV)-oxides are also known to form during weathering of laterites (Dublet et al., 2017). The XANES spectra for the Çaldağ and Shevchenko laterites as supplied show a broader peak profile around 4 – 5 eV in width spanning the range of values for Co(II) and Co(III), and suggesting that they contained a mixture of Co(II) and Co(III). Similar profiles were observed for less-weathered laterites found at depth and interpreted as containing Co present in olivine and serpentinite (Dublet et al., 2017). Post-reduction, the main Co peak shifted towards lower energies in each laterite (Figure A1.9), indicating reduction of Co(III) to Co(II), which has a main absorption edge at 7725 eV (Dublet et al., 2017).

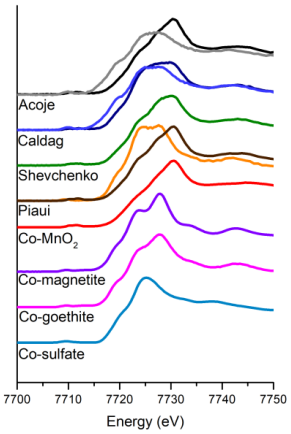


**Figure A1.9**– Co K-edge XANES of laterites as supplied (darker colours) and at the end of the sediment microcosm study (lighter colours) compared to standards. The peak of Co-doped $MnO_2$

at 7730 eV represents Co(III) and Co-sulphate at 7725 eV represents Co(II), similar to the standards reported in Dublet et al. (2017). Co speciation in the doped magnetite and goethite standards is similar, and resembles the Co-serpentinite and Co-olivine reported in Dublet et al. (2017).

## A1.5 Discussion

### A1.5.1 Microbial metal reduction in sediment microcosms

Metal-reducing conditions were stimulated in the Natural History Museum laterite sediment microcosms by adding acetate, or acetate and *Geobacter sulfurreducens*, leading to Mn(IV), Fe(III) and in some cases, sulphate reduction. Although this did not cause the liberation of Co and Ni to the aqueous phase, sequential extractions showed that the amount of easily recoverable Co increased from < 1 % to up to 45 % (closely mirroring Mn behaviour) and Ni from < 1.5 % to up to 11 %. Sequencing of the prokaryotic community showed that the addition of acetate stimulated the growth of indigenous bacteria closely related to known nitrate, Mn(IV)/Fe(III) and sulphate/thiosulphate reducers from the Clostridiales, *Anaeromyxobacter, Desulfurispora, Thermincola* and *Azoarcus* spp.

Metal-reducing conditions were also stimulated in the Piauí laterite sediment microcosms by adding glucose, which led to Mn(IV) reduction and liberation of Co and Ni. Sequential extractions showed the amount of easily recoverable Co increased from < 0.5 % to up to 64 % (closely mirroring Mn behaviour) and Ni from < 5 % to up to 12 %. Fe(III) reduction was observed in two of the five Piauí 23 replicates, demonstrating heterogeneity in the sediment, which was also reflected in the composition of the prokaryotic communities. Known Mn(IV)/Fe(III) reducers (e.g. *Paenibacillus*) were initially present in all of the samples. In Sample A the proportion of *Paenibacillus* remained high at Day 76 (unlike in the no electron donor control), suggesting it might have been responsible for metal reduction, but in Sample B glucose biostimulation appeared to promote fermentative metabolisms which generated an increased quantity of VFAs rather than Fe(II).

### A1.5.2 The impact of microbial metal reduction on laterite mineralogy

All four laterites were dominated by goethite, both before and after incubation in sediment microcosms. It appeared that microbial Fe(III)-reduction did not occur substantially in these experiments, with iron predominantly present as Fe(III) both before and after incubation in sediment microcosms (Figs. A1.7, A1.S16). Most of the signal from *L*-edge XAS occurs from the surface 3 - 4 nm of a sample (Byrne et al., 2013), and therefore any reduced Fe(II)-containing minerals ought to have been identifiable using this technique. Previous work showed both XRD patterns and TEM images for immature and crystalline goethite were similar before and after incubation with *G. sulfurreducens*, suggesting goethite is relatively recalcitrant to microbial Fe(III)-reduction (Cutting et al., 2009). Moreover, the sequential extraction data showed that 97 – 99 % of Fe in the laterites as supplied was present in the aqua regia extractable "residual" phase (Figs. A1.2, A1.5, A1.S5, A1.S6) and therefore was unlikely to be bioavailable. Although small increases in the acetic-acid extractable "exchangeable" phase were observed in the laterites after incubation in sediment microcosms, and the proportion of Fe(II) increased during the course of the experiment (Figs. A1.1, A1.4, A1.S1, A1.S2), overall the mineralogy remained dominated by the large quantities of goethite present.

The Ni $L_{II}$ and $L_{III}$ edge and *K* edge XAS spectra for each laterite were very similar before and after the development of metal-reducing conditions (Figs. A1.7, A1.8), demonstrating that (in the solid phase) Ni remained in association with the microbiologically-recalcitrant goethite throughout the course of the experiment.

The Co *K* edge XAS spectra showed that it was initially present as Co(III), likely incorporated into Mn-oxide minerals that formed < 1.5 % (w/w) of the laterites (Figure A1.9). After reducing conditions were stimulated by the addition of an organic substrate, Co was shown to be reduced to Co(II) or a mixed Co(II)/Co(III) phase. This corresponds with the sequential extraction data that showed a significant proportion of Co was transformed from a hydroxylamine hydrochloride extractable "reducible" form to an acetic acid extractable "exchangeable" phase, considered to represent the sorbed fraction (Figs. A1.2, A1.5, A1.S5, A1.S6, A1.S13). The mechanism by which this occurred during the development of reducing conditions in sediment microcosms is likely to be linked to the microbial reduction of Mn(IV) oxides to Mn(II), releasing Co(III) from the crystal

structure, which then sorbs back to the laterite as Co(II) (Tanaka et al., 2013). It was not possible to infer from this dataset whether Co(III) was reduced to Co(II) as a result of thermodynamic equilibration upon dissolution of Mn-oxides via microbial Mn(IV) reduction, or whether direct microbial reduction of Co(III) had occurred (previously observed by Gorby *et al.*, 1998).

### A1.5.3 Implications for Co and Mn biogeochemical cycling

Co and Mn concentrations were positively correlated in the laterites (Figure A1.S1) and Co was likely present as Co(III) incorporated into Mn oxides (Figure A1.9). This corresponds with previous data showing Co being associated with Mn-oxide enriched horizons in laterites (Elias et al., 1981; Yongue-Fouateu et al., 2006; Dublet et al., 2017), and in soil environments (Taylor and McKenzie, 1966; Uren, 2013).

Here we stimulated the natural microbial community in the laterites to develop metal-reducing conditions by adding acetate or glucose. The results showed very similar geochemical behaviour for Co and Mn; neither metal was released to solution in the acetate biostimulated NHM laterites (Figs. A1.1, A1.S2, A1.S3), while in the glucose biostimulated Piauí laterite the time series plots showed that Co and Mn were released to the aqueous phase at remarkably similar rates, indicating a close association and that the mechanism of Co release was likely to be microbial Mn(IV) reduction (Figure A1.4). The distributions of Co and Mn in the laterites observed using sequential extractions were again very comparable (Figs. A1.2, A1.5, A1.S5, A1.S6) both before and after microbial metal reduction. Together, these results show that redox cycling plays a dynamic and defining role in controlling the fate of Co and Mn in these sediment systems.

### A1.5.4 Applying microbial metal reduction to bioprocess laterites

Biostimulation of laterites with acetate or glucose dramatically increased the proportion of easily recoverable Co (and to a lesser extent Ni), without transforming the majority of the iron oxides. Therefore a new two-step bioprocessing strategy to recover Co from laterite ores is proposed. First, the laterites should be treated with organic substrates such as glucose or acetate (or potentially similar simple sources of cheaply available or waste carbon) and left for a period of time to allow metal-reducing conditions to develop, after which they should be rinsed with acetic acid. This will mobilise up to 64 % of the Co, with minimal dissolution of Fe. Different organic substrates may stimulate respirative or fermentative metabolisms; which although both capable

of mobilising Co, should be taken into account when assessing their cost-effectiveness. It appears that glucose biostimulation may be a more promising for use in a laterite processing technique compared to acetate biostimulation as it generated both aqueous and “exchangeable” Co and Ni, and extracted a higher proportion of metals from the laterite.

The results presented here showed that up to 64 % of the Co present in these laterites could be recovered by this process. Further benefits are gained from the minimal amount of Fe-based crystalline minerals mobilised during the process, which will negate the need to separate Fe from the processed product, and lessen the requirement for dealing with large quantities of associated iron oxide wastes. Additional work is ongoing to assess the suitability of this two-step laterite treatment process under flowing conditions that more closely represent the conditions that would be employed in an industrial scenario.

### A1.6 Conclusions

Microbial metal reduction was stimulated in laterites using organic substrates. Large quantities of Co were transformed from a ‘reducible’ phase to a more labile ‘exchangeable’ phase, which was leachable using acetic acid. The organic substrates stimulated the growth of indigenous metal reducing prokaryotes which were likely responsible for Mn(IV) reduction and Co mobilisation. Increases in the proportion of fungi that produce beneficial organic acids previously shown to leach Co and Ni were also observed, and could also play a role in metal solubilisation. These results are compelling given that similar behaviour observed in four laterites (Acoje, Çaldağ, Piauí and Shevchenko) from different continents. In addition to generating new data on how the solubility of Co is controlled during microbial redox cycling in lateritic soils, this also informs a new two-step bioprocessing strategy that is proposed to recover Co from laterites.

The results presented here demonstrate that Co can be biogeochemically cycled in sediments. Co and Mn association has previously been observed in many different environments, and here Co behaviour was closely linked to that of Mn, suggesting Co mobility will consequently be controlled by Mn(IV)-reducing and Mn(II)-oxidising bacteria. These groups are ubiquitous in sediments, and indeed were observed to be present in each of the four laterites analysed. This

highlights the important role of microbial processes in the weathering of laterites, and their contribution to the enrichment of Co within Mn oxide minerals.

### A1.7 Supplementary material

Supplementary material comprising Tables A1.S1 – A1.S7 and Figures A1.S1 – A1.S17 is provided online.

### A1.8 Funding

This work was supported by the Natural Environment Research Council (CoG3 NE/M011518/1). Beamtime at beamline I20 was funded by grants SP16735 and SP17313 from Diamond Light Source. This research used resources of the Advanced Light Source, which is a DOE Office of Science User Facility under contract no. DE-AC02-05CH11231.

### A1.9 Acknowledgements

We are very grateful to Paul Lythgoe, Alastair Bewsher, John Waters, Heath Bagshaw and Roseanna Byrne (University of Manchester) for analytical support with ICP-AES, ion chromatography, XRF, TOC, XRD, TEM and qPCR. We thank Sulaiman Mulroy (University of Manchester) for collecting the Co XANES spectra at Diamond Light Source, and Shusaka Hayama (I20, Diamond Light Source) and Alpha N'Diaye (6.3.1, Advanced Light Source) for their advice on how to use their beamlines. We would additionally like to thank Mike and Ann Oxley (Brazilian Nickel) for allowing LN to collect samples from the Piauí deposit, and the Natural History Museum for access to their sample collection.

### A1.10 References

Bacon J. R. and Davidson C. M. (2008) Is there a future for sequential chemical extraction? *Analyst* 133, 25–46.

British Geological Survey (2009) *Cobalt*. British Geological Survey, Keyworth, Nottingham.

Brown A. E., Muthumeenakshi S., Sreenivasaprasad S., Mills P. R. and Swinburne T. R. (1993) A PCR primer-specific to *Cylindrocarpon heteronema* for detection of the pathogen in apple wood. *FEMS Microbiol. Lett.* 108, 117–120.

Byrne J. M., Coker V. S., Moise S., Wincott P. L., Vaughan D. J., Tuna F., Arenholz E., Van Der Laan G., Pattrick R. A. D., Lloyd J. R. and Telling N. D. (2013) Controlled cobalt doping in biogenic magnetite nanoparticles. *J. R. Soc. Interface* 10, 20130134.

Caporaso J. G., Kuczynski J., Stombaugh J., Bittinger K., Bushman F. D., Costello E. K., Fierer N., Peña A. G., Goodrich J. K., Gordon J. I., Huttley G. A., Kelley S. T., Knights D., Koenig J. E., Ley R. E., Lozupone C. A., McDonald D., Muegge B. D., Pirrung M., Reeder J., Sevinsky J. R., Turnbaugh P. J., Walters W. A., Widmann J., Yatsunenko T., Zaneveld J. and Knight R. (2010) QIIME allows analysis of high-throughput community sequencing data. *Nat. Methods* 7, 335–336.

Caporaso J. G., Lauber C. L., Walters W. A., Berg-Lyons D., Huntley J., Fierer N., Owens S. M., Betley J., Fraser L., Bauer M., Gormley N., Gilbert J. A., Smith G. and Knight R. (2012) Ultra-high-throughput microbial community analysis on the Illumina HiSeq and MiSeq platforms. *ISME J.* 6, 1621–1624.

Caporaso J. G., Lauber C. L., Walters W. A., Berg-Lyons D., Lozupone C. A., Turnbaugh P. J., Fierer N. and Knight R. (2011) Global patterns of 16S rRNA diversity at a depth of millions of sequences per sample. *Proc. Natl. Acad. Sci. USA* 108, 4516–4522.

Chen G., Yang H., Li H. and Tong L. (2016) Recovery of cobalt as cobalt oxalate from cobalt tailings using moderately thermophilic bioleaching technology and selective sequential extraction. *Minerals* 6, 67.

Coker V. S., Bell A. M. T., Pearce C. I., Pattrick R. A. D., van der Laan G. and Lloyd J. R. (2008) Time-resolved synchrotron powder X-ray diffraction study of magnetite formation by the Fe(III)-reducing bacterium *Geobacter sulfurreducens*. *Am. Mineral.* 93, 540–547.

Crowe S. A., O'Neill A. H., Weisener C. G., Kulczycki E., Fowle D. A. and Roberts J. A. (2007) Reductive dissolution of trace metals from sediments. *Geomicrobiol. J.* 24, 157–165.

Cutting R. S. S., Coker V. S. S., Fellowes J. W. W., Lloyd J. R. R. and Vaughan D. J. J. (2009) Mineralogical and morphological constraints on the reduction of Fe(III) minerals by *Geobacter sulfurreducens*. *Geochim. Cosmochim. Acta* 73, 4004–4022.

Ding L. and Yokota A. (2004) Proposals of *Curvibacter gracilis* gen. nov., sp. nov. and *Herbaspirillum putei* sp. nov. for bacterial strains isolated from well water and reclassification of [*Pseudomonas*] *huttiensis*, [*Pseudomonas*] *lanceolata*, [*Aquaspirillum*] *delicatum* and [*Aquaspirillum*] *autotrophicum* as *Herbaspirillum huttiense* comb. nov., *Curvibacter lanceolatus* comb. nov., *Curvibacter delicatus* comb. nov. and *Herbaspirillum autotrophicum* comb. nov.. *Int. J. Syst. Evol. Microbiol.* 54, 2223–2230.

Downward L., Booth C. H., Lukens W. W. and Bridges F. (2007) A variation of the F-Test for determining statistical relevance of particular parameters in EXAFS fits. *AIP Conf. Proc.* 882, 129–131.

Dublet G., Juillot F., Brest J., Noël V., Fritsch E., Proux O., Olivi L., Ploquin F. and Morin G. (2017) Vertical changes of the Co and Mn speciation along a lateritic regolith developed on peridotites (New Caledonia). *Geochim. Cosmochim. Acta* 217, 1–15.

Edgar R. C. (2010) Search and clustering orders of magnitude faster than BLAST. *Bioinformatics* 26, 2460–2461.

Edgar R. C. (2013) UPARSE: highly accurate OTU sequences from microbial amplicon reads. *Nat. Methods* 10, 996–998.

Edgar R. C., Haas B. J., Clemente J. C., Quince C. and Knight R. (2011) UCHIME improves sensitivity and speed of chimera detection. *Bioinformatics* 27, 2194–2200.

Elias M., Donaldson M. J. and Giorgetta N. (1981) Geology, mineralogy and chemistry of lateritic nickel-cobalt deposits near Kalgoorlie, Western Australia. *Econ. Geol.* 76, 1775–1783.

Gardes M. and Bruns T. D. (1993) ITS primers with enhanced specificity for basidiomycetes--application to the identification of mycorrhizae and rusts. *Mol. Ecol.* 2, 113–118.

Gorby Y. A., Caccavo F. J. and Bolton H. J. (1998) Microbial reduction of cobalt$^{III}$EDTA$^{-}$ in the presence and absence of manganese(IV) oxide. *Environ. Sci. Technol.* 32, 244–250.

Gweon H. S., Oliver A., Taylor J., Booth T., Gibbs M., Read D. S., Griffiths R. I. and Schonrogge K. (2015) PIPITS: an automated pipeline for analyses of fungal internal transcribed spacer sequences from the Illumina sequencing platform. *Methods Ecol. Evol.* 6, 973–980.

Haas B. J., Gevers D., Earl A. M., Feldgarden M., Ward D. V, Giannoukos G., Ciulla D., Tabbaa D., Highlander S. K., Sodergren E., Methé B., DeSantis T. Z., Human Microbiome Consortium T. H. M., Petrosino J. F., Knight R. and Birren B. W. (2011) Chimeric 16S rRNA sequence formation and detection in Sanger and 454-pyrosequenced PCR amplicons. *Genome Res.* 21, 494–504.

Hem J. D. (1985) *Study and interpretation of the chemical characteristics of natural water.* US Geological Survey, Alexandria, VA.

Heyrman J., Vanparys B., Logan N. A., Balcaen A., Rodríguez-Díaz M., Felske A. and Vos P. De (2004) *Bacillus novalis* sp. nov., *Bacillus vireti* sp. nov., *Bacillus soli* sp. nov., *Bacillus bataviensis* sp. nov. and *Bacillus drentensis* sp. nov., from the Drentse A grasslands. *Int. J. Syst. Evol. Microbiol.* 54, 47–57.

Johnson D., Grail B., Hallberg K., Johnson D. B., Grail B. M. and Hallberg K. B. (2013) A new direction for biomining: extraction of metals by reductive dissolution of oxidized ores. *Minerals* 3, 49–58.

Joshi N. A. and Fass J. N. (2011) Sickle: A sliding-window, adaptive, quality-based trimming tool for FastQ files [Software]. Available at http://github.com/najoshi/sickle.

Joshi N., Filip J., Coker V. S., Sadhukhan J., Safarik I., Bagshaw H. and Lloyd J. R. (2018) Microbial reduction of natural Fe(III) minerals; toward the sustainable production of functional magnetic nanoparticles. *Front. Environ. Sci.* 6, 127.

Keith-Roach M. J., Morris K. and Dahlgaard H. (2003) An investigation into technetium binding in sediments. *Mar. Chem.* 81, 149–162.

Kirchhof G., Eckert B., Stoffels M., Ivo Baldani J., Reis V. M. and Hartmann A. (2001) *Herbaspirillum frisingense* sp. nov., a new nitrogan-fixing bacterial species that occurs in C4-fibre plants. *Int. J. Syst. Evol. Microbiol.* 51, 157–168.

Kozich J. J., Westcott S. L., Baxter N. T., Highlander S. K. and Schloss P. D. (2013) Development of a dual-index sequencing strategy and curation pipeline for analyzing amplicon sequence data on the MiSeq Illumina sequencing platform. *Appl. Environ. Microbiol.* 79, 5112–5120.

Kursunoglu S. and Kaya M. (2016) Atmospheric pressure acid leaching of Caldag lateritic nickel ore. *Int. J. Miner. Process.* 150, 1–8.

Laan G. van der and Kirkman I. W. (1992) The 2p absorption spectra of 3d transition metal compounds in tetrahedral and octahedral symmetry. *J. Phys. Condens. Matter* 4, 4189–4204.

Landers M., Gräfe M., Gilkes R. J., Saunders M. and Wells M. A. (2011) Nickel distribution and speciation in rapidly dehydroxylated goethite in oxide-type lateritic nickel ores: XAS and TEM spectroscopic (EELS and EFTEM) investigation. *Aust. J. Earth Sci.* 58, 745–765.

Lane D. J. (1991) 16S/23S rRNA sequencing. In *Nucleic Acid Techniques in Bacterial Systematics* (eds. E. Stackebrant and M. Goodfellow). John Wiley & Sons Ltd, London. pp. 115–175.

Lovley D. R., Holmes D. E. and Nevin K. P. (2004) Dissimilatory Fe(III) and Mn(IV) reduction. In

*Advances in Microbial Physiology* (ed. R. K. Poole). Academic Press. pp. 219–286.

Lovley D. R. and Phillips E. J. (1986) Organic matter mineralization with reduction of ferric iron in anaerobic sediments. *Appl. Environ. Microbiol.* 51, 683–9.

Lovley D. R. and Phillips E. J. P. (1988) Novel mode of microbial energy metabolism: Organic carbon oxidation coupled to dissimilatory reduction of iron or manganese. *Appl. Environ. Microbiol.* 54, 1472–1480.

Lovley D. R. and Phillips E. J. P. (1987) Rapid assay for microbially reducible ferric iron in aquatic sediments. *Appl. Environ. Microbiol.* 53, 1536–1540.

Lovley D. R., Phillips E. J. P., Gorby Y. A. and Landa E. R. (1991) Microbial reduction of uranium. *Nature* 350, 413–416.

Loyaux-Lawniczak S., Vuilleumier S. and Geoffroy V. A. (2019) Efficient reduction of iron oxides by *Paenibacillus* spp. strains isolated from tropical soils. *Geomicrobiol. J.*, 1–10.

Manceau A., Schlegel M. ., Musso M., Sole V. ., Gauthier C., Petit P. . and Trolard F. (2000) Crystal chemistry of trace elements in natural and synthetic goethite. *Geochim. Cosmochim. Acta* 64, 3643–3661.

Marrero J., Coto O., Goldmann S., Graupner T. and Schippers A. (2015) Recovery of nickel and cobalt from laterite tailings by reductive dissolution under aerobic conditions using *Acidithiobacillus* species. *Environ. Sci. Technol.* 49, 6674–6682.

Martin M. (2011) Cutadapt removes adapter sequences from high-throughput sequencing reads. *EMBnet.journal* 17, 10.

Masella A. P., Bartram A. K., Truszkowski J. M., Brown D. G. and Neufeld J. D. (2012) PANDAseq: paired-end assembler for Illumina sequences. *BMC Bioinformatics* 13, 31.

Murray J. W. and Dillard J. G. (1979) The oxidation of cobalt(II) adsorbed on manganese dioxide. *Geochim. Cosmochim. Acta* 43, 781–787.

Myers C. R. and Nealson K. H. (1988) Bacterial manganese reduction and growth with manganese oxide as the sole electron acceptor. *Science (80-. ).* 240, 1319–1321.

Nurk S., Bankevich A., Antipov D., Gurevich A. A., Korobeynikov A., Lapidus A., Prjibelski A. D., Pyshkin A., Sirotkin A., Sirotkin Y., Stepanauskas R., Clingenpeel S. R., Woyke T., Mclean J. S., Lasken R., Tesler G., Alekseyev M. A. and Pevzner P. A. (2013) Assembling single-cell genomes and mini-metagenomes from chimeric MDA products. *J. Comput. Biol.* 20, 714–737.

Oxley A., Smith M. E. and Caceres O. (2016) Why heap leach nickel laterites? *Miner. Eng.* 88, 53–60.

Pattrick R. A. D., Van Der Laan G., Henderson C. M. B., Kuiper P., Dudzik E. and Vaughan D. J. (2002) Cation site occupancy in spinel ferrites studied by X-ray magnetic circular dichroism: developing a method for mineralogists. *Eur. J. Mineral.* 14, 1095–1102.

Perez O. C., Coto J. M. and Schippers A. (2013) Quantification of the microbiaI community in lateritic deposits. *Integr. Sci. Ind. Knowl. Biohydrometall.* 825, 33–36.

Petrie L., North N. N., Dollhopf S. L., Balkwill D. L. and Kostka J. E. (2003) Enumeration and characterization of iron(III)-reducing microbial communities from acidic subsurface sediments contaminated with uranium(VI). *Appl. Environ. Microbiol.* 69, 7467–7479.

Pohlmann A., Fricke W. F., Reinecke F., Kusian B., Liesegang H., Cramm R., Eitinger T., Ewering C., Pötter M., Schwartz E., Strittmatter A., Voß I., Gottschalk G., Steinbüchel A., Friedrich B. and Bowien B. (2006) Genome sequence of the bioplastic-producing “Knallgas” bacterium *Ralstonia eutropha* H16. *Nat. Biotechnol.* 24, 1257–1262.

Rauret G., López-Sánchez J. F., Sahuquillo A., Rubio R., Davidson C., Ure A., Quevauviller P. and F. Lopez-Sanchez J. (1999) Improvement of the BCR three step sequential extraction procedure prior to the certification of new sediment and soil reference materials. *J. Environ. Monit.* 1, 57–61.

Ravel B. and Newville M. (2005) ATHENA, ARTEMIS, HEPHAESTUS: data analysis for X-ray absorption spectroscopy using IFEFFIT. *J. Synchrotron Radiat.* 12, 537–541.

Reinhold-Hurek B. and Hurek T. (2006) The genera *Azoarcus, Azovibrio, Azospira* and *Azonexus*. In *The Prokaryotes* Springer New York, New York, NY. pp. 873–891.

Roqué-Rosell J., Mosselmans J. F. W., Proenza J. A., Labrador M., Galí S., Atkinson K. D. and Quinn P. D. (2010) Sorption of Ni by “lithiophorite-asbolane” intermediates in Moa Bay lateritic deposits, eastern Cuba. *Chem. Geol.* 275, 9–18.

Roqué-Rosell J., Villanova-de-Benavent C. and Proenza J. A. (2017) The accumulation of Ni in serpentines and garnierites from the Falcondo Ni-laterite deposit (Dominican Republic) elucidated by means of μXAS. *Geochim. Cosmochim. Acta* 198, 48–69.

Rowe A. R., Yoshimura M., LaRowe D. E., Bird L. J., Amend J. P., Hashimoto K., Nealson K. H. and Okamoto A. (2017) *In situ* electrochemical enrichment and isolation of a magnetite-reducing bacterium from a high pH serpentinizing spring. *Environ. Microbiol.* 19, 2272–2285.

Salter S. J., Cox M. J., Turek E. M., Calus S. T., Cookson W. O., Moffatt M. F., Turner P., Parkhill J., Loman N. J. and Walker A. W. (2014) Reagent and laboratory contamination can critically impact sequence-based microbiome analyses. *BMC Biol.* 12, 87.

Shaheen S. M., Rinklebe J., Frohne T., White J. R. and DeLaune R. D. (2014) Biogeochemical factors governing cobalt, nickel, selenium, and vanadium dynamics in periodically flooded Egyptian North Nile Delta rice soils. *Soil Sci. Soc. Am. J.* 78, 1065.

da Silva K., Florentino L. A., da Silva K. B., de Brandt E., Vandamme P. and de Souza Moreira F. M. (2012) *Cupriavidus necator* isolates are able to fix nitrogen in symbiosis with different legume species. *Syst. Appl. Microbiol.* 35, 175–182.

Simanova A. A. and Peña J. (2015) Time-resolved investigation of cobalt oxidation by Mn(III)-rich δ-$MnO_2$ using quick X-ray absorption spectroscopy. *Environ. Sci. Technol.* 49, 10867–10876.

Singh R., Dong H., Liu D., Marts A. R., Tierney D. L. and Almquist C. B. (2015) [Cobalt(III)–EDTA]− reduction by thermophilic methanogen *Methanothermobacter thermautotrophicus*. *Chem. Geol.* 411, 49–56.

Smith S. L., Grail B. M. and Johnson D. B. (2017) Reductive bioprocessing of cobalt-bearing limonitic laterites. *Miner. Eng.* 106, 86–90.

Tanaka K., Yu Q., Sasaki K. and Ohnuki T. (2013) Cobalt(II) oxidation by biogenic Mn oxide produced by *Pseudomonas* sp. strain NGY-1. *Geomicrobiol. J.* 30, 874–885.

Taylor D. L., Walters W. A., Lennon N. J., Bochicchio J., Krohn A., Caporaso J. G. and Pennanen T. (2016) Accurate estimation of fungal diversity and abundance through improved lineage-specific primers optimized for Illumina amplicon sequencing. *Appl. Environ. Microbiol.* 82, 7217–7226.

Taylor R. and McKenzie R. (1966) The association of trace elements with manganese minerals in Australian soils. *Aust. J. Soil Res.* 4, 29.

The Cobalt Institute (2019) The Cobalt Institute. *Webpage*. Available at: https://www.cobaltinstitute.org/ [Accessed January 22, 2019].

Tzeferis P. G., Agatzini S. and Nerantzis E. T. (1994) Mineral leaching of non-sulphide nickel ores using heterotrophic micro-organisms. *Lett. Appl. Microbiol.* 18, 209–213.

Uren N. (2013) Cobalt and manganese. In *Heavy Metals in Soils: Trace Metals and Metalloids in Soils and their Bioavailability* (ed. B. J. Alloway). Springer Netherlands. pp. 335–366.

US Geological Survey (2018) *Mineral commodity summaries: Cobalt*, US Geological Survey, Reston, Virginia.

Valix M., Usai F. and Malik R. (2001) Fungal bio-leaching of low grade laterite ores. *Miner. Eng.* 14, 197–203.

Villemur R., Lanthier M., Beaudet R. and Lépine F. (2006) The *Desulfitobacterium* genus. *FEMS Microbiol. Rev.* 30, 706–733.

Vos P. De, Garrity G. M., Jones D., Krieg N. R., Ludwig W., Rainey F. A., Schleifer K.-H. and Whitman W. B. (2009) *Bergey's Manual of Systematic Bacteriology, Volume 3, The Firmicutes*. 2nd Edition., Springer Dordrecht Heidelberg London New York.

Wang Q., Garrity G. M., Tiedje J. M. and Cole J. R. (2007) Naive Bayesian classifier for rapid assignment of rRNA sequences into the new bacterial taxonomy. *Appl. Environ. Microbiol.* 73, 5261–5267.

Wilkins M. J., Livens F. R., Vaughan D. J., Beadle I. and Lloyd J. R. (2007) The influence of microbial redox cycling on radionuclide mobility in the subsurface at a low-level radioactive waste storage site. *Geobiology* 5, 293–301.

Yongue-Fouateu R., Ghogomu R. T., Penaye J., Ekodeck G. E., Stendal H. and Colin F. (2006) Nickel and cobalt distribution in the laterites of the Lomié region, south-east Cameroon. *J. African Earth Sci.* 45, 33–47.

Zavarzina D. G., Sokolova T. G., Tourova T. P., Chernyh N. A., Kostrikina N. A. and Bonch-Osmolovskaya E. A. (2007) *Thermincola ferriacetica* sp. nov., a new anaerobic, thermophilic, facultatively chemolithoautotrophic bacterium capable of dissimilatory Fe(III) reduction. *Extremophiles* 11, 1–7.

Zhang X., Li G.-X., Chen S.-C., Jia X.-Y., Wu K., Cao C.-L. and Bao P. (2016) Draft genome sequence of *Desulfitobacterium hafniense* strain DH, a sulfate-reducing bacterium isolated from paddy soils. *Genome Announc.* 4, e01693-15.

# Appendix 2. Exploratory experimental beamtime work on lateritic soils from Santa Elena Peninsula and microcosms

---

## A2.1 X-ray absoprtion spectroscopy (XAS) in soils after anaerobic biostimulation in microcosm

X-ray absorption spectroscopy (XAS) exploratory work was done using the 6.3.1 beamline at the Advance Light Source (ALS). Lawrence Berkeley National Laboratory. Berkeley, California, United States of America (March 2018). Here 4 microcosm soil samples after anoxic incubation were analysed:

1. Mountain soil from ES location biostimulated with glucose
2. Mountain soil from CEI location biostimulated with cellulose
3. North Lowland soil from BES location, dry season, biostimulated with cellulose
4. North Lowland soil from BES location, wet season, biostimulated with cellulose

Samples were analysed for Fe, Ni, Mn and Co. However, only Fe XAS data was successfully recorded for all the samples. Mn and Co concentrations were too low for detection in some of them, while Ni was not detected in any of the samples analysed. In general, XAS data showed that after anoxic incubation with glucose and cellulose (Figure A2.1 and A2.2), Fe(II) and Mn(II) likely were the dominant species. Iron the mountain soil samples resembled to magnetite minerals, while Fe(III) minerals like those originally present in soil samples were diminished (Joshi et al., 2018; Kubin et al., 2018; M. et al., 2015). This information supported all the data discussed in Chapters 5 and 6 of this thesis.

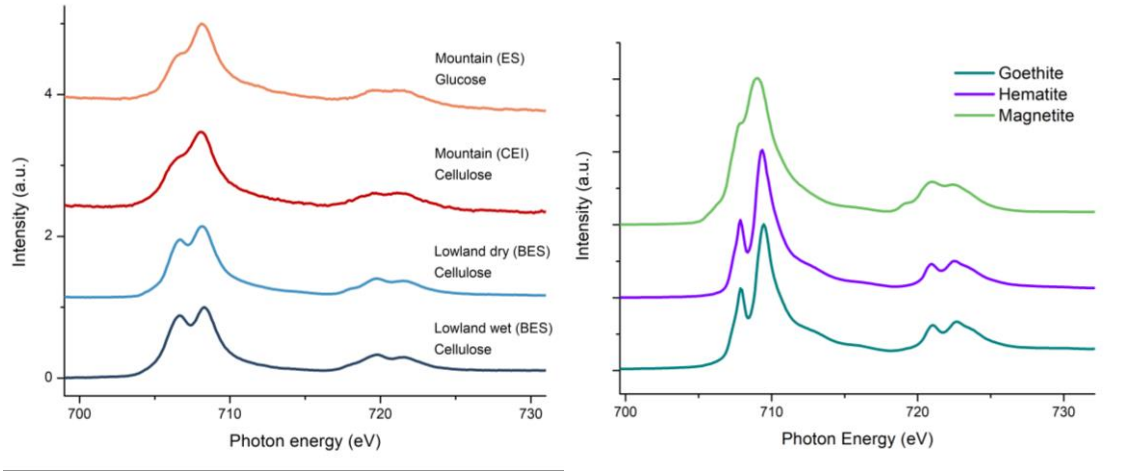


**Figure A2.1.** Fe L-edge XAS collected for different soil samples from the Santa Elena Peninsula after anaerobic biostimulation in redox cycling microcosm experiments (left), and for Fe standards (right).

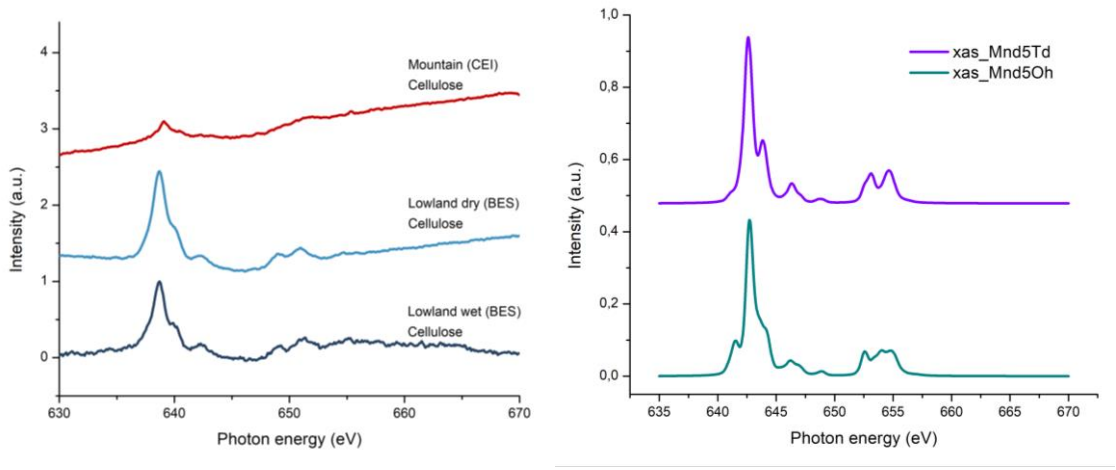


**Figure A2.2.** Mn L-edge XAS collected for different soil samples from the Santa Elena Peninsula after anaerobic biostimulation in redox cycling microcosm experiments (left), and L-edge XAS calculations for Mn(II).

Cobalt was only detected in one of the samples after anoxic incubation, the microcosm containing mountain soils from ES locations and stimulated with glucose, likely as Co(II) (Figure A2.3) (Bora et al., 2015). In the three other three samples analysed in ALS, those stimulated with cellulose, Co was not detected in the soils, presumably due to the high mobilisation of cobalt to the aqueous phase when these microcosm soils were amended with cellulose, as shown in Chapter 6.

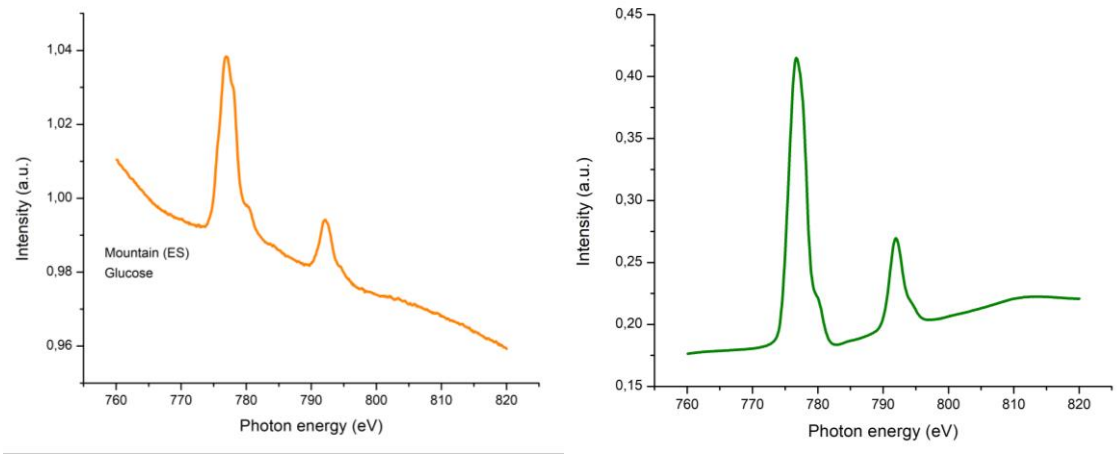


**Figure A2.3.** Co L-edge XAS collected for Mountain (ES) soil sample collected during dry season from the Santa Elena Peninsula after anaerobic biostimulation with glucose in redox cycling microcosm experiments (left), and for standard cobalt sulphate (right).

### A2.2 K-edge XANES in aqueous solution after anaerobic biostimulation in microcosm

Additional exploratory work with X-ray Apsorption Near Edge Spectroscopy (XANES) was done using the I20 beamline at Diamond Light Source (DLS), Oxfordshire, United Kingdom (September 2018). Here the aqueous solution of 4 microcosm soil samples after anoxic incubation with cellulose were analysed:

1. Mountain soil from CEI location biostimulated with cellulose
2. Mountain soil from ES location, dry season, biostimulated with cellulose
3. Mountain soil from ES location, wet season, biostimulated with cellulose
4. North Lowland soil from BES location, wet season, biostimulated with cellulose

Samples were analysed for Fe, Mn and Co. However, only Fe and Mn XANES data were successfully recorded for all the samples. Co concentrations were too low for detection. In general, Fe and Mn were found as reduced species in solution (Figure A2.4) (Henderson et al., 2014), supporting all the data shown in Chapter 6, where reductive conditions were imposed in the microcosm soils. Therefore microbially-mediated solubilisation of Fe(II) and Mn(II) occurred coupled to cellulose degradation in these soils. However, two soil samples (Mountain ES wet and

Mountain CEI) were re-oxidised, but this was more likely due to accidental oxidation of samples during sampling and/or transport.

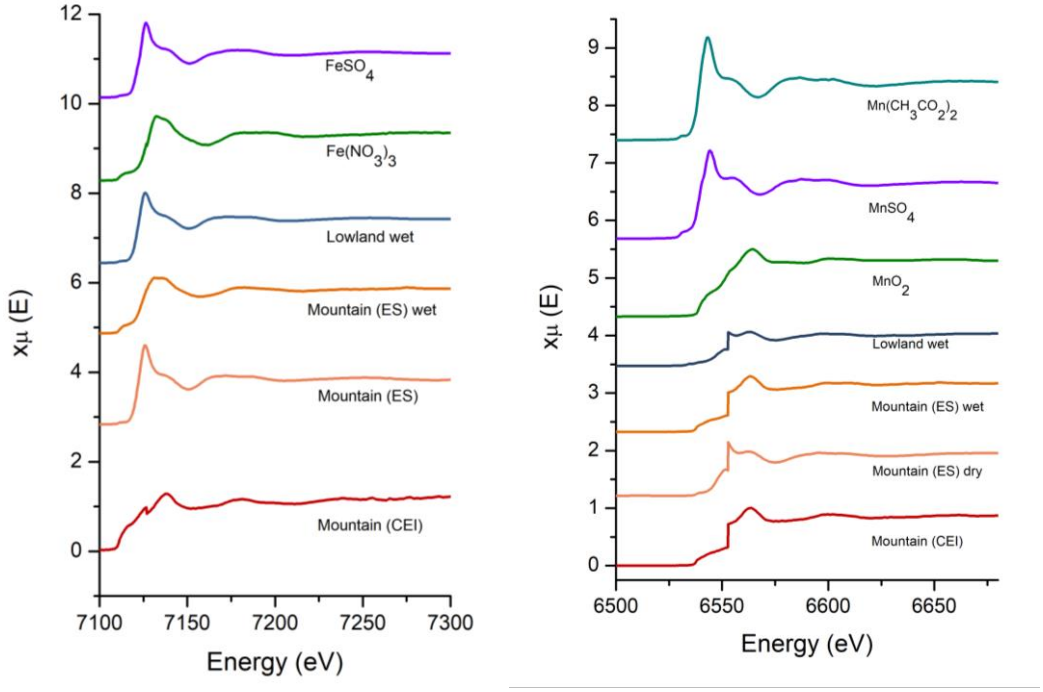


**Figure A2.4.** Fe (left) and Mn (right) K-edge XANES collected for the aqueous phase of the redox cycling microcosm experiments with soils from the Santa Elena Peninsula after anoxic biostimulation with cellulose and for their respective standards.

### A2.3 Cobalt K-edge XANES in lateritic soils from the Santa Elena Peninsula

Some exploratory work using K-edge XANES was done using the I20 beamline at Diamond Light Source (DLS). Oxfordshire, United Kingdom (January 2018), to study the natural chemistry of Co in those soils. Here 3 soil samples from Santa Elena Peninsula were analysed:

1. Mountain soil from CEI location
2. North Lowland soil from BES location
3. Serpentinite clast collected from the soil from Mountain LN location

In all the samples tested (Figure A2.5), cobalt was not likely to be as its reduced form (Bresson et al., 2006) presumably due to the natural oxidative conditions of the soils, reflected in the mineralogy dominated by Fe(III) (Chapter 4).

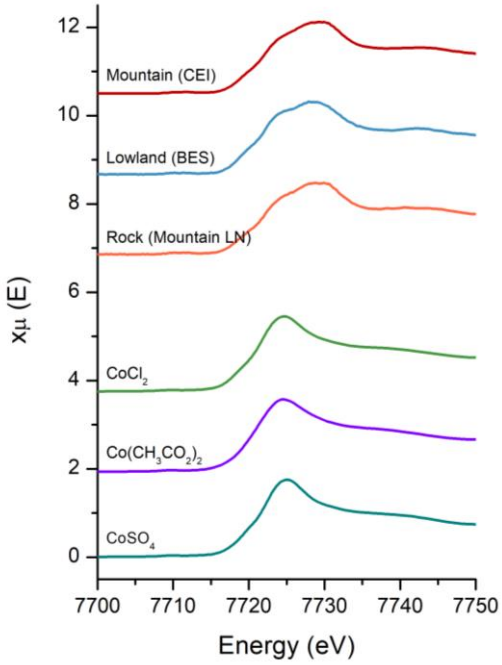


**Figure A2.5.** Co K-edge XANES collected for the aqueous phase of the redox cycling microcosm experiments with soils from the Santa Elena Peninsula after anaerobic biostimulation with cellulose and for Mn standards.

### A2.4 References

Bora, D.K., Cheng, X., Kapilashrami, M., Glans, P.A., Luo, Y., Guo, J.-H., 2015. Influence of crystal structure, ligand environment and morphology on Co L-edge XAS spectral characteristics in cobalt compounds. J. Synchrotron Radiat. 22, 1450–1458.

Bresson, C., Esnouf, S., Lamouroux, C., Solari, P.L., Den Auwer, C., 2006. XAS Investigation of biorelevant cobalt complexes in aqueous media. New J. Chem. 30, 416–424. https://doi.org/10.1039/B514454J

Henderson, G., De Groot, F., Moulton, B., 2014. X-ray Absorption Near-Edge Structure (XANES) Spectroscopy. Rev. Mineral. Geochemistry 78, 75–138. https://doi.org/10.2138/rmg.2014.78.3

Joshi, N., Filip, J., Coker, V.S., Sadhukhan, J., Safarik, I., Bagshaw, H., Lloyd, J.R., 2018. Microbial Reduction of Natural Fe(III) Minerals; Toward the Sustainable Production of Functional Magnetic Nanoparticles . Front. Environ. Sci. .

Kubin, M., Guo, M., Kroll, T., Löchel, H., Källman, E., Baker, M.L., Mitzner, R., Gul, S., Kern, J., Föhlisch, A., Erko, A., Bergmann, U., Yachandra, V., Yano, J., Lundberg, M., Wernet, P., 2018. Probing the oxidation state of transition metal complexes: a case study on how charge and spin densities determine Mn L-edge X-ray absorption energies. Chem. Sci. 9, 6813–6829. https://doi.org/10.1039/C8SC00550H

M., B.J., H., M., S., C. V, J., C., R., L.J., 2015. Scale-up of the production of highly reactive biogenic magnetite nanoparticles using Geobacter sulfurreducens. J. R. Soc. Interface 12, 20150240. https://doi.org/10.1098/rsif.2015.0240

# Appendix 3. Conference presentations, external experimental work collaboration, fieldwork and outreach.

---

### A3.1 Awards

**Best poster award.** 1st The geochemistry and mineralogy of contaminated environments meeting. London, United Kingdom, organised by the Royal Society of Chemistry. 2018, June. **Poster**: "Natural biogeochemistry of Co, Ni and Cr in Costa Rican Lateritic soils".

### A3.2 Conferences

#### A3.2.1 Oral presentations

1. 2019, August. Goldschmidt Conference 2019. Barcelona, Spain, organised by the European Association of Geochemistry. Flash talk.
2. 2018, December. 9th SEES Postgraduate Research Conference. Manchester, UK, organised by the SEES University of Manchester. Oral talk.
3. 2018, August. Goldschmidt Conference 2018. Boston, United States of America, organised by the European Association of Geochemistry. Oral talk.

#### A3.2.2 Poster presentations

1. 2019, August. Goldschmidt Conference 2019. Barcelona, Spain, organised by the European Association of Geochemistry.
2. 2019, May. Security of Supply of Mineral Resources Finale Meeting 2019. London, UK, organised by the British Geological Survey.
3. 2018, June. 1st The geochemistry and mineralogy of contaminated environments meeting. London, United Kingdom, organised by the Royal Society of Chemistry and the Mineralogical Society of Great Britain and Ireland.
4. 2017, December. 8th SEES Postgraduate Research Conference. Manchester, UK, organised by the SEES University of Manchester.

5. 2017, August. Goldschmidt Conference 2017. Paris, France, organised by the European Association of Geochemistry.
6. 2017, April. Microbiological Society Annual Conference 2017. Edinburgh, United Kingdom, organised by the Microbiological Society of United Kingdom.
7. 2016, December. 7th SEES Postgraduate Research Conference. Manchester, UK, organised by the SEES University of Manchester.

### A3.3 External experimental work: laboratory beamtime

1. Diamond Light Source (DLS). Oxfordshire, United Kingdom. 2018, September. Beamtime at beamline I20 was funded by grant SP17313 from DLS.
2. Advance Light Source (ALS). Lawrence Berkeley National Laboratory. Berkeley, California, United States of America. March 2018. Used 6.3.1 beamline for XAS and XMCD, with resources of ALS, which is a Department of Energy Office of Science User Facility under contract no. DE-AC02-05CH11231.
3. Diamond Light Source (DLS). Oxfordshire, United Kingdom. 2018, January. Beamtime at beamline I20 was funded by grant SP16735 from DLS.

### A3.4 CoG$^3$ Meetings

These were CoG$^3$ project meetings where I had to present an update of my research (as oral talk) in every one of them:

1. Camborne School of Mines, Penryn, Cornwall, 12$^{th}$ April 2019.
2. National Oceanography Centre (NOC), Southampton, 1$^{st}$ November 2018.
3. University of Edinburgh, Edinburgh, 22$^{nd}$ March 2018.
4. University of Manchester, Manchester, 17$^{th}$ October 2017
5. University of Dundee, Dundee, 29$^{th}$ June 2017
6. Natural History Museum, London, 24$^{th}$ March 2017
7. University of Manchester, Manchester, 27$^{th}$ October 2016
8. Natural History Museum, London, 21$^{st}$ March 2016

### A3.5 Outreach

Outreach expositor. Bluedot Festival, co-organised by the University of Manchester. **Stand:** “Life at the Extremes”. Jodrell Bank Observatory, Cheshire, United Kingdom. 2018. July.

### A3.6 Fieldwork in Costa Rica

Several field campaigns were done to Costa Rica, in all of them the Santa Rosa National Park in the Área de Conservación Guanacaste was visited. The Peninsula of Santa Elena is inside this National Park. In all fieldtrips the Unidad de Recursos Forestales Laboratory in the University of Costa Rica was used as local research laboratory.

1. Fifth fieldtrip (Rock sampling): del 3rd-26th April 2018.
2. Fourth fieldtrip (Rock sampling): 1st-25th September 2017.
3. Third fieldtrip (Dry season soil sampling): 19th April to 12th May 2017.
4. Second fieldtrip (Wet season soil sampling): 7th-25th September 2016.
5. First fieldtrip (Exploratory work of sampling locations): 18th May to 5th June 2016. In this field campaign some exploratory work was also done in the Páramo of Cerro de la Muerte, within the Tapantí-Macizo de la Muerte National Park from the Área de Conservación La Amistad Pacífico.